STRESS ANALYSIS OF POROELASTIC SEABED SLOPES UNDER WAVE LOADING USING THE BOUNDARY ELEMENT METHOD

WAYNE W. RAMAN-NAIR, B Sc (Math), B Sc (Eng), M Eng

STRESS ANALYSIS OF POROELASTIC SEABED SLOPES UNDER WAVE LOADING USING THE BOUNDARY ELEMENT METHOD

by

© Wayne W. Raman-Nair, B.Sc. (Math.), B. Sc. (Eng.), M. Eng.

A thesis submitted to the School of Graduate
Studies in partial fulfillment of the
requirements for the degree of
Doctor of Philosophy

Faculty of Engineering and Applied Science
Memorial University of Newfoundland
October 1990

St. John's Newfoundland Canada

ISBN 0-315-61801-9

SUBJECT CATEGORIES

Dissertation Abstracts International is arranged by broad, general subject categories. Choose the *one* listed below (capital letters) which most nearly describes the general content of your dissertation. If the major subject category has sub-fields under it, and *only* if it does, please choose *one* (small letters). (Ex.: ECONOMICS, Theory). Enter subject category on Item 7 of Agreement Form.

HUMANITIES

IA COMMUNICATIONS AND THE ARTS
- ARCHITECTURE
- CINEMA
- FINE ARTS
- INFORMATION SCIENCE
- JOURNALISM
- LIBRARY SCIENCE
- MASS COMMUNICATIONS
- MUSIC
- SPEECH
- THEATER

IIA EDUCATION
- EDUCATION
  - General
  - Administration
  - Adult
  - Agricultural
  - Art
  - Audiovisual
  - Business
  - Community and Social
  - Community Colleges
  - Curriculum and Instruction
  - Early Childhood
  - Elementary
  - Finance
  - Guidance and Counseling
  - Health
  - Higher
  - History
  - Home Economics
  - Industrial
  - Language and Languages
  - Mathematics
  - Middle School
  - Minorities
  - Music
  - Personality Development and Mental Hygiene
  - Philosophy
  - Physical
  - Preschool
  - Programmed Instruction
  - Psychology
  - Religion
  - Sciences
  - Secondary
  - Social Sciences
  - Special
  - Teacher Training
  - Teaching Machines
  - Tests and Measurements
  - Theory and Practice
  - Vocational

IIIA LANGUAGE, LITERATURE AND LINGUISTICS
- LANGUAGE
  - General
  - Ancient
  - Linguistics
  - Modern
- LITERATURE
  - General
  - Classical
  - Comparative
  - Medieval
  - Modern
  - American
  - Asian
  - Dutch and Scandinavian
  - English
  - Germanic
  - Latin American
  - Romance
  - Russian and East European
  - Slavic and Finno-Ugrian

IVA PHILOSOPHY, RELIGION AND THEOLOGY
- PHILOSOPHY
- RELIGION
  - General
  - Clergy
  - History
  - Music
  - Philosophy
- THEOLOGY

VA SOCIAL SCIENCES
- ACCOUNTING
- AMERICAN STUDIES
- ANTHROPOLOGY
  - Archaeology
  - Cultural
  - Physical
- BANKING
- BUSINESS ADMINISTRATION
- ECONOMICS
  - General
  - Agricultural
  - Commerce-Business
  - Finance (includes Public Finance)
  - History
  - Theory
- FOLKLORE
- HISTORY
  - General
  - Ancient
  - Medieval
  - Modern
  - Black
  - Church
  - Africa
  - Asia
  - Australia and Oceania
  - Canada
  - Europe
  - Latin America
  - United States
- HISTORY OF SCIENCE
- LAW
- MANAGEMENT
- MARKETING
- POLITICAL SCIENCE
  - General
  - International Law and Relations
  - Public Administration
- PUBLIC RELATIONS
- RECREATION
- SOCIAL GEOGRAPHY
- SOCIAL STRUCTURE
- SOCIAL WORK
- SOCIOLOGY
  - General
  - Community Organization
  - Criminology
  - Demography
  - Educational
  - Individual and Family Studies
  - Industrial
  - Labor Relations
  - Public Welfare
  - Race Relations
  - Social Problems
  - Statistics–Research Methods
  - Theory
- TRANSPORTATION
- URBAN AND REGIONAL PLANNING
- WOMEN'S STUDIES

SCIENCES

IB BIOLOGICAL SCIENCES
- AGRICULTURE
  - General
  - Animal Culture
  - Animal Pathology
  - Forestry & Wildlife
  - Plant Culture
  - Plant Pathology
  - Plant Physiology
  - Range Management
  - Wood Technology
- AGRONOMY
- ANATOMY
- BIOLOGICAL OCEANOGRAPHY
- BIOLOGY
- BIOPHYSICS
  - General
  - Medical
- BIOSTATISTICS
- BOTANY
- ECOLOGY
- ENTOMOLOGY
- GENETICS
- LIMNOLOGY
- MICROBIOLOGY
- PHYSIOLOGY
- RADIATION BIOLOGY
- VETERINARY SCIENCE
- ZOOLOGY

IIB EARTH SCIENCES
- GEOCHEMISTRY
- GEODESY
- GEOLOGY
- GEOPHYSICS
- HYDROLOGY
- MINERALOGY
- PALEOBOTANY
- PALEONTOLOGY
- PALEOZOOLOGY
- PHYSICAL GEOGRAPHY
- PHYSICAL OCEANOGRAPHY

IIIB HEALTH AND ENVIRONMENTAL SCIENCES
- ENVIRONMENTAL SCIENCES
- FOOD TECHNOLOGY
- HEALTH SCIENCES
  - General
  - Audiology
  - Chemotherapy
  - Dentistry
  - Education
  - Hospital Management
  - Human Development
  - Hygiene
  - Immunology
  - Medicine & Surgery
  - Mental Health
  - Nursing
  - Nutrition
  - Pathology
  - Pharmacy
  - Public Health
  - Radiology
  - Recreation
  - Speech Pathology
- HOME ECONOMICS
- PHARMACOLOGY

IVB PHYSICAL SCIENCES
- PURE SCIENCES
  - CHEMISTRY
    - General
    - Analytical
    - Biological
    - Inorganic
    - Nuclear
    - Organic
    - Pharmaceutical
    - Physical
    - Polymer
    - Radiation
    - Water
  - MATHEMATICS
  - PHYSICS
    - General
    - Acoustics
    - Astronomy & Astrophysics
    - Atmospheric Science
    - Atomic
    - Electronics and Electricity
    - Elementary Particles and High Energy
    - Fluid and Plasma
    - Molecular
    - Nuclear
    - Optics
    - Radiation
    - Solid State
  - STATISTICS
- APPLIED SCIENCES
  - APPLIED MECHANICS
  - ASTRONAUTICS
  - COMPUTER SCIENCE
  - ENGINEERING
    - General
    - Aerospace
    - Agricultural
    - Automotive
    - Biomedical
    - Chemical (includes ceramics and fuel)
    - Civil
    - Electronics and Electrical
    - Heat and Thermodynamics
    - Hydraulic
    - Industrial
    - Marine
    - Materials Science
    - Mechanical
    - Metallurgy
    - Mining
    - Nuclear
    - Petroleum
    - Sanitary and Municipal
    - System Science
  - OPERATIONS RESEARCH
  - PLASTICS TECHNOLOGY
  - TEXTILE TECHNOLOGY

VB PSYCHOLOGY
- PSYCHOLOGY
  - General
  - Clinical
  - Experimental
  - Industrial
  - Physiological
  - Psychobiology
  - Social

Abstract

The effect of wave forces on the stability of a sloping seabed is investigated using linear wave theory and Biot's theory of poroelasticity. The wave forces on the slope, the wave-induced effective stresses and pore pressures are all computed by the boundary element method. Full derivations are presented for the boundary integral equations and fundamental solutions of the poroelastic theory for the case of sinusoidal loading conditions. The wave-induced stress field is combined with the in-situ stress field and the Mohr-Coulomb failure criterion is used to determine the zone of incipient failure. It is found that wave induced stresses must be analysed throughout an entire wave cycle in order to assess the likelihood of failure and also that the stability of a slope under waves is strongly dependent on the initial stress distribution.

Acknowledgements

I would like to thank my supervisor, Dr. Gary Sabin, for his guidance and encouragement throughout the development of this thesis. His insight and experience as a mathematician were invaluable in overcoming many of the hurdles present in an endeavour such as this. For typing the manuscript on Latex I owe sincere thanks to Cyril Mullins and his wife Elizabeth. For the drawings in chapters 3, 4, 6, 7 and in appendices B, C and I, I am indebted to Daryl Thompson. The contour plots in chapter 8 and appendix J were cut out and arranged by Brian Titus and his wife Colina, and to them I express my warmest appreciation. For assistance with the labeling of these plots I am deeply grateful to my brother-in-law, Mr. Darrell Warren. To my wife Catherine Anne I express my deepest appreciation for her patience and understanding in tolerating a largely absentee husband during the preparation of the work. In addition, I would like to acknowledge the financial support of the School of Graduate Studies, the Faculty of Engineering and Applied Science and my supervisor Dr. Gary Sabin.

Finally, I express my thanks to God for His guidance in my work and in my life.

Contents

List of Figures

List of Tables

List of Symbols

Latin symbols

a	parameter dependent on soil properties and wave frequency (equation 5.81)
c	parameter related to a by a multiplicative constant (equation 6.15)
$D_{\alpha kj}$	kernels for the evaluation of interior stresses
e	dilatation of solid skeleton
e_{ij}	strain tensor of solid skeleton
f	porosity of soil
F_{ij}	sum of all inter-granular forces vector on an area δA of soil normal to the j axis
g	acceleration due to gravity
G	shear modulus of soil skeleton
G_{ik}	part of the fundamental solution $\tilde{\tilde{u}}_i^{*k}$
h_0	water depth at slope base
h_0'	water depth at slope top
H	wave height; an elastic modulus of soil (equation 5.52)
H_{ik}	part of the fundamental solution $\tilde{\tilde{u}}_i^{*k}$
i	$\sqrt{-1}$
k	soil parameter (equation 3.21); wave number
k_0	permeability of soil in ms^{-1}
K	conjugate stress ratio
K_0	coefficient of lateral earth pressure at rest
K_0, K_1, K_2	modified Bessel functions of the second kind of orders 0,1,2 respectively
K_b	bulk modulus of soil skeleton
K_f	bulk modulus of water
K_r	bulk modulus of soil grains
l_0	soil depth at slope base
l_0'	soil depth at slope top
L	wavelength
M	soil parameter (equation 3.2)
n_i	unit outward normal to a curve or surface
p	pore pressure
$\bar{p}$	frequency independent part of pore pressure
$\bar{p}^0, \bar{p}^{01}, \bar{p}^{*k}$	fundamental solutions
$\underline{\rho}, \underline{P}$	position vector of a point P

P_0	amplitude of wave pressure at the mudline
P_{ik}	part of the fundamental solution $\tilde{\overline{T}}_i^{*k}$
Q	soil parameter (equation 3.14)
Q_{ik}	part of the fundamental solution $\tilde{\overline{T}}_i^{*k}$
r	distance from node j to an arbitrary point
R	soil parameter (equation 3.14)
$S_{\alpha kj}$	kernels for the evaluation of interior stresses
t	time
T_i for $i = 1,2$	surface tractions
T_3	$= -p$
$\overline{T}_i$ for $i = 1,2,3$	frequency independent part of T_i
$\tilde{\overline{T}}_i$ $(i = 1,2,3)$	dimensionless form of $\overline{T}_i$
$\overline{T}_i^e, \tilde{\overline{T}}_i^e$	nodal values of $\overline{T}_i, \tilde{\overline{T}}_i$
$\overline{T}_i^0, \overline{T}_i^{01}, \overline{T}_i^{*k}, \tilde{\overline{T}}_i^{*k}$	fundamental solutions
$\underline{u}, u_i$ $(i = 1,2)$	displacement vector of the soil skeleton
u_3	$= f(U_i - u_i)$
$\overline{u}_i$ for $i = 1,2,3$	frequency independent part of u_i
$\tilde{\overline{u}}_i$ $(i = 1,2,3)$	dimensionless form of $\overline{u}_i$
$\overline{u}_i^e, \tilde{\overline{u}}_i^e$	nodal values of $\overline{u}_i, \tilde{\overline{u}}_i$
$\overline{u}_i^0, \overline{u}_i^{01}, \overline{u}_i^{*k}, \tilde{\overline{u}}_i^{*k}$	fundamental solutions
$\underline{U}, U_i$ $(i = 1,2)$	displacement vector of the pore water
$\overline{U}_i$ for $i = 1,2$	frequency independent part of U_i
$\overline{U}_i^0, \overline{U}_i^{01}, \overline{U}_i^{*k}, \tilde{\overline{U}}_i^{*k}$	fundamental solutions
$\overline{v}_n$	$= \overline{u}_3$
$\overline{v}_n^{01}, \overline{v}_n^{*k}$	fundamental solutions
$\underline{X}, X_i$	body force per unit mass
Z_{ik}	part of the fundamental solution $\tilde{\overline{T}}_i^{*k}$

Greek symbols

α	soil parameter (equation 3.2)
β	slope angle in degrees; function of μ and ν (equation 5.63)
γ_d	dry unit weight of soil
γ'	buoyant unit weight of soil

Γ	boundary of soil region
Γ_e	boundary segment of soil region
Δ	Dirac delta function
δ_{ij}	Kronecker delta
ε	fluid dilatation
η_0	incident wave amplitude
θ	stress angle (degrees)
λ	Lame' constant of soil skeleton
λ_c	soil parameter (equation 3.2)
μ	shear modulus of soil skeleton
ν	Poisson's ratio of soil skeleton
ξ	local coordinate on boundary element
ρ	density of soil (bulk)
ρ_s	density of soil grains
ρ_f	density of pore water
$\sigma = -fp$	fluid part of total stress tensor (equation 3.11)
σ_{ij}	solid part of total stress tensor (equation 3.11)
$\overline{\sigma}_{ij}^{*k}, \overline{\sigma}^{0}$	fundamental solutions
σ_x', σ_z'	x, z components of effective stress
τ_{ij}	total stress tensor
τ_{ij}'	effective stress tensor
τ_{xz}	(effective) shear stress
Φ	wave velocity potential
ϕ	frequency independent part of wave velocity potential
ϕ^*	fundamental solution (potential problem)
ϕ'	angle of internal friction of soil in degrees (effective stress parameter)
ω	wave frequency (circular)
Ω	a region of soil or water

Chapter 1

INTRODUCTION

Engineering interest in the stability of the seafloor has been motivated by the presence of petroleum beneath the submarine soil. The necessity of locating bottom-mounted structures, pipelines and cables on or in the vicinity of seabed slopes has made the analysis of submarine slope stability a matter of great importance. One of the factors contributing to submarine slope failures is the effect of the loading due to water waves. A well known example is the failure of two Shell jacket pile platforms in the Gulf of Mexico during Hurricane Camille (1969). Other areas susceptible to wave-induced slope instabilities are the Gulf of Alaska and the Nova Scotian shelf. Although many researchers (including the author) have presented stability analyses of a flat seabed under wave loading, few have attempted comprehensive theoretical studies of seabed slopes. It has been long recognised that there is a need for a stress analysis approach to problems of slope stability to supplement existing limit equilibrium analyses. In performing such a study the important first step is the choice of a soil model. Unfortunately, there is at present no soil model

which by itself completely describes the complex behaviour of soil. In choosing a model one must therefore identify those aspects of soil behaviour which are most pertinent to the problem being addressed. Several researchers (Yamamoto et al., 1978-1985; Mynett and Mei, 1982; Zienkiewicz et al., 1984; Cheng and Liu, 1986) have pointed out that in determining the seabed response to wave loading, the coupling between the soil skeleton and pore water is of primary significance. In light of this fact, Biot's poroelastic model will be used as the basis for the theoretical analysis. This model has been experimentally verified for the wave loading of sand beds (Yamamoto, 1978 ; Cheng and Liu, 1986). In order to determine the wave forces on the slope we shall use linear (Airy) wave theory and the boundary element method. The problem of wave propagation over a slope has been studied analytically by Stoker (1957) for certain values of the slope angle. For our purposes it is necessary to determine the wave forces on an arbitrary slope, and to this end the boundary element method furnishes a quick and efficient procedure. The boundary conditions on the surface of the slope are thus provided in a natural way.

We distinguish between two features of soil response under wave loading. In the terminology of Finn et al., (1983) these are due to "transient" and "residual" stresses respectively. The "transient" stresses and pore pressures are the instantaneous soil response to the passing wave as determined by the constitutive laws and equations of motion. This response vanishes when the wave passes. The "residual" stresses and pore pressures are due to the cumulative effects of the passage of several waves. These induce permanent strains and "residual" pore pressures which depend on the relative rates of generation and dissipation. In this thesis only the problem of "transient" instability will be addressed. We would emphasise that

although the term "transient" is used, we actually determine the steady-state solution to the governing equations under sinusoidal loading. Biot's poroelastic model is thus adopted in its basic form i.e. with constant soil properties. Even with these simplifications the problem is intractable by analytic methods and we employ the boundary element method (BEM) to compute the wave-induced effective stresses and pore pressures. These are combined with the in-situ stresses and the Mohr-Coulomb failure criterion is used to determine the incipient zone of failure. The manner in which such failure progresses is a matter which requires further research and the methods presented herein may be used as a starting point in this regard.

Chapter 2

LITERATURE SURVEY

We have already mentioned that in the analysis of seabed stability it is important to choose an appropriate soil model. We review some of the approaches taken by various authors for modelling the saturated submarine sediments.

2.1 Soil Models

Some of the early attempts at soil modelling (Putnam, 1949; Sleath, 1970; Moshagen and Torum, 1975) neglected soil deformation under loading and thus do not provide a complete model. Oner and Janbu (1975) presented an analysis of the seabed under offshore storage tanks, in which the soil is modelled by springs and dashpots. Bell et al. (1976) performed both stochastic and deterministic analyses assuming homogeneous, isotropic, and elastic soil. Moshagen and Monkmeyer (1979) have used potential theory to describe the flow within the seabed (as did Putnam and Sleath). The soil is assumed to be homogeneous, isotropic, coarse-

grained and rigid. They have also computed the wave-induced pressure distribution on the surface of a vertical embedded cylinder, as well as the total horizontal force and overturning moment generated by the hydrodynamic seepage pressure. O'Donnell (1982) has determined the wave-induced pore pressure fields around a variety of structures (buried pipelines, breakwaters, seawalls, sheetpile bulkhead, offshore foundation) using a potential theory and the Boundary Integral Equation Method. Potential theory has also been used by Lai et al. (1975) and Macpherson (1978) to determine the wave-induced pore pressure around a buried pipeline, and by Liu (1985) to compute the wave-induced pore pressure under a gravity structure. The latter considers the soil skeleton and pore water to be incompressible and he has employed the Riemann-Hilbert technique to compute the pore pressures. Rahman, Seed and Booker (1977) have computed the wave-induced pore pressure history under an axisymmetric tank assuming Darcy's Law and by incorporating a mechanism for pore-pressure generation and dissipation. Munro et al. (1985) have used an elasto-plastic soil model that includes foundation stratigraphy and embedment of an offshore structure. They have developed equivalent spring stiffnesses of soil for vertical, horizontal and moment loading. An elasto-plastic soil model has also been suggested by Prevost et al. (1980). This model incorporates both drained and undrained behavior. It describes the anisotropic, elastoplastic, path dependent, non-linear stress-strain-strength properties of inviscid saturated soils. It is assumed that the elasticity of the material is linear and isotropic and that non-linearity and anisotropy result from its plasticity.

Potts and Windle (1985) did a numerical study of the foundation behavior of a gravity platform using concepts from critical state soil mechanics (Drammen clay

model). Meimon and Lassoudiere (1985) have proposed an elastoplastic model with multiple yield surfaces and kinematical hardening, and involving eleven material constants. Zienkiewicz et al. (1982) have also adopted an elastoplastic model for describing soil behavior. Bouckovalas et al. (1984) have used an empirical model describing the cumulative effects of cyclic loading of sands. He draws upon an analogy between accumulation of strain during cyclic loading and viscoelastic creep, and uses equations and rules derived from the behavior of actual sands. A viscoelastic model was adopted by Schapery and Dunlap (1978) who, in addition, considered non-linear soil properties and the variation of soil properties with depth. Using the linear dynamic theory by Biot (1965), Schapery and Dunlap solved the elastic-viscous problem of wave-seabed interaction. Kraft et al. (1985) have compared this model with field data and have observed good agreement.

While the above approaches have their individual merits, they do not account for an important feature of wave-soil interaction, viz. the coupled responses of the soil 'skeleton' and pore water. Such behaviour must also be considered in problems of soil consolidation. The earliest attempt at modelling soil consolidation is due to Terzaghi. In this theory the effective stresses (in the soil skeleton) and the pore pressure are regarded as autonomous stress systems linked only through the general equations of equilibrium (Zaretskii, 1972) . It has been generally recognised that a more accurate picture of the coupled interaction between the solid and fluid phases is provided by the Biot theory of three dimensional consolidation, first presented by M.A. Biot in 1941 for quasi-static phenomena and later extended by him in a series of papers to include soil anisotropy and visco-elasticity (Biot, 1955, 1956, 1963). A general poroelastic theory including dynamical terms was presented in

1962 (Biot,1962). In Biot's formulation the interaction between the soil skeleton and pore water is represented through body forces. The coupling between soil skeleton and pore water is also considered in a 'mixture' theory by Katsube and Carroll (1987). This theory reduces to Biot's when certain terms involving velocity gradient are suppressed. These terms account for part of the shear interaction between the solid and fluid constituents. However, as pointed out by Katsube and Carroll (1987), these terms are unimportant for most practical applications requiring the solution of steady state boundary value problems, and Biot's model does in fact account for the most significant shear interaction effects (which are due to fluid viscosity).

2.2 The Poroelastic Model of Biot

This theory has been used by a number of authors for analysing seabed stability. The first appears to be Yamamoto et al. (1978) and Madsen (1978) who developed an analytical solution for wave-induced effective stresses and pore pressures in homogeneous isotropic seabeds. They have analysed beds of infinite depth, while Yamamoto (1978) has considered beds of finite depth. Yamamoto et al. (1978) have substantiated their theoretical findings for sand beds by extensive laboratory experiments. Subsequently, however, Clukey et al. (1984) and Davies (1985) have indicated discrepancies between their experimental results and Yamamoto's theoretical findings. They suggest the incorporation of additional features in the Biot model, among them hydraulic anisotropy (as done by Madsen, 1978), layering and damping. Yamamoto et al. (1983,1985) introduced into the Biot model the effects

of Coulomb damping and non-linear shear modulus via the Hardin-Drnevich (1972) formulas and have obtained good correlation with experiments.

Several other authors have adopted the Biot poroelastic model. Spierenburg (1985) has used the analytic solutions of Yamamoto to determine the wave-induced forces on a buried pipeline. He has also used these solutions together with a one dimensional version of Biot's pore pressure equation to develop a model for pore pressure generation. Silvestri et al. (1985) have included the effect of soil anisotropy and found that the soil is closer to failure than when considered isotropic. Simon, Zienkiewicz and Paul (1984) have developed an analytical solution to Biot's equations for the transient response of a one-dimensional column of fluid-saturated poroelastic solid. Mei (1982) has solved Biot's equations using a boundary layer approximation method, his argument being that relative motion between pore water and soil skeleton is significant only within a boundary layer at the mudline. He has considered the problem of waves propagating over a horizontal seabed, waves passing over a pipe laid on the seabed, waves normally incident on a long caisson, and the lifting of a large object from the seafloor. Kokkinowrachos (1985) has determined the wave-induced pore pressure below an offshore structure resting directly on the seabed or embedded in the soil. The two-dimensional problem is considered and both the cross-section of the structure and the contour of the seabottom can be of arbitrary shape. He has used the macroelement approach to solve Biot's equations. In this method the cross-section of the structure and the seabed contour are approximated by step curves, and the flow field around the structure and in the soil is subdivided into macro-elements. The method can be extended for stratified and inelastic soil. Mynett and Mei (1982) have considered the wave-

induced stresses in a saturated, homogeneous, isotropic poro-elastic seabed beneath a rectangular caisson. They have analyzed the two-dimensional problem and have used Mei's boundary layer approximation in conjunction with Biot's equations. A complex variable technique is used to achieve an analytic solution for stresses and pore pressure. Barends and Calle (1985) have used the solution of Yamamoto et al. (1978) to determine the response of the seabed to wave loading. They then establish a procedure for the assessment of cyclic pore pressure build-up and liquefaction of seabeds under random wave loading using a one-dimensional equation for pore pressure. Finn et al. (1983) have used Biot's equations for the transient response of the seabed, and the Seed-Rahman model of pore pressure generation and dissipation (Seed and Rahman, 1978) to assess residual pore pressures. Ishihara and Yamazaki (1984) have used the Yamamoto-Madsen solution of Biot's equations and have done a liquefaction analysis in terms of cyclic stress ratio. Okusa (1985) has used Biot's equations to analyze the wave-induced stresses in unsaturated soils. Mei and McTigue (1984) have performed an analysis of a submarine ridge and canyon under wave loading using the Biot theory. Sabin (1989) has presented analytic formulae for effective stresses and pore pressures in a poroelastic seabed under normal and shear loads. The author's M.Eng thesis (1985) deals with the analytic solution of Biot's equations for wave loading for both the dynamic (i.e. inertia terms included) and quasi-static cases. A homogeneous, isotropic seabed is assumed. It is shown that the response of sandbeds is essentially quasi-static, i.e. the inertia terms in the governing equations may be ignored.

For many problems an analytic approach is either too difficult or impossible and it is necessary to resort to numerical methods. The finite element method (FEM)

has been used by a number of authors to solve Biot's equations for analyzing various problems of soil consolidation and flow through porous media (Sandhu and Wilson,1969 ; Yokoo et al.,1971 ; Ghaboussi and Wilson,1973 ; Smith and Hobbs,1976). Zienkiewicz and Shiomi (1984) have used the FEM to solve Biot's equations and have introduced various approximations for 'fast' and 'slow' phenomena and for the cases of compressible and incompressible fluid. In recent years the boundary element method (BEM) has emerged as a significant challenger to the finite element method and has been successfully applied in many areas of solid and fluid mechanics. One of the advantages of the BEM is that the field equations in the region of interest are transformed into integral equations on the boundary of the region, thus reducing the dimension of the problem by one. Only the boundary of the region needs to be discretised and the user has control over the number of interior points at which the solution of the governing equations are found. This contrasts with the FEM which requires domain discretisation and necessarily produces solutions at all interior nodes. Further, for many problems, the BEM gives greater accuracy than the FEM for the same level of discretisation (Mukherjee et al.,1984). The BEM is still undergoing development and it is certain that further research will extend the power and range of applicability of the method. Kuroki et al.(1982) and Aramaki et al.(1985) have used the BEM in conjunction with Biot's theory but only after uncoupling the soil deformation and pore pressure equations. The fully coupled equations were solved using the BEM by Cheng and Liggett (1984). They have assumed homogeneous, isotropic soil and constant soil properties and they have used Laplace transformed space to deal with time dependent problems. Cheng and Liu (1986) have used the boundary element method and the Biot theory to deter-

mine wave induced seepage forces on a buried pipeline. They have obtained good agreement with experimental results . They have also investigated the sensitivity of the pore pressure response to several soil and fluid parameters . A boundary element formulation for Biot's equations including viscoelastic behaviour of the soil skeleton has been presented by Predeleanu (1981).

2.3 Slope Stability under Waves

The stability of underwater slopes was discussed by Terzaghi (1956) who pointed out that slope failures occur when the average shearing stress on the potential surface of sliding becomes equal to the average shearing resistance along this surface. One of the first analyses of slope stability under waves is due to Henkel (1970). He presented a total stress analysis (i.e. neglecting pore pressures) based on the principle of limiting equilibrium and the assumption of a circular failure surface. He used a standing wave as the loading on the slope. Henkel used his model to show that the overturning moment produced by large waves on a sloping bed in the Gulf of Mexico could exceed the resisting moment provided by the soft sediments. Bea (1971) used the same model to investigate the failures of the Shell platforms in the Gulf of Mexico during Hurricane Camille in 1969. Rahman et al. (1985) have developed a probabilistic analysis for slope stability in which the waves are considered as a random process and the undrained shear strength of sediments is treated as a random variable. In this paper Henkel's approach is extended to develop a method for evaluating the probability of soil failure. Mitchell et al. (1972) proposed that slope failures were caused by strength reductions due to wave

remoulding, rather than additional driving moments or shear stresses. An effective stress method of slices for the stability of seabed slopes has been presented by Finn and Lee (1979), which includes both wave and earthquake loading. Wright (1976) developed a finite element model which included gravity stresses and utilized a hyperbolic stress-strain relationship. Wave forces were estimated from linear wave theory using a constant water depth. The major limitation of the above studies is that the interaction between soil skeleton and pore water is not taken into account. We therefore choose the poroelastic model for our present study. As mentioned previously, Mei and McTigue (1984) have used Biot's poroelastic model to analyse the effects of wave loading on a gentle slope. They use an analytic solution valid for flat beds with a modified wave pressure which approximates the slow variation in the wave forces over a gentle slope. For certain values of the slope angle the analytic techniques of Stoker (1957) may be used to determine the wave forces on the slope, but for an arbitrary slope numerical methods are required. Alliney (1981) has used linear wave theory and the BEM to determine the wave velocity potential over an arbitrary coastal planar slope. In this thesis we determine (via the BEM) the wave forces on an arbitrary planar slope in the open ocean. The major difference between these two problems is that the latter has an additional boundary for which appropriate conditions must be specified. We have defined the side boundary conditions using the techniques illustrated by Alliney. The wave-induced stress field in the sloping bed is also computed by the BEM using Biot's poroelastic model. To provide boundary conditions on the side boundaries of the poroelastic medium we use an analytic solution for flat beds.

Chapter 3

Theoretical Background

The theory of poroelasticity presented by M.A. Biot in 1962 will be used to model the soil medium. Here we present the final equations with an explanation of the notation.

3.1 The Biot Soil Model (Theory of Poroelasticity)

The saturated soil is modelled as a solid, porous, deformable skeleton, the pores being completely filled with water. We assume that the soil is homogeneous and isotropic. The Cartesian coordinates are denoted by x_1, x_2 and x_3. Subscripts 1, 2, and 3 refer to the Cartesian coordinate directions, unless otherwise specified. A repeated suffix indicates summation with respect to that suffix over the range 1, 2, 3 unless otherwise specified. A comma followed by a suffix indicates partial

differentation with respect to the appropriate coordinate direction, e.g. $A_{,i} \equiv \frac{\partial A}{\partial x_i}$.

We let $u = (u_1, u_2, u_3)$ be the displacement of the solid matrix at any point; $U = (U_1, U_2, U_3)$ be the displacement of the fluid at any point; and f be the porosity of the soil. We denote by τ_{ij} the total stress components on the bulk material; τ_{ij} is a j-direction stress acting on a plane normal to the i-axis. The pore pressure is denoted by p. For the present, we use the usual sign convention adopted in the theory of elasticity, i.e.;

(a) tensile stresses are positive and,

(b) a shear stress is reckoned positive when acting in a positive coordinate direction on a plane whose outward normal points in a positive coordinate direction; or when acting in a negative coordinate direction on a plane whose outward normal points in a negative coordinate direction. We defer until a later section the use of the conventional soil mechanics sign convention, which is exactly opposite to that described above.

We now present the constitutive laws as (Biot, 1962)

$$\begin{aligned} \tau_{ij} &= 2\mu e_{ij} + (\lambda_c e - \alpha M \zeta)\delta_{ij} \quad \text{(a)} \\ p &= -\alpha M e + M\zeta \qquad\qquad\quad \text{(b)} \end{aligned} \tag{3.1}$$

where

$$e_{ij} = \tfrac{1}{2}(u_{i,j} + u_{j,i})$$

$$e = e_{kk}$$

$$\zeta = -f(U_k - u_k)_{,k}$$

δ_{ij} is the Kronecker delta.

The constant μ is the shear modulus of the soil skeleton. The other constants λ_c,α

and M appearing in (3.1) may be expressed in terms of the following familiar elastic moduli :

K_r = bulk modulus of soil grain

K_b = bulk modulus of soil skeleton

K_f = bulk modulus of water

It can be shown that (Biot and Willis, 1957; Stoll,1974)

$$\begin{aligned} \lambda_c &= \frac{(K_r - K_b)^2}{D - K_b} + K_b - \frac{2\mu}{3} \\ \alpha &= 1 - \frac{K_b}{K_r} \\ M &= \frac{K_r^2}{D - K_b} \end{aligned} \tag{3.2}$$

where

$$D = K_r \left[1 + f\left(\frac{K_r}{K_f} - 1\right)\right]$$

It is of interest to examine the relationship between (3.1) and Hooke's Law. From equation (3.1) (b) we have

$$\zeta = \frac{1}{M}(p + \alpha M e)$$

Substituting this into (3.1) (a) gives

$$\tau_{ij} = 2\mu e_{ij} + \delta_{ij}[(\lambda_c - \alpha^2 M)e - \alpha p] \tag{3.3}$$

From (3.2) we find that

$$\lambda_c - \alpha^2 M = K_b - \frac{2\mu}{3} \equiv \lambda \tag{3.4}$$

Here, λ is the standard Lamé constant of the theory of elasticity. Equation (3.3) may now be re-written as:

$$\tau_{ij} = 2\mu e_{ij} + \delta_{ij}\lambda e - \delta_{ij}\alpha p \tag{3.5}$$

We shall show that this reduces to Hooke's Law when written in terms of effective stress. To define the effective stress tensor, we consider a plane area δA of saturated soil normal to the i axis, shown schematically in Figure (3.1).

We denote by F_{ij} the sum of all inter-granular forces acting on the area δA in the j direction. The pore pressure p exerts a force $p\delta A$ in opposition to the normal inter-granular forces. Since τ_{ij} is the net total stress in the j direction we have the following balance of forces on the area δA :

$$\tau_{ij}\,\delta A = F_{ij} - p\,\delta A\,\delta_{ij}$$

We define the effective stress components τ'_{ij} by

$$\tau'_{ij} = \frac{F_{ij}}{\delta A} \tag{3.6}$$

Hence the above equation becomes

$$\tau_{ij} = \tau'_{ij} - p\delta_{ij} \tag{3.7}$$

Writing (3.5) in terms of effective stress gives

$$\tau'_{ij} = 2\mu e_{ij} + \delta_{ij}\lambda e + \delta_{ij}(1-\alpha)p \tag{3.8}$$

For most soils the ratio $\frac{K_b}{K_r}$ is negligible (of the order 10^{-4}) so that α is effectively equal to unity (equation 3.2). Thus (3.8) reduces to

$$\tau'_{ij} = 2\mu e_{ij} + \delta_{ij}\lambda e \tag{3.9}$$

which is Hooke's Law for the soil skeleton.

We now re-write the constitutive laws (3.1) in a form suitable for deriving the boundary integral equations. It is first necessary to write the total stress tensor in terms of stresses on the solid and liquid portions of an element of soil :

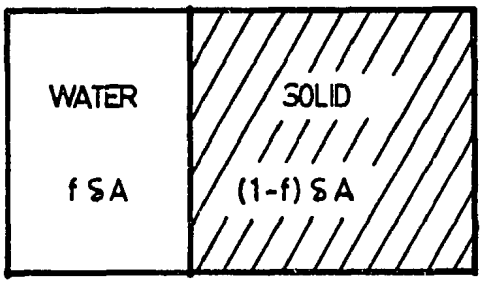

Fig.(3.1) Plane area δA normal to i-axis

Referring again to Figure (3.1) we define σ_{ij} as the net j-direction stress on the solid area averaged over the entire area δA i.e. $\sigma_{ij}\,\delta A$ is the j-direction resultant of intergranular and pore pressure forces on the solid area. With this definition we find

$$\sigma_{ij}\delta A = F_{ij} - \delta_{ij}(1-f)\delta A\, p$$

which simplifies to (using 3.6)

$$\sigma_{ij} = \tau'_{ij} - \delta_{ij}(1-f)p \tag{3.10}$$

Eliminating τ'_{ij} between (3.7) and (3.10) gives

$$\tau_{ij} = \sigma_{ij} + \delta_{ij}\,\sigma \tag{3.11}$$

where

$$\sigma = -fp \tag{3.12}$$

We proceed to re-write the constitutive equations (3.1) in terms of σ_{ij} and σ : Writing $\varepsilon = U_{k,k}$ we note that

$$\zeta = -f(\varepsilon - e)$$

Multiplying equation (3.1) (b) by $-f$ gives

$$\sigma = Qe + R\varepsilon \tag{3.13}$$

where

$$Q = (\alpha - f)fM \quad ; \quad R = f^2 M \tag{3.14}$$

Substituting equation (3.1) into (3.11) gives, using (3.4)

$$\begin{aligned} \sigma_{ij} &= 2\mu e_{ij} + \delta_{ij}\left[\{\lambda + M(\alpha - f)^2\}e + fM(\alpha - f)\varepsilon\right] \\ &= 2\mu e_{ij} + (\lambda + \frac{Q^2}{R})e\delta_{ij} + Q\varepsilon\delta_{ij} \end{aligned} \tag{3.15}$$

Since the soil grain is practically incompressible we may make the assumption $K_r \rightarrow \infty$, and thus $\alpha \rightarrow 1$. Then, substituting for M (from 3.2) in (3.14) we have

$$R = fK_f \quad ; \quad \frac{Q}{R} = \frac{1-f}{f} \tag{3.16}$$

To complete the model we present the equations of motion as (Biot, 1962)

$$\tau_{ij,j} + \rho X_i = \rho \ddot{u}_i + \rho_f \ddot{w}_i \tag{3.17}$$

$$-p_{,i} + \rho_f X_i = \rho_f \ddot{u}_i + m\ddot{w}_i + \frac{\rho_f g}{k_0}\dot{w}_i \tag{3.18}$$

where

$$w_i = f(U_i - u_i)$$

$$\rho = (1-f)\rho_s + f\rho_f$$

$\rho_s =$ density of soil grains

$\rho_f =$ density of pore water

$f =$ porosity

$k_0 =$ soil permeability in ms^{-1}

$m =$ added mass parameter

The "added mass" parameter m is due to the coupling of soil grains and fluid in relative motion. In (3.17) and (3.18) we have included the body force per unit mass X_i. Differentiation with respect to time is denoted by dots. As demonstrated in the author's M. Eng. thesis, the terms in $\ddot{u}_i$ and $\ddot{w}_i$ may be deleted from the equations of motion for problems of water wave loading on sand beds. This is due to the low frequency of the loading and the relative stiffness of sand beds (as compared to clay beds, for example). Then using (3.11) and (3.12) we write the

governing equations (3.17) and (3.18) as

$$\sigma_{ij,j} + \sigma_{,i} = -\rho X_i \tag{3.19}$$

$$\sigma_{,i} + f\rho_f X_i = fk(\dot{U}_i - \dot{u}_i) \tag{3.20}$$

where

$$k = \frac{\rho_f g f}{k_0} \tag{3.21}$$

For convenience we record again the constitutive laws from (3.15) and (3.13) :

$$\sigma_{ij} = 2\mu e_{ij} + (\lambda + \frac{Q^2}{R})e\delta_{ij} + Q\varepsilon\delta_{ij} \tag{3.22}$$

$$\sigma = Qe + R\varepsilon \tag{3.23}$$

where

$$\begin{aligned} R &= fK_f \\ Q &= (1-f)K_f \end{aligned} \tag{3.24}$$

and

$\mu =$ shear modulus of soil skeleton ; $\lambda =$ Lamé constant of soil skeleton

The relationships between σ_{ij}, σ and effective stresses τ'_{ij} and pore pressure p are given by (3.10) and (3.12).

3.2 The Biot Model in Conventional Notation

It is instructive to write the basic equations of the Biot soil model in the notation used in conventional soil mechanics. The Cartesian coordinate axes are such that the x and y axes are horizontal and z axis points vertically downward. Normal

stresses in the x, y and z directions are denoted by σ_x, σ_y and σ_z respectively, and shear stresses are denoted by τ_{xy}, τ_{yz} and τ_{zx}. The sign convention is exactly opposite to that used in classical elasticity, i.e.

(1) for normal stresses, compression is positive

(2) a shear stress is considered positive if (a) it points in a positive coordinate direction when acting on a plane whose outward normal points in a negative coordinate direction, or (b) it points in a negative coordinate direction when acting on a plane whose outward normal points in a positive coordinate direction.

Effective stresses are denoted by $\sigma_x^{'}$, $\sigma_y^{'}$, $\sigma_z^{'}$, $\tau_{xy}^{'}$, $\tau_{yz}^{'}$, and $\tau_{zx}^{'}$. In equation (3.7) we identify subscripts 1, 2, 3 with the x, y, z coordinates axes respectively. Then, allowing for the change in sign convention (3.7) becomes

$$\sigma_x^{'} = \sigma_x - p,\ \sigma_y^{'} = \sigma_y - p,\ \sigma_z^{'} = o_z - p$$

$$\tau_{xy}^{'} = \tau_{xy},\ \tau_{yz}^{'} = \tau_{yz},\ \tau_{zx}^{'} = \tau_{zx} \tag{3.25}$$

We have already shown that the constitutive law (3.1) (a) or (3.22), when written in terms of effective stress, is equivalent to Hooke's law for the soil skeleton, equation (3.9). Writing

$$G \equiv \mu,\ \lambda = \frac{2G\nu}{1-2\nu}$$

this becomes

$$\sigma_x^{'} = -2Ge_x - (\frac{2G\nu}{1-2\nu})e$$
$$\sigma_y^{'} = -2Ge_y - (\frac{2G\nu}{1-2\nu})e$$
$$\sigma_z^{'} = -2Ge_z - (\frac{2G\nu}{1-2\nu})e$$

$$\tau'_{xy} = -2\mu e_{xy}$$

$$\tau'_{yz} = -2\mu e_{yz}$$

$$\tau'_{zx} = -2\mu e_{zx}$$

where

$$e_x = \frac{\partial u}{\partial x},\ e_y = \frac{\partial v}{\partial y},\ e_z = \frac{\partial w}{\partial z}$$

$$e_{xy} = \frac{1}{2}\left(\frac{\partial u}{\partial y} + \frac{\partial v}{\partial x}\right)$$

$$e_{yz} = \frac{1}{2}\left(\frac{\partial v}{\partial z} + \frac{\partial w}{\partial y}\right)$$

$$e_{zx} = \frac{1}{2}\left(\frac{\partial w}{\partial x} + \frac{\partial u}{\partial z}\right)$$

u, v, w are displacements u_1, u_2, u_3 of the soil skeleton in the x, y, z directions respectively.

The parameter G is the shear modulus of the soil skeleton, and the Lamé constant λ is expressed in terms of the more familiar Poisson's ratio ν. The constitutive law for pore pressure is written from (3.23) and (3.24) as

$$p = -\frac{K_f}{f}[(1-f)e + f\varepsilon] \tag{3.26}$$

where

$$e = \frac{\partial u}{\partial x} + \frac{\partial v}{\partial y} + \frac{\partial w}{\partial z}$$

$$\varepsilon = \frac{\partial U}{\partial x} + \frac{\partial V}{\partial y} + \frac{\partial W}{\partial z}$$

$(U, V, W) = (U_1, U_2, U_3)$, the displacements of the pore water.

The governing equations (3.17) and (3.18) become, neglecting the acceleration terms and using (3.25) :

$$\begin{aligned} \frac{\partial \sigma_x'}{\partial x} + \frac{\partial \tau_{xy}'}{\partial y} + \frac{\partial \tau_{xz}'}{\partial z} - \rho X &= -\frac{\partial p}{\partial x} \\ \frac{\partial \tau_{xy}'}{\partial y} + \frac{\partial \sigma_y'}{\partial y} + \frac{\partial \tau_{yz}'}{\partial y} - \rho Y &= -\frac{\partial p}{\partial y} \\ \frac{\partial \tau_{xz}'}{\partial z} + \frac{\partial \tau_{yz}'}{\partial z} + \frac{\partial \sigma_z'}{\partial z} - \rho Z &= -\frac{\partial p}{\partial z} \end{aligned} \tag{3.27}$$

$$-\underline{\nabla} p + \rho_f \underline{X} = \frac{\rho_f g f}{k_0} \frac{\partial}{\partial t}(\underline{U} - \underline{u}) \tag{3.28}$$

where $\underline{X} = (X, Y, Z)$ is the body force per unit mass; $\underline{U} = (U, V, W)$; $\underline{u} = (u, v, w)$. Equation (3.28) is recognised as Darcy's Law. It reduces to a more familiar form by considering no body force $\underline{X}$,zero displacement of the soil skeleton ($\underline{u} = \underline{0}$) and by defining the fluid velocity $\underline{U}^* = f\underline{U}$.

It is possible to define a coefficient of consolidation analogous to that defined in Terzaghi's consolidation theory. It has been shown by the author (Raman-Nair,1985) that the pore pressure p can be written as the sum of an harmonic function r and a function q which satisfies the "heat equation" form . Specifically,

$$p(x, z, t) = q(x, z, t) + r(x, z, t) \tag{3.29}$$

where

$$\nabla^2 r = 0 \tag{3.30}$$

$$c_v \nabla^2 q = \frac{\partial q}{\partial t} \tag{3.31}$$

with

$$c_v = \frac{k_0}{\rho_f g} \left(\frac{f}{K_f} + \frac{1 - 2\nu}{2\mu(1 - \nu)} \right)^{-1} \tag{3.32}$$

Equation (3.31) is of the same form as Terzaghi's consolidation equation and the coefficient c_v may thus be defined as a consolidation coefficient . To the author's knowledge , equations (3.29) to (3.31) have not previously appeared in the literature. The formula for c_v has been presented without derivation by Cheng and Liu (1986), and in different notation using a different analysis by Yamamoto (1978).

It will not be convenient to use the notation of this section in the following development. We shall, however, return to this notation when we consider the failure analysis.

Chapter 4

Wave Forces on a Sloping Bed

4.1 Problem Formulation and Boundary Conditions

According to Sleath (1984) viscous effects are unimportant when considering the wave loading of the seafloor in the absence of strong currents. We shall therefore assume that the flow is essentially irrotational. Further, we may ignore shear stresses at the mudline since these are due primarily to the fluid viscosity. For the free surface, we employ the assumptions of linear wave theory i.e. that the wave amplitude is small relative to the wavelength so that boundary conditions may be applied at the still water level. It is worth noting that for the purpose of determining the wave forces on the seabed, the error involved in using linear wave theory versus higher order wave theories is negligible. For example, in evaluating the dynamic

wave pressure on the seabed under a wave crest, we find that for a wave of length $300m.$,height $24m.$ in $80m.$ of water, the linear theory estimate is only 1.3 per cent higher than the estimate using Stokes' second order theory.

We shall assume that there is negligible flow into the seabed i.e. the fluid velocity normal to the bed is essentially zero. There have been some attempts in the literature to account for flow into the seabed . For example,using Darcy's law Dean and Dalrymple (1984) write

$$-\frac{\partial \Phi}{\partial y} = -\frac{K}{\mu}\frac{\partial p}{\partial y} \text{ at seabed}$$

where

$$\begin{aligned} \frac{K}{\mu} &= \frac{k_0}{\rho_f g} \\ \Phi &= \text{wave velocity potential} \\ k_0 &= \text{soil permeability} \\ \mu &= \text{shear modulus of soil} \\ \rho_f &= \text{density of water} \\ y &= \text{vertical coordinate} \end{aligned}$$

However, the pore pressure p on the right hand side is not known until the soil equations are solved . Dean and Dalrymple obtain an approximate picture of the pore pressure by employing a simplified model,viz., the assumption that p obeys Laplace's equation in the soil and decays exponentially with soil depth. They deduce that for a wave of amplitude η_0,wave number k and frequency ω in water

of depth h, the wave pressure P at the mudline is given by

$$P = \frac{\rho_f g \eta_0}{\cosh kh \left[1 - \frac{i\omega k_0}{g} \tanh kh\right]} e^{i(kx-\omega t)}$$

We note that for 10 second waves in $80m.$ of water propagating over sandy beds the imaginary term in the denominator is of the order 10^{-4} to 10^{-6} so that the above equation may be approximated by

$$P = \frac{\rho_f g \eta_0}{\cosh kh} e^{i(kx-\omega t)} \tag{4.1}$$

which is the same as would be obtained by assuming negligible flow into the seabed. Further support for this assumption comes from the fact that good agreement with experimentally measured wave-induced pore pressure was obtained by Yamamoto et al. (1978) and Cheng et. al. (1986). They used (4.1) to provide boundary conditions at the mudline for the poroelastic soil model .

It is reasonable to assume that the problem is two dimensional i.e. the slope is planar and conditions are uniform in the direction normal to the direction of propagation of the wave. The problem domain $OABC$ and incident wave direction are shown in Figure (4.1). The condition of irrotationality guarantees the existence of a velocity potential $\Phi(x, y, t)$, where x and y are spatial coordinates as shown (Figure (4.1)), and t is time. The wave forces on the seabed will be computed from the function Φ. The flow above the seabed may be considered incompressible and the continuity equation then requires that

$$\nabla^2 \Phi = 0 \tag{4.2}$$

where

$$\nabla^2 \equiv \frac{\partial^2}{\partial x^2} + \frac{\partial^2}{\partial y^2}$$

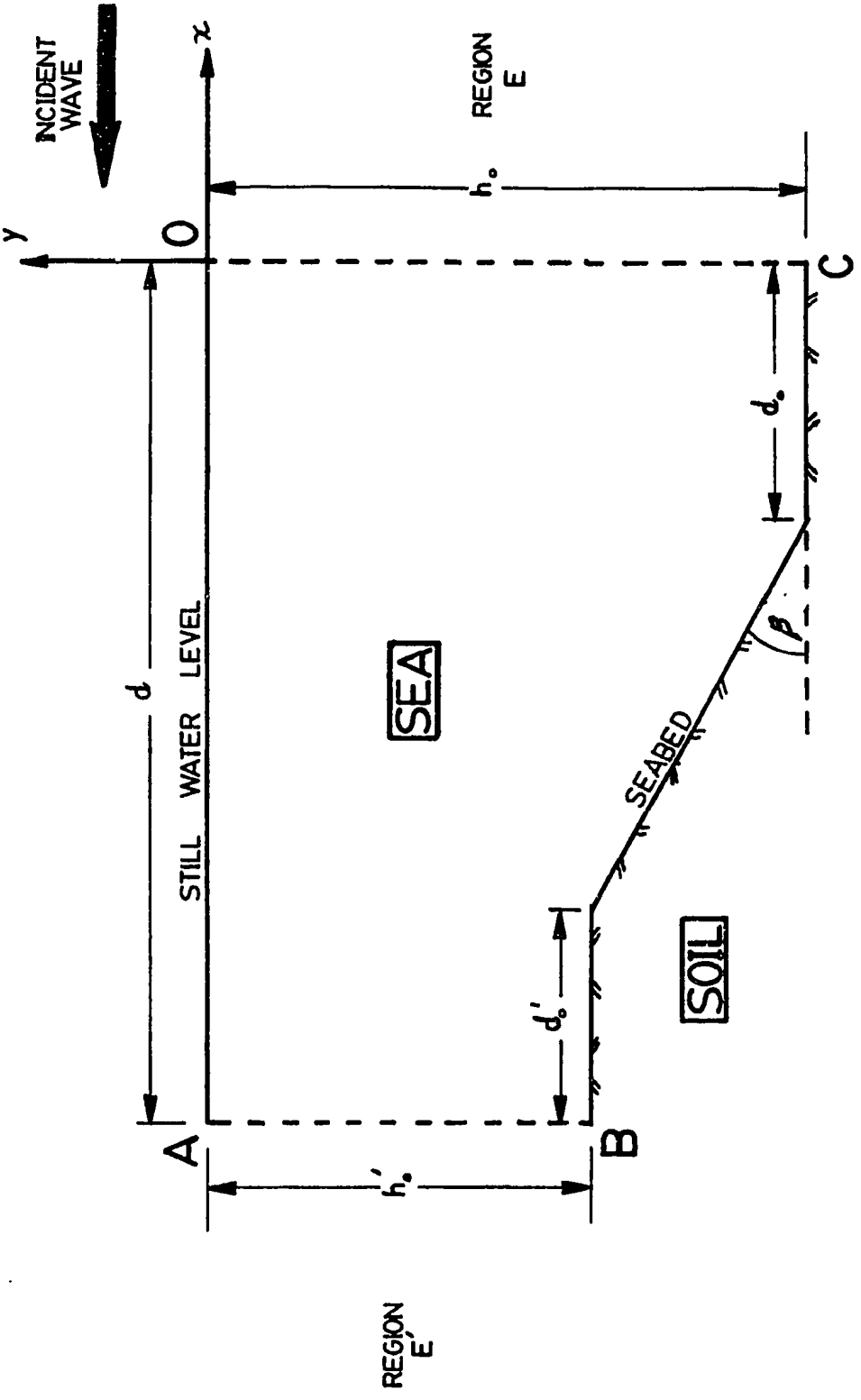

Fig. (4.1) Wave Propagation over Slope

The boundary conditions are

$$\frac{\partial \Phi}{\partial n} = 0 \quad \text{on BC} \tag{4.3}$$

$$\frac{\partial^2 \Phi}{\partial t^2} + g\frac{\partial \Phi}{\partial y} = 0 \quad \text{on OA} \tag{4.4}$$

where we have made the assumptions of classical linear wave theory (see **Appendix A**); $\frac{\partial \Phi}{\partial n}$ is the normal derivative on BC.

Since the wave frequency ω does not change with water depth, the function Φ may be written

$$\Phi(x, y, t) = \phi(x, y)e^{-i\omega t} \tag{4.5}$$

where $\phi(x, y)$ is a complex function and it is understood that the physical situation is represented by the real part of equation (4.5). Thus, equation (4.2) with boundary conditions (4.3) and (4.4) may be re-written:

$$\nabla^2 \phi = 0 \quad \text{in } OABC \tag{4.6}$$

$$\frac{\partial \phi}{\partial n} = 0 \quad \text{on } BC \tag{4.7}$$

$$\frac{\partial \phi}{\partial y} - \frac{\omega^2 \phi}{g} = 0 \quad \text{on } OA \tag{4.8}$$

The boundary OC (Fig. 4.1) experiences waves progressing from the right (incident waves) as well as reflected waves from the slope coming from the left. The boundary AB ,however, experiences waves travelling in one direction only i.e. towards the left. To obtain the boundary conditions on the interfaces OC and AB we follow the approach of Alliney (1981). In the problem considered by Alliney the boundary AB (Fig. 4.1) is absent since he considered a coastal situation (i.e. $h_0' = 0$). Here we need to determine the boundary condition on AB. First, we obtain the general solution ϕ_a of equation (4.6) in an open-ended two-dimensional domain of constant

depth h. The boundary conditions are :

$$\frac{\partial \phi_a}{\partial n} = 0 \quad \text{at } y = -h \tag{4.9}$$

$$\frac{\partial \phi_a}{\partial y} - \frac{\omega^2 \phi_a}{g} = 0 \quad \text{at } y = 0 \tag{4.10}$$

Using the technique of separation of variables we assume that

$$\phi_a(x, y) = X(x)Y(y)$$

Substitution into (4.6) gives, for sinusoidal behaviour in X,

$$\frac{d^2X}{dx^2} + k^2X = 0 \text{ and } \frac{d^2Y}{dy^2} - k^2Y = 0$$

where k is a complex constant. The general solutions of these equations are

$$X = ae^{ikx} + be^{-ikx}$$

$$Y = C\cosh(ky + \alpha)$$

where a, b, C and α are complex constants. From boundary condition (4.9) we find that $\alpha = kh$ and hence the solution is of the form

$$\phi_a = \cosh(ky + kh)[ce^{ikx} + de^{-ikx}] \tag{4.11}$$

Using (4.10) we have the dispersion relation

$$\frac{\omega^2}{g} = k\tanh(kh) \tag{4.12}$$

This equation has two real roots $\pm k_0$ and an infinity of purely imaginary roots $\pm ik_1, \pm ik_2, \ldots$, where $k_i \geq 0$, $i = 0, 1, 2\cdots$ (see **Appendix B**). Since (4.6) is a

linear equation we obtain its general solution from (4.11) as

$$\begin{aligned}\phi_a &= \cosh(k_0y+k_0h)[c_0e^{ik_0x}+d_0e^{-ik_0x}]\\ &\quad+\cosh(-k_0y-k_0h)[c_0'e^{-ik_0x}+d_0'e^{ik_0x}]\\ &\quad+\sum_{n=1}^{\infty}\cosh[ik_n(y+h)][c_ne^{-k_nx}+d_ne^{k_nx}]\\ &\quad+\sum_{n=1}^{\infty}\cosh[-ik_n(y+h)][c_n'e^{k_nx}+d_n'e^{-k_nx}]\end{aligned}$$

This may be written more concisely as

$$\begin{aligned}\phi_a &= A\cosh[k_0(y+h)][a_0e^{ik_0x}+e^{-ik_0x}]\\ &\quad+\sum_{n=1}^{\infty}\cos[k_n(y+h)][a_ne^{-k_nx}+b_ne^{k_nx}]\end{aligned}\tag{4.13}$$

The constants A, a_0, a_n, b_n appearing in (4.13) must be interpreted for the external regions E and E' which lie outside the problem domain, as illustrated in Figure (4.1).

In the region E to the right of OC in Figure (4.1) we consider an incident wave of amplitude η_0, wave number k_0 and frequency ω propagating in the negative x direction. It is easily shown (see **Appendix A**) that the velocity potential corresponding to the incident wave is:

$$\phi_I(x,y) = -\frac{ig\eta_0}{\omega}\frac{\cosh[k_0(y+h_0)]}{\cosh(k_0h_0)}e^{-ik_0x}\tag{4.14}$$

By putting $h = h_0$ in (4.13) we see that the term $A\cosh[k_0(y+h_0)]e^{-ik_0x}$ represents the incident wave, so that for the region E,

$$A = \frac{-ig\eta_0}{\omega\cosh(k_0h_0)}$$

The term $a_0A\cosh[k_0(y+h_0)]e^{ik_0x}$ represents the right running reflected wave, and a_0 can be interpreted as the reflection coefficient. In order that the velocity potential

remain finite as $x \rightarrow \infty$ we must have $b_n = 0$ for all n. Hence from (4.13) we have the velocity potential ϕ_E in region E :

$$\begin{aligned}\phi_E(x,y) &= -\frac{ig\eta_0}{\omega}\frac{\cosh[k_0(y+h_0)]}{\cosh(k_0h_0)}\left[a_0e^{ik_0x}+e^{-ik_0x}\right] \\ &+ \sum_{n=1}^{\infty} a_n\cos[k_n(y+h_0)]e^{-k_nx} \qquad (4.15)\end{aligned}$$

For the region E' to the left of AB we put $h = h_0'$ in equation (4.12) and denote the roots by $\pm k_0', \pm ik_n', n = 1, 2\cdots$ where $k_0', k_n' \geq 0$. Since there is no right running wave in this region, the coefficient a_0 in (4.13) must be zero. Also, in order that the velocity potential be finite as $x \rightarrow -\infty$ we must have $a_n = 0$ for all n. Thus, from (4.13), we have the velocity potential $\phi_{E'}$ in region E' as

$$\phi_{E'}(x,y) = a_0'\cosh[k_0'(y+h_0')]e^{-ik_0'x} + \sum_{n=1}^{\infty} a_n'e^{k_n'x}\cos[k_n'(y+h_0')] \qquad (4.16)$$

We can now obtain expressions for ϕ and its normal derivative on the lateral boundaries OC and AB. For OC, we put $x = 0$ in (4.15) and its derivative with respect to x :

$$\phi_{|OC} = f_0(y) + \sum_{n=1}^{N+1} a_nf_n(y), \quad y \in OC \qquad (4.17)$$

$$\frac{\partial\phi}{\partial n}|_{OC} = -g_0(y) + \sum_{n=1}^{N+1} a_ng_n(y), \quad y \in OC \qquad (4.18)$$

where we have used N terms of the infinite series and :

$$\begin{aligned}f_0(y) &= \frac{-ig\eta_0}{\omega}\frac{\cosh[k_0(y+h_0)]}{\cosh(k_0h_0)} \\ f_n(y) &= \cos[k_n(y+h_0)], \quad n = 1, 2, \cdots, N \\ g_0(y) &= \frac{g\eta_0k_0}{\omega}\frac{[k_0(y+h_0)]}{\cosh(k_0h_0)} \qquad (4.19) \\ g_n(y) &= -k_n\cos[k_n(y+h_0)], \quad n = 1, 2, \cdots, N\end{aligned}$$

$$f_{N+1}(y) = f_0(y), \; g_{N+1}(y) = g_0(y), \; a_{N+1} = a_0 \qquad (4.20)$$

For AB we have

$$\begin{aligned}\phi\,|_{AB} &= \phi_{E'}(-d,y)\\ &= a_0' e^{ik_0' d}\cosh[k_0'(y+h_0')] + \sum_{n=1}^{N} a_n' e^{-k_n' d}\cos[k_n'(y+h_0')]\end{aligned}$$

$$\begin{aligned}\frac{\partial\phi}{\partial n}\,|_{AB} &= -\frac{\partial\phi}{\partial x}\,|_{AB}\\ &= ik_0' a_0' e^{ik_0' d}\cosh[k_0'(y+h_0')] + \sum_{n=1}^{N'} -a_n' k_n' e^{-k_n' d}\cos[k_n'(y+h_0')]\end{aligned}$$

Since the horizontal distance d is large, the terms in $e^{-k_n' d}$ are effectively zero and these equations reduce to

$$\begin{aligned}\phi\,|_{AB} &= a_0' e^{ik_0' d}\cosh[k_0'(y+h_0')]\\ \frac{\partial\phi}{\partial n}\,|_{AB} &= ik_0' a_0' e^{ik_0' d}\cosh[k_0'(y+h_0')]\end{aligned}$$

Thus we have the relation

$$\frac{\partial\phi}{\partial n}\,|_{AB} = ik_0'\phi\,|_{AB} \tag{4.21}$$

which is a well known radiation condition.

4.2 The Boundary Integral Equation

The problem defined by (4.6) with boundary conditions (4.7), (4.8), (4.17), (4.18) and (4.21), may be solved by the boundary element method with a view to determining ϕ, and hence the wave pressure, on the seabed BC. The following derivation of the boundary integral equation is standard (Brebbia et al. 1984) but is presented here for completeness. For an arbitrary function $\phi^*(x,y)$ we may write,

from (4.6):

$$\int_{\Omega} \phi^* \nabla^2 \phi \, d\Omega = 0$$

where Ω denotes the region $OABC$.

Assuming that ϕ, ϕ^* are continuous and have continuous first and second partial derivatives in Ω we use Green's second identity (Sokolnikoff et al., 1966) to get

$$\int_{\Omega} \phi \nabla^2 \phi^* d\Omega + \int_{\Gamma} (\phi^* \frac{\partial \phi}{\partial n} - \phi \frac{\partial \phi^*}{\partial n}) d\Gamma = 0 \tag{4.22}$$

where Γ denotes the boundary $OABC$. We choose ϕ^* to be the solution of the equation

$$\nabla^2 \phi^* + \Delta(\underline{x}, \underline{x}_p) = 0 \tag{4.23}$$

where Δ denotes the Dirac delta function, $\underline{x}_p$ is the position vector of the point P at which the delta function is non-zero, and $\underline{x}$ is the position vector of an arbitrary point. The solution of equation (4.23) for the case of two dimensions is

$$\phi^* = -\frac{1}{2\pi} \ln r \tag{4.24}$$

where $r = |\underline{x} - \underline{x}_p|$ (see **Appendix D**). Using (4.23) we have

$$\int_{\Omega} \phi \nabla^2 \phi^* d\Omega = -\int_{\Omega} \phi \Delta(\underline{x}, \underline{x}_p) d\Omega = -\phi(\underline{x}_p) \tag{4.25}$$

by the sifting property of the delta function. Substituting (4.25) into (4.22) gives

$$-\phi(\underline{x}_p) + \int_{\Gamma} \left(\phi^* \frac{\partial \phi}{\partial n} - \phi \frac{\partial \phi^*}{\partial n} \right) d\Gamma = 0 \tag{4.26}$$

We now take the point P (position vector $\underline{x}_p$) to the boundary Γ. Since ϕ^* is singular at P, integration along the section of Γ containing P requires special consideration. For generality, we consider P at a corner point on the boundary and draw a circular

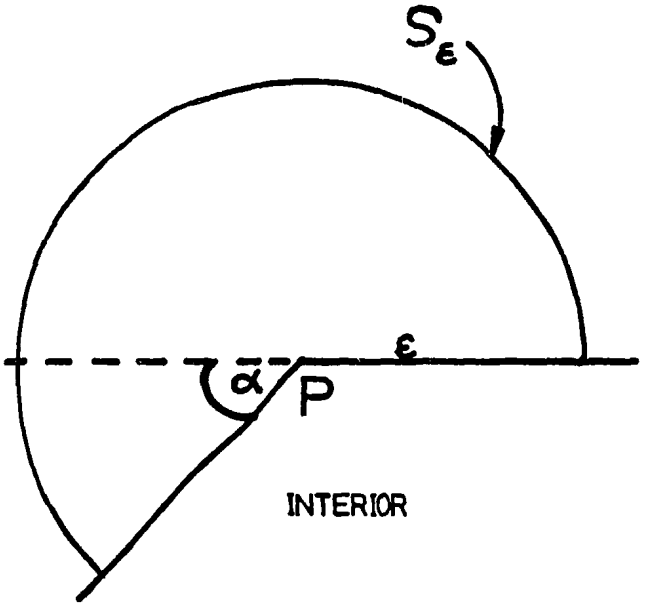

Fig.(4.2) Boundary Point P.

arc S_ϵ of radius ϵ, centre P as shown in Figure (4.2). We now write equation (4.26) for a **boundary** point $\underline{x}_p$:

$$\begin{aligned} -\phi(\underline{x}_p) \;+\; & \lim_{\epsilon\to 0}\int_{\Gamma-S_\epsilon}(\phi^*\frac{\partial\phi}{\partial n}-\phi\frac{\partial\phi^*}{\partial n})\,d\Gamma \\ +\; & \lim_{\epsilon\to 0}\int_{S_\epsilon}(\phi^*\frac{\partial\phi}{\partial n}-\phi\frac{\partial\phi^*}{\partial n})\,d\Gamma \;=\; 0 \end{aligned} \tag{4.27}$$

Now,

$$\begin{aligned} \lim_{\epsilon\to 0}\int_{S_\epsilon}\phi^*\frac{\partial\phi}{\partial n}\,d\Gamma &= \lim_{\epsilon\to 0}\int_{S_\epsilon}-\frac{1}{2\pi}\ln r\frac{\partial\phi}{\partial n}\,d\Gamma \\ &= -\frac{1}{2\pi}\frac{\partial\phi}{\partial n}\,|_{S_\epsilon}\lim_{\epsilon\to 0}[\ln\epsilon\int_{S_\epsilon}d\Gamma] \\ &= -\frac{1}{2\pi}\frac{\partial\phi}{\partial n}\,|_{S_\epsilon}\lim_{\epsilon\to 0}[(\pi+\alpha)\epsilon\ln\epsilon]=0 \end{aligned} \tag{4.28}$$

where we have assumed that $\dfrac{\partial\phi}{\partial n}$ is approximately constant on the small arc S_ϵ. Also,

$$\begin{aligned} \lim_{\epsilon\to 0}\int_{S_\epsilon}\phi\frac{\partial\phi^*}{\partial n}\,d\Gamma &= \lim_{\epsilon\to 0}\int_{S_\epsilon}\phi\frac{\partial}{\partial r}(-\frac{1}{2\pi}\ln r)\,d\Gamma \\ &= -\frac{\phi(\underline{x}_p)}{2\pi}\lim_{\epsilon\to 0}\int_{S_\epsilon}\frac{1}{r}d\Gamma \\ &= \frac{-\phi(\underline{x}_p)}{2\pi}\lim_{\epsilon\to 0}[\frac{1}{\epsilon}\int_{S_\epsilon}d\Gamma] \\ &= \frac{-\phi(\underline{x}_p)}{2\pi}(\pi+\alpha) \end{aligned} \tag{4.29}$$

where α is the angle illustrated in Figure (4.2). Substituting (4.28) and (4.29) into (4.27) we have for a **boundary** point P :

$$\phi(\underline{x}_p)(\frac{1}{2}-\frac{\alpha}{2\pi})+\int_\Gamma(\phi\frac{\partial\phi^*}{\partial n}-\phi^*\frac{\partial\phi}{\partial n})d\Gamma=0 \tag{4.30}$$

where it is understood that the domain of integration does not include the point $\underline{x}_p$.

4.3 Boundary Element Procedure

The boundary Γ is discretised into M straight line segments or "elements" and a node is located at the mid-point of each element. We shall assume that ϕ and $\frac{\partial \phi}{\partial n}$ are constant and take their nodal values on each element. The use of these "constant" elements gives very good accuracy, when the boundary does not exhibit a significant degree of curvature. The "constant" element is the simplest type of discontinous element and avoids the ambiguities present in the value of $\frac{\partial \phi}{\partial n}$ at corner points.

The boundary element technique involves writing the boundary integral equation (4.30) for each of the M nodes, i.e. putting $\underline{x}_p$ equal to each node in turn. This produces M equations in $2M$ variables, these being the nodal values of ϕ and $\frac{\partial \phi}{\partial n}$. In a well posed problem we know either ϕ, $\frac{\partial \phi}{\partial n}$ or a relationship between them at each node, which thus reduces the number of unknowns to M.

We let ϕ_e and ϕ'_e denote the values of ϕ and $\frac{\partial \phi}{\partial n}$ respectively at node e, which lies at the mid-point of element e as noted above. In equation (4.30) we let the point $\underline{x}_p$ lie at the j th node, so that $\phi(\underline{x}_p) = \phi_j$ and $r = |\underline{x} - \underline{x}_j|$, where $\underline{x}_j$ is the position vector of the j th node and $\underline{x}$ is the position vector of an arbitrary point on the boundary.

Since $\underline{x}_p$ is not a corner point, $\alpha = 0$ and the discretisation of (4.30) leads to

$$\frac{1}{2}\phi_j + \sum_{e=1}^{M} \int_{\Gamma_e} (\phi_e \frac{\partial \phi^*}{\partial n} - \phi'_e \phi^*)\, d\Gamma_e = 0 \qquad (4.31)$$

where Γ_e denotes element e and we recall that ϕ^* is given by (4.24). Since ϕ_e and ϕ'_e are constant on Γ_e we can take them outside the integral sign and (4.31) takes

the form :

$$\sum_{e=1}^{M}(A_e\phi_e - B_e\phi'_e) = 0 \tag{4.32}$$

where

$$A_e = \begin{cases} \int_{\Gamma_e} \frac{\partial \phi^*}{\partial n} d\Gamma_e & e \neq j \\ \int_{\Gamma_j} \frac{\partial \phi^*}{\partial n} d\Gamma_j + \frac{1}{2} & e = j \end{cases}$$

$$B_e = \int_{\Gamma_e} \phi^* d\Gamma_e \tag{4.33}$$

The evaluation of the integrals A_e and B_e is described in **Appendix C.**

We choose M_1, M_2, M_3, M_4 elements on OA, AB, BC and CO respectively (Figure (4.1)), the elements (and nodes) being numbered in an anti-clockwise direction starting from O, i.e. O is the first point of element 1 and the second point of element M, where $M = M_1 + M_2 + M_3 + M_4$. From boundary conditions (4.7), (4.8) and (4.21) we find that

$$\text{on } OA \quad \phi'_e = \frac{\omega^2}{g}\phi_e \quad e = 1, 2, \cdots, M_1 \tag{4.34}$$

$$\text{on } AB \quad \phi'_e = ik'_0\phi_e \quad e = M_1 + 1, \cdots, M_1 + M_2 \tag{4.35}$$

$$\text{on } BC \quad \phi'_e = 0 \quad e = M_1 + M_2 + 1, \cdots, M_1 + M_2 + M_3 \tag{4.36}$$

On CO we deduce the relationship between ϕ and $\frac{\partial \phi}{\partial n}$ as follows. We must first choose $M_4 = N + 1$ which is the number of coefficients a_n appearing in equations (4.17) and (4.18). The y coordinates of the M_4 nodes on CO will be denoted by $y_1, y_2, \cdots y_{M_4}$ corresponding to nodes $M_1 + M_2 + M_3 + 1, \cdots, M$. We write equations

(4.17) and (4.18) at each of these nodes :

$$\begin{aligned} \phi(y_k) - f_0(y_k) &= \sum_{n=1}^{M_4} a_n f_n(y_k) \\ \phi'(y_k) + g_0(y_k) &= \sum_{n=1}^{M_4} a_n g_n(y_k) \\ k &= 1, 2, \cdots, M_4 \end{aligned}$$

These may be written in matrix form :

$$\{\phi\}_{CO} - \{f\} = [F]\{a\} \tag{4.37}$$

$$\{\phi'\}_{CO} + \{g\} = [G]\{a\} \tag{4.38}$$

where

$$\begin{aligned} \{\phi\}_{CO} &= \{\phi(y_k)\}, \quad k = 1, 2, \cdots, M_4 \\ &= \{\phi_e\}, \quad e = M_1 + M_2 + M_3 + 1, \cdots, M \\ \{\phi'\}_{CO} &= \{\phi'(y_k)\}, \quad k = 1, 2, \cdots, M_4 \\ &= \{\phi'_e\}, \quad e = M_1 + M_2 + M_3 + 1, \cdots, M \\ \{f\} &= \{f_0(y_k)\} \quad k = 1, 2, \cdots, M_4 \\ \{g\} &= \{g_0(y_k)\} \quad k = 1, 2, \cdots, M_4 \\ \{a\} &= \{a_n\} \quad n = 1, 2, \cdots, M_4 \\ f_{M_4} = f_0, &\quad g_{M_4} = g_0, \quad a_{M_4} = a_0 \end{aligned}$$

Also, $F_{kn} = f_n(y_k), G_{kn} = g_n(y_k)$ are the $k - n$ elements of the $M_4 \times M_4$ matrices $[F]$ and $[G]$ respectively.

From (4.37)

$$\{a\} = [F]^{-1}(\{\phi\}_{CO} - \{f\})$$

Substituting in (4.38) gives

$$\{\phi'\}_{CO} = [H](\{\phi\}_{CO} - \{f\}) - \{g\} \tag{4.39}$$

where

$$[H] = [G][F]^{-1}$$

We now note that equation (4.32) may be written in vector form as

$$\{A_e\}_\Gamma^T \{\phi_e\}_\Gamma - \{B_e\}_\Gamma^T \{\phi_e'\}_\Gamma = 0 \tag{4.40}$$

where $\{A_e\}_\Gamma, \{B_e\}_\Gamma, \{\phi_e\}_\Gamma, \{\phi_e'\}_\Gamma$ denote the M-dimensional vectors of the quantities $A_e, B_e, \phi_e, \phi_e'$ on the closed curve Γ; the superscript "T" denotes the transpose of a vector. In order to apply the boundary conditions we write equation (4.40) explicitly in terms of quantities defined on each section of the boundary Γ, i.e.

$$\begin{aligned} \{A_e\}_{OA}^T\{\phi_e\}_{OA} &- \{B_e\}_{OA}^T\{\phi_e'\}_{OA} \\ +\{A_e\}_{AB}^T\{\phi_e\}_{AB} &- \{B_e\}_{AB}^T\{\phi_e'\}_{AB} \\ +\{A_e\}_{BC}^T\{\phi_e\}_{BC} &- \{B_e\}_{BC}^T\{\phi_e'\}_{BC} \\ +\{A_e\}_{CO}^T\{\phi_e\}_{CO} &- \{B_e\}_{CO}^T\{\phi_e'\}_{CO} = 0 \end{aligned} \tag{4.41}$$

From (4.34) - (4.36) we have

$$\begin{aligned} \{\phi_e'\}_{OA} &= \frac{\omega^2}{g}\{\phi_e\}_{OA} \\ \{\phi_e'\}_{AB} &= ik_0'\{\phi_e\}_{AB} \\ \{\phi_e'\}_{BC} &= 0 \end{aligned} \tag{4.42}$$

Substituting equations (4.42) together with (4.39) into equation (4.41) gives

$$\{A_e - \frac{\omega^2}{g}B_e\}_{OA}^T\{\phi_e\}_{OA} + \{A_e - ik_0'B_e\}_{AB}^T\{\phi_e\}_{AB}$$

$$+\{A_e\}^T_{BC}\{\phi_e\}_{BC} + (\{A_e\}^T_{CO} - \{B_e\}^T_{CO}[H])\{\phi_e\}_{CO}$$
$$= -\{B_e\}^T_{CO}([H]\{f\} + \{g\})$$

This equation may be written :

$$[\{A_e - \frac{\omega^2}{g}B_e\}^T_{OA} \quad \{A_e - ik'_0 B_e\}_{AB} \quad \{A_e\}^T_{BC} \quad \{A_e\}^T_{CO} - \{B_e\}^T_{CO}[H]] \begin{pmatrix} \{\phi_e\}_{OA} \\ \{\phi_e\}_{AB} \\ \{\phi_e\}_{BC} \\ \{\phi_e\}_{CO} \end{pmatrix}$$

$$= -\{B_e\}^T_{CO}([H]\{f\} + \{g\}) \tag{4.43}$$

Equation (4.43) is the j th row of the complete matrix equation

$$[C]\{\phi\} = \{b\} \tag{4.44}$$

The (j,k) -th element of matrix $[C]$ is

$$C_{jk} = \begin{cases} A_k - \dfrac{\omega^2}{g}B_k & k = 1,\cdots,M_1 \\ A_k - ik'_0 B_k & k = M_1+1,\cdots,M_1+M_2 \\ A_k & k = M_1+M_2+1,\cdots,M_1+M_2+M_3 \\ A_k - \sum_{r=1}^{M_4} B_{M_1+M_2+M_3+r}\, H_{r,k-M_1-M_2-M_3} & \\ & k = M_1+M_2+M_3+1,\cdots,M \end{cases} \tag{4.45}$$

The j th element of vector $\{b\}$ is

$$b_j = -\sum_{r=1}^{M_4} B_{M_1+M_2+M_3+r}\, h_r$$

Table 4.1: Comparison of BEM with Analytic Formula for ϕ on a Flat Seabed

x coord. of point on Flat Seabed	$\phi(BEM) \times 10^2 m^2 s^{-1}$		$\phi(Analytic) \times 10^2 m^2 s^{-1}$	
	Real	Imag	Real	Imag
-63.5	0.94559	-0.23239	0.94492	-0.23209
-50.65	0.84967	-0.47520	0.84919	-0.47499
-20.95	0.41352	-0.88093	0.41336	-0.88084
-5.55	0.11285	-0.96644	0.11285	-0.96644

where h_r is the r th component of the vector $[H]\{f\} + \{g\}$ i.e.

$$h_r = \sum_{i=1}^{M_4} H_{ri} f_0(y_i) + g_0(y_r)$$

The solution vector is

$$\{\phi\} = \{\phi_e\}, \ e = 1, 2, \cdots, M$$

The wave pressure P is determined from Bernoulli's equation as

$$P = -\rho_f \frac{\partial \phi}{\partial t} = i\omega\rho_f \phi e^{-i\omega t} \tag{4.46}$$

The accuracy of the computer program was checked by running it for the case of a flat seabed under a wave of length $300m.$ and height $24m.$ in $80m.$ of water. The boundary values of ϕ were compared with those computed from the analytic formula (4.14). Excellent agreement was obtained as illustrated in Table (4.1) .

Chapter 5

Boundary Integral Formulation for Two Dimensional Poroelasticity - Sinusoidal Loading Conditions

As noted previously, the boundary element method has been applied to Biot's equations by a number of authors. The boundary element formulation for Laplace transformed space was accomplished by Cheng and Liggett(1984). Although the use of Laplace transforms is convenient for treating the time derivatives, such a formulation is not practical for the present problem owing to the difficulty of numerically inverting the transforms for problems involving sinusoidal loading. Cheng

and Liu (1986) have presented the boundary integral equations and fundamental solutions for sinusoidal loading conditions but without derivation. We present here these derivations and in addition, the functions required for determining interior effective stresses and pore pressure.

5.1 The Boundary Integral Equations

The governing equations (3.19) and (3.20) are recorded again for convenience :

$$\sigma_{ij,j} + \sigma_{,i} = -\rho X_i \tag{5.1}$$

$$\sigma_{,i} + f\rho_f X_i = fk(\dot{U}_i - \dot{u}_i) \tag{5.2}$$

The problem is to solve (5.1) and (5.2) in a domain Ω bounded by a closed curve Γ, in two dimensions. Either the displacements u_i, U_i or the tractions T_i is known on Γ. The tractions are given by (Sokolnikoff, 1956)

$$T_i = \tau_{ij} n_j \tag{5.3}$$

and using (3.11) this becomes

$$T_i = \sigma_{ij} n_j + \sigma n_i \tag{5.4}$$

where n_i is the i th component of the unit outward normal on Γ. A reciprocal theorem may be deduced as follows. We note that the constitutive laws (3.22) and (3.23) are of the form

$$\sigma_{ij} = Ae_{ij} + (Be + Q\varepsilon)\delta_{ij}$$

$$\sigma = Qe + R\varepsilon$$

If we consider two independent states of stress, denoted by primed and unprimed symbols, we have

$$\begin{aligned}\sigma_{ij}e'_{ij} + \sigma\varepsilon' &= Ae_{ij}e'_{ij} + (Be + Q\varepsilon)e'_{ii} + (Qe + R\varepsilon)\varepsilon' \\ &= Ae_{ij}e'_{ij} + Bee' + (Q\varepsilon e' + Qe\varepsilon') + R\varepsilon\varepsilon'\end{aligned}$$

since $e'_{ii} = e'$

Since the right hand side is symmetric with respect to primed and un-primed symbols, the left hand side must also be symmetric i.e.

$$\sigma_{ij}e'_{ij} + \sigma\varepsilon' = \sigma'_{ij}e_{ij} + \sigma'\varepsilon \tag{5.5}$$

which is the reciprocal theorem for poroelasticity (Cleary,1977). We shall seek the steady state solution of the governing equations under sinusoidal loading of frequency ω, i.e. we shall assume that a quantity A, be it stress or displacement, takes the form $A = \bar{A}e^{-i\omega t}$ where t is time. Equations (5.1),(5.2),(5.4) and (5.5) then take the form

$$\bar{\sigma}_{ij,j} + \bar{\sigma}_{,i} = -\rho\bar{X}_i \quad \text{in } \Omega \tag{5.6}$$

$$\bar{\sigma}_{,i} + f\rho_f\bar{X}_i = -i\omega fk(\bar{U}_i - \bar{u}_i) \quad \text{in } \Omega \tag{5.7}$$

$$\bar{T}_i = \bar{\sigma}_{ij}n_j + \bar{\sigma}n_i \quad \text{on } \Gamma \tag{5.8}$$

$$\bar{\sigma}_{ij}\bar{e}'_{ij} + \bar{\sigma}\bar{\varepsilon}' = \bar{\sigma}'_{ij}\bar{e}_{ij} + \bar{\sigma}'\bar{\varepsilon} \tag{5.9}$$

Assuming continuity of the first partial derivatives, we apply the divergence theorem to the product $\bar{\sigma}_{ij}\bar{u}'_i$:

$$\int_\Omega (\bar{\sigma}_{ij}\bar{u}'_i)_{,j}\, d\Omega = \int_\Gamma \bar{\sigma}_{ij}\bar{u}'_i n_j\, d\Gamma$$

i.e.

$$\int_\Omega (\bar{\sigma}_{ij}\bar{u}'_{i,j} + \bar{\sigma}_{ij,j}\ \bar{u}'_i)\, d\Omega = \int_\Gamma \bar{\sigma}_{ij}\bar{u}'_i n_j\, d\Gamma \qquad (5.10)$$

Since i and j are dummy indices we can write

$$\begin{aligned} \bar{\sigma}_{ij}\bar{u}'_{i,j} &= \frac{1}{2}(\bar{\sigma}_{ij}\bar{u}'_{i,j} + \bar{\sigma}_{ji}\bar{u}'_{j,i}) \\ &= \frac{1}{2}\bar{\sigma}_{ij}(\bar{u}'_{i,j} + \bar{u}'_{j,i}) = \bar{\sigma}_{ij}\bar{e}'_{ij} \end{aligned}$$

since $\bar{\sigma}_{ij} = \bar{\sigma}_{ji}$

Hence (5.10) becomes

$$\int_\Omega (\bar{\sigma}_{ij}\bar{e}'_{ij} + \bar{\sigma}_{ij,j}\bar{u}'_i)\, d\Omega = \int_\Gamma \bar{\sigma}_{ij}\bar{u}'_i n_j\, d\Gamma \qquad (5.11)$$

Similarly, we may apply the divergence theorem to $\bar{\sigma}'_{ij}\bar{u}_i$ to get :

$$\int_\Omega (\bar{\sigma}'_{ij}\bar{e}_{ij} + \bar{\sigma}'_{ij,j}\bar{u}_i)\, d\Omega = \int_\Gamma \bar{\sigma}'_{ij}\bar{u}_i n_j\, d\Gamma \qquad (5.12)$$

Applying the divergence theorem to the product $\bar{\sigma}\bar{U}'_i$ gives

$$\int_\Omega (\bar{\sigma}\bar{U}'_i)_{,i}\, d\Omega = \int_\Gamma \bar{\sigma}\bar{U}'_i n_i\, d\Gamma$$

i.e.

$$\int_\Omega (\bar{\sigma}\bar{\varepsilon}' + \bar{\sigma}_{,i}\bar{U}'_i)\, d\Omega = \int_\Gamma \bar{\sigma}\bar{U}'_i n_i\, d\Gamma \qquad (5.13)$$

Similarly, by applying the divergence theorem to $\bar{\sigma}'\bar{U}_i$ we have

$$\int_\Omega (\bar{\sigma}'\bar{\varepsilon} + \bar{\sigma}'_{,i}\bar{U}_i)\, d\Omega = \int_\Gamma \bar{\sigma}'\bar{U}_i n_i\, d\Gamma \qquad (5.14)$$

We now add equations (5.11) and (5.13) to get

$$\begin{aligned} &\int_\Omega (\bar{\sigma}_{ij}\bar{e}'_{ij} + \bar{\sigma}\bar{\varepsilon}' + \bar{\sigma}_{ij,j}\bar{u}'_i + \bar{\sigma}_{,i}\bar{U}'_i)\, d\Omega \\ &\qquad = \int_\Gamma [\bar{T}_i\bar{u}'_i + \bar{\sigma}(\bar{U}'_j - \bar{u}'_j)n_j]\, d\Gamma \end{aligned} \qquad (5.15)$$

Adding (5.12) and (5.14) gives

$$\int_\Omega (\bar{\sigma}'_{ij}\bar{e}_{ij} + \bar{\sigma}'\bar{\varepsilon} + \bar{\sigma}'_{ij,j}\bar{u}_i + \bar{\sigma}'_{,i}\bar{U}_i)\, d\Omega$$
$$= \int_\Gamma [\bar{T}'_i\bar{u}_i + \bar{\sigma}'(\bar{U}_j - \bar{u}_j)n_j]\, d\Gamma \tag{5.16}$$

We subtract (5.16) from (5.15) and use the reciprocal relation (5.5) to get

$$\int_\Omega [\,(\bar{\sigma}_{ij,j}\bar{u}'_i - \bar{\sigma}'_{ij,j}\bar{u}_i) + (\bar{\sigma}_{,i}\bar{U}'_i - \bar{\sigma}'_{,i}\bar{U}_i)\,]\, d\Omega$$
$$= \int_\Gamma [\,\bar{T}_i\bar{u}'_i - \bar{T}'_i\bar{u}_i + \bar{\sigma}(\bar{U}'_j - \bar{u}'_j)n_j$$
$$-\bar{\sigma}'(\bar{U}_j - \bar{u}_j)n_j\,]\, d\Gamma \tag{5.17}$$

We now let the primed stresses and displacements correspond to certain special loading conditions prescribed via the body force per unit mass X_i. Referring to Figure (3.1) we note that the masses of the solid and fluid portions of the area δA are respectively $(1-f)\rho_s\delta A$ and $f\rho_f\delta A$, where ρ_s is the density of the soil grains and ρ_f is the density of the pore water. The bulk density ρ of the soil is given by :

$$\rho = \rho_1 + \rho_2 \tag{5.18}$$

where $\rho_1 = (1-f)\rho_s$ and $\rho_2 = f\rho_f$.

The body force on the mass $\rho\delta A$ shown in Figure (3.1) is

$$\rho X_i\delta A \equiv (\rho_1 X_i + \rho_2 X_i)\delta A$$

Here we interpret the terms $\rho_1 X_i$ and $\rho_2 X_i$ as the body forces (per unit volume) acting on the solid and fluid portions of soil respectively. We let the primed stresses and displacements correspond to the loading

$$\rho_1 X_i^k = 2\pi\delta_{ik}\Delta(\underline{x}, p)e^{-i\omega t} \tag{5.19}$$

$$\rho_2 X_i^k = 0 \tag{5.20}$$

$$i, k = 1, 2$$

Here $\Delta(\underline{x},\underline{p})$ denotes the Dirac delta function, points $\underline{x},\underline{p}$ being on the solid skeleton. The superscript k on the left hand side indicates the direction of the point load and equations (5.19), (5.20) thus describe two loading situations. This represents sinusoidal point loading on the solid skeleton and is analogous to the loading commonly used for deriving the fundamental solutions for elasticity problems (Brebbia et al.,1984). A similar approach was taken by Cheng and Liggett (1984) for Laplace transformed space. Since $X_i = \bar{X}_i e^{-i\omega t}$, we have from (5.19) and (5.20) :

$$\rho_1 \bar{X}_i^k = 2\pi\delta_{ik}\Delta(\underline{x},\underline{p}) \tag{5.21}$$

$$\rho_2 \bar{X}_i^k = 0 \tag{5.22}$$

$$i,k = 1,2$$

The stresses and displacements due to the loading (5.21) and (5.22) will be denoted by asterisks and referred to as **fundamental** quantities. Substituting (5.21) and (5.22) into the governing equations (5.6) and (5.7), and noting (5.18) we have

$$\bar{\sigma}_{ij,j}^{*k} = -i\omega f k(\bar{U}_i^{*k} - \bar{u}_i^{*k}) - 2\pi\delta_{ik}\Delta(\underline{x},\underline{p}) \tag{5.23}$$

$$\bar{\sigma}_{,i}^{*k} = -i\omega f k(\bar{U}_i^{*k} - \bar{u}_i^{*k}) \tag{5.24}$$

Also, for an arbitrary body force $X_i = \bar{X}_i e^{-i\omega t}$ we have from (5.6) and (5.7)

$$\bar{\sigma}_{ij,j} = -\rho_1 \bar{X}_i + i\omega f k(\bar{U}_i - \bar{u}_i) \tag{5.25}$$

$$\bar{\sigma}_{,i} = -\rho_2 \bar{X}_i - i\omega f k(\bar{U}_i - \bar{u}_i) \tag{5.26}$$

We replace the primes in equation (5.17) by asterisks and use equations (5.23) to (5.26) to get

$$\int_\Omega \{[-\rho_1 \bar{X}_i + i\omega f k(\bar{U}_i - \bar{u}_i)]\bar{u}_i^{*k} - [i\omega f k(\bar{U}_i^{*k} - \bar{u}_i^{*k}) - 2\pi\delta_{ik}\Delta(\underline{x},\underline{p})]\bar{u}_i$$

$$+[-\rho_2\bar{X}_i - i\omega fk(\bar{U}_i - \bar{u}_i)]\bar{U}_i^{*k} + i\omega fk(\bar{U}_i^{*k} - \bar{u}_i^{*k})\bar{U}_i\}\, d\Omega$$
$$= \int_\Gamma \{(\bar{T}_i\bar{u}_i^{*k} - \bar{T}_i^{*k}\bar{u}_i) + \bar{\sigma}(\bar{U}_i^{*k} - \bar{u}_i^{*k})n_i - \bar{\sigma}^{*k}(\bar{U}_i - \bar{u}_i)n_i\}\, d\Gamma \quad (5.27)$$

By the sifting property of the delta function,

$$\int_\Omega 2\pi\delta_{ik}\Delta(\underline{x},\underline{p})\bar{u}_i\, d\Omega = 2\pi\delta_{ik}\bar{u}_i(\underline{p}) \quad (5.28)$$

where the integration has been performed with respect to $\underline{x}$, and $\underline{p}$ is the position vector of the point of application of the point load. Both sides of equation (5.27) are thus functions of $\underline{p} \in \Omega$ and this equation takes the form

$$\begin{aligned} 2\pi\delta_{ik}\bar{u}_i(\underline{p}) &= \int_\Gamma (\bar{T}_i\bar{u}_i^{*k} - \bar{T}_i^{*k}\bar{u}_i) + \bar{\sigma}(\bar{U}_i^{*k} - \bar{u}_i^{*k})n_i \\ &\quad -\bar{\sigma}^{*k}(\bar{U}_i - \bar{u}_i)n_i\, d\Gamma \\ &\quad + \int_\Omega \bar{X}_i(\rho_1\bar{u}_i^{*k} + \rho_2\bar{U}_i^{*k})\, d\Omega \end{aligned} \quad (5.29)$$

In order to write (5.29) for a boundary point $\underline{p}$ it is necessary to evaluate the Cauchy principal value of integrals involving the fundamental quantities (denoted by asterisks), since the quantities are singular at $\underline{p}$. This operation results in modifications to the term in $\bar{u}_k(\underline{p})$ and the general form of this term is $2\pi\alpha_{ik}\bar{u}_i(\underline{p})$, which resembles (5.28) in form.

Thus for any point $\underline{p} \in \Gamma$, (5.29) becomes

$$\begin{aligned} 2\pi\alpha_{ik}\bar{u}_i(\underline{p}) &= PV\int_\Gamma [(\bar{T}_i\bar{u}_i^{*k} - \bar{T}_i^{*k}\bar{u}_i) + \bar{\sigma}(\bar{U}_i^{*k} - \bar{u}_i^{*k})n_i \\ &\quad -\bar{\sigma}^{*k}(\bar{U}_i - \bar{u}_i)n_i]\, d\Gamma \\ &\quad + PV\int_\Omega \bar{X}_i(\rho_1\bar{u}_i^{*k} + \rho_2\bar{U}_i^{*k})\, d\Omega \end{aligned} \quad (5.30)$$

The symbol PV denotes the Cauchy principal value of an integral. The coefficient α_{ik} must be evaluated either from the Cauchy principal value of the integrals or by using a "rigid body motion" analogy (Brebbia et al.,1984).

Equation (5.30) is the integral equation for the soil displacements. To derive a similar equation for pore pressure we consider the fundamental solutions corresponding to the loading

$$\begin{aligned} \rho X_i &= 0 \\ (\rho_2 X_i)_{,i} &= -2\pi f k \Delta(\underline{x}, \underline{\nu}) e^{-i\omega t} \end{aligned}$$

i.e.

$$\rho \bar{X}_i = 0 \tag{5.31}$$

$$(\rho_2 \bar{X}_i)_{,i} = -2\pi f k \Delta(\underline{x}, \underline{p}) \tag{5.32}$$

Since $\rho = \rho_1 + \rho_2$, equation (5.31) implies that $\rho_2 \bar{X}_i = -\rho_1 \bar{X}_i$, i.e. the body forces on the solid and fluid portions of soil cancel each other. Equation (5.32) describes the loading on the fluid portion of soil. We assume that there exists a scalar function χ such that

$$\rho_2 \bar{X}_i = \chi_{,i} \tag{5.33}$$

and hence from (5.32) we have

$$\nabla^2 \chi = -2\pi f k \Delta(\underline{x}, \underline{\nu}) \tag{5.34}$$

We shall denote the stresses and displacements corresponding to the loading (5.31), (5.32) by superscript 0. These are also called fundamental quantities. From the governing equations (5.6) and (5.7) and the loading described by (5.31) and (5.32) we have

$$\bar{\sigma}^0_{ij,j} = i\omega f k(\bar{U}^0_i - \bar{u}^0_i) + \chi_{,i} \tag{5.35}$$

$$\bar{\sigma}^0_{,i} = -i\omega f k(\bar{U}^0_i - \bar{u}^0_i) - \chi_{,i} \tag{5.36}$$

Using equations (5.25), (5.26), (5.35) and (5.36) we have from (5.17)

$$\begin{aligned}\int_\Omega \{ [-\rho_1 \bar{X}_i + i\omega f k(\bar{U}_i - \bar{u}_i)]\bar{u}_i^0 - [i\omega f k(\bar{U}_i^0 - \bar{u}_i^0) + \chi_{,i}]\bar{u}_i \\ +[-\rho_2 \bar{X}_i - i\omega f k(\bar{U}_i - \bar{u}_i)]\bar{U}_i^0 + [i\omega f k(\bar{U}_i^0 - \bar{u}_i^0) + \chi_{,i}]\bar{U}_i \} \, d\Omega \\ = \int_\Gamma \{ (\bar{T}_i \bar{u}_i^0 - \bar{T}_i^0 \bar{u}_i) + \bar{\sigma}(\bar{U}_j^0 - \bar{u}_j^0) n_j \\ -\bar{\sigma}^0(\bar{U}_j - \bar{u}_j) n_j \} \, d\Gamma \end{aligned} \tag{5.37}$$

By collecting terms we find that the left side (L.H.S.) of (5.37) reduces to

$$\text{L.H.S. of (5.37)} = \int_\Omega \{ \bar{X}_i[-\rho \bar{u}_i^0 - \rho_2(\bar{U}_i^0 - \bar{u}_i^0)] + \chi_{,i}(\bar{U}_i - \bar{u}_i) \} \, d\Omega \tag{5.38}$$

From (5.36) :

$$\bar{U}_i^0 - \bar{u}_i^0 = \frac{i}{\omega f k}(\bar{\sigma}_{,i}^0 + \chi_{,i})$$

From (5.7) :

$$\bar{U}_i - \bar{u}_i = \frac{i}{\omega f k}(\bar{\sigma}_{,i} + f \rho_f \bar{X}_i)$$

Substituting these expressions into (5.38) gives

$$\text{L.H.S. of (5.37)} = \int_\Omega \left[-\bar{X}_i(\rho \bar{u}_i^0 + \frac{i\rho_f}{\omega k}\bar{\sigma}_{,i}^0) + \frac{i\chi_{,i}\bar{\sigma}_{,i}}{\omega f k} \right] d\Omega \tag{5.39}$$

By applying the divergence theorem to the product $\psi \eta_i$ it is easy to establish the identity

$$\int_\Omega \eta_i \psi_{,i} d\Omega = -\int_\Omega \psi \eta_{i,i} d\Omega + \int_\Gamma \psi \eta_i n_i d\Gamma \tag{5.40}$$

By putting $\eta_i = \chi_{,i}$ and $\psi = \bar{\sigma}$ we have

$$\begin{aligned}\int_\Omega \chi_{,i}\bar{\sigma}_{,i} \, d\Omega &= -\int_\Omega \bar{\sigma}\nabla^2\chi \, d\Omega + \int_\Gamma \bar{\sigma}\chi_{,i} n_i \, d\Gamma \\ &= 2\pi f k \int_\Omega \bar{\sigma}\Delta(\underline{x}, \underline{p}) \, d\Omega + \int_\Gamma \bar{\sigma}\chi_{,i} n_i \, d\Gamma \\ &= 2\pi f k \bar{\sigma}(\underline{p}) + \int_\Gamma \bar{\sigma}\chi_{,i} n_i d\Gamma \end{aligned} \tag{5.41}$$

using (5.34) and the sifting property of the delta function.

We now substitute (5.41) into (5.39) :

$$\text{L.H.S. of (5.37)} = \int_\Omega -\bar{X}_i(\rho\bar{u}_i^0 + \frac{i\rho_f}{\omega k}\bar{\sigma}_{,i}^0)\,d\Omega + \frac{2\pi i}{\omega}\bar{\sigma}(\underline{p}) + \frac{i}{\omega f k}\int_\Gamma \bar{\sigma}\chi_{,i}n_i\,d\Gamma \tag{5.42}$$

Equation (5.37) thus becomes

$$\begin{aligned}\frac{2\pi i}{\omega}\bar{\sigma}(\underline{p}) &= \int_\Gamma [(\bar{T}_j\bar{u}_j^0 - \bar{T}_j^0\bar{u}_j) + \bar{\sigma}(\bar{U}_j^0 - \bar{u}_j^0)n_j \\ &\quad -\bar{\sigma}^0(\bar{U}_j - \bar{u}_j)n_j - \frac{i}{\omega f k}\bar{\sigma}\chi_{,j}n_j]\,d\Gamma \\ &\quad + \int_\Omega \bar{X}_j(\rho\bar{u}_j^0 + \frac{i\rho_f}{\omega k}\bar{\sigma}_{,j}^0)\,d\Omega \qquad (5.43) \\ j &= 1,2\end{aligned}$$

If equation (5.43) is written for a boundary point $\underline{p}$ the singular integrals involving fundamental quantities must be interpreted as Cauchy principal values and extra terms in $\bar{\sigma}(\underline{p})$ appear. Thus for a boundary point $\underline{p}$:

$$\begin{aligned}\frac{2\pi i\theta}{\omega}\bar{\sigma}(\underline{p}) &= PV\int_\Gamma [(\bar{T}_j\bar{u}_j^0 - \bar{T}_j^0\bar{u}_j) + \bar{\sigma}(\bar{U}_j^0 - \bar{u}_j^0)n_j \\ &\quad -\bar{\sigma}^0(\bar{U}_j - \bar{u}_j)n_j - \frac{i}{\omega f k}\bar{\sigma}\chi_{,j}n_j]\,d\Gamma \\ &\quad + PV\int_\Omega \bar{X}_j(\rho\bar{u}_j^0 + \frac{i\rho_f}{\omega k}\bar{\sigma}_{,j}^0)\,d\Omega \qquad (5.44) \\ j &= 1,2\end{aligned}$$

The coefficient θ must be determined from the evaluation of the Cauchy principal value of the singular integrals or from a "rigid body motion" analogy. For the purpose of determining wave-induced stresses and pore pressures we assume that there are no body forces present. Thus from (5.30) and (5.44) we write the

boundary integral equations as for $\underline{p} \in \Gamma$ as

$$2\pi\alpha_{ik}\bar{u}_i(\underline{p}) = PV\int_\Gamma [(\bar{T}_i\bar{u}_i^{*k} - \bar{T}_i^{*k}\bar{u}_i) + \bar{\sigma}(\bar{U}_i^{*k} - \bar{u}_i^{*k})n_i - \bar{\sigma}^{*k}(\bar{U}_i - \bar{u}_i)n_i]\, d\Gamma \tag{5.45}$$

$$\frac{2\pi i\theta}{\omega}\bar{\sigma}(\underline{p}) = PV\int_\Gamma [(\bar{T}_i\bar{u}_i^{0} - \bar{T}_i^{0}\bar{u}_i) + \bar{\sigma}(\bar{U}_i^{0} - \bar{u}_i^{0})n_i - \bar{\sigma}^{0}(\bar{U}_i - \bar{u}_i)n_i - \frac{i}{\omega f k}\bar{\sigma}\chi_{,i}n_i]\, d\Gamma \tag{5.46}$$

where subscripts $i, k = 1, 2$, and as previously noted, a repeated subscript indicates summation.

5.2 The Fundamental Solutions

As indicated earlier, the fundamental solutions are the stresses and displacements corresponding to the loadings described by equations (5.21), (5.22) and (5.31), (5.32) . In order to determine these solutions the governing equations (5.6) and (5.7) must be written in terms of displacements via the constitutive relations (3.22) and (3.23). This renders (5.6) and (5.7) as

$$\mu\bar{u}_{i,jj} + (\lambda + \mu + \frac{Q^2}{R} + Q)\bar{u}_{j,ji} + (Q + R)\bar{U}_{j,ji} = -\rho\bar{X}_i \tag{5.47}$$

$$Q\bar{u}_{j,ji} + R\bar{U}_{j,ji} + f\rho_f\bar{X}_i = -i\omega f k(\bar{U}_i - \bar{u}_i) \tag{5.48}$$

where, we recall, Q and R are given by (3.24). The first set of fundamental solutions, denoted by asterisks, is obtained by substituting (5.21) and (5.22) into (5.47) and (5.48) to give

$$\mu\bar{u}_{i,jj}^{*k} + (\lambda + \mu + \frac{Q^2}{R} + Q)\bar{u}_{j,ji}^{*k} + (Q + R)\bar{U}_{j,ji}^{*k} = -2\pi\delta_{ik}\Delta(\underline{x}, \underline{p}) \tag{5.49}$$

$$Q\bar{u}_{j,ji}^{*k} + R\bar{U}_{j,ji}^{*k} + i\omega f k(\bar{U}_i^{*k} - \bar{u}_i^{*k}) = 0 \tag{5.50}$$

Following Biot (1956) we define

$$\bar{v}_i^{*k} = \left(\frac{H-Q-R}{H}\right)\bar{u}_i^{*k} + \left(\frac{Q+R}{H}\right)\bar{U}_i^{*k} \tag{5.51}$$

where

$$H = \lambda + 2\mu + \frac{(Q+R)^2}{R} \tag{5.52}$$

and

$$\bar{w}_i^{*k} = \bar{U}_i^{*k} - \bar{u}_i^{*k} \tag{5.53}$$

from which we have

$$\bar{u}_i^{*k} = \bar{v}_i^{*k} - \left(\frac{Q+R}{H}\right)\bar{w}_i^{*k} \tag{5.54}$$

$$\bar{U}_i^{*k} = \bar{v}_i^{*k} + \left(1 - \frac{Q+R}{H}\right)\bar{w}_i^{*k} \tag{5.55}$$

In terms of $\bar{v}_i^{*k}$ and $\bar{w}_i^{*k}$ equations (5.49) and (5.50) become

$$\mu\bar{v}_{i,jj}^{*k} + (H-\mu)\bar{v}_{j,ji}^{*k} - \frac{\mu(Q+R)}{H}(\bar{w}_{i,jj}^{*k} - \bar{w}_{j,ji}^{*k}) = -2\pi\delta_{ik}\Delta(\underline{x},\underline{p}) \tag{5.56}$$

$$(Q+R)\bar{v}_{j,ji}^{*k} + \frac{R(\lambda+2\mu)}{H}\bar{w}_{j,ji}^{*k} + i\omega f k\bar{w}_i^{*k} = 0 \tag{5.57}$$

But we note from (5.24) that

$$\bar{w}_i^{*k} = \frac{\bar{\sigma}_i^{*k}}{-i\omega f k}$$

so that

$$\bar{w}_{j,ji}^{*k} = \bar{w}_{i,jj}^{*k}$$

Substituting this into (5.56) and (5.57) gives

$$\mu\bar{v}_{i,jj}^{*k} + (H-\mu)\bar{v}_{j,ji}^{*k} = -2\pi\delta_{ik}\Delta(\underline{x},\underline{p}) \tag{5.58}$$

$$(Q+R)\bar{v}_{j,ji}^{*k} + \frac{R(\lambda+2\mu)}{H}\bar{w}_{i,jj}^{*k} + i\omega f k\bar{w}_i^{*k} = 0 \tag{5.59}$$

Equation (5.58) may be compared to the elasticity equation

$$\mu u^k_{i,jj} + (\lambda + \mu) u^k_{j,ji} = -2\pi\delta_{ik}\Delta(\underline{x},\underline{p}) \tag{5.60}$$

Employing the Papkovitch-Neuber technique we write

$$u^k_i = \frac{\partial}{\partial z_i}(\psi^k_0 + z_j\psi^k_j) - 4(1-\nu)\psi^k_i \tag{5.61}$$

where

$$\nu = \frac{\lambda}{2(\lambda+\mu)} \tag{5.62}$$

The quantities ψ^k_0,ψ^k_i are functions of the spatial coordinates z_i . We may take any one of these functions to be zero without loss of completeness (Eubanks and Sternberg,1956). Accordingly, we set $\psi^k_0 \equiv 0$. We define the coordinate system by

$$z_i = x_i - p_i$$

where x_i, p_i are the coordinates of the points $\underline{x}$ and $\underline{p}$ respectively . Using (5.61) and writing

$$\beta = \frac{2\mu(1-\nu)}{1-2\nu} \tag{5.63}$$

we find that (5.60) becomes

$$\beta\frac{\partial}{\partial x_i}[(x_j - p_j)\nabla^2\psi^k_j] - 2(1-2\nu)\beta\nabla^2\psi^k_i = -2\pi\delta_{ik}\Delta(\underline{x},\underline{p})$$

We now integrate over a circular region Ω,centre $\underline{p}$ and radius ϵ :

$$\beta\int_\Omega \frac{\partial}{\partial x_i}[(x_j - p_j)\nabla^2\psi^k_j]\,d\Omega - 2(1-2\nu)\beta\int_\Omega \nabla^2\psi^k_i\,d\Omega = -2\pi\delta_{ik} \tag{5.64}$$

since

$$\int_\Omega \Delta(\underline{x},\underline{p})\,d\Omega = 1$$

We may define local polar coordinates with $\underline{p}$ as origin by letting

$$x_1 - p_1 = r\cos\theta$$

$$x_2 - p_2 = r\sin\theta$$

Then,assuming ψ_i^k is independent of θ , we find that the second integral on the left hand side of (5.64) is easily evaluated as

$$\begin{aligned}\int_\Omega \nabla^2\psi_i^k\, d\Omega &= \int_\Omega (\psi_{i,j}^k)_{,j}\, d\Omega \\ &= \int_\Gamma \psi_{i,j}^k n_j\, d\Gamma \\ &= \int_\Gamma \frac{\partial\psi_i^k}{\partial n}\, d\Gamma \\ &= \int_0^{2\pi} \left(\frac{\partial\psi_i^k}{\partial r}\right)_{r=\epsilon} \epsilon\, d\theta \\ &= 2\pi\epsilon\left(\frac{\partial\psi_i^k}{\partial r}\right)_{r=\epsilon} \end{aligned} \tag{5.65}$$

where Γ is the circular boundary of Ω .

The first integral on the left hand side of (5.64) is evaluated by noting that for any continuously differentiable function ϕ

$$\int_\Omega \frac{\partial\phi}{\partial x_i}\, d\Omega = \int_\Gamma \phi n_i\, d\Gamma$$

Thus

$$\int_\Omega \frac{\partial}{\partial x_i}[(x_j - p_j)\nabla^2\psi_j^k]\, d\Omega = \int_\Gamma (x_j - p_j)\nabla^2\psi_j^k n_i\, d\Gamma \tag{5.66}$$

Changing to polar coordinates and recalling that ψ_i^k is independent of θ ,(5.66) becomes

$$\int_\Omega \frac{\partial}{\partial x_i}[(x_j - p_j)\nabla^2\psi_j^k]\, d\Omega$$

$$= \int_\Gamma [r\cos\theta\nabla^2\psi_1^k + r\sin\theta\nabla^2\psi_2^k] \begin{pmatrix} \cos\theta \\ \sin\theta \end{pmatrix} d\Gamma$$

$$= \begin{bmatrix} \int_0^{2\pi} [\epsilon\cos\theta(\nabla^2\psi_1^k)_{r=\epsilon} + \epsilon\sin\theta(\nabla^2\psi_2^k)_{r=\epsilon}]\cos\theta.\epsilon\, d\theta \\ \int_0^{2\pi} [\epsilon\cos\theta(\nabla^2\psi_1^k)_{r=\epsilon} + \epsilon\sin\theta(\nabla^2\psi_2^k)_{r=\epsilon}]\sin\theta.\epsilon\, d\theta \end{bmatrix}$$

$$= \pi\epsilon^2 \begin{bmatrix} (\nabla^2\psi_1^k)_{r=\epsilon} \\ (\nabla^2\psi_2^k)_{r=\epsilon} \end{bmatrix} = \pi\epsilon^2(\nabla^2\psi_i^k)_{r=\epsilon} \tag{5.67}$$

Then using (5.65) and (5.67),equation (5.64) simplifies to

$$\beta\pi\epsilon^2(\nabla^2\psi_i^k)_{r=\epsilon} - 4(1-2\nu)\beta\pi\epsilon(\frac{\partial\psi_i^k}{\partial r})_{r=\epsilon} = -2\pi\delta_{ik} \tag{5.68}$$

We choose ψ_i^k such that

$$\nabla^2\psi_i^k = 0 \text{ at least when } \underline{x} \neq \underline{p} \text{ i.e. } r \neq 0 \tag{5.69}$$

Then (5.68) becomes

$$2(1-2\nu)\beta\left(\frac{\partial\psi_i^k}{\partial r}\right)_{r=\epsilon} = \frac{1}{\epsilon}\delta_{ik} \tag{5.70}$$

This equation is satisfied by

$$\begin{aligned} \psi_i^k &= \frac{1}{2(1-2\nu)\beta}\ln r\delta_{ik} \\ &= \frac{1}{4\mu(1-\nu)}\ln r\delta_{ik} \end{aligned} \tag{5.71}$$

which also satifies condition (5.69) . We thus have from (5.61) a solution of (5.60) as

$$\begin{aligned} u_i^k &= \frac{1}{4\mu(1-\nu)}(z_j\ln r\delta_{jk})_{,i} - \frac{1}{\mu}\ln r\delta_{ik} \\ &= \frac{1}{4\mu(1-\nu)}[r_{,i}r_{,k} + (-3+4\nu)\ln r\delta_{ik}] \end{aligned} \tag{5.72}$$

where we have used $r^2 = z_i z_i$, $z_{i,j} = \delta_{ij}$ and $z_i = r r_{,i}$.

By comparing (5.60) with (5.58) we have the analogy :

$$\begin{aligned} u_i^k &\longrightarrow \bar{v}_i^{*k} \\ \mu &\longrightarrow \mu \\ \lambda + \mu &\longrightarrow H - \mu \end{aligned}$$

Hence

$$\begin{aligned} \lambda &\longrightarrow H - 2\mu \\ \nu = \frac{\lambda}{2(\lambda+\mu)} &\longrightarrow \frac{H-2\mu}{2(H-\mu)} \end{aligned}$$

We thus construct from (5.72) the function $\bar{v}_i^{*k}$ as

$$\bar{v}_i^{*k} = \left(\frac{H-\mu}{2\mu H}\right) r_{,i} r_{,k} - \left(\frac{H+\mu}{2\mu H}\right) \ln r \delta_{ik} \tag{5.73}$$

To determine $\bar{w}_i^{*k}$ (defined by 5.53) we again note from (5.24) that $\bar{w}_i^{*k}$ is the gradient of a scalar function. Writing

$$\bar{w}_i^{*k} = \phi_{,i}^k \tag{5.74}$$

we have from (5.59)

$$(Q+R)\frac{\partial}{\partial x_i}(\bar{v}_{j,j}^{*k}) + \frac{R(\lambda+2\mu)}{H}\frac{\partial}{\partial x_i}(\nabla^2 \phi^k) + i\omega f k \frac{\partial}{\partial x_i}(\phi^k) = 0$$

Integrating with respect to x_i and setting the integration constant equal to zero (since we are only interested in a particular solution) gives

$$(Q+R)\bar{v}_{j,j}^{*k} + \frac{R(\lambda+2\mu)}{H}\nabla^2 \phi^k + i\omega f k \phi^k = 0 \tag{5.75}$$

To evaluate $\bar{v}^{*k}_{j,j}$ we make use of the following results :

$$\begin{aligned} r_{,i} &= \frac{x_i - p_i}{r} \\ r_{,i}r_{,i} &= 1 \\ r_{,ij} &= \frac{\delta_{ij}}{r} - \frac{r_{,i}r_{,j}}{r} \\ (r_{,j}r_{,k})_{,j} &= \frac{r_{,k}}{r} \end{aligned}$$

which are easily deduced from the definition

$$r^2 = (x_i - p_i)(x_i - p_i)$$

Then differentiating $\bar{v}^{*k}_j$ (from (5.73)) with respect to x_j we get

$$\bar{v}^{*k}_{i,i} = -\frac{1}{H}(\ln r)_{,k}$$

Substituting in (5.75) gives

$$\nabla^2\phi^k + \frac{i\omega fkH}{R(\lambda+2\mu)}\phi^k = \left[\frac{Q+R}{R(\lambda+2\mu)}\right](\ln r)_{,k} \tag{5.76}$$

We let

$$\phi^k = \phi^k_1 + \phi^k_2 \tag{5.77}$$

where

$$\begin{aligned} \phi^k_1 &= \left(\frac{Q+R}{i\omega fkH}\right)(\ln r)_{,k} \\ &= \frac{-i(Q+R)}{wfkH}\frac{r_{,k}}{r} \end{aligned} \tag{5.78}$$

Since (see Appendix D)

$$\nabla^2(\ln r) = 2\pi\Delta(x,p)$$

we have

$$\begin{aligned}\nabla^2\phi_1^k &= \left(\frac{Q+R}{i\omega fkH}\right)(\nabla^2 \ln r)_{,k} \\ &= \frac{2\pi(Q+R)}{i\omega fkH}\frac{\partial}{\partial x_k}[\Delta(\underline{x},\underline{p})] \end{aligned} \tag{5.79}$$

where the right hand side must be interpreted as the derivative of a generalized function. Substituting (5.77) into (5.76) and then using (5.78) and (5.79) gives

$$\nabla^2\phi_2^k + \frac{i\omega fkH}{R(\lambda+2\mu)}\phi_2^k = -\frac{2\pi(Q+R)}{i\omega fkH}\frac{\partial}{\partial x_k}[\Delta(\underline{x},\underline{p})] \tag{5.80}$$

We define the constant a by

$$a^2 = -\frac{i\omega fkH}{R(\lambda+2\mu)} \tag{5.81}$$

This will be expressed in a more convenient form later. Equation (5.80) becomes

$$\nabla^2\phi_2^k - a^2\phi_2^k = \frac{2\pi i(Q+R)}{\omega fkH}\frac{\partial}{\partial x_k}[\Delta(\underline{x},\underline{p})] \tag{5.82}$$

Integration with respect to x_k gives

$$\nabla^2\eta^k - a^2\eta^k = 2\pi\Delta(\underline{x},\underline{p}) \tag{5.83}$$

where

$$\eta^k = \frac{\omega fkH}{i(Q+R)}\int \phi_2^k dx_k \text{ (no sum on } k) \tag{5.84}$$

A solution to (5.83) is (Bleistein, 1984)

$$\eta^k = -K_0(ar) \tag{5.85}$$

where K_0 is the modified Bessel function of the second kind of order zero, and $r = |\underline{x}-\underline{p}|$. From (5.83) and (5.84) it is clear that

$$\begin{aligned}\phi_2^k &= \frac{-i(Q+R)}{\omega fkH}\frac{\partial}{\partial x_k}[K_0(ar)] \\ &= \frac{i(Q+R)}{\omega fkH}ar_{,k}K_1(ar) \end{aligned} \tag{5.86}$$

where K_1 is the modified Bessel function of the second kind of order 1. Now substituting (5.77) and (5.85) into (5.76) we have

$$\phi^k = \frac{i(Q+R)}{\omega f k H} a r_{,k} [K_1(ar) - \frac{1}{ar}] \tag{5.87}$$

The function $\bar{w}_i^{*k}$ may now be obtained from (5.74) as

$$\begin{aligned} \bar{w}_i^{*k} &= \frac{i(Q+R)a^2}{\omega f k H} \{ [\frac{2}{a^2 r^2} - K_2(ar)] r_{,i} r_{,k} \\ &\quad + \delta_{ik} [\frac{K_1(ar)}{ar} - \frac{1}{a^2 r^2}] \} \end{aligned} \tag{5.88}$$

where we have used the results

$$K_2(ar) = K_0(ar) + \frac{2}{ar} K_1(ar)$$

$$\frac{\partial}{\partial x_i} [K_1(ar)] = -\frac{1}{2} a r_{,i} [K_0(ar) + K_2(ar)]$$

Using (5.73) and (5.88) we recover $\bar{u}_i^{*k}$ and $\bar{U}_i^{*k}$ from (5.54) and (5.55) :

$$\begin{aligned} \bar{u}_i^{*k} &= \left(\frac{H-\mu}{2\mu H} \right) r_{,i} r_{,k} - \left(\frac{H+\mu}{2\mu H} \right) \ln r \delta_{ik} \\ &\quad - \frac{i(Q+R)^2 a^2}{\omega f k H^2} \{ [\frac{2}{a^2 r^2} - K_2(ar)] r_{,i} r_{,k} \\ &\quad + \delta_{ik} [\frac{K_1(ar)}{ar} - \frac{1}{a^2 r^2}] \} \end{aligned} \tag{5.89}$$

$$\begin{aligned} \bar{U}_i^{*k} &= \left(\frac{H-\mu}{2\mu H} \right) r_{,i} r_{,k} - \left(\frac{H+\mu}{2\mu H} \right) \ln r \delta_{ik} \\ &\quad + \frac{i(H-Q-R)(Q+R)a^2}{\omega f k H^2} \{ [\frac{2}{a^2 r^2} - K_2(ar)] r_{,i} r_{,k} \\ &\quad + \delta_{ik} [\frac{K_1(ar)}{ar} - \frac{1}{a^2 r^2}] \} \end{aligned} \tag{5.90}$$

The tractions $\bar{T}_i^{*k}$ and $\bar{\sigma}^{*k}$ are now obtained from (5.8) and the constitutive laws (3.22) and (3.23) i.e.

$$\bar{T}_i^{*k} = 2\mu \bar{e}_{ij}^{*k} n_j + (\lambda + \frac{Q^2}{R} + Q) \bar{e}^{*k} n_i + (Q+R) \bar{\varepsilon}^{*k} n_i \tag{5.91}$$

$$\bar{\sigma}^{*k} = Q \bar{e}^{*k} + R \bar{\varepsilon}^{*k} \tag{5.92}$$

where

$$\begin{aligned}\bar{e}_{ij}^{*k} &= \frac{1}{2}(\bar{u}_{i,j}^{*k} + \bar{u}_{j,i}^{*k}) \\ \bar{e}^{*k} &= \bar{u}_{i,i}^{*k} \\ \bar{\varepsilon}^{*k} &= \bar{U}_{i,i}^{*k}\end{aligned}$$

Thus substituting (5.89) and (5.90) into (5.91) and (5.92) we obtain after some manipulations

$$\begin{aligned}\bar{T}_i^{*k} &= -2\left(\frac{H-\mu}{H}\right)\frac{r_{,i}r_{,k}}{r}\frac{\partial r}{\partial n} + \frac{\mu}{H}\frac{1}{r}(r_{,k}n_i - r_{,i}n_k - \frac{\partial r}{\partial n}\delta_{ik}) \\ &\quad -\frac{i2\mu(Q+R)^2a^3}{\omega fkH^2}\{\frac{\partial r}{\partial n}\delta_{ik}[\frac{2}{a^3r^3} - \frac{K_2(ar)}{ar}] \\ &\quad +\frac{\partial r}{\partial n}r_{,i}r_{,k}[K_3(ar) - \frac{8}{a^3r^3}] \\ &\quad +r_{,k}n_i[\frac{2}{a^3r^3} + \frac{3K_2(ar)}{ar} - K_3(ar)] \\ &\quad +r_{,i}n_k[\frac{2}{a^3r^3} - \frac{K_2(ar)}{ar}]\} \qquad (5.93) \\ \bar{\sigma}^{*k} &= a\left(\frac{Q+R}{H}\right)r_{,k}[K_1(ar) - \frac{1}{ar}] \qquad (5.94)\end{aligned}$$

In these derivations the following relations were used

$$K_{n+1}(z) = K_{n-1}(z) + \frac{2n}{z}K_n(z)$$

$$K_n'(z) = -\frac{1}{2}[K_{n-1}(z) + K_{n+1}(z)]$$

The second set of fundamental solutions, denoted by superscript 0, is obtained by substituting (5.31) and (5.33) into (5.47) and (5.48). This gives

$$\mu\nabla^2\bar{u}_i^0 + (\lambda+\mu+\frac{Q^2}{R}+Q)\bar{u}_{j,ji}^0 + (Q+R)\bar{U}_{j,ji}^0 = 0 \qquad (5.95)$$

$$Q\bar{u}_{j,ji}^0 + R\bar{U}_{j,ji}^0 + \chi_{,i} + i\omega fk(\bar{U}_i^0 - \bar{u}_i^0) = 0 \qquad (5.96)$$

where χ is found from (5.34). The solution of (5.34) is (see Appendix D)

$$\chi = -fk \ln r \tag{5.97}$$

We define

$$\bar{v}_i^0 = \bar{u}_i^0 + \left(\frac{Q+R}{H}\right)(\bar{U}_i^0 - \bar{u}_i^0) \tag{5.98}$$

$$\bar{w}_i^0 = \bar{U}_i^0 - \bar{u}_i^0 \tag{5.99}$$

from which we have

$$\bar{u}_i^0 = \bar{v}_i^0 - \left(\frac{Q+R}{H}\right)\bar{w}_i^0 \tag{5.100}$$

$$\bar{U}_i^0 = \bar{v}_i^0 + \left(1 - \frac{Q+R}{H}\right)\bar{w}_i^0 \tag{5.101}$$

From (5.36) we note that

$$\bar{w}_i^0 = \left(\frac{\bar{\sigma}^0 + \chi_{,i}}{-i\omega fk}\right)_{,i}$$

which implies that

$$\nabla^2 \bar{w}_i^0 = \bar{w}_{j,ji}^0 \tag{5.102}$$

Using (5.100), (5.101) and (5.102) we express (5.95) and (5.96) in terms of $\bar{v}_i^0, \bar{w}_i^0$:

$$\mu \nabla^2 \bar{v}_i^0 + (H - \mu)\bar{v}_{j,ji}^0 = 0 \tag{5.103}$$

$$(Q+R)\bar{v}_{j,ji}^0 + \frac{R(\lambda+2\mu)}{H}\nabla^2 \bar{w}_i^0 + i\omega fk\bar{w}_i^0 - \frac{fkr_{,i}}{r} = 0 \tag{5.104}$$

We note that $\bar{v}_i^0 = 0$ is a solution of (5.103), and (5.104) then becomes

$$\nabla^2 \bar{w}_i^0 - a^2 \bar{w}_i^0 + \frac{a^2}{i\omega}\frac{r_{,i}}{r} = 0 \tag{5.105}$$

where we have used (5.81). We let

$$\bar{w}_i^0 = \frac{r_{,i}}{i\omega r} + \eta_i \tag{5.106}$$

By using the results

$$r_{,ij} = \frac{\delta_{ij}}{r} - \frac{r_{,i}r_{,j}}{r} \; ; \; r_{,jj} = \frac{1}{r} \; ; \; r_{,j}r_{,j} = 1$$

$$(r_{,i}r_{,j})_{,j} = \frac{r_{,i}}{r} \; ; \; r_{,ijj} = -\frac{r_{,i}}{r^2}$$

it is easily shown that

$$\nabla^2 \left(\frac{r_{,i}}{r}\right) = 0$$

Hence from (5.106) we have

$$\nabla^2 \bar{w}_i^c = \nabla^2 \eta_i \tag{5.107}$$

We substitute (5.106) and (5.107) into (5.105) to find

$$\nabla^2 \eta_i - a^2 \eta_i = 0 \tag{5.108}$$

From (5.106) we see that it would be convenient to seek a solution of (5.108) of the form

$$\eta_i = r_{,i} f(r)$$

Substituting this into (5.108) gives

$$r^2 \frac{\mathrm{d}^2 f}{\mathrm{d}r^2} + r \frac{\mathrm{d}f}{\mathrm{d}r} - (a^2 r^2 + 1) f = 0$$

Putting $x = ar$ and $g(x) = f(\frac{x}{a})$ this equation becomes

$$x^2 \frac{\mathrm{d}^2 g}{\mathrm{d}x^2} + x \frac{\mathrm{d}g}{\mathrm{d}x} - (x^2 + 1) g = 0 \tag{5.109}$$

We recognise (5.109) as the modified Bessel equation of order 1 and hence we can write a solution as

$$g(x) = K_1(x)$$

Thus $f(r) = K_1(ar)$ and we write a solution of (5.108) as

$$\eta_i = r_{,i} K_1(ar)$$

In Appendix E we verify by direct substitution that this is a solution of (5.108). It is clear that

$$\eta_i = \frac{-ar_{,i}}{i\omega} K_1(ar) \tag{5.110}$$

also satisfies (5.108) so that from (5.106) we have

$$\bar{w}_i^0 = \frac{-ar_{,i}}{i\omega}[K_1(ar) - \frac{1}{ar}] \tag{5.111}$$

The fundamental solutions $\bar{u}_i^0$ and $\bar{U}_i^0$ can now be written from (5.100) and (5.101):

$$\bar{u}_i^0 = \left(\frac{Q+R}{i\omega H}\right) ar_{,i}[K_1(ar) - \frac{1}{ar}] \tag{5.112}$$

$$\bar{U}_i^0 = \left(\frac{Q+R}{H} - 1\right) \frac{ar_{,i}}{i\omega}[K_1(ar) - \frac{1}{ar}] \tag{5.113}$$

since $\bar{v}_i^0 = 0$.

Equation (5.8) and the constitutive laws (3.22), (3.23) imply

$$\bar{T}_i^0 = 2\mu \bar{e}_{ij}^0 n_j + (\lambda + \frac{Q^2}{R} + Q)\bar{e}^0 n_i + (Q+R)\bar{\varepsilon}^0 n_i \tag{5.114}$$

$$\bar{\sigma}^0 = Q\bar{e}^0 + R\bar{\varepsilon}^0 \tag{5.115}$$

where

$$\bar{e}_{ij}^0 = \frac{1}{2}(\bar{u}_{i,j}^0 + \bar{u}_{j,i}^0)$$

$$\bar{e}^0 = \bar{u}_{i,i}^0$$

$$\bar{\varepsilon}^0 = \bar{U}_{i,i}^0$$

Using (5.112) and (5.113) in (5.114) and (5.115) gives, after the necessary algebra,

$$\begin{aligned}\bar{T}_i^0 &= -i\frac{2\mu a^2}{\omega}\left(\frac{Q+R}{H}\right)\{r_{,i}\frac{\partial r}{\partial n}[\frac{2}{a^2r^2}-K_2(ar)] \\ &\quad +n_i[\frac{1}{2}K_2(ar)+\frac{1}{2}K_0(ar)-\frac{1}{a^2r^2}]\} \qquad (5.116)\\ \bar{\sigma}^0 &= -fkK_0(ar) \qquad (5.117)\end{aligned}$$

It is desirable to express the fundamental solutions in terms of familiar material constants. We first recall that

$$k=\frac{\rho_f g f}{k_0} \qquad (5.118)$$

where k_0 is the soil permeability is ms^{-1}, f is the soil porosity, ρ_f is the density of the pore water and g is the gravitational acceleration. Also, from (3.24) we write the constant H, defined in (5.52), as

$$H=\lambda+2\mu+\frac{K_f}{f} \qquad (5.119)$$

where λ and μ are the Lamé constant and shear modulus respectively of the soil skeleton, and K_f is the bulk modulus of the pore water. The parameter λ may be written in terms of the more familiar Poisson's ratio ν:

$$\lambda=\frac{2\mu\nu}{1-2\nu} \qquad (5.120)$$

and equation (5.119) may be re-written:

$$H=\frac{2\mu(1-\nu)}{1-2\nu}+\frac{K_f}{f} \qquad (5.121)$$

Using (3.24), (5.118), (5.120) and (5.121) we express the parameter a^2, defined in (5.81), as

$$a^2=\frac{-i\omega\rho_f g}{k_0}[\frac{1-2\nu}{2\mu(1-\nu)}+\frac{f}{K_f}] \qquad (5.122)$$

We can now summarize all the fundamental solutions as follows :

$$\begin{aligned}
\bar{u}_i^{*k} &= \left(\frac{H-\mu}{2\mu H}\right) r_{,i}r_{,k} - \left(\frac{H+\mu}{2\mu H}\right) \ln r\delta_{ik} \\
&\quad -\frac{ik_0K_f^2a^2}{\omega f^2\rho_f g H^2}\{[\frac{2}{a^2r^2} - K_2(ar)]r_{,i}r_{,k} \\
&\quad +\delta_{ik}[\frac{K_1(ar)}{ar} - \frac{1}{a^2r^2}]\} \qquad (5.123) \\
\bar{U}_i^{*k} &= \left(\frac{H-\mu}{2\mu H}\right) r_{,i}r_{,k} - \left(\frac{H+\mu}{2\mu H}\right) \ln r\delta_{ik} \\
&\quad +\frac{i(H-K_f)K_f k_0a^2}{\omega f^2\rho_f g H^2}\{[\frac{2}{a^2r^2} - K_2(ar)]r_{,i}r_{,k} \\
&\quad +\delta_{ik}[\frac{K_1(ar)}{ar} - \frac{1}{a^2r^2}]\} \qquad (5.124) \\
\bar{T}_i^{*k} &= -2\left(\frac{H-\mu}{H}\right)\frac{r_{,i}r_{,k}}{r}\frac{\partial r}{\partial n} + \frac{\mu}{H}\frac{1}{r}(r_{,k}n_i - r_{,i}n_k - \frac{\partial r}{\partial n}\delta_{ik}) \\
&\quad -\frac{i2\mu K_f^2k_0a^3}{\omega f^2\rho_f g H^2}\{\frac{\partial r}{\partial n}\delta_{ik}[\frac{2}{a^3r^3} - \frac{K_2(ar)}{ar}] \\
&\quad +\frac{\partial r}{\partial n}r_{,i}r_{,k}[K_3(ar) - \frac{8}{a^3r^3}] \\
&\quad +r_{,k}n_i[\frac{2}{a^3r^3} + \frac{3K_2(ar)}{ar} - K_3(ar)] \\
&\quad +r_{,i}n_k[\frac{2}{a^3r^3} - \frac{K_2(ar)}{ar}]\} \qquad (5.125) \\
\bar{\sigma}^{*k} &= \left(\frac{aK_f}{H}\right) r_{,k}[K_1(ar) - \frac{1}{ar}] \qquad (5.126) \\
\bar{u}_i^0 &= -\left(\frac{iK_f a}{\omega H}\right) r_{,i}[K_1(ar) - \frac{1}{ar}] \qquad (5.127) \\
\bar{U}_i^0 &= \frac{i}{\omega}(1 - \frac{K_f}{H})ar_{,i}[K_1(ar) - \frac{1}{ar}] \qquad (5.128) \\
\bar{T}_i^0 &= -i\frac{2\mu K_f a^2}{\omega H}\{r_{,i}\frac{\partial r}{\partial n}[\frac{2}{a^2r^2} - K_2(ar)] \\
&\quad +n_i[\frac{1}{2}K_2(ar) + \frac{1}{2}K_0(ar) - \frac{1}{a^2r^2}]\} \qquad (5.129) \\
\bar{\sigma}^0 &= \frac{-\rho_f g f^2}{k_0}K_0(ar) \qquad (5.130)
\end{aligned}$$

where the constants H and a are given by (5.121) and (5.122) respectively, and

suffixes i and k take the values 1 and 2.

5.3 Evaluation of α_{ik} and θ

As previously mentioned,the coefficients α_{ik} and θ appearing in the boundary integral equations (5.45) and (5.46) may be determined from the evaluation of the Cauchy principal values of the integrals. However,as will be seen below, it is not necessary to know these quantities explicitly. They will be determined by a method known as the " rigid body motion" analogy,which is frequently used in the boundary element literature. First we rewrite the boundary integral equations (5.45) and (5.46) so that pore pressure p appears explicitly. To do this we substitute $\bar{\sigma} = -f\bar{p}$ and define the fundamental solutions $\bar{p}^{*k}$ and $\bar{p}^{o}$ by

$$\bar{\sigma}^{*k} = -f\bar{p}^{*k}$$

$$\bar{\sigma}^{o} = -f\bar{p}^{o}$$

Substituting these in (5.45) and (5.46), multiplying (5.46) by $\frac{-\omega}{if}$ and using (5.97) gives the boundary integral equations in the form

$$2\pi\alpha_{ik}\bar{u}_i(\underline{P}) = PV\int_{\Gamma}(\bar{T}_i\bar{u}_i^{*k} - \bar{T}_i^{*k}\bar{u}_i) - (\bar{p}\bar{v}_n^{*k} - \bar{p}^{*k}\bar{v}_n)\,d\Gamma \qquad (5.131)$$

$$i,k = 1,2$$

$$2\pi\theta\bar{p}(\underline{P}) = PV\int_{\Gamma}(\bar{T}_i\bar{u}_i^{01} - \bar{T}_i^{01}\bar{u}_i) - (\bar{p}\bar{v}_n^{01} - \bar{p}^{01}\bar{v}_n)d\Gamma \qquad (5.132)$$

$$i = 1,2$$

where we have written

$$\begin{aligned}
\bar{v}_n &= f(\bar{U}_j - \bar{u}_j)n_j \\
\bar{v}_n^{*k} &= f(\bar{U}_j^{*k} - \bar{u}_j^{*k})n_j \\
\bar{u}_i^{01} &= \frac{-\omega}{if}\bar{u}_i^0 \\
\bar{U}_i^{01} &= \frac{-\omega}{if}\bar{U}_i^0 \\
\bar{T}_i^{01} &= \frac{-\omega}{if}\bar{T}_i^0 \\
\bar{p}^{01} &= \frac{-\omega}{if}\bar{p}^0 = \frac{\omega\bar{\sigma}^0}{if^2} \\
\bar{v}_n^{01} &= f(\bar{U}_i^{01} - \bar{u}_i^{01})n_i - \frac{1}{r}\frac{\partial r}{\partial n}
\end{aligned} \tag{5.133}$$

The position vector of the point P on the boundary (at which r is zero) is denoted by $\underline{P}$. To determine the coefficient α_{ik} we notice that the governing equations (5.47) and (5.48) admit the following trivial constant solutions for the case of zero body forces:

$$\text{(a) } \bar{u}_1 = \bar{U}_1 = 1 \text{ and } \bar{u}_2 = \bar{U}_2 = 0 \Rightarrow \bar{v}_n = 0$$

$$\text{(b) } \bar{u}_1 = \bar{U}_1 = 0 \text{ and } \bar{u}_2 = \bar{U}_2 = 1 \Rightarrow \bar{v}_n = 0$$

where it is implicit that $\omega = 0$. No stresses or pore pressures are induced by these cases, as is easily verified from the constitutive relations, i.e. $\bar{T}_i = 0$ and $\bar{p} = 0$. Substituting the first case (a) into (5.131) gives :

$$2\pi\alpha_{1k} = -\int_\Gamma \bar{T}_1^{*k} d\Gamma$$

Similarly, the second case (b) produces from (5.131)

$$2\pi\alpha_{2k} = -\int_\Gamma \bar{T}_2^{*k} d\Gamma$$

Thus we have

$$2\pi c_{ik} = -\int_\Gamma \bar{T}_i^{*k} d\Gamma \quad i,k = 1,2 \tag{5.134}$$

To determine the parameter θ we consider (again for no body forces) the case of unit pore pressure and zero displacement of the soil skeleton, i.e.,$\bar{p} = 1$, $\bar{u}_i = 0$ and $\omega = 0$. From the constitutive laws (3.22) and (3.23) we have (using $\bar{\sigma} = -f\bar{p}$)

$$\bar{\epsilon} = -\frac{1}{K_f} \text{ and } \bar{\sigma}_{ij} = -(1-f)\delta_{ij}$$

Thus for a compressible fluid ($K_f \neq \infty$),the fluid displacement $\bar{U}_i$ is non-zero. We note also ,from (5.8),that the tractions $\bar{T}_i$ are non-zero. Since $\omega = 0$,the parameter a defined in (5.122) is zero. Hence,in the boundary integral equations we must use the limit of the fundamental solutions as $a \to 0$. We now examine the fundamental solutions appearing in (5.132). It will be shown in section (6.2) that the functions $\bar{u}_i^{01}$, $\bar{T}_i^{01}$, $\bar{p}^{01}$ possess logarithmic singularity at $ar = 0$,(See 6.29). From the definitions (5.133) and (5.127),(5.128), (5.130),it is clear that $\bar{u}_i^{01}$, $\bar{T}_i^{01}$, $\bar{p}^{01}$ all approach zero as $a \to 0$. The function $\bar{v}_n^{01}$,on the other hand, behaves differently. From (5.133), (5.127) and (5.128) we have

$$\bar{v}_n^{01} = -ar_{,i}[K_1(ar) - 1/ar]n_i - \frac{1}{r}\frac{\partial r}{\partial n}$$

The first term tends to zero as $a \to 0$, as can be seen from (6.22). Thus putting $\bar{p} = 1$, $\bar{u}_i = 0$ in (5.132) and taking limits of the fundamental solutions as $a \to 0$ we have

$$2\pi\theta = \int_\Gamma \frac{1}{r}\frac{\partial r}{\partial n} d\Gamma \tag{5.135}$$

Chapter 6

Boundary Element Procedure

In this chapter we outline the numerical details of the boundary element method used for solving a boundary value problem. The accuracy of the method is illustrated by comparison with the analytic solution for the wave loading of a horizontal isotropic poroelastic seabed which is briefly described in **Appendix I**

6.1 Discretisation of Boundary Integral Equations

Using (5.134) and (5.135), the boundary integral equations (5.45) and (5.46) become

$$\int_{\Gamma} \left\{ \tilde{\overline{T}}_i \tilde{\overline{u}}_i^{*k} + \tilde{\overline{T}}_i^{*k} \left[\tilde{\overline{u}}_i (\underline{P}) - \tilde{\overline{u}}_i \right] - \tilde{\overline{p}} \tilde{\overline{v}}_n^{*k} + \tilde{\overline{p}}^{*k} \tilde{\overline{v}}_n \right\} d\Gamma = 0 \qquad (6.1)$$

$$\int_\Gamma \left\{ \tilde{\overline{T}}_i \, \tilde{\overline{u}}_i^{01} - \tilde{\overline{T}}_i^{01} \, \tilde{\overline{u}}_i - \tilde{\overline{p}} \, f \left(\tilde{\overline{U}}_i^{01} - \tilde{\overline{u}}_i^{01} \right) n_i + \tilde{\overline{p}}^{01} \, \tilde{\overline{v}}_n + \frac{r_0}{r} \frac{\partial r}{\partial n} \left[\tilde{\overline{p}} - \tilde{\overline{p}}(\underline{P}) \right] \right\} d\Gamma = 0 \tag{6.2}$$

where (5.46) was multiplied by $\frac{r_0}{\mu}$ (r_0 is an arbitrary length) and we have defined the following dimensionless quantities :

$$\begin{aligned} \tilde{\overline{u}}_i^{*k} &= \mu \overline{u}_i^{*k} & \tilde{\overline{v}}_n^{*k} &= \mu \overline{v}_n^{*k} \\ \tilde{\overline{T}}_i^{*k} &= r_0 \overline{T}_i^{*k} & \tilde{\overline{p}}^{*k} &= r_0 \overline{p}^{*k} \end{aligned} \tag{6.3}$$

$$\begin{aligned} \tilde{\overline{u}}_i^{01} &= r_0 \overline{u}_i^{01} & \tilde{\overline{U}}_i^{01} &= r_0 \overline{u}_i^{01} \\ \tilde{\overline{T}}_i^{01} &= \frac{r_0^2}{\mu} \overline{T}_i^{01} & \tilde{\overline{p}}^{01} &= \frac{r_0^2}{\mu} \overline{p}^{01} \end{aligned}$$

It is understood that the integrals are evaluated in the Cauchy principal value sense and we recall that $\underline{P}$ denotes the position vector of the point at which $r = 0$. We now discretise the boundary Γ into M straight line segments Γ_e, $e = 1$ *to* M. Each segment is termed a "boundary element" and a node is located at its midpoint. On each element we make the assumption

$$\tilde{\overline{T}}_i = \tilde{\overline{T}}_i^e, \quad \tilde{\overline{u}}_i = \tilde{\overline{u}}_i^e$$

where $\tilde{\overline{T}}_i^e$ and $\tilde{\overline{u}}_i^e$ denote the values of $\tilde{\overline{T}}_i$ and $\tilde{\overline{u}}_i$ at node e. For this reason the elements are termed "constant" elements.

If we let point $\underline{P}$ be the jth node (i.e. $r = 0$ at node j) then equation (6.1) becomes

$$\begin{aligned} &\sum_{e=1}^{M} \tilde{\overline{T}}_i^e \int_{\Gamma_e} \tilde{\overline{u}}_i^{*k} \, d\Gamma_e + \sum_{e=1}^{M} \left(\tilde{\overline{u}}_i^j - \tilde{\overline{u}}_i^e \right) \int_{\Gamma_e} \tilde{\overline{T}}_i^{*k} \, d\Gamma_e \\ &+ \sum_{e=1}^{M} -\tilde{\overline{p}}^e \int_{\Gamma_e} \tilde{\overline{v}}_n^{*k} \, d\Gamma_e + \sum_{e=1}^{M} \tilde{\overline{v}}_n^e \int_{\Gamma_e} \tilde{\overline{p}}^{*k} \, d\Gamma_e \quad = 0 \end{aligned} \tag{6.4}$$

The second term on the left hand side is

$$\begin{aligned}\sum_{e=1}^{M}\left(\tilde{\tilde{u}}_i^j-\tilde{\tilde{u}}_i^e\right)\int_{\Gamma_e}\tilde{\tilde{T}}_i^{*k}\,d\Gamma_e &= \sum_{\substack{e=1\\e\neq j}}^{M}\left(\tilde{\tilde{u}}_i^j-\tilde{\tilde{u}}_i^e\right)\int_{\Gamma_e}\tilde{\tilde{T}}_i^{*k}\,d\Gamma_e\\ &= \tilde{\tilde{u}}_i^j\sum_{\substack{e=1\\e\neq j}}^{M}\int_{\Gamma_e}\tilde{\tilde{T}}_i^{*k}\,d\Gamma_e-\sum_{\substack{e=1\\e\neq j}}^{M}\tilde{\tilde{u}}_i^e\int_{\Gamma_e}\tilde{\tilde{T}}_i^{*k}\,d\Gamma_e\\ &= \sum_{e=1}^{M}S_{ki}^e\tilde{\tilde{u}}_i^e\end{aligned}$$

where we have defined S_{ki}^e as

$$S_{ki}^e = \begin{cases} -\int_{\Gamma_e}\tilde{\tilde{T}}_i^{*k}\,d\Gamma_e & e\neq j\\ \sum_{\substack{r=1\\r\neq j}}^{M}\int_{\Gamma_r}\tilde{\tilde{T}}_i^{*k}\,d\Gamma_r & e=j\end{cases}$$

$$i,k=1,2$$

We now note that (6.1) may be written in the form

$$\sum_{e=1}^{M}\left(R_{ki}^e\tilde{\tilde{T}}_i^e+S_{ki}^e\tilde{\tilde{u}}_i^e\right)=0 \qquad (6.5)$$

$$i=1\ to\ 3,\qquad k=1,2$$

where we have defined $\tilde{\tilde{u}}_3=\tilde{\tilde{v}}_n$ and

$$S_{k3}^e=\int_{\Gamma_e}\tilde{\tilde{p}}^{*k}\,d\Gamma_e \qquad k=1,2$$

$$R_{ki}^e = \begin{cases}\int_{\Gamma_e}\tilde{\tilde{u}}_i^{*k}\,d\Gamma_e & i=1,2\\ \int_{\Gamma_e}\tilde{\tilde{v}}_n^{*k}\,d\Gamma_e & i=3\end{cases}$$

$$k=1,2$$

Writing $\tilde{\bar{T}}_3 = -\tilde{\bar{p}}$ and discretising (6.2), we obtain

$$\begin{aligned}
&\sum_{e=1}^{M} \tilde{\bar{T}}_i^e \int_{\Gamma_e} \tilde{\bar{u}}_i^{01}\, d\Gamma_e + \sum_{e=1}^{M} \tilde{\bar{u}}_i^e \int_{\Gamma_e} -\tilde{\bar{T}}_i^{01}\, d\Gamma_e \\
&\mp \sum_{e=1}^{M} \tilde{\bar{T}}_3^e \int_{\Gamma_e} f\left(\tilde{\bar{U}}_i^{01} - \tilde{\bar{u}}_i^{01}\right) n_i\, d\Gamma_e \\
&+ \sum_{e=1}^{M} \tilde{\bar{u}}_3^e \int_{\Gamma_e} \tilde{\bar{p}}^{01}\, d\Gamma_e + \sum_{e=1}^{M} \left(\tilde{\bar{T}}_3^e - \tilde{\bar{T}}_3^j\right) \int_{\Gamma_e} -\frac{r_0}{r}\frac{\partial r}{\partial n}\, d\Gamma_e \;=\; 0
\end{aligned} \tag{6.6}$$

Proceeding as done earlier we write the last term on the left hand side as

$$\begin{aligned}
\sum_{e=1}^{M} \left(\tilde{\bar{T}}_3^e - \tilde{\bar{T}}_3^j\right) \int_{\Gamma_e} -\frac{r_0}{r}\frac{\partial r}{\partial n}\, d\Gamma_e &= \sum_{\substack{e=1 \\ e\neq j}}^{M} \left(\tilde{\bar{T}}_3^e - \tilde{\bar{T}}_3^j\right) \int_{\Gamma_e} -\frac{r_0}{r}\frac{\partial r}{\partial n}\, d\Gamma_e \\
&= \sum_{\substack{e=1 \\ e\neq j}}^{M} \tilde{\bar{T}}_3^e \int_{\Gamma_e} -\frac{r_0}{r}\frac{\partial r}{\partial n} d\Gamma_e + \tilde{\bar{T}}_3^j \sum_{\substack{e=1 \\ e\neq j}}^{M} \int_{\Gamma_e} \frac{r_0}{r}\frac{\partial r}{\partial n}\, d\Gamma_e \\
&= \sum_{e=1}^{M} \tilde{\bar{T}}_3^e V^e
\end{aligned}$$

where V^e is defined as

$$V^e = \begin{cases} \displaystyle\int_{\Gamma_e} -\frac{r_0}{r}\frac{\partial r}{\partial n}\, d\Gamma_e & e \neq j \\[2ex] \displaystyle\sum_{\substack{e=1 \\ e\neq j}}^{M} \int_{\Gamma_e} \frac{r_0}{r}\frac{\partial r}{\partial n}\, d\Gamma_e & e = j \end{cases} \tag{6.7}$$

Equation (6.6) may thus be written in the form

$$\sum_{e=1}^{M} R_{3i}^e \tilde{\bar{T}}_i^e \;+\; \sum_{e=1}^{M} S_{3i}^e \tilde{\bar{u}}_i^e = 0 \tag{6.8}$$

$$i = 1 \text{ to } 3$$

where

$$R^e_{3i} = \begin{cases} \int_{\Gamma_e} \tilde{\bar{u}}_i^{01}\, d\Gamma_e & i = 1,2 \\ \\ \int_{\Gamma_e} f\left(\tilde{\bar{U}}_i^{01} - \tilde{\bar{u}}_i^{01}\right) n_i\, d\Gamma_e + V^e & i = 3 \end{cases}$$

$$S^e_{3i} = \begin{cases} \int_{\Gamma_e} -\tilde{\bar{T}}_i^{01}\, d\Gamma_e & i = 1,2 \\ \\ \int_{\Gamma_e} \tilde{\bar{p}}^{01}\, d\Gamma_e & i = 3 \end{cases}$$

Combining (6.5) and (6.8) we have

$$\sum_{e=1}^{M} \left(R^e_{ki}\, \tilde{\bar{T}}_i^e + S^e_{ki} \tilde{\bar{u}}_i^e \right) = 0 \qquad (6.9)$$

$$i,k = 1 \text{ to } 3$$

where we recall that $\tilde{\bar{u}}_3 = \tilde{\bar{v}}_n$ and $\tilde{\bar{T}}_3 = -\tilde{\bar{p}}$. Equation (6.9) is in fact the discretised boundary integral equation. The formulae for R^e_{ki} and S^e_{ki} may be written more compactly if we make the following definitions:

$$\tilde{\bar{u}}_i^{*3} = \tilde{\bar{u}}_i^{01}, \qquad \tilde{\bar{T}}_i^{*3} = \tilde{\bar{T}}_i^{01}, \qquad for\ i = 1,2 \qquad (6.10)$$

$$\tilde{\bar{u}}_3^{*k} = \begin{cases} \tilde{\bar{v}}_n^{*k} & k = 1,2 \\ \\ f\left(\tilde{\bar{U}}_i^{01} - \tilde{\bar{u}}_i^{01}\right) n_i & k = 3 \end{cases} \qquad (6.11)$$

$$\tilde{\bar{T}}_3^{*k} = \begin{cases} -\tilde{\bar{p}}^{*k} & k = 1,2 \\ \\ -\tilde{\bar{p}}^{01} & k = 3 \end{cases} \qquad (6.12)$$

Then

$$R^e_{ki} = \begin{cases} \int_{\Gamma_e} \tilde{\bar{u}}^{*3}_3 \, d\Gamma_e + V^e & i = k = 3 \\ \\ \int_{\Gamma_e} \tilde{\bar{u}}^{*k}_i \, d\Gamma_e & otherwise \end{cases} \tag{6.13}$$

$$S^e_{ki} = \begin{cases} \sum_{\substack{s=1 \\ s \neq j}}^{M} \int_{Gamma_s} \tilde{\bar{T}}^{*k}_i \, d\Gamma_s & i,k = 1,2 \\ & e = j \\ \\ -\int_{\Gamma_e} \tilde{\bar{T}}^{*k}_i \, d\Gamma_e & otherwise \end{cases} \tag{6.14}$$

6.2 Function Approximations

To evaluate integrals R^e_{ki}, S^e_{ki} we need to take a closer look at the integrands. It will be noted that the fundamental solutions are functions of $ar, r_{,i}$ and n_i, these quantities being defined in Chapter 5. From (5.81) we note that a^2 may be written in the form

$$a^2 = -ic^2 \tag{6.15}$$

where

$$c = \frac{\omega f k H}{R(\lambda + 2\mu)} \tag{6.16}$$

The constant c is real and positive and has dimensions of (length)$^{-1}$. From (6.15) we have

$$ar = cre^{-i\frac{\pi}{4}} \tag{6.17}$$

The Bessel functions of argument ar may now be separated into real and imaginary parts via the relations (Abramowitz and Stegun, 1970).

$$K_0(xe^{-i\frac{\pi}{4}}) \;=\; ker\, x - i\, kei\, x \tag{6.18}$$

$$\begin{aligned} K_1(xe^{-i\frac{\pi}{4}}) &= -(kei_1\, x + i\, ker_1\, x) \\ &= -\frac{1}{\sqrt{2}}(ker'\, x + kei'\, x) - \frac{i}{\sqrt{2}}(ker'\, x - kei'\, x) \end{aligned} \tag{6.19}$$

and

$$K_{n+1}(z) = K_{n-1}(z) + \frac{2n}{z}K_n(z) \tag{6.20}$$

n integer, z real or complex

To evaluate the Kelvin functions ker, kei, ker', kei' we use the polynomial approximations given by Abramowitz and Stegun, Sec. 9.11. These have been tested against IMSL routines for the Kelvin functions and have been found to be extremely accurate. The use of the IMSL routines directly in the BEM program is not computationally efficient owing to the large number of function evaluations required. Using the polynomial representations,therefore, we write expressions for the following functional groups involving the Bessel functions, which appear in the fundamental solutions. The algebra involved is quite extensive and is not recorded. The final results are

$$K_0(ar) = \ln(\frac{cr}{2})\tilde{u}_0(cr) + \tilde{v}_0(cr) \tag{6.21}$$

$$\frac{K_1(ar)}{ar} - \frac{1}{a^2r^2} = \ln(\frac{cr}{2})\tilde{u}_1(cr) + \tilde{v}_1(cr) \tag{6.22}$$

$$K_2(ar) - \frac{2}{a^2r^2} = \ln(\frac{cr}{2})\tilde{u}_2(cr) + \tilde{v}_2(cr) \tag{6.23}$$

$$\frac{K_2(ar)}{ar} - \frac{2}{a^3r^3} = \ln(\frac{cr}{2})\tilde{u}_3(cr) + \tilde{w}_3(cr) + \frac{1}{cr}\tilde{z}_3(cr) \tag{6.24}$$

$$K_3(ar) - \frac{3K_2(ar)}{ar} - \frac{2}{a^3r^3} = \ln(\frac{cr}{2})\tilde{u}_4(cr) + \tilde{w}_4(cr) + \frac{1}{cr}\tilde{z}_4(cr) \tag{6.25}$$

$$\frac{1}{2}K_2(ar) + \frac{1}{2}K_0(ar) - \frac{1}{a^2r^2} = \ln(\frac{cr}{2})\tilde{u}_5(cr) + \tilde{v}_5(cr) \tag{6.26}$$

$$K_3(ar) - \frac{8}{a^3r^3} = \ln(\frac{cr}{2})\tilde{u}_6(cr) + \tilde{w}_6(cr) + \frac{1}{cr}\tilde{z}_6(cr) \tag{6.27}$$

where for any n

$$\begin{aligned}
\tilde{u}_n(x) &= u_n(x) + iu_n'(x) \\
\tilde{v}_n(x) &= v_n(x) + iv_n'(x) \\
\tilde{w}_n(x) &= w_n(x) + iw_n'(x) \\
\tilde{z}_n(x) &= z_n(x) + iz_n'(x)
\end{aligned} \tag{6.28}$$

The functions $u_n, u_n', v_n, v_n', w_n, w_n', z_n, z_n'$ are recorded in **Appendix F**. These expressions enable us to express the fundamental solutions $\tilde{\tilde{u}}_i^{*k}$ and $\tilde{\tilde{T}}_i^{*k}$ as

$$\begin{aligned}
\tilde{\tilde{u}}_i^{*k} &= \ln(\frac{cr}{2})\tilde{H}_{ik} + \tilde{G}_{ik} \\
\tilde{\tilde{T}}_i^{*k} &= \ln(\frac{cr}{2})\tilde{P}_{ik} + \tilde{Q}_{ik} + \frac{1}{cr}\tilde{Z}_{ik}(cr)
\end{aligned} \tag{6.29}$$

where

$$\begin{aligned}
\tilde{H}_{ik} &= H_{ik} + iH_{ik}' \quad \tilde{G}_{ik} = G_{ik} + iG_{ik}' \\
\tilde{P}_{ik} &= P_{ik} + iP_{ik}' \quad \tilde{Q}_{ik} = Q_{ik} + iQ_{ik}' \\
\tilde{Z}_{ik} &= Z_{ik} + iZ_{ik}'
\end{aligned} \tag{6.30}$$

These functions (6.30) are defined in **Appendix G.**

6.3 Evaluation of Integrals

As can be seen from **Appendix F** and **Appendix G** the functions $\tilde{H}_i^{*k}$,$\tilde{G}_i^{*k}$,$\tilde{P}_i^{*k}$, $\tilde{Q}_i^{*k}$, $\tilde{Z}_i^{*k}$, defined in (6.30), possess no singularities. We see from (6.7) and (6.29)

that the integrands of R^e_{ki} and S^e_{ki} (equations 6.13 and 6.14) possess terms of order $\frac{1}{r}$ for certain values of i and k. It will be noted,however, that it is not neccessary to integrate these expressions over the element on which $r = 0$ (element j). Hence all integrals may be considered of the form

$$I = \int_{\Gamma_e} [\ln(\frac{cr}{2}) f(\frac{r}{r_0}; r_{,i}; n_i) + g(\frac{r}{r_0}; r_{,i}; n_i)] \, d\Gamma_e \qquad (6.31)$$

where the functions f and g are non-singular at $r = 0$ and Γ_e is an arbitrary element e. Special procedures are required for the case $e = j$, owing to the presence of the logarithmic singularity on this element. In addition, we make note of the following facts concerning the nature of functions f and g in (6.31). The functional approximations used (**Appendix F**) change form at the value $cr = 8$. When writing an integral in the form (6.31) we have employed the following programming device. For the range $cr > 8$ the function f has been set to zero and the entire functional form of the integrand has been assigned to the function g. The result is that both f and g are discontinuous at $cr = 8$, while the entire form of the integrand in (6.31) is not. This must be taken into consideration only on element j, since it is only on this element that it is necessary to separate the integrands into logarithmic and non-logarithmic parts.

We now describe the details of the integration procedure. We consider that the boundary Γ lies in the $x - z$ plane with the x and z coordinate axes directed to the right and vertically downward respectively. We recall that the problem is two dimensional, i.e. conditions are uniform in the y direction. We denote the coordinates of the end points of an arbitrary element Γ_e by (x_e, z_e) and (x_{e+1}, z_{e+1}) and define the integration direction from the former point to the latter. Since there are M elements, $(x_{M+1}, z_{M+1}) \equiv (x_1, z_1)$. The x and z coordinates of a point on Γ_e

are represented parametrically as

$$x = \frac{1}{2}(1-\xi)x_e + \frac{1}{2}(1+\xi)x_{e+1}$$
$$z = \frac{1}{2}(1-\xi)z_e + \frac{1}{2}(1+\xi)z_{e+1}$$
$$\text{where } -1 \leq \xi \leq 1$$

The point $\underline{p}$ from which r is measured is located at node j (mid-point of element Γ_j). Denoting the coordinates of $\underline{p}$ by (x_0, z_0) we have

$$x_0 = \frac{1}{2}(x_j + x_{j+1}) \qquad z_0 = \frac{1}{2}(z_j + z_{j+1}) \tag{6.32}$$

Since $r = |\underline{x} - \underline{p}|$ we have

$$r = [(x-x_0)^2 + (z-z_0)^2]^{\frac{1}{2}}$$
$$r_{,1} \equiv \frac{\partial r}{\partial x} = \frac{x-x_0}{r} \tag{6.33}$$
$$r_{,2} \equiv \frac{\partial r}{\partial z} = \frac{z-z_0}{r}$$

It is easily verified that the unit outward normal n_i for anticlockwise integration around Γ is given by

$$n_1 = \frac{1}{2J_e}(z_e - z_{e+1}) \quad ; \quad n_2 = \frac{1}{2J_e}(x_{e+1} - x_e) \tag{6.34}$$

where

$$J_e = \frac{1}{2}[(x_{e+1}-x_e)^2 + (z_{e+1}-z_e)^2]^{\frac{1}{2}} \tag{6.35}$$

The line element $d\Gamma_e$ is given by

$$d\Gamma_e = J_e d\xi \tag{6.36}$$

For the case $e \neq j$ it is thus quite easy to express (6.31) in the form

$$I = \int_{-1}^{1} F(\xi)d\xi \tag{6.37}$$

by using (6.32) through (6.36). Standard Gaussian quadrature can now be applied to (6.37). Integration along element Γ_j must be considered in two cases, viz. integration before and after the mid-point (x_0, z_0), at which the logarithmic singularity occurs. We shall denote these two integrals by I_a and I_b respectively.

Case(a): Integration from (x_j, z_j) to (x_0, z_0)

We define r_{max} to be the distance from (x_j, z_j) to (x_0, z_0), i.e.

$$r_{max} = \frac{1}{2}[(x_j - x_0)^2 + (z_j - z_0)^2]^{\frac{1}{2}} \tag{6.38}$$

We find by putting $(x_e, z_e) \equiv (x_j, z_j)$ and $(x_{e+1}, z_{e+1}) \equiv (x_0, z_0)$ in (6.32) to (6.36) that

$$\begin{aligned} r &= \frac{1}{2}(1-\xi)r_{max} \\ r_{,1} &= \frac{x_j - x_0}{r_{max}} \qquad r_{,2} = \frac{z_j - z_0}{r_{max}} \\ n_1 &= r_{,2} \qquad\qquad n_2 = -r_{,1} \\ \frac{\partial r}{\partial n} &\equiv r_{,i}n_i = 0 \end{aligned} \tag{6.39}$$

Hence we have

$$\begin{aligned} I_a \;=\; & \frac{1}{2}r_{max}\int_{-1}^{1}\{\ln[\frac{c(1-\xi)r_{max}}{\pm}]f[\frac{(1-\xi)r_{max}}{2r_0}; r_{,i}; n_i] \\ & + g[\frac{(1-\xi)r_{max}}{2r_0}; r_{,i}; n_i]\}d\xi \end{aligned} \tag{6.40}$$

We note that $r_{,i}$ and n_i are constant on Γ_j. Because of the discontinuities in the functions f and g at $cr = 8$, the integral I_a must be evaluated in two cases also :

(1) $cr_{max} < 8$

In this case the discontinuity does not lie in the range of the integration. By isolating the logarithmic singularity (at $\xi = 1$) and making appropriate changes of

variable we can express (6.40) as

$$\begin{aligned} I_a &= \frac{1}{2}r_{max}\int_{-1}^{1}\ln[\frac{cr_{max}}{4}]f[\frac{(1-\xi)r_{max}}{2r_0};r_{,i};n_i]+g[\frac{(1-\xi)r_{max}}{2r_0};r_{,i};n_i]d\xi \\ &+\frac{1}{4}r_{max}\int_{-1}^{1}\ln(\frac{3-\xi}{2})f[\frac{(3-\xi)r_{max}}{4r_0};r_{,i};n_i]d\xi \\ &-\frac{1}{2}r_{max}\int_{0}^{1}\ln(\frac{1}{\xi})f[\frac{\xi r_{max}}{2r_0};r_{,i};n_i]d\xi \end{aligned} \tag{6.41}$$

(2) $cr_{max} > 8$

The discontinuity at $cr = 8$ now lies within the range of integration. We define the value ξ_0 such that $cr = 8$ at $\xi = \xi_0$. From (6.39) we thus have

$$\xi_0 = 1 - \frac{16}{cr_{max}} \tag{6.42}$$

We express (6.40) as the sum of two integrals: one from -1 to ξ_0 and the other from ξ_0 to 1, making use of the fact that for $\xi < \xi_0$ (i.e. $cr > 8$), f is identically zero. Again by isolating the logarithmic singularity and making appropriate changes of variable we write (6.40) as

$$\begin{aligned} I_a &= \frac{1}{4}(1+\xi_0)r_{max}\int_{-1}^{1}g[\frac{(1-s)r_{max}}{2r_0};r_{,i};n_i]d\xi \\ &+\frac{1}{4}(1-\xi_0)r_{max}\int_{-1}^{1}\ln(\frac{cr_{max}}{4})f[\frac{(1-t)r_{max}}{2r_0};r_{,i};n_i]+g[\frac{(1-t)r_{max}}{2r_0};r_{,i};n_i]d\xi \\ &+\frac{1}{4}r_{max}(1-\xi_0)\ln(1-\xi_0)\int_{-1}^{1}f[\frac{(u\,r_{max}}{2r_0};r_{,i};n_i]d\xi \\ &-\frac{1}{2}r_{max}(1-\xi_0)\int_{0}^{1}\ln(\frac{1}{\xi})f[\frac{v\,r_{max}}{2r_0};r_{,i};n_i]d\xi \end{aligned} \tag{6.43}$$

where

$$s = \tfrac{1}{2}(1+\xi_0)(1+\xi) - 1$$

$$t = \tfrac{1}{2}[1+\xi_0+\xi(1-\xi_0)]$$

$$u = \tfrac{1}{2}(1-\xi_0)(1+\xi)$$

$$v = \xi(1-\xi_0)$$

Case (b): Integration from (x_0, z_0) to (x_{j+1}, z_{j+1})

Here we define r_{max} as the distance from (x_0, z_0) to (x_{j+1}, z_{j+1}) so that

$$r_{max} = [(x_{j+1} - x_0)^2 + (z_{j+1} - z_0)^2]^{\frac{1}{2}} \tag{6.44}$$

We put $(x_e, z_e) = (x_0, z_0)$ and $(x_{e+1}, z_{e+1}) = (x_{j+1}, z_{j+1})$ in (6.32) to (6.36) to find

$$\begin{aligned} r &= \frac{1}{2}(1+\xi)r_{max} \\ r_{,1} &= \frac{x_{j+1} - x_0}{r_{max}} \quad r_{,2} = \frac{z_{j+1} - z_0}{r_{max}} \\ n_1 &= -r_{,2} \qquad n_2 = r_{,1} \\ \frac{\partial r}{\partial n} &\equiv r_{,i} n_i = 0 \end{aligned} \tag{6.45}$$

As before, it is necessary to consider two sub-cases :

(1) $cr_{max} < 8$

The result is

$$\begin{aligned} I_b \;=\; & \frac{1}{2} r_{max} \int_{-1}^{1} \ln(\frac{cr_{max}}{4}) f[\frac{(1+\xi)r_{max}}{2r_0}; r_{,i}; n_i] + g[\frac{(1+\xi)r_{max}}{2r_0}; r_{,i}; n_i] d\xi \\ & + \frac{1}{4} r_{max} \int_{-1}^{1} \ln(\frac{3+\xi}{2}) f[\frac{(3+\xi)r_{max}}{4r_0}; r_{,i}; n_i] d\xi \\ & - \frac{1}{2} r_{max} \int_{0}^{1} \ln(\frac{1}{\xi}) f[\frac{(\xi r_{max}}{2r_0}; r_{,i}; n_i] d\xi \end{aligned} \tag{6.46}$$

(2) $cr_{max} > 8$

Again, we define ξ_0 by the relation $cr = 8$ at $\xi = \xi_0$. From (6.45) we find that

$$\xi_0 = \frac{16}{cr_{max}} - 1 \tag{6.47}$$

Noting again that $f \equiv 0$ when $\xi > \xi_0$ we have the final result as

$$I_b \;=\; \frac{1}{4}(1 - \zeta_0) r_{max} \int_{-1}^{1} g[\frac{(1+s)r_{max}}{2r_0}; r_{,i}; n_i] d\xi$$

$$+\frac{1}{4}(1+\xi_0)r_{max}\int_{-1}^{1}\ln(\frac{cr_{max}}{4})f[\frac{(1+t)r_{max}}{2r_0};r_{,i};n_i]+g[\frac{(1+t)r_{max}}{2r_0};r_{,i};n_i]d\xi$$
$$+\frac{1}{4}(1+\xi_0)\ln(1+\xi_0)r_{max}\int_{-1}^{1}f[\frac{(u\,r_{max}}{2r_0};r_{,i};n_i]d\xi$$
$$-\frac{1}{2}(1+\xi_0)r_{max}\int_{0}^{1}\ln(\frac{1}{\xi})f[\frac{(v\,r_{max}}{2r_0};r_{,i};n_i]d\xi \qquad (6.48)$$

where

$$s=\tfrac{1}{2}[\xi(1-\xi_0)+1+\xi_0]$$

$$t=\tfrac{1}{2}[\xi(1+\xi_0)-1+\xi_0]$$

$$u=\tfrac{1}{2}(1+\xi_0)(1+\xi)$$

$$v=\xi(1+\xi_0)$$

We now write (6.31) for the case $e=j$, i.e.

$$I \text{ on } \Gamma_j = I_a + I_b$$

where I_a is given by (6.41) or (6.43) and I_b is given by (6.46) or (6.48) depending on whether cr_{max} is less than or greater than 8. We note that in (6.41) and (6.43) the quantities r, $r_{,i}$, n_i and ξ_0 are given by (6.38), (6.39) and (6.42); whereas in (6.46) and (6.48) these quantities are given by (6.44), (6.45), and (6.47). The integrals I_a and I_b are evaluated by standard Gaussian quadrature. We draw attention to the fact that the last term in the expressions for I_a and I_b involves a logarithmic singularity. These terms are written in a form suitable for the application of the quadrature rules designed for such cases (Brebbia et al., 1984).

6.4 Determination of Unknown Boundary Data

The discretised form (6.9) of the boundary integral equation may be written

$$\sum_{e=1}^{M}(R_{ki}^{e}(j)\tilde{\tilde{T}}_{i}^{e} + S_{ki}^{e}(j)\tilde{\tilde{u}}_{i}^{e}) = 0 \qquad (6.49)$$
$$i,k = 1 \text{ to } 3;\ j = 1 \text{ to } M$$

where the argument j has been included to emphasize the fact that (6.49) must be written for each node on the boundary Γ, i.e. each node must serve in turn as node j, the node at which $r = 0$. The coefficients R_{ki}^{e} and S_{ki}^{e} are determined using the methods described in the previous section. In a well posed problem, exactly half of the boundary data is known. At each node the boundary data consists of six quantities : $\{\tilde{\tilde{T}}_{i}^{e},\ \tilde{\tilde{u}}_{i}^{e},\ i = 1 \text{ to } 3\}$.

We let $\{x_{i}^{'e},\ i = 1 \text{ to } 3\}$ denote the three known values at node e, and $\{x_{i}^{e},\ i = 1 \text{ to } 3\}$ denote the three unknown values at node e. We denote the coefficients of $x_{i}^{'e}$ and x_{i}^{e} in (6.49) by $F_{ki}^{'e}$ and F_{ki}^{e} respectively. Then equation (6.49) may be written

$$\sum_{e=1}^{M} F_{ki}^{e}(j)x_{i}^{e} = b_{k}(j) \qquad (6.50)$$
$$i,k = 1 \text{ to } 3;\ j = 1 \text{ to } M$$

where

$$b_{k}(j) = -\sum_{e=1}^{M} F_{ki}^{'e}(j)x_{i}^{'e} \qquad (6.51)$$

For a given value of j, equation (6.50) generates three rows of the final matrix equation as k takes the values 1 to 3. Specifically, (6.50) is the n th row of the matrix equation, where

$$n = 3j - (3 - k) \quad k = 1 \text{ to } 3;\ j = 1 \text{ to } M$$

The final $3M \times 3M$ matrix equation may be written in the form

$$[G]\{y\} = \{c\} \tag{6.52}$$

It can be verified that the elements of the matrix $[G]$ and vector $\{c\}$ are produced by the following algorithm :

For $j = 1$ to M

For $k = 1$ to 3

$n = 3j - (3 - k)$

$$c_n = -\sum_{e=1}^{M} F'^{e}_{ki} x'^{e}_{i}$$

For $t = 1$ to M

For $p = 3t - 2$ to $3t$

$G_{np} = F^{t}_{k,p-3(t-1)}$

A given input value x'^{e}_{i} must be identified either as $\tilde{\tilde{T}}^{e}_{i}$ or $\tilde{\tilde{u}}^{e}_{i}$ so that proper assignments can be made to the quantities F'^{e}_{ki} and F^{e}_{ki}. The solution vector $\{y\}$ consists of the $3M$ unknown nodal values $\{x^{e}_{i}, i = 1 \text{ to } 3, e = 1 \text{ to } M\}$.

6.5 Determination of Interior Stresses and Pore Pressure

We recall that for an interior point $\underline{x}$ the coefficients α_{ik} and θ in equations (5.131) and (5.132) respectively become

$$\alpha_{ik} = \delta_{ik}$$

$$\theta = 1$$

Using the definitions (6.3) and (6.10),(6.11), (6.12) we write (5.131) and (5.132) for an interior point $\underline{x}$:

$$2\pi \bar{u}_k(\underline{x}) = \int_\Gamma \tilde{\bar{T}}_\alpha(\underline{x}')\, \tilde{\bar{u}}^{*k}_\alpha(r, \frac{\partial r}{\partial \underline{x}'}, \underline{n}) - \tilde{\bar{T}}^{*k}_\alpha(r, \frac{\partial r}{\partial \underline{x}'}, \underline{n}) \tilde{\bar{u}}_\alpha(\underline{x}')\, d\Gamma \qquad (6.53)$$

$$k = 1, 2$$

$$\frac{2\pi r_0}{\mu} \bar{p}(\underline{x}) = \int_\Gamma \tilde{\bar{T}}_\alpha(\underline{x}')\, \tilde{\bar{u}}^{*3}_\alpha(r, \frac{\partial r}{\partial \underline{x}'}, \underline{n}) - \tilde{\bar{T}}^{*3}_\alpha(r, \frac{\partial r}{\partial \underline{x}'}, \underline{n}) \tilde{\bar{u}}_\alpha(\underline{x}')\, d\Gamma \qquad (6.54)$$

where $r = |\underline{x}' - \underline{x}|$. In the above equations the integration is performed with respect to $\underline{x}' \in \Gamma$, and the subscript α is summed from 1 to 3. In order to determine the effective stresses at point $\underline{x}$, we must evaluate derivatives of $\bar{u}_k$ with respect to $\underline{x}$ and then use the constitutive laws. We note that a comma followed by a subscript denotes differentiation with respect to one of the coordinates of $\underline{x}' = (x_1', x_2')$. Differentiation with respect to $\underline{x}$ will be written explicitly. For example, since $r^2 = (x_j' - x_j)(x_j' - x_j)$, we have

$$r_{,i} = \frac{x_i' - x_i}{r} \ , \ \frac{\partial r}{\partial x_i} = -r_{,i}$$

$$\text{and } \frac{\partial}{\partial x_j}(r_{,i}) = \frac{1}{r}(r_{,i} r_{,j} - \delta_{ij})$$

Again, repeated suffixes denotes summation. Using the constitutive relation (3.9) with

$$\lambda = \frac{2\mu\nu}{1-2\nu}$$

we can write from (6.53)

$$\frac{2\pi}{\mu}\bar{\tau}'_{kj} = \int_\Gamma (\tilde{\bar{T}}_\alpha D_{\alpha kj} - \tilde{\bar{u}}_\alpha S_{\alpha kj})\, d\Gamma$$
$$k,j = 1,2\ ,\ \alpha = 1,2,3 \tag{6.55}$$

where

$$D_{\alpha kj} = \frac{\partial \tilde{\bar{u}}^{*k}_\alpha}{\partial x_j} + \frac{\partial \tilde{\bar{u}}^{*j}_\alpha}{\partial x_k} + \left(\frac{2\nu}{1-2\nu}\right)\frac{\partial \tilde{\bar{u}}^{*i}_\alpha}{\partial x_i}\delta_{kj} \tag{6.56}$$

$$S_{\alpha kj} = \frac{\partial \tilde{\bar{T}}^{*k}_\alpha}{\partial x_j} + \frac{\partial \tilde{\bar{T}}^{*j}_\alpha}{\partial x_k} + \left(\frac{2\nu}{1-2\nu}\right)\frac{\partial \tilde{\bar{T}}^{*i}_\alpha}{\partial x_i}\delta_{kj} \tag{6.57}$$

Using the definitions (6.29), (6.30) and **Appendix G** we can perform the differentiations indicated in (6.56) and (6.57). The algebra involved is again quite extensive. The results are listed in **Appendix H.**

Discretisation of (6.55) leads to

$$\frac{2\pi}{\mu}\bar{\tau}'_{kj}(\underline{x}) = \sum_{e=1}^{M}(\tilde{\bar{T}}^e_\alpha P^e_{\alpha kj} - \tilde{\bar{u}}^e_\alpha Q^e_{\alpha kj}) \tag{6.58}$$

where

$$P^e_{\alpha kj} = \int_{\Gamma_e} D_{\alpha kj}\, d\Gamma_e$$
$$Q^e_{\alpha kj} = \int_{\Gamma_e} S_{\alpha kj}\, d\Gamma_e \tag{6.59}$$
$$k,j = 1,2;\ \alpha = 1,2,3;\ e = 1 \text{ to } M$$

Similarly, the pore pressure at $\underline{x}$ is found by discretising (6.54):

$$\frac{2\pi r_0}{\mu}\bar{p}(\underline{x}) = \sum_{e=1}^{M}\tilde{\bar{T}}^e_\alpha A^e_\alpha - \tilde{\bar{u}}^e_\alpha B^e_\alpha \tag{6.60}$$

where

$$A_\alpha^e = \int_{\Gamma_e} \tilde{\bar{u}}_\alpha^{*3} d\Gamma_e$$
$$B_\alpha^e = \int_{\Gamma_e} \tilde{\bar{T}}_\alpha^{*3} d\Gamma_e$$
$$\alpha = 1 \text{ to } 3 \ , e = 1 \text{ to } M \tag{6.61}$$

Since $\underline{x}$ is not on the boundary Γ, the integrals (6.60) and (6.61) are all non-singular and are evaluated by standard Gaussian quadrature.

6.6 Wave loading of Flat Homogeneous Isotropic Seabed. Comparison with Analytic Solution.

We consider a horizontal distance of one quarter of the wavelength L, as illustrated in Figure (6.1). The x axis is at the mudline as shown and the z axis is vertically downward. The wave pressure on OC is of the form

$$P = P_0 e^{i(kx-\omega t)}$$

where $k = \frac{2\pi}{L}$ and ω is the circular frequency. Hence

$$\bar{P} = P_0 e^{ikx} \tag{6.62}$$

From linear wave theory, the formula for P_0 is given by

$$P_0 = \frac{\rho_f(\frac{H}{2})g}{\cosh(kh)} \tag{6.63}$$

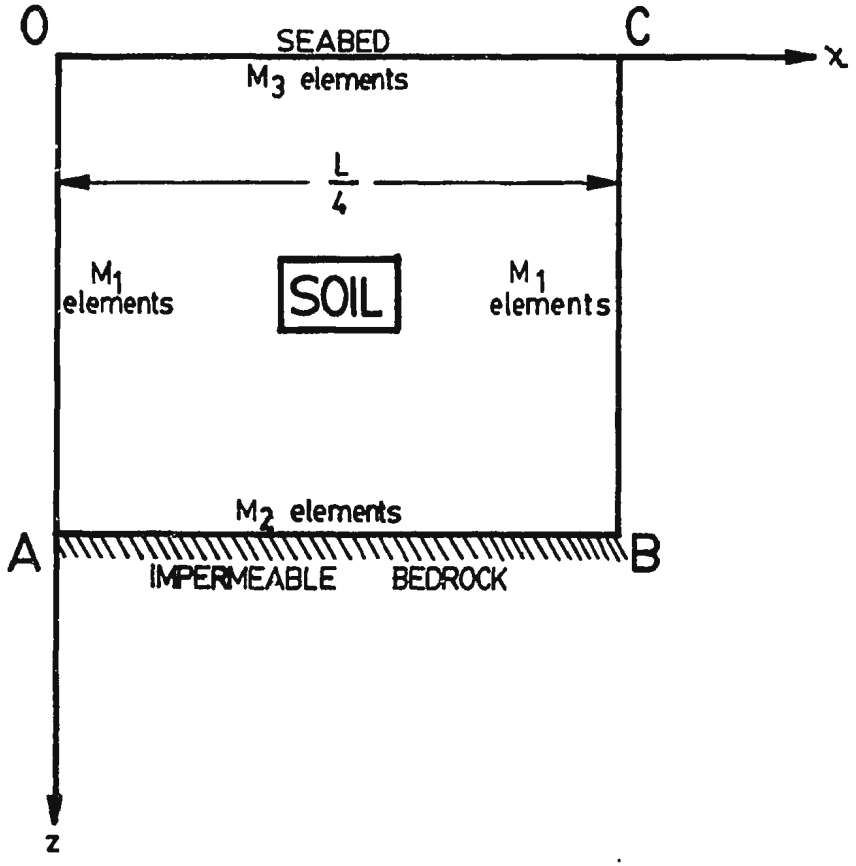

Fig. (6.1) BEM Test for Flat Seabed.

where H is the wave height and h is the water depth. From (3.7) and (5.3) we have

$$T_i = \tau'_{ij} n_j - p n_i \qquad (i = 1,2) \tag{6.64}$$

and we recall that

$$T_3 = -p \tag{6.65}$$

The boundary conditions are as follows :

On OC, $\bar{\tau}'_{12} = 0$, $\bar{\tau}'_{22} = 0$, $\bar{p} = P_0 e^{ikx}$.

In terms of $\tilde{\bar{T}}_i$ these become

$$\tilde{\bar{T}}_1 = 0,\ \tilde{\bar{T}}_2 = \frac{P_0}{\mu} e^{ikx},\ \tilde{\bar{T}}_3 = -\frac{P_0}{\mu} e^{ikx} \tag{6.66}$$

On AB:

$$\tilde{\bar{u}}_i = 0 \text{ for } i = 1,2,3 \tag{6.67}$$

Periodicity conditions must be used on the side boundaries OA and BC. A given function $f(x,z)$ may be expressed as

$$f(x,z) = F(z) e^{ikx} \tag{6.68}$$

where $f(x,z)$ represents $\bar{u}_i, \bar{U}_i, \bar{\tau}'_{ij}$ or $\bar{p}$. From (6.68) we deduce that since $k = \frac{2\pi}{L}$

$$f(\frac{L}{4}, z) = i f(0,z) \tag{6.69}$$

Equation (6.69) can be used to express the boundary conditions on BC in terms of those on OA. It is easy to show that

$$\begin{aligned} \tilde{\bar{u}}_i(\tfrac{L}{4}, z) &= \alpha_u^i \tilde{\bar{u}}_i(0,z) \text{ no sum on } i \\ \tilde{\bar{T}}_i(\tfrac{L}{4}, z) &= \alpha_T^i \tilde{\bar{T}}_i(0,z) \text{ no sum on } i \end{aligned} \tag{6.70}$$

where α_u^n and α_T^n are complex constants defined by

$$\alpha_u^n = \begin{cases} i & n = 1,2 \\ -i & n = 3 \end{cases}$$

$$\alpha_T^n = \begin{cases} -i & n = 1,2 \\ i & n = 3 \end{cases}$$

Conditions (6.66), (6.67) and (6.70) must now be used in the discretised boundary integral equation (6.9). Since the boundary conditions on BC are expressed in terms of those on OA we choose the same number of elements M_1 on each of these boundary segments. On AB and CO we choose M_2 and M_3 elements respectively. The total number of elements is thus $M = 2M_1 + M_2 + M_3$. The first element is taken on OA and the last one on CO. The direction of integration is anticlockwise around the boundary.

Using (6.70) we have

$$\begin{aligned} \tilde{\tilde{T}}_i^{M_1+M_2+e} &= \alpha_T^i \tilde{\tilde{T}}_i^{M_1+1-e} \\ \tilde{\tilde{u}}_i^{M_1+M_2+e} &= \alpha_u^i \tilde{\tilde{u}}_i^{M_1+1-e} \\ e &= 1 \text{ to } M_1, \quad \text{no sum on } i \end{aligned}$$

We let

$$\begin{aligned} R_{ki}^{M_1+M_2+e} &= R_{ki}'^{M_1+1-e} \\ S_{ki}^{M_1+M_2+e} &= S_{ki}'^{M_1+1-e} \\ e &= 1 \text{ to } M_1 \end{aligned}$$

Then it is easily shown that

$$\sum_{e=1}^{M_1} R_{ki}^{M_1+M_2+e} \tilde{\tilde{T}}_i^{M_1+M_2+e} = \sum_{e=1}^{M_1} \alpha_T^i R_{ki}^{'e} \tilde{\tilde{T}}_i^e$$

$$\sum_{e=1}^{M_1} S_{ki}^{M_1+M_2+e} \tilde{\tilde{u}}_i^{M_1+M_2+e} = \sum_{e=1}^{M_1} \alpha_u^i S_{ki}^{'e} \tilde{\tilde{u}}_i^e$$

Substituting into (6.9) gives

$$\begin{aligned} &\sum_{e=1}^{M_1} (R_{ki}^e + \alpha_T^i R_{ki}^{'e}) \tilde{\tilde{T}}_i^e + (S_{ki}^e + \alpha_u^i S_{ki}^{'e}) \tilde{\tilde{u}}_i^e \\ &+ \sum_{e=i}^{M_2} (R_{ki}^{M_1+e} \tilde{\tilde{T}}_i^{M_1+e} + S_{ki}^{M_1+e} \tilde{\tilde{u}}_i^{M_1+e}) \\ &+ \sum_{e=1}^{M_3} (R_{ki}^{2M_1+M_2+e} \tilde{\tilde{T}}_i^{2M_1+M_2+e} + S_{ki}^{2M_1+M_2+e} \tilde{\tilde{u}}_i^{2M_1 M_2+e}) = 0 \end{aligned} \tag{6.71}$$

We now define the following

For $e = 1$ to M_1

$$R_{ki}^{*e} = R_{ki}^e + \alpha_T^i R_{ki}^{'e}$$

$$S_{ki}^{*e} = S_{ki}^e + \alpha_u^i S_{ki}^{'e}$$

$$T_i^{*e} = \tilde{\tilde{T}}_i^e$$

$$u_i^{*e} = \tilde{\tilde{u}}_i^e$$

For $e = 1$ to M_2:

$$R_{ki}^{*M_1+e} = R_{ki}^{M_1+e}$$

$$S_{ki}^{*M_1+e} = S_{ki}^{M_1+e}$$

$$T_i^{*M_1+e} = \tilde{\tilde{T}}_i^{M_1+e}$$

$$u_i^{*M_1+e} = \tilde{\tilde{u}}_i^{M_1+e}$$

For $e = 1$ to M_3

$$R_{ki}^{*M_1+M_2+e} = R_{ki}^{2M_1+M_2+e}$$

$$S_{ki}^{*M_1+M_2+e} = S_{ki}^{2M_1+M_2+e}$$

$$T_i^{*M_1+M_2+e} = \tilde{T}_i^{2M_1+M_2+e}$$

$$u_i^{*M_1+M_2+e} = \tilde{u}_i^{2M_1+M_2+e}$$

With these definitions, equation (6.71) becomes

$$\sum_{e=1}^{M^*} R_{ki}^{*e}(j)T_i^{*e} + S_{ki}^{*e}(j)u_i^{*e} = 0 \quad i,k = 1 \text{ to } 3 \tag{6.72}$$

where $M^* = M_1 + M_2 + M_3$

The unknowns are

$$\begin{aligned} &\{T_i^{*e},\ u_i^{*e},\ \ e = 1 \text{ to } M_1\} \\ &\{T_i^{*M_1+e},\ \ e = 1 \text{ to } M_2\} \\ &\{u_i^{*M_1+M_2+e},\ \ e = 1 \text{ to } M_3\} \end{aligned} \tag{6.73}$$

where $i = 1$ to 3, i.e. a total of $(6M_1 + 3M_2 + 3M_3)$ or $3M$ unknowns. Equation (6.72) must be written with each boundary node serving as $r = 0$, i.e. as j takes the values 1 to M. This produces $3M$ equations. For a given j, row number $3j-(3-k)$ of the matrix equation is generated.

For $e = 1$ to $(M_2 + M_3)$ we define

$$\left.\begin{aligned} x_i'^e &= T_i^{*M_1+e} \\ F_{ki}'^e &= R_{ki}^{*M_1+e} \\ x_i^e &= u_i^{*M_1+e} \\ F_{ki}^e &= S_{ki}^{*M_1+e} \end{aligned}\right\} \text{ if } T_i^{*M_1+e} \text{ is known}$$

and

$$\left.\begin{aligned} x_i'^e &= u_i^{*M_1+e} \\ F_{ki}'^e &= \quad {}^{*M_1+e}_{ki} \\ x_i^e &= T_i^{*M_1+e} \\ F_{ki}^e &= R_{ki}^{*M_1+e} \end{aligned}\right\} \text{ if } u_i^{*M_1+e} \text{ is known}$$

Then equation (6.72) becomes

$$\sum_{e=1}^{M_1}(R_{ki}^{*e}\, T_i^{*e} + S_{ki}^{*e}\, u_i^{*e}) + \sum_{e=1}^{M_2+M_3} F_{ki}\, x_i^e = -\sum_{e=1}^{M_2+M_3} F_{ki}'^e\, x_i'^e \qquad (6.74)$$

This may be written in matrix form

$$[G]\{y\} = \{b\} \qquad (6.75)$$

It can be verified that the following algorithm generates the matrix $[G]$ and vector $\{b\}$:

For j = 1 to M

For k = 1 to 3

$$n = 3j - (3-k)$$

$$b_n = -\sum_{e=1}^{M_2+M_3} F_{ki}'^e x_i'^e$$

$$G_{np} = \begin{cases} R_{k,p-3t+3}^{*t} & p = 3t-2 \text{ to } 3t, t = 1 \text{ to } M_1 \\ S_{k,p-3(M_1+t-1)}^{*t} & p = 3M_1+3t-2 \text{ to } (3M_1+3t), t = 1 \text{ to } M_1 \\ F_{k,p-3(2M_1+t-1)}^{t} & p = (6M_1+3t-2) \text{ to } (6M_1+3t), t = 1 \text{ to } (M_2+M_3) \end{cases}$$

The solution vector is given by (6.73). The interior stresses are computed as described in Section (6.5). In order to test the accuracy of the BEM we compare

Table 6.1: Comparison of BEM with Analytic Solution at (1,2)

Stresses	BEM (200 elements)		Analytic	
$\times 10^4\ Nm^{-2}$	Real	Imag	Real	Imag
$\bar{\tau}'_{11}$	0.9047	0.1253	0.9068	0.1310
$\bar{\tau}'_{22}$	-0.9104	0.2007	-0.9064	0.1952
$\bar{\tau}'_{12}$	-0.0075	0.1535	-0.0075	0.1527
$\bar{p}$	4.5129	0.3004	4.5116	0.3044

Table 6.2: Comparison of BEM with Analytic Solution at (5,5)

Stresses	BEM (200 elements)		Analytic	
$\times 10^4\ Nm^{-2}$	Real	Imag	Real	Imag
$\bar{\tau}'_{11}$	0.8639	0.0845	0.8639	0.0852
$\bar{\tau}'_{22}$	-0.9307	-0.1081	-0.9310	-0.1088
$\bar{\tau}'_{12}$	-0.0431	0.3670	-0.0430	0.3666
$\bar{p}$	4.4466	0.4330	4.4449	0.4342

the results with the analytic solution which is briefly described in **Appendix I.** The data for the test case was $OA = 25m$, water depth $=70m$, wave period $=$ 15 sec. (which corresponds to a wavelength L of $311.812m$), wave height $= 24m$. Details of the input data for the soil (fine sand) can be found in **Chapter 8.** Tables (6.1), (6.2) and (6.3) show the stresses in N/m^2 at three interior points (coordinates defined by axes in Figure (6.1)) obtained by the two methods . There is excellent agreement between the BEM and the analytic solution. The BEM results were obtained with eight point Gaussian quadrature.

Table 6.3: Comparison of BEM with Analytic Solution at (35,12)

Stresses	BEM (200 elements)		Analytic	
$\times 10^4\ Nm^{-2}$	Real	Imag	Real	Imag
$\bar{\tau}'_{11}$	0.5517	0.4725	0.5517	0.4725
$\bar{\tau}'_{22}$	-0.5790	-0.4955	-0.5790	-0.4955
$\bar{\tau}'_{12}$	-0.5811	0.6753	-0.5809	0.6749
$\bar{p}$	3.4689	2.9490	3.4686	2.9489

Chapter 7

Stress Analysis of Sloping Seabed Under Wave Loading

7.1 Wave Induced Effective Stresses and Pore Pressure in a Bed of Arbitrary Slope

The problem domain is illustrated in Figure (7.1). The x and z axes are chosen with origin at O' as shown. The incident wave is travelling in the negative x direction. The boundary conditions on the seabed $BDEC$ are that the normal and shear effective stresses are zero (there is no applied inter-granular load) and the pore pressure $\overline{p}$ is equal to the wave pressure $\overline{P}$ acting normal to the bed (determined from equation 4.46). In terms of the tractions $\bar{T}_i$, these become :

On BD : $\bar{T}_1 = 0,\ \bar{T}_2 = i\omega\rho_f\bar{\phi}\,|_{BD},\ \bar{T}_3 = -i\omega\rho_f\bar{\phi}\,|_{BD}$

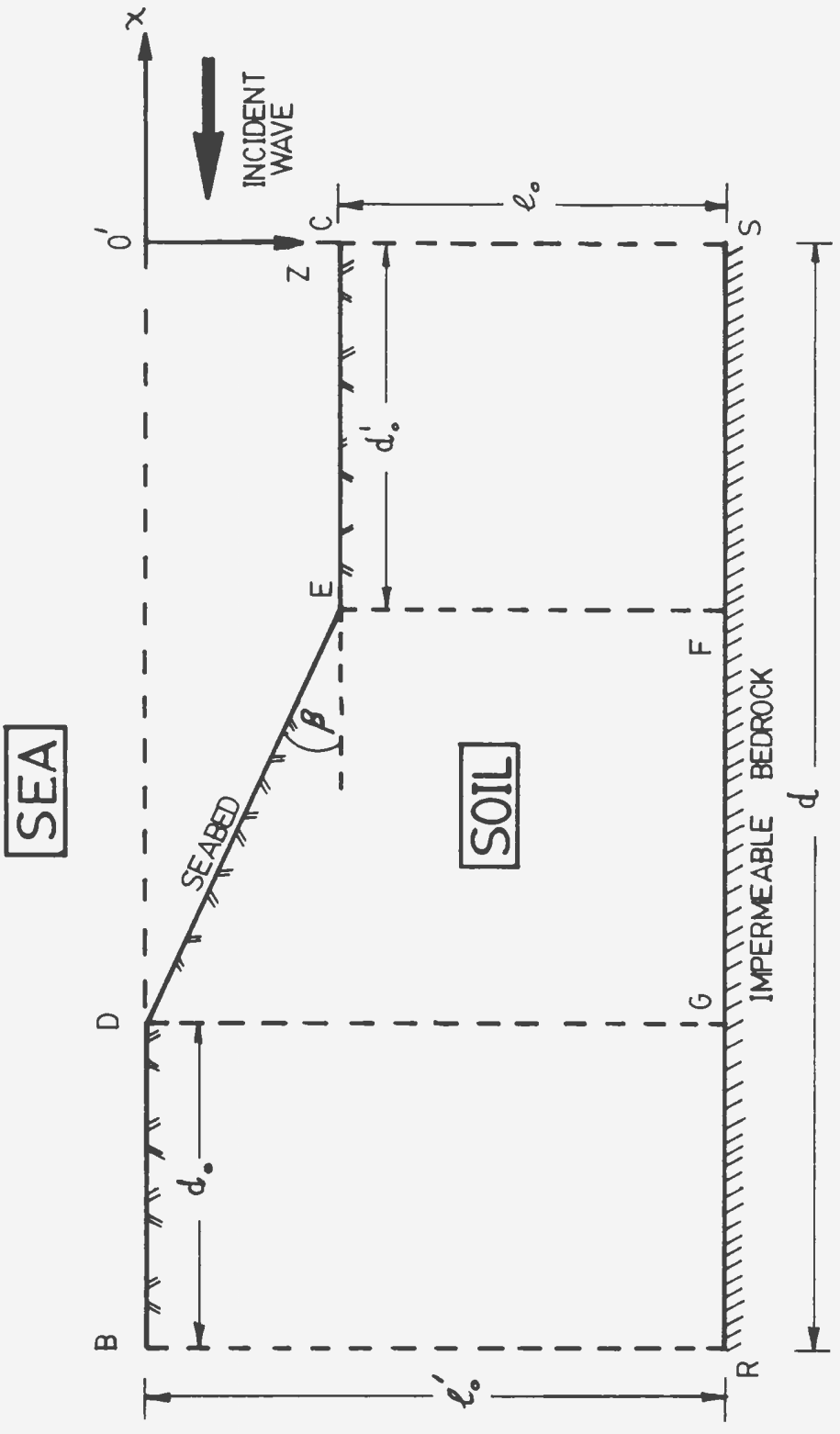

Fig.(7.1) Sloping Seabed

On DE : $\bar{T}_1 = -i\omega\rho_f\bar{\phi}\,|_{DE}\sin\beta$, $\bar{T}_2 = i\omega\rho_f\bar{\phi}\,|_{DE}\cos\beta$, $\bar{T}_3 = -i\omega\rho_f\bar{\phi}\,|_{DE}$

On EC : $\bar{T}_1 = 0$, $\bar{T}_2 = i\omega\rho_f\bar{\phi}\,|_{EC}$, $\bar{T}_3 = -i\omega\rho_f\bar{\phi}\,|_{EC}$

where $\bar{\phi}$ is the velocity potential in the sea as determined from the techniques of Chapter 4. At the interface with the bedrock base RS we have :

$$\bar{u}_1 = \bar{u}_2 = \bar{u}_3 = 0$$

To provide boundary conditions on the side boundaries BR and SC we make use of the author's analytic solution (hereafter referred to as A.S.) described in Appendix I. We first determine from (4.15) the velocity potential on the seabed in the region to the right of $O'C$. The coefficients a_n in (4.15) are determined by solving (4.37) for the vector $\{a\}$. The numerical results indicate that the infinite sum on the right hand side of (4.15) is negligible compared to the other terms. Neglecting this term, we write the velocity potential on the seabed to the right of $O'C$ as :

$$\Phi\,|_{bed} = \frac{-ig\eta_0}{\omega\cosh(k_0h_0)}[a_0e^{ik_0x} + e^{-ik_0x}]e^{-i\omega t} \tag{7.1}$$

Hence from (4.46) the wave pressure on the seabed in this region is :

$$P\,|_{bed} = \frac{\rho_f g\eta_0}{\cosh(k_0h_0)}[a_0e^{ik_0x} + e^{-ik_0x}]e^{-i\omega t} \tag{7.2}$$

which is in a form suitable for applying the A.S. We can determine the effective stresses and pore pressure (and hence $\bar{T}_i$) on SC by superposing the results obtained from the A.S. for the following two cases:

(1) Incident Wave conditions :

$$k = -k_0$$

$$P_0 = \frac{\rho_f g\eta_0}{\cosh(k_0h_0)}$$

(2) Reflected Wave conditions :

$$k = k_0$$
$$P_0 = \frac{a_0 \rho_f g \eta_0}{\cosh(k_0 h_0)}$$

The $\bar{\tau}'_{ij}$ and $\bar{p}$ at desired soil depths are evaluated at $x = 0$ in each case. We can now write the boundary conditions on SC, noting that $(n_1, n_2) = (1, 0)$:

$$\bar{T}_1 = \bar{\tau}'_{11} - \bar{p}, \;\; \bar{T}_2 = \bar{\tau}'_{21}, \;\; \bar{T}_3 = -\bar{p}$$

For the region to the left of BR, the wave velocity potential on the seabed is, from (4.16)

$$\Phi \mid_{bed} = a'_0 e^{-ik'_0 x} e^{-i\omega t} \tag{7.3}$$

where we have neglected the infinite sum on the right hand side of (4.16). The coefficient a'_0 may be determined from the numerically determined value of $\bar{\phi}$ at B:

$$\bar{\phi} \mid_B = a'_0 e^{ik'_0 d} \tag{7.4}$$

Again, from (4.46) and (7.3) the wave pressure on the seabed in this region is :

$$\begin{aligned} P \mid_{bed} &= i\omega \rho_f a'_0 e^{-ik'_0 x} e^{-i\omega t} \\ &= i\omega \rho_f \bar{\phi} \mid_B e^{-ik'_0 d} e^{-i(k'_0 x + \omega t)} \end{aligned} \tag{7.5}$$

where we have used (7.4).

The effective stresses and pore pressure on BR may thus be determined from the A.S. using

$$k = -k'_0, \;\; P_0 = i\omega \rho_f \bar{\phi} \mid_B e^{-ik'_0 d}, \;\; x = -d$$

On BR, $(n_1, n_2) = (-1, 0)$ and we write the boundary conditions as

$$\bar{T}_1 = -\bar{\tau}'_{11} + \bar{p}, \quad \bar{T}_2 = -\bar{\tau}'_{21}, \quad \bar{T}_3 = -\bar{p}$$

With the boundary conditions thus specified, we determine the unknown boundary data and wave-induced interior stresses as described in Chapter 6.

7.2 Initial Stresses

The in-situ stresses in soil depend not only on gravitational forces, but also on the stress history due to the geological processes involved in the formation of the soil deposit. Thus the standard constants of elasticity theory must be modified to adequately model the in-situ stress field. For example, for a flat seabed under hydrostatic conditions the effective stresses at depth z are, in conventional notation,

$$\begin{aligned} \sigma'_z &= \gamma' z \\ \sigma'_x &= K_0 \gamma' z \\ \tau'_{xz} &= 0 \end{aligned} \tag{7.6}$$

where γ' is the buoyant unit weight of the saturated soil and $\sigma'_z, \sigma'_x, \tau'_{xz}$ are the effective vertical, horizontal and shear stresses respectively at depth z (soil mechanics sign convention). The parameter K_0 is the coefficient of lateral earth pressure at rest which attempts to account for the stress history of the soil. It is usually empirically determined. For a sloping bed it is possible to determine the gravitational stress field from the theory of elasticity using a numerical technique (finite element or boundary element method) since no analytic solution exists for the geometry

of the problem considered. In this approach it would be necessary to modify the elastic constants for the reasons discussed above. However, no adequate method of doing this is currently available and we employ the concept of conjugate stresses introduced by Taylor (1948) in which it is possible to account for the stress history of the soil via a parameter analogous to K_0. The concept is strictly valid only for infinite slopes. Accordingly, the representation of in-situ stresses by this method in the vicinity of the lines DG and EF (Figure 7.1) is only approximate.

We shall first consider an infinite slope of dry soil inclined at an angle β as illustrated in Figure (7.2).

The element $ABCD$, located at distance z below the surface of the slope as shown, has sides AB and CD parallel to the slope. Taylor (1948) has shown that the total stresses on the element may be represented by σ_v in the vertical direction and σ_β parallel to the slope. The stresses σ_v and σ_β are called conjugate stresses. Considering the weight of material above AB it is easily seen that

$$\sigma_v = \gamma_d z \cos\beta \tag{7.7}$$

where γ_d is the unit weight of the dry soil. Following Chowdhury (1977), we assume that there exists a constant K, called the conjugate stress ratio, such that

$$\sigma_\beta = K\sigma_v$$

i.e.

$$\sigma_\beta = K\gamma_d z \cos\beta \tag{7.8}$$

We now determine the Cartesian stress tensor τ_{ij} at a point. As before, the unit outward normal on a plane is denoted by (n_1, n_2) and the tractions T_i are given by

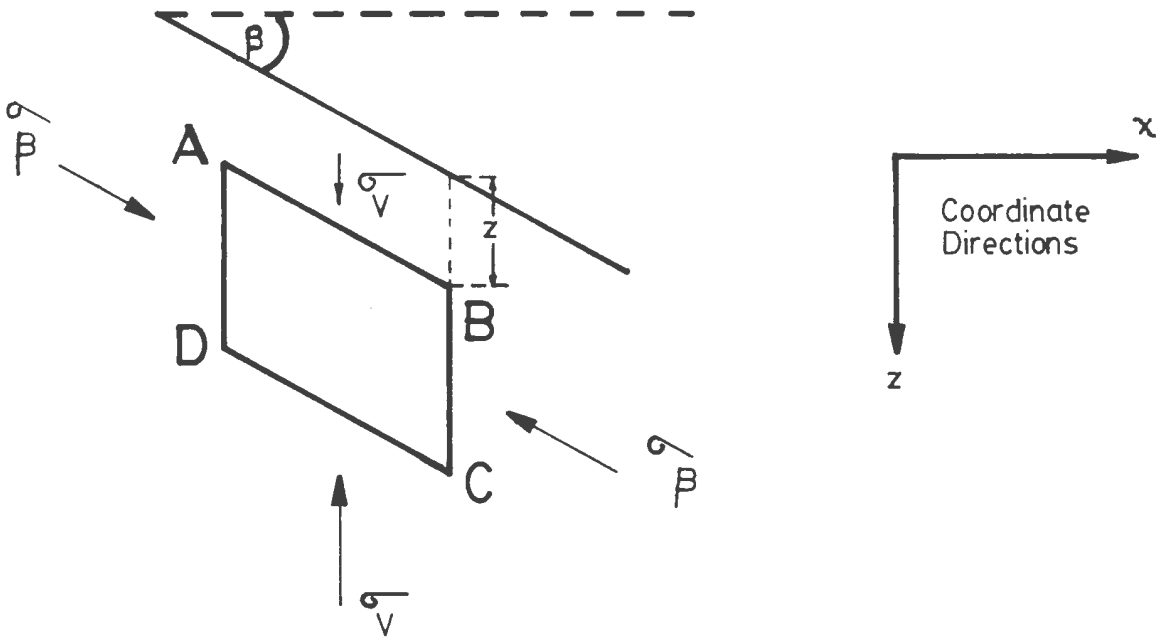

Fig. (7.2) Conjugate Stresses in Infinite Slope

(5.3). On AB, Figure (7.2),

$$T_1 = 0,\ T_2 = \sigma_v,\quad n_1 = \sin\beta, n_2 = -\cos\beta$$

This gives

$$\tau_{11}\sin\beta - \tau_{12}\cos\beta = 0 \qquad (i)$$

$$\tau_{21}\sin\beta - \tau_{22}\cos\beta = \gamma_d z\cos\beta \qquad (ii)$$

On BC,

$$T_1 = -\sigma_\beta\cos\beta,\ T_2 = -\sigma_\beta\sin\beta,\quad n_1 = 1, n_2 = 0$$

This gives

$$\tau_{11} = -K\gamma_d z\cos^2\beta \qquad (iii)$$

$$\tau_{21} = -K\gamma_d z\sin\beta\cos\beta \qquad (iv)$$

From (ii) and (iv) we have

$$\tau_{22} = -\gamma_d z(1 + K\sin^2\beta) \qquad (v)$$

It is easily verified that the expressions given by (iii),(iv) and (v) satisfy (i).

The above expressions give the effective stress tensor at a point in a slope of dry soil. If we now consider the effective stress field in a submerged slope we note that γ_d is now replaced by γ', the buoyant unit weight of the soil. Hence the effective stress tensor in a submerged slope is given by expressions (iii), (iv) and (v) above with γ_d replaced by γ'. Using the conventional soil mechanics notation and sign conventions (described in Section 3.2) we have the in-situ effective stress field in the region $DEFG$ (Figure 7.1) as

$$\sigma_x' = \gamma' z(1 + K\sin^2\beta)$$

$$\begin{aligned} \sigma_x' &= K\gamma' z\cos^2\beta \\ \tau_{xz}' &= K\gamma' z\sin\beta\cos\beta \end{aligned} \tag{7.9}$$

where we recall that z denotes depth below the sloping surface DE. We can define K_0 ,the coefficient of earth pressure at rest, in the usual way as the ratio of the horizontal to vertical effective stress ,i.e.

$$K_0 = \frac{K\cos^2\beta}{1+K\sin^2\beta}$$

The value of K can thus be determined from measurements of K_0, or from commonly accepted empirical formulae for K_0 (Bowles, 1984).

The principal stresses σ_1', σ_3' are given by :

$$\sigma_{1,3}' = \frac{1}{2}(\sigma_x' + \sigma_x' \pm \sqrt{\frac{1}{4}(\sigma_x' - \sigma_z')^2 + \tau_{xz}'^2}$$

which gives

$$\sigma_{1,3}' = \frac{1}{2}\gamma' z[1+K \pm \sqrt{K^2 - 2K\cos 2\beta + 1}] \tag{7.10}$$

The limiting values of the conjugate stress ratio K are determined by the Mohr-Coulomb failure criterion which is written for cohesionless soils as

$$\sigma_1' - \sigma_3' = (\sigma_1' + \sigma_3')\sin\phi' \tag{7.11}$$

where ϕ' is the (effective) angle of internal friction of the soil. From (7.10) and (7.11) we have

$$K^2\cos^2\phi' - 2K(\cos 2\beta + \sin^2\phi') + \cos^2\phi' = 0 \tag{7.12}$$

which has roots

$$K_1, K_2 = \frac{1}{\cos^2\phi'}[\cos 2\beta + \sin^2\phi' \pm 2\cos\beta\sqrt{\sin^2\phi' - \sin^2\beta}] \tag{7.13}$$

Table 7.1: Limiting Values of K

Slope Angle β (deg.)	Limits for K	
	$\phi' = 30°$	$\phi' = 35°$
5	0.34 - 2.95	0.27 - 3.64
10	0.35 - 2.82	0.29 - 3.50.
15	0.39 - 2.59	0.31 - 3.25
20	0.44 - 2.27	0.34 - 2.92
25	0.54 - 1.84	0.40 - 2.50

We note that the roots are real if $\phi' \geq \beta$. Equation (7.13) gives the limiting values of K, i.e. the range of values of K for which the in-situ stresses do not violate the Mohr-Coulomb failure criterion. These values are presented in Table (7.1) for various slope angles and values of the angle ϕ'. The upper and lower limits for K correspond to states of passive and active failure respectively in the undisturbed soil. The initial stresses in the regions $BDGR$ and $ECSF$ (Figure (7.2)) are estimated from equations (7.6),where z is depth below BD and EC respectively.

7.3 Failure Analysis

The basis for the failure analysis will be the Mohr-Coulomb failure criterion which is widely accepted in the geotechnical community. We shall identify "zones of overstress" in the soil, i.e. regions of soil in which the failure criterion is violated. It should be noted, however, that when such violation of the failure criterion has taken place,the stress field is, strictly speaking, invalid. The zone of overstress must

therefore be regarded as the approximate region of failure. Further, we note that owing to the effect of stress transfer when the failure condition is violated, the zone of overstress denotes the minimum region of soil failure. An elastoplastic analysis is then required to determine the failure zone more accurately. In this thesis we provide the first stage of such an analysis, via the location of the overstressed zones determined by a single application of the failure criterion. This type of failure analysis has also been employed by Yamamoto (1978), Mynett and Mei (1982) and Mei and McTigue (1984). The limitations of such analysis was also pointed out by Mei and McTigue (1984) who nevertheless recognised the utility of the approach in providing a good first approximation of the extent of the failure zone.

We employ the conventional soil mechanics notation and sign convention described in Section (3.2). The initial effective stresses determined from Section (7.2) will be denoted by $\sigma_x'^{(0)}, \sigma_z'^{(0)}, \tau_{xz}'^{(0)}$. The wave-induced effective stresses will be denoted by $\sigma_x'^{(1)}, \sigma_z'^{(1)}, \tau_{xz}'^{(1)}$ where we take the real part of the complex stresses computed by the BEM.

The resultant effective stresses $\sigma_x', \sigma_z', \tau_{xz}'$ are thus given by :

$$\begin{aligned} \sigma_x' &= \sigma_x'^{(0)} + \sigma_x'^{(1)} \\ \sigma_z' &= \sigma_z'^{(0)} + \sigma_z'^{(1)} \\ \tau_{xz}' &= \tau_{xz}'^{(0)} + \tau_{xz}'^{(1)} \end{aligned} \tag{7.14}$$

These stresses may be plotted on a Mohr circle as illustrated in Figure (7.3). The coordinates (σ, τ) of any point D on the circle are the normal and shear stress acting on a particular plane, the inclination of which is determined from the angle $D\hat{C}A$ in Figure (7.3).

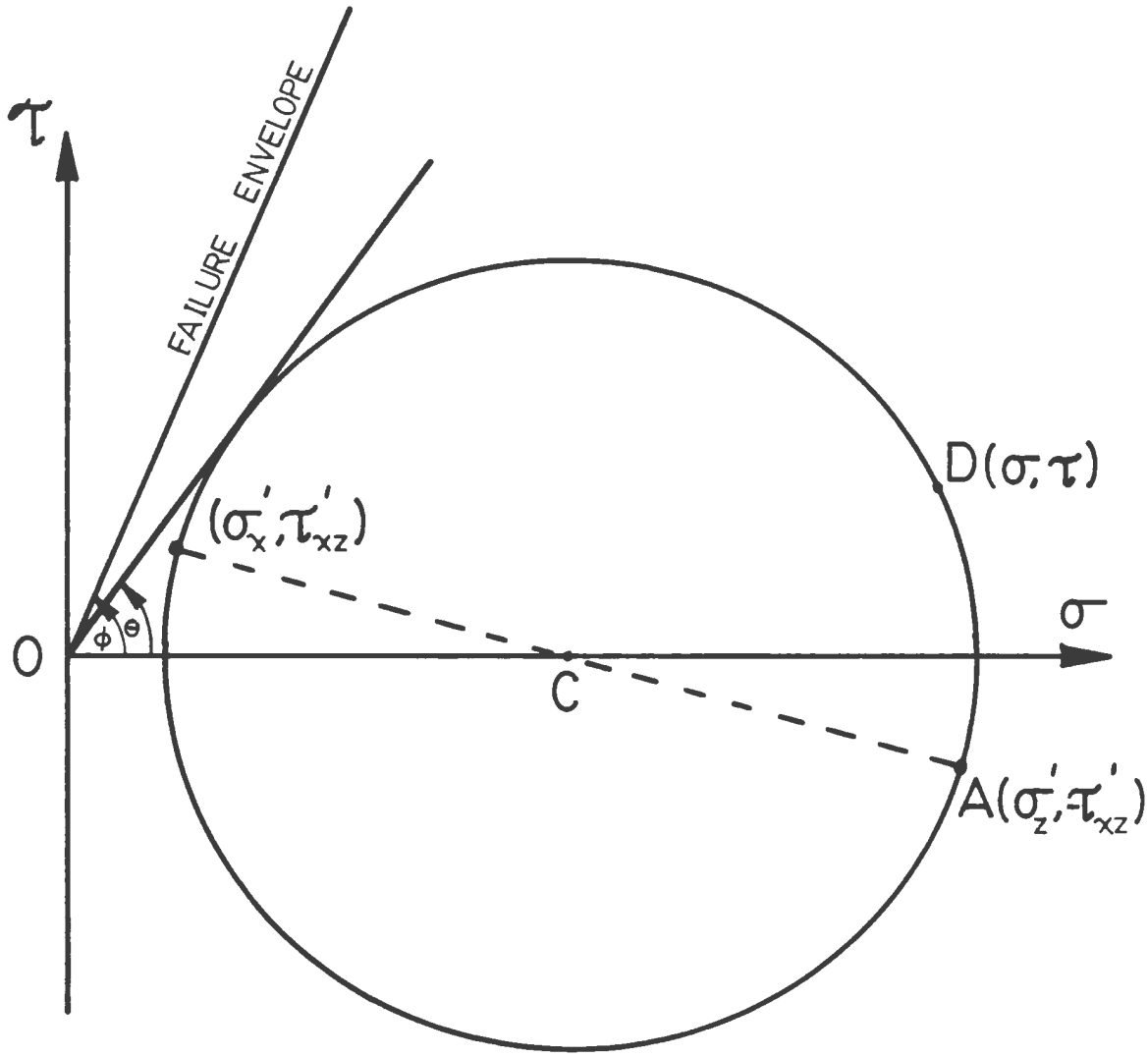

Fig.(7.3) The Stress Angle θ

The Mohr-Coulomb failure envelope is the line

$$\tau = \sigma \tan \phi' \tag{7.15}$$

and is illustrated in the figure. It intersects the τ axis at the origin O. We define the stress angle θ as the angle between the σ axis and the tangent to the circle from the failure envelope intercept O. The stress angle is a function of the stress state $(\sigma_x', \sigma_z', \tau_{xz})$, and by comparing its value with ϕ' we determine the "distance" between the current stress state and the failure state. The condition of failure is thus conveniently expressed as

$$\theta \geq \phi' \tag{7.16}$$

From the geometry of Figure (7.3) we find that

$$\sin \theta = \frac{[(\sigma_z' - \sigma_x')^2 + 4\tau_{xz}'^2]^{\frac{1}{2}}}{\sigma_x' + \sigma_z'} \tag{7.17}$$

from which θ can be calculated. The overstressed zones are then determined from (7.16). We would comment at this point that for the purpose of determining the stress angle no significant reduction in accuracy is observed by using four point Gaussian quadrature (instead of eight point quadrature) when computing the wave-induced effective stresses by the BEM.

Chapter 8

Results and Discussion

We first present the wave pressures on a sloping seabed as computed by the methods of **Chapter 4**. Figures (8.1) and (8.2) illustrate the wave pressures on a 12 degree slope due to wave lengths (L) of $300m$ and $150m$ respectively. The coordinates of the points on the slope are as defined in Figure (7.1). The bed slopes upward between $x = -5m$ and $x = -60m$ (points E and D in Figure (7.1)). The incident wave height is $24m$ and the water depth between $x = 0m$ and $x = -5m$ is $80m$. At time $t = 0$, the wave crest is vertically above the point $x = 0m$ (point C in Figure (7.1)). The graphs illustrate the progression in time of the wave pressures, the maximum pressures being experienced by points under the wave crest. The maxima at the left end of the slope are slightly greater than at the right end owing to the smaller water depth at the left end. We note also that negative pressures are experienced at certain instants of the wave cycle. At $\omega t = \pi$ and $\omega t = \frac{3\pi}{2}$ the wave pressures are the negative of those illustrated for $\omega t = 0$ and $\omega t = \frac{\pi}{2}$ respectively.

Thus we would expect, for example, positive wave-induced pore pressures at $\omega t = \frac{\pi}{2}$ and negative wave-induced pore pressures at $\omega t = \frac{3\pi}{2}$. We have also investigated the wave pressures on a 12 degree slope in shallower water. A wave of length $150m$ in $80m$ of water would have a length of $133.5m$ in $30m$ of water over a flat bed. Figure (8.3) illustrates the wave pressures on a 12 degree slope, the wave length and water depth at the base of the slope being $133.5m$ and $30m$ respectively. The incident wave height is set at $16m$. Even at this reduced wave height, the maximum wave pressures are more than twice those illustrated in Figure (8.2), owing to the smaller water depths.

We now examine the wave-induced failure zones in the soil. As described in Section (7.3), the approximate extent of the failure zone may be determined by computing the stress angle θ at several points in the soil and comparing with the angle of friction ϕ'. For this purpose it is convenient to plot contours of the stress angle. If the angle of friction of the soil is, for example, $\phi' = 30°$, we can determine the failure zone approximately as the region in which $\theta \geq 30°$. We emphasize again that this provides only an estimate of the minimum failure zone, owing to the fact that violation of the Mohr-Coulomb criterion invalidates the stress field. The meaning of "failure" in the Mohr-Coulomb sense is that frictional resistance in the soil has been exceeded on some plane. The failure zone is thus an unstable region and further research is needed to study the manner in which failure progresses.

Stress angle contours for a fine sand and coarse sand with slope angles of $\beta = 2°, 5°, 12°, 20°$ and wave lengths of $L = 150m, 225m, 300m$ are given in this chapter and in Appendix J. The contours were produced by the graphics package SURFACE II at Memorial University. Because of the interpolation and smoothing performed

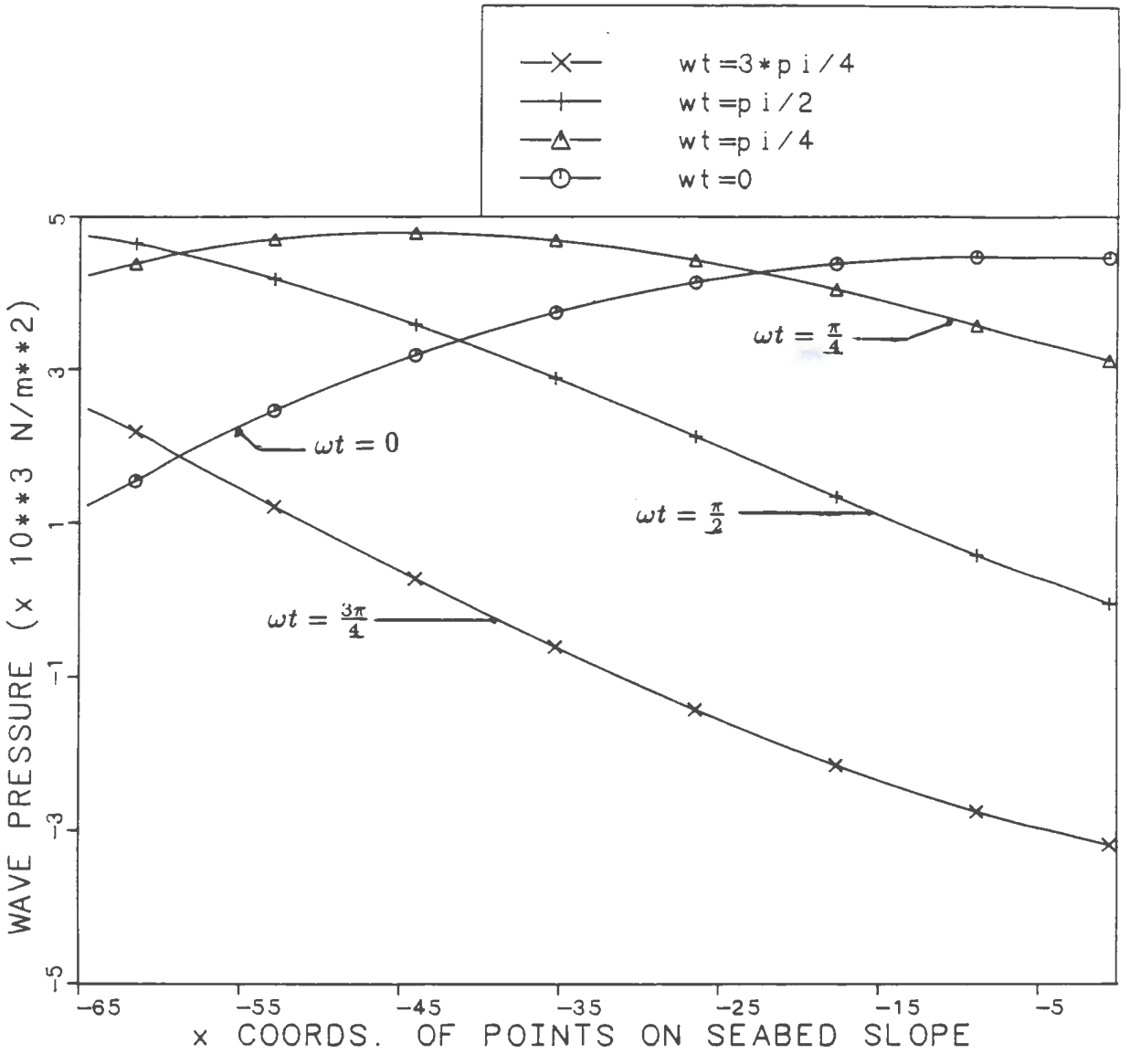

Figure 8.1: Wave Pressure on 12 deg. Slope : $L = 300m.$, $H = 24m.$
Water Depth at Slope Base ($x = 0$) $= 80\,m.$

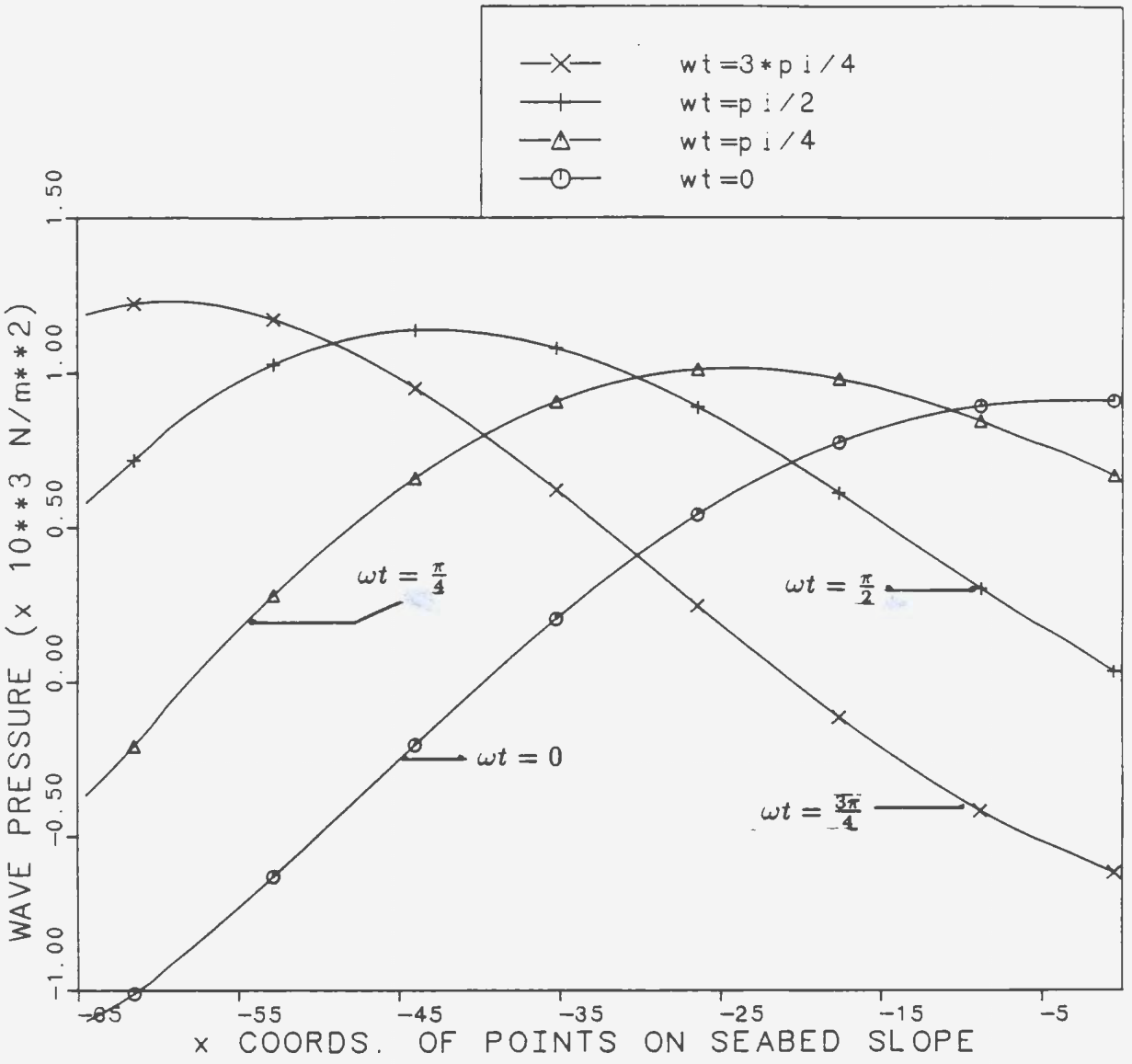

Figure 8.2: Wave Pressure on 12 deg. Slope : $L = 150m.$, $H = 24m.$
Water Depth at Slope Base ($x = 0$) $= 80\,m.$

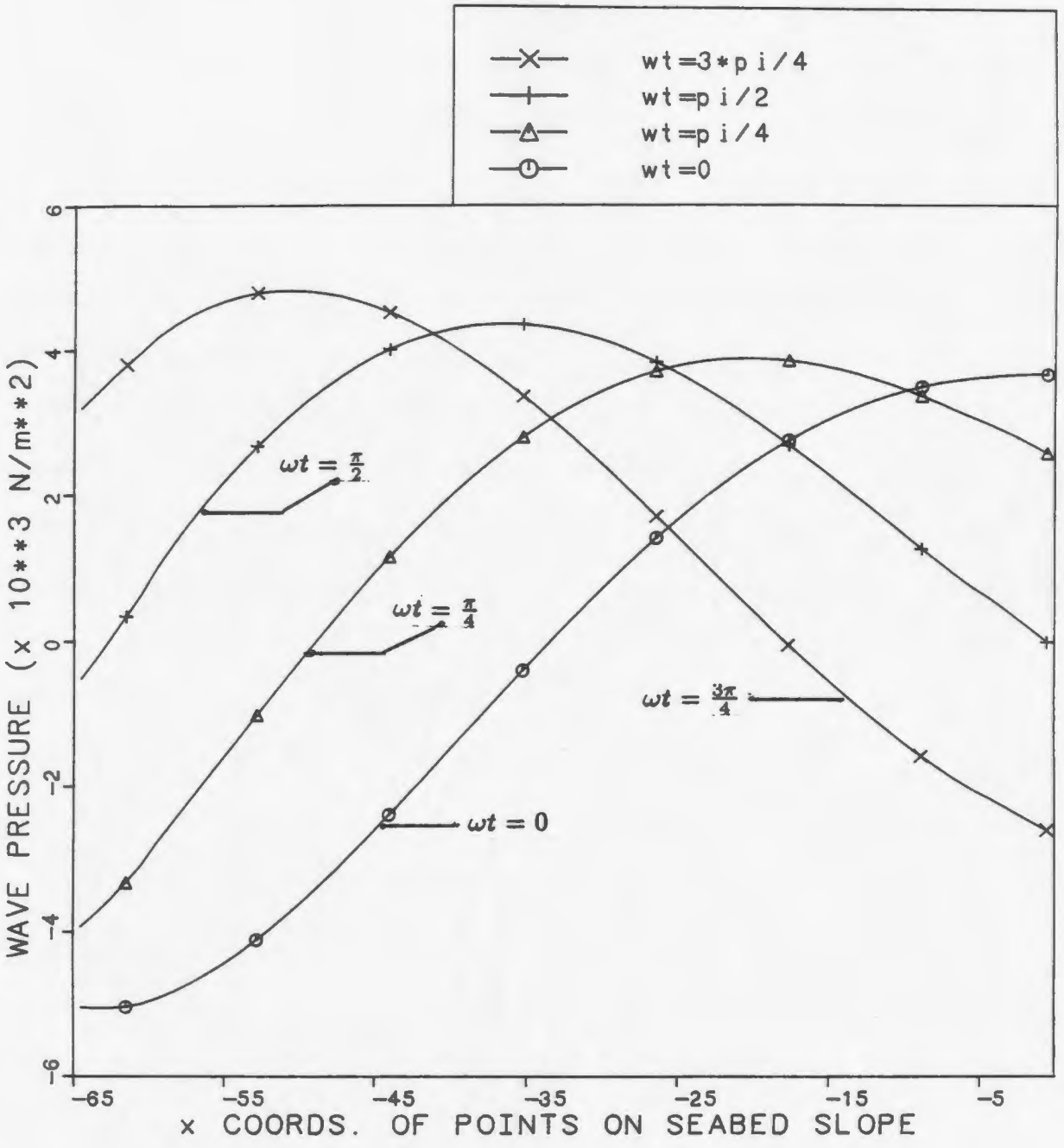

Figure 8.3: Wave Pressure on 12 deg. Slope : $L = 133.5m.$, $H = 16m.$
Water Depth at Slope Base ($x = 0$) $= 30\,m.$

by SURFACE II the contours are to be regarded as an approximate representation of the actual numerical results. In all cases (except figure 8.11) a wave height of $24m$ was used. The conjugate stress ratio K was taken to be 0.5 except in figures (8.13) to (8.15). The distances d, d_0, d_0' in Figure (7.1) are $65m, 5m$ and $5m$ respectively. The water depth at C (Figure 7.1) was kept at $80m$ and the depth at B varied from $78m$ for the 2° slope to $60m$ for the 20° slope. Similarly, the soil depth l_0 at C was kept at $20m$, with the depth l_0' at B varying from $22m$ for the 2° slope to $40m$ for the 20° slope. In only two cases was it necessary to deviate from this pattern, viz. the cases of fine sand, $\beta = 20^\circ$ with $L = 225m$ and $150m$. In these cases we chose $l_0 = 17m, l_0' = 37m$ and $l_0 = 14m, l_0' = 34m$ respectively. The reason for these changes is that numerical overflow problems were encountered when generating the boundary conditions on BR (using the method of Appendix I). The effect of the changes is that the boundary conditions on RS (Figure 7.1) is applied at a smaller depth than would otherwise have been the case. In order to investigate this further we have tested the case of Figure (8.4) (fine sand, $L = 300m, \beta = 20^\circ$) with the location of the boundary RS determined by $l_0 = 14m$ and $l_0' = 34m$. The contours obtained (shown in Figure J.1) are of the same pattern as in Figure (8.4), although in some places the failure zone ($\theta \geq 30^\circ$) is not as deep.

The soil data is as follows :

Shear modulus G (Nm^{-2})	1.0×10^7
Poisson's ratio ν	0.33
Porosity f	0.3
Permeability k_0 (ms^{-1})	1.0×10^{-4}(fine sand)
	1.0×10^{-2} (coarse sand)
Density of soil grains $\rho_s(kgm^{-3})$	2.7×10^3

The bulk modulus of the pore water, K_f, was taken as $2.3 \times 10^9 Nm^{-2}$.

As expected, the plots indicate that for a given slope angle the longer wavelengths produce the greater failure zones, and for a given wavelength the greater failures are observed in the steeper slopes. In most cases, there is no significant difference in the extent of the failure zones (hereafter termed the failure profile) for fine sand ($k_0 = 10^{-4} ms^{-1}$) and coarse sand ($k_0 = 10^{-2} ms^{-1}$). We observe, however, for $\beta = 20°, L = 300m$ and $225m$ the failure zones ($\theta \geq 30°$) in fine sand (Figures 8.4 and 8.5) are slightly deeper than in coarse sand (Figures 8.6 and 8.7). Also, in these cases, failure conditions in fine sand persist at $\omega t = \pi$, whereas this is not so in coarse sand.

The plots also illustrate the variation in the failure profile throughout the course of a wave cycle. The contours are shown for the instants $\omega t = 0, \frac{\pi}{2}, \pi, \frac{3\pi}{2}$. As the wave cycle progresses in time the responses of the soil skeleton and pore water also go through a cycle, out of phase with the wave cycle. The phase lag is quite easily computed from the arguments of the complex effective stresses and pore pressures determined by the boundary element method. We emphasize that the skeleton and pore water do not respond independently : the responses are coupled as described

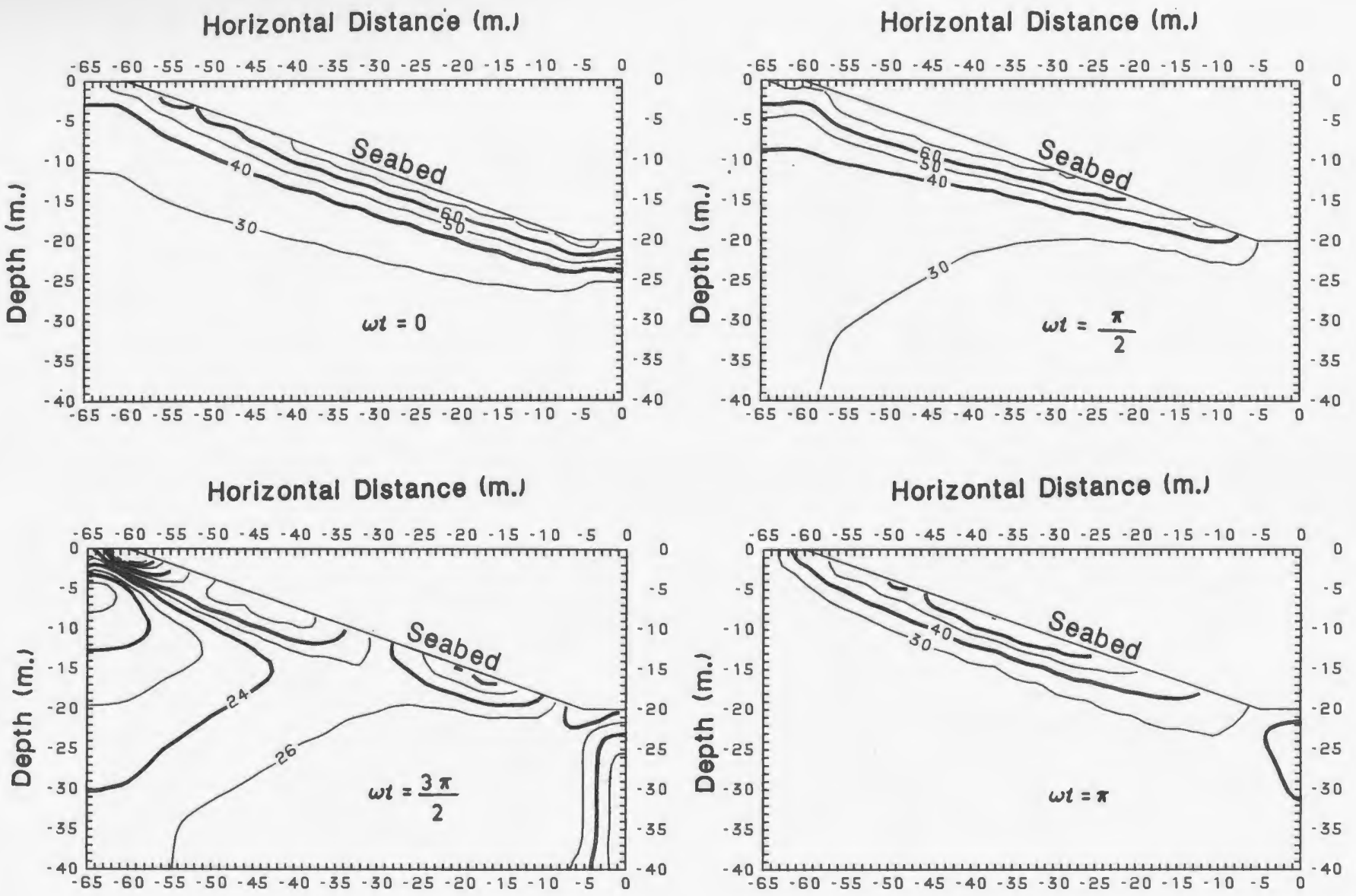

Figure 8.4: Stress Angle Contours(degrees): Fine Sand, $K = 0.5$, $L = 300$ m, $\beta = 20^o$

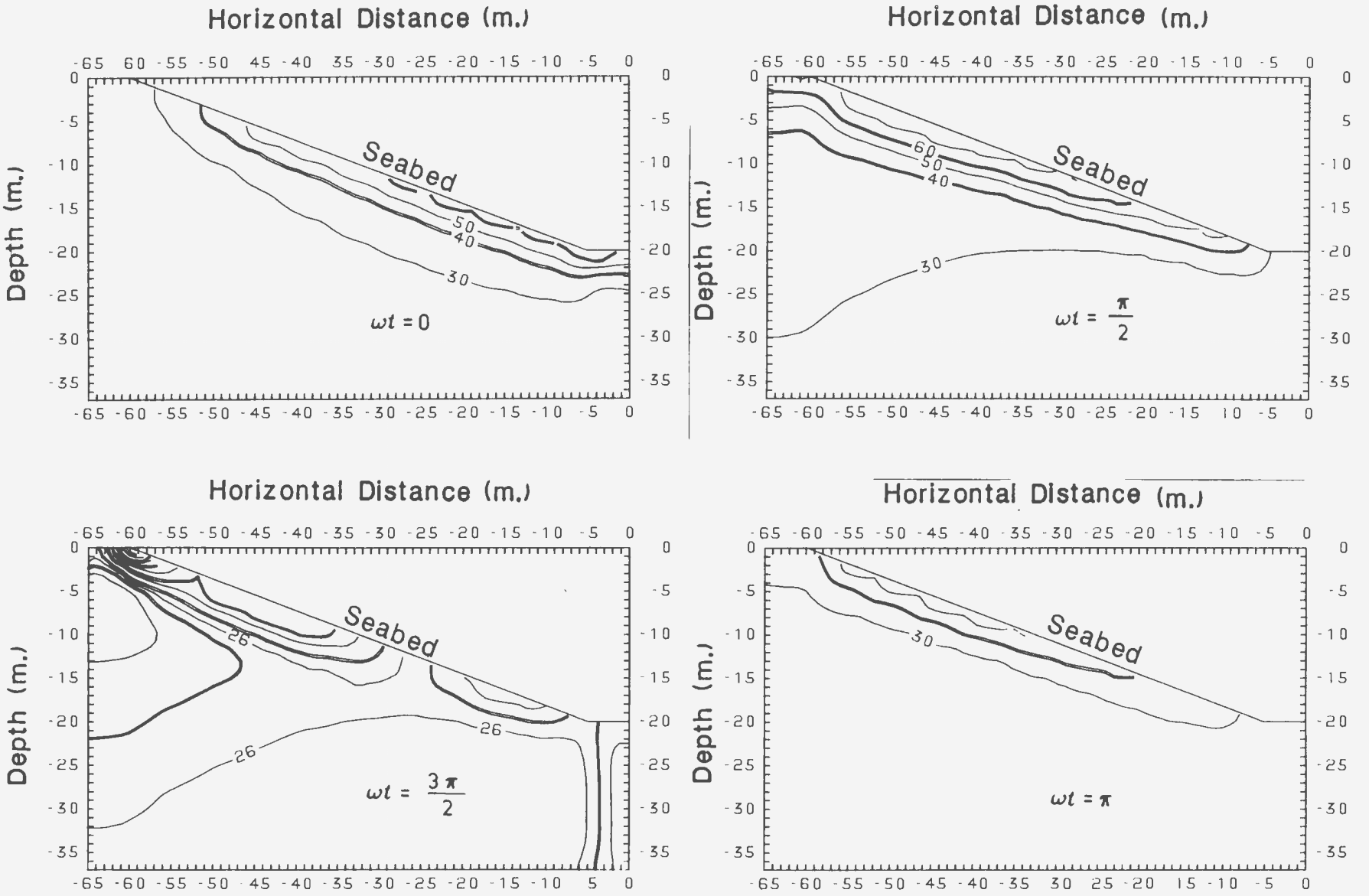

Figure 8.5: Stress Angle Contours(degrees): Fine Sand, $K = 0.5$, $L = 225$ m, $\beta = 20^o$

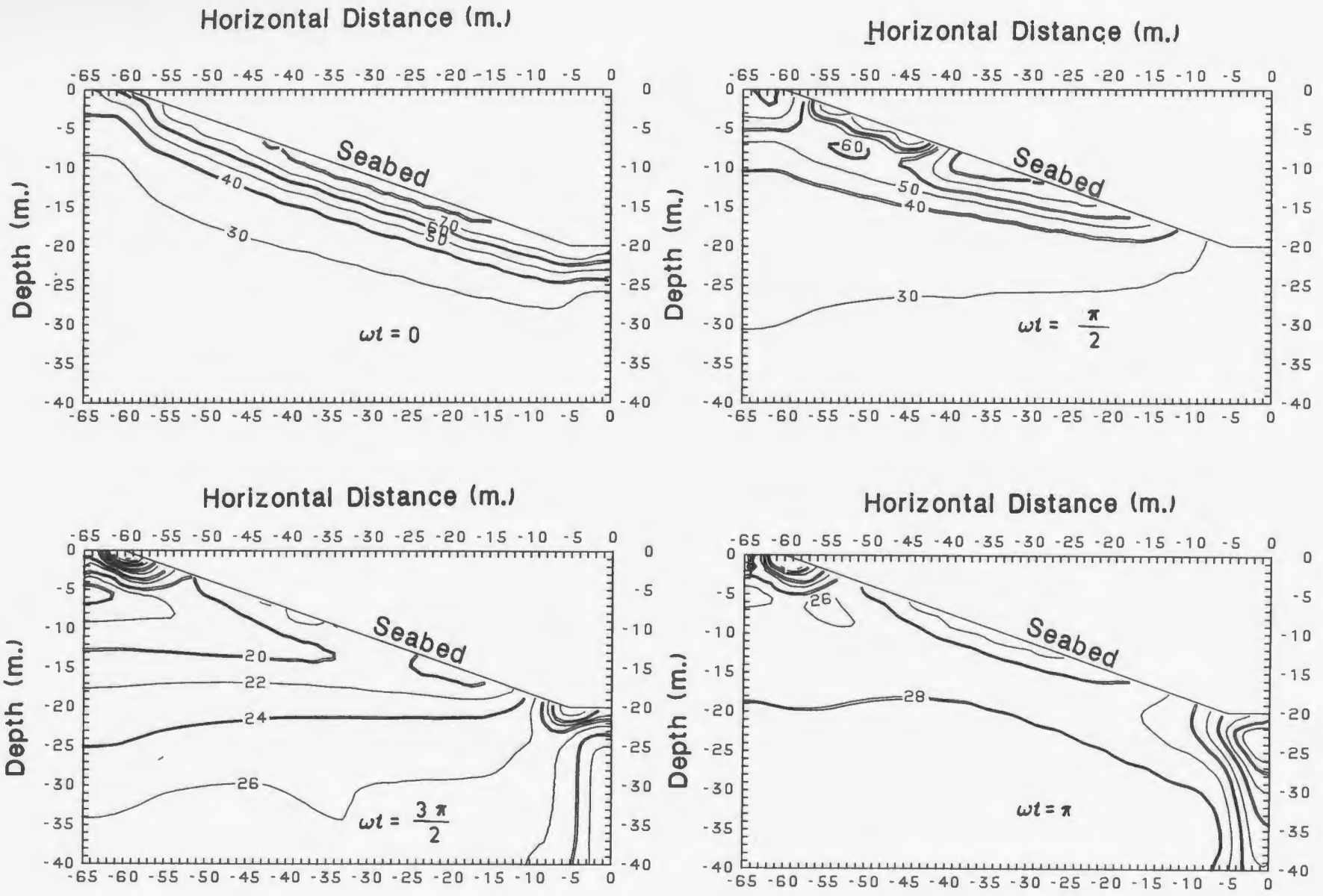

Figure 8.6: Stress Angle Contours(degrees):Coarse Sand,$K = 0.5$, $L = 300$ m, $\beta = 20^o$

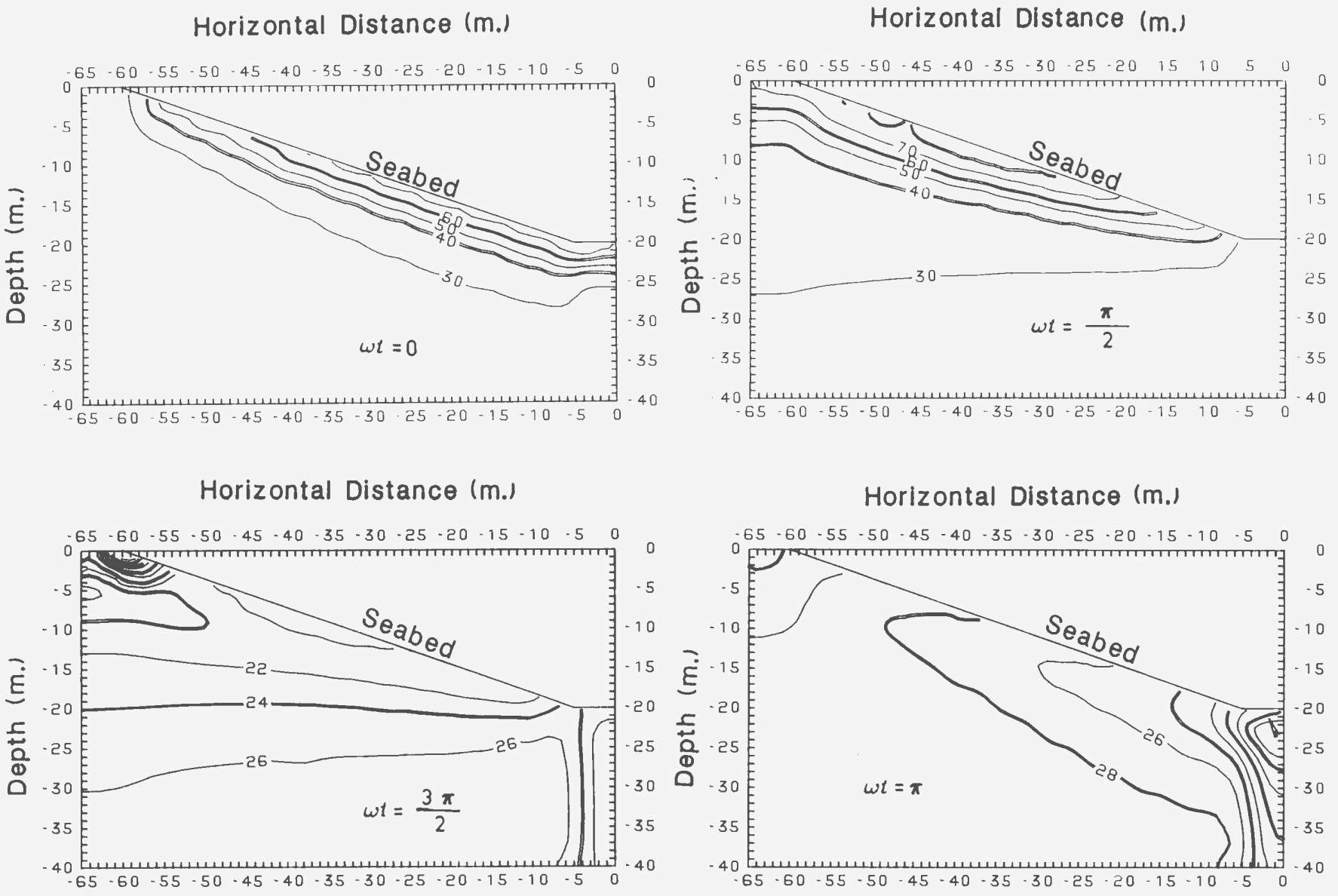

Figure 8.7: Stress Angle Contours(degrees): Coarse Sand, $K = 0.5$, $L = 225$ m, $\beta = 20^o$

by the Biot equations. At certain instants in the wave cycle the effective stresses at several points are such that the Mohr circles touch or cross the failure criterion. At other instants the effective stresses produce Mohr circles which are quite distant from the failure criterion, this being the result of negative wave-induced pore pressures. It is therefore necessary to examine the stability characterisitcs of the slope throughout the wave cycle in order to assess the likelihood of failure. For the time instants plotted, the greatest failure zones are observed at $\omega t = \frac{\pi}{2}$ in most cases.

The stress angle contours in a flat bed of coarse sand (computed from the analytic solution), with $L = 300m, K = K_0 = 0.5$ are shown in Figure (8.8). If we compare this with the plots for slopes of 5^o and 2^o in coarse sand with $L = 300m$ (Figures 8.9 and 8.10) we notice that the failure profiles and failure depths are similar. This means that for gentle slopes of the order of 5^o or less we can determine approximately the extent of the failure zones by using the analytic solution for a flat seabed described in Appendix I.

In Figure(8.11), we illustrate the stress angle contours in coarse sand corresponding to the wave loading described by Figure (8.3), i.e. a wave of length $133.5m$ and $16m$ height in $30m$ of water incident on a 12^o slope. We have already noted that such a wave would produce more than twice the maximum pressures than it would in $80m$ of water at a wavelength of $150m$, and a greater height of $24m$. The stress angle contours for this latter case are illustrated in Figure(8.12). Accordingly, the failure zones illustrated in Figure (8.11) are much greater than those illustrated in Figure (8.12).

We have also investigated the effect of the initial stress distribution as determined by the value of the conjugate stress ratio K. Stress angle contours in coarse

Table 8.1: In Situ Stress Angle θ_0 (deg)

β (deg)	$K = 0.5$	$K = 0.7$	$K = 1.0$
2	19.6	10.4	2.0
5	20.1	11.3	5.0
12	22.7	15.7	12.0
20	27.6	22.3	20.0

sand at $\omega t = \frac{\pi}{2}$ ($L = 300m$) are shown in Figures (8.13) and (8.14) for $K = 0.7$ and 1.0. We find that at these values of K the extent of the failure zones is considerably smaller than at $K = 0.5$ (compare, for example, Figures (8.13),(8.14), $\beta = 20°$ with Figure (8.6), $\omega t = \frac{\pi}{2}$). The reason for this becomes obvious when we examine the stress angle θ_0 under in-situ stress conditions. This is easily computed from equations (7.9) and (7.17) as

$$\theta_0 = \sin^{-1}[\frac{(K^2 - 2K\cos 2\beta + 1)^{\frac{1}{2}}}{K+1}] \tag{8.1}$$

For normally consolidated soils the in-situ horizontal effective stress is less than the vertical effective stress, i.e. $\sigma_x'^{(0)} < \sigma_z'^{(0)}$. From (7.9) we find that

$$\sigma_x'^{(0)} < \sigma_z'^{(0)} \Longrightarrow K < \frac{1}{\cos 2\beta} \tag{8.2}$$

Values of θ_0 for different values of K and β satisfying (8.2) are given in table (8.1). During the parts of the wave cycle in which the horizontal effective stress is decreased and the vertical effective stress is increased, the stress angle θ increases above its in-situ value. If it increases to the extent that $\theta \geq \phi'$, failure occurs in a manner analogous to "active" failure, e.g. at $\omega t = \frac{\pi}{2}$. We note from table (8.1) that the in-situ stress angle θ_0 decreases as K goes from 0.5 to 1.0. This means that

at $K = 0.5$ the unloaded slope is closer to wave induced failure than at $K = 1.0$. In some cases, e.g. $L = 150m, \beta = 12°, K = 0.7$ and 1.0, there is only minimal failure (Figures J.21 and J.22).

In some soils the in-situ horizontal effective stress is larger than the vertical effective stress i.e. $\sigma_x'^{(0)} > \sigma_z'^{(0)}$. Such a situation may occur if the soil has been subjected in the past to heavy overburden stresses which have since been removed over the course of its history. In this case the stress angle is increased during the parts of the wave cycle in which the horizontal effective stresses are increased and the vertical effective stresses reduced. Again if $\theta \geq \phi'$ failure occurs, but this time in a manner analogous to "passive" failure. Such a situation is shown in Figure (8.15) for a coarse sand, $L = 300m$, $\beta = 20°$ at $\omega t = \pi$, where we have taken $K = 2$. As an example we examine the stress state at the point with horizontal and vertical coordinates of (-54.5, -7.6) in Figure (8.15). The in-situ stresses are (for $K = 2$)

$$\sigma_x'^{(0)} = 0.1155 \times 10^6 Nm^{-2}$$

$$\sigma_z'^{(0)} = 0.8064 \times 10^5 Nm^{-2}$$

$$\tau_{xz}'^{(0)} = 0.4199 \times 10^5 Nm^{-2}$$

We note that $\sigma_x'^{(0)} > \sigma_z'^{(0)}$. The in-situ stress angle θ_0 is 27.6°. The wave induced stresses are shown in table (8.2) at several instants in the wave cycle. At $\omega t = 0$ and $\frac{\pi}{2}$ the wave reduces the horizontal effective stresses and increases the vertical effective stresses thus tending to reduce the stress angle from its in-situ value. The resultant stress angles are in fact 21.7° and 25.1° at $\omega t = 0$ and $\frac{\pi}{2}$ respectively. At $\omega t = \pi$ and $\frac{3\pi}{2}$ the wave pressures are reversed and the Mohr circle expands as the horizontal stress increases and the vertical stress decreases. The resultant

Table 8.2: Wave Induced Stresses ($\times 10^4\, Nm^{-2}$) at (-54.5,-7.6) in Figure (8.15)

Stress Component	$\omega t = 0$	$\omega t = \frac{\pi}{2}$	$\omega t = \pi$	$\omega t = \frac{3\pi}{2}$
σ'_x	-0.9694	-2.143	0.9694	2.143
σ'_z	0.5819	0.3287	-0.5819	-0.3287
τ'_{xz}	-0.7634	-0.4510	0.7634	0.4510

stress angles are 33.8° and 31.0° respectively, indicating that the failure criterion ($\theta \geq 30°$) has been violated. The failure zone at $\omega t = \pi$ is particularly extensive as shown in Figure (8.15).

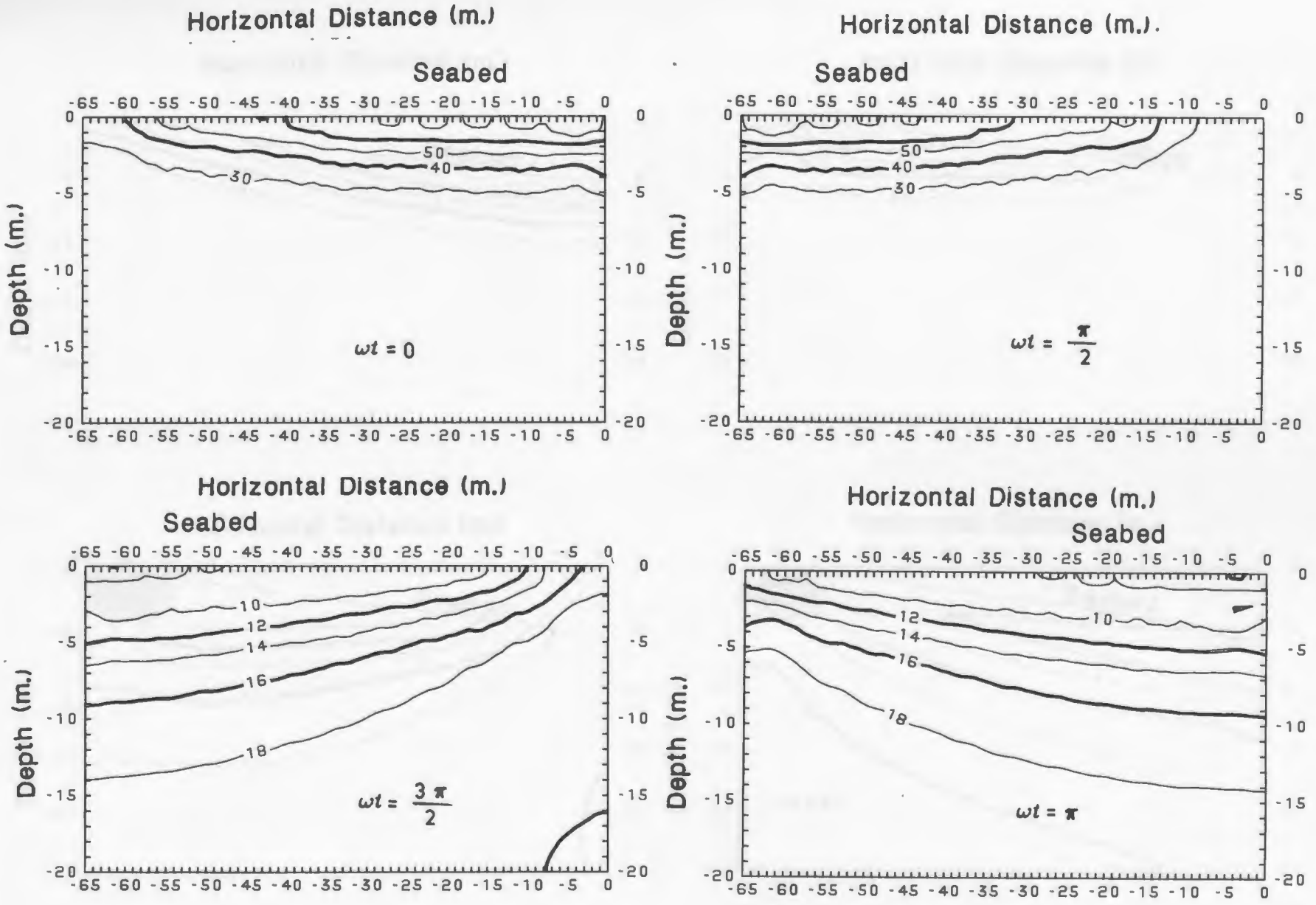

Figure 8.8: Stress Angle Contours(degrees),Analytic Solution for Flat Bed :Coarse Sand,$K = 0.5, L = 300$ m

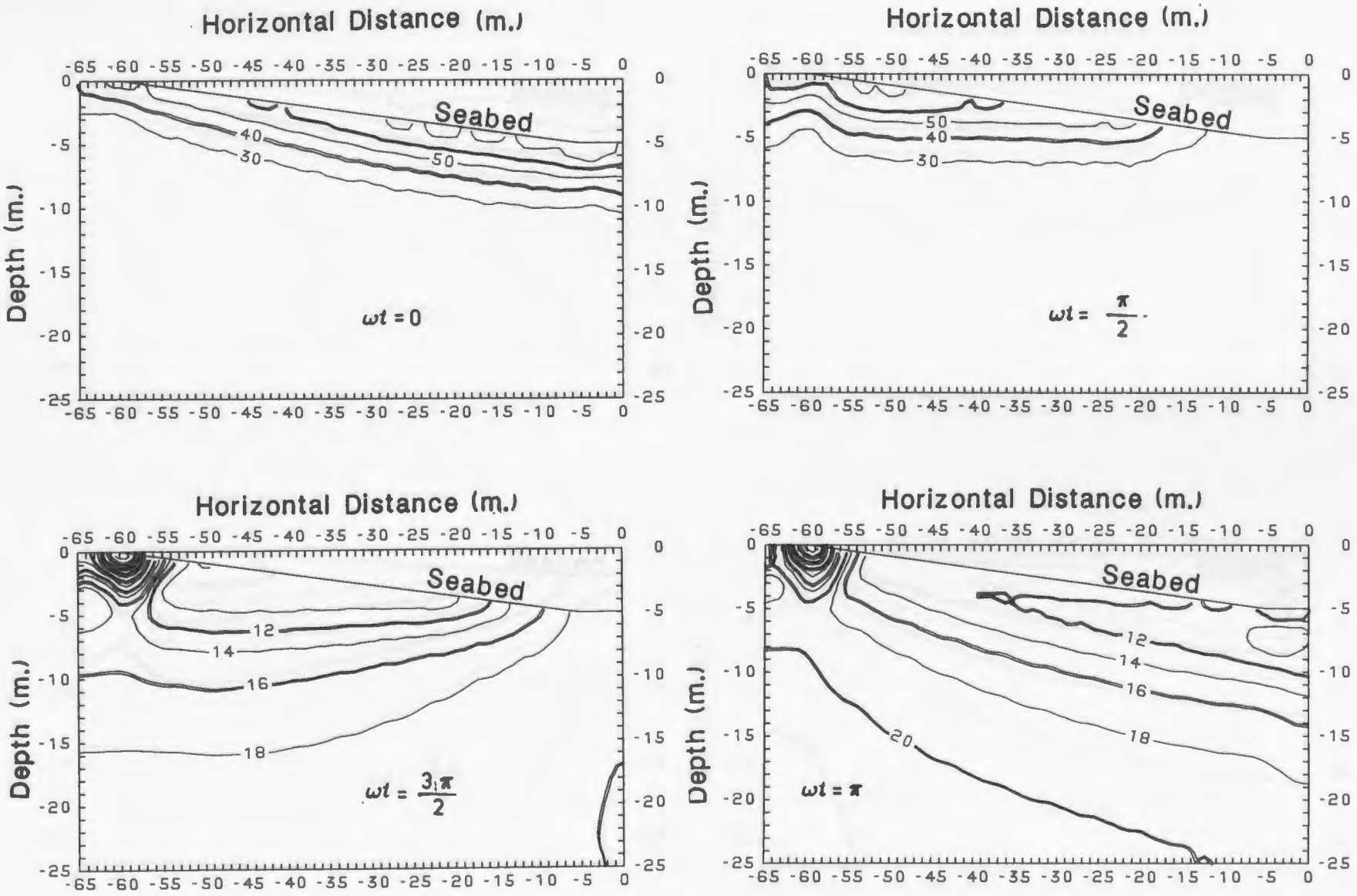

Figure 8.9: Stress Angle Contours(degrees): Coarse Sand,$K = 0.5$, $L = 300$ m, $\beta = 5^o$

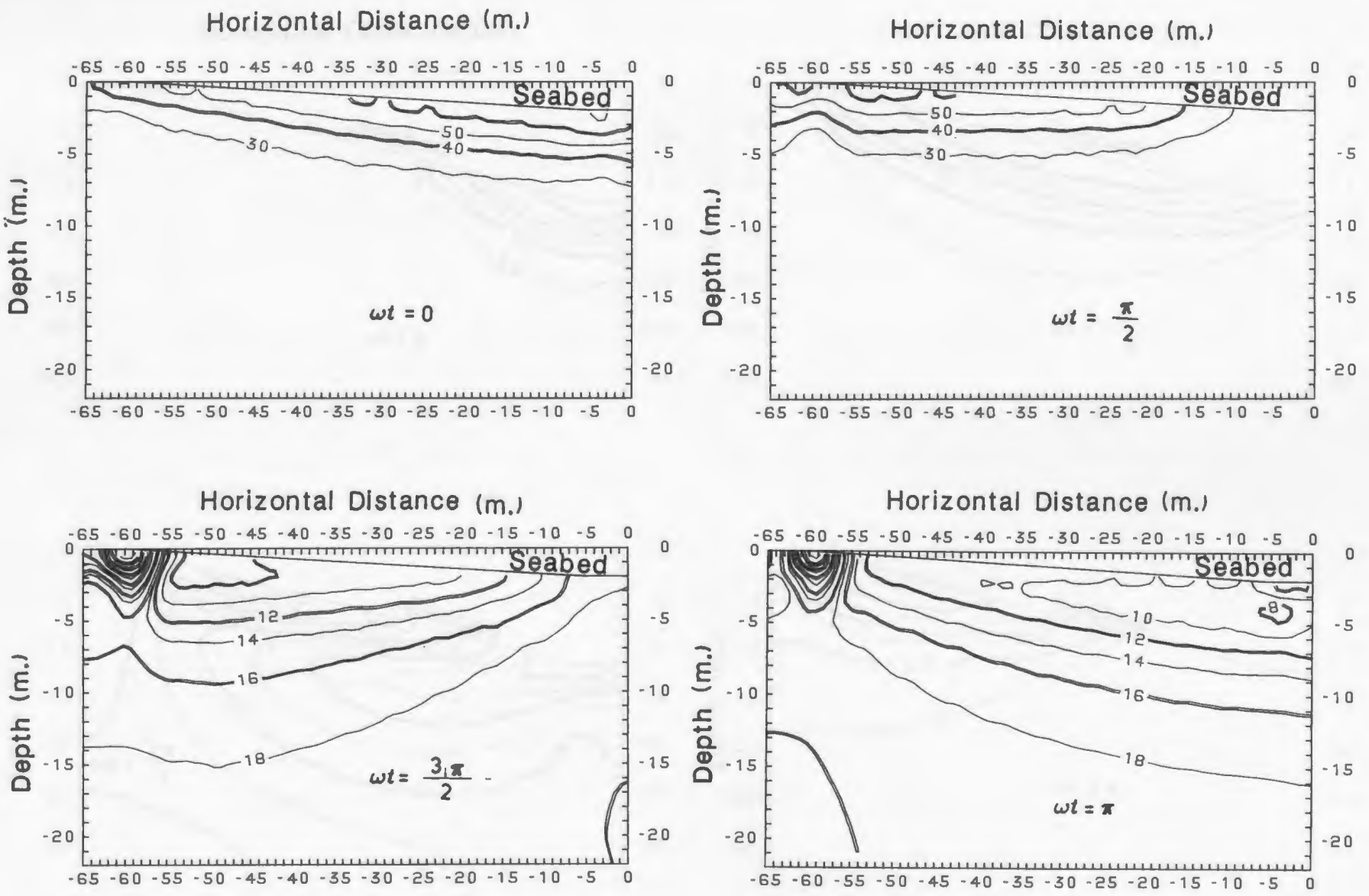

Figure 8.10: Stress Angle Contours(degrees): Coarse Sand,$K = 0.5$, $L = 300$ m, $\beta = 2^o$

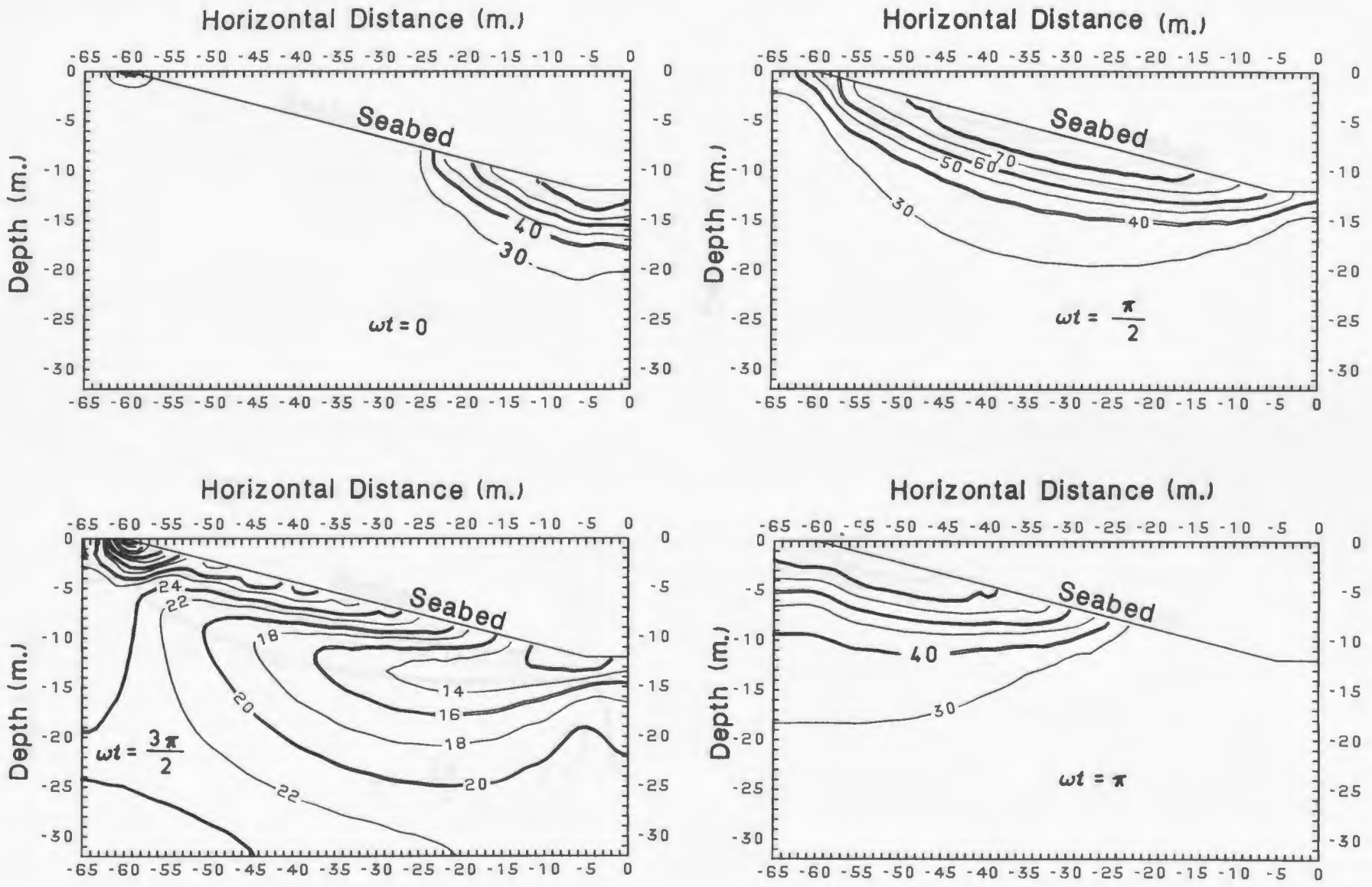

Figure 8.11: Stress Angle Contours(degrees): Coarse Sand, $K = 0.5$, $L = 133.5$ m, $\beta = 12^o$
$h_0 = 30$ m, $h_0' = 18$ m, $\eta_0 = 8$ m

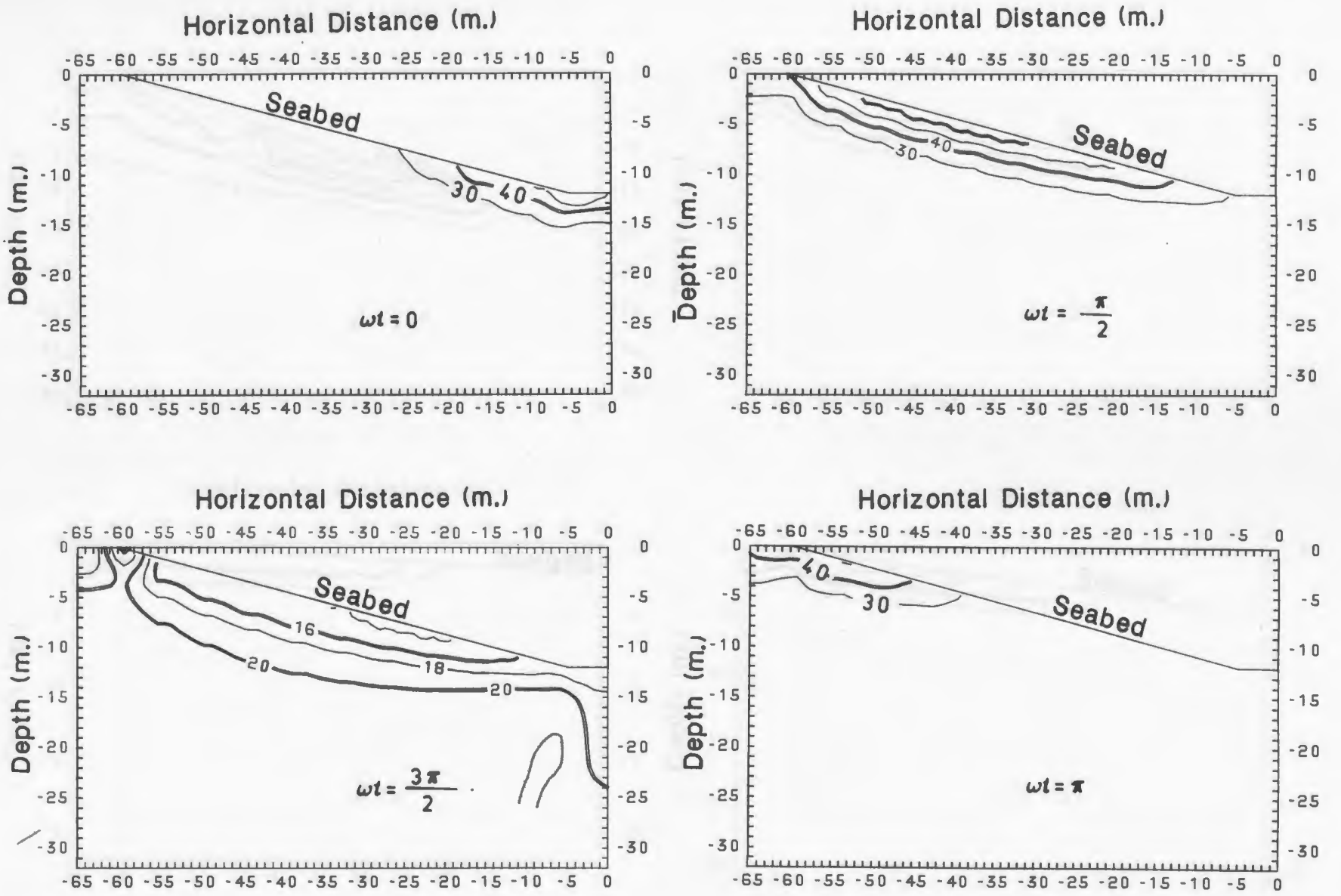

Figure 8.12: Stress Angle Contours(degrees): Coarse Sand, $K = 0.5$, $L = 150$ m, $\beta = 12^o$
$h_0 = 80$ m, $h_0' = 68$ m, $\eta_0 = 12$ m

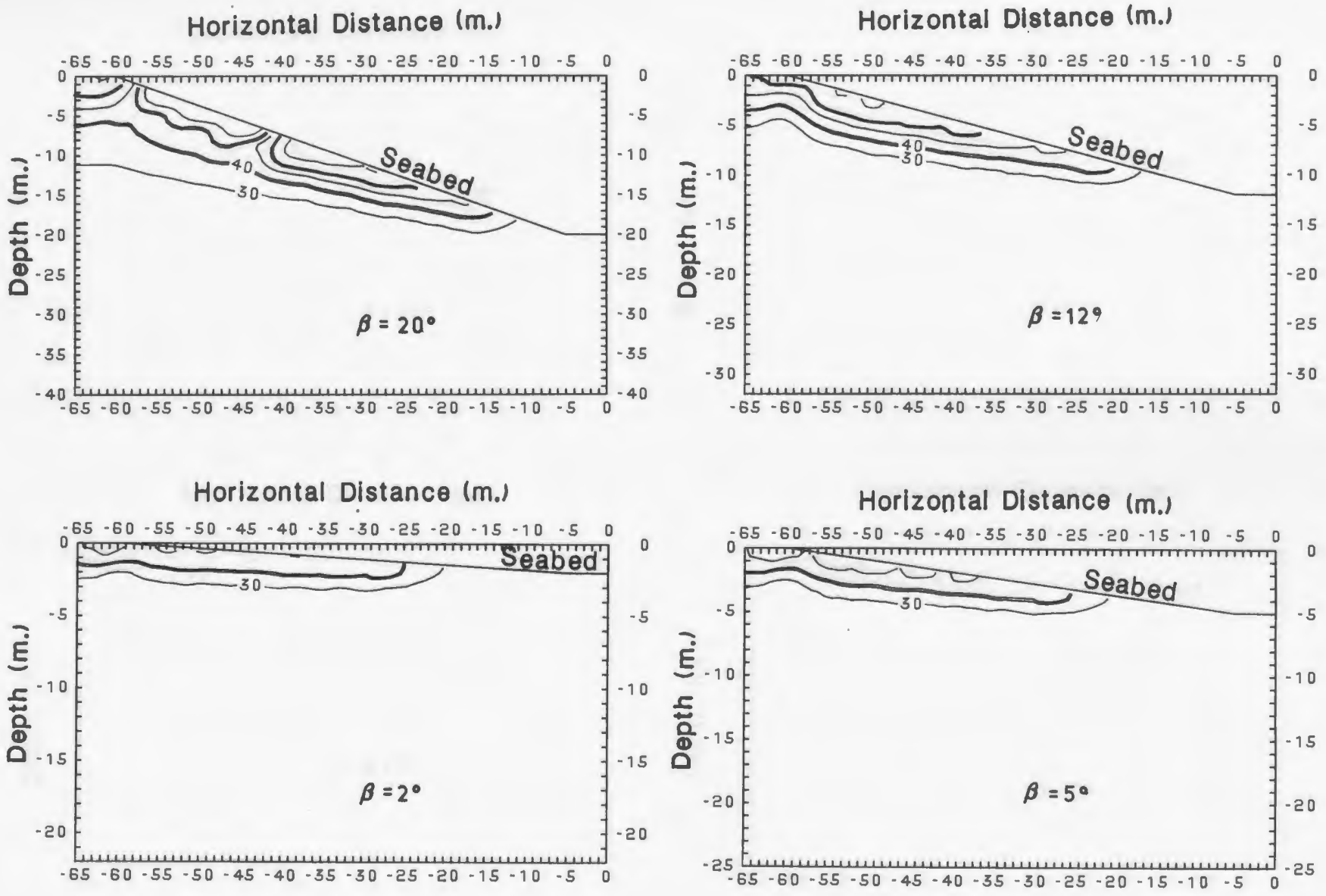

Figure 8.13: Stress Angle Contours(degrees): Coarse Sand, $L = 300$ m, $\omega t = \frac{\pi}{2}$, $K = 0.7$

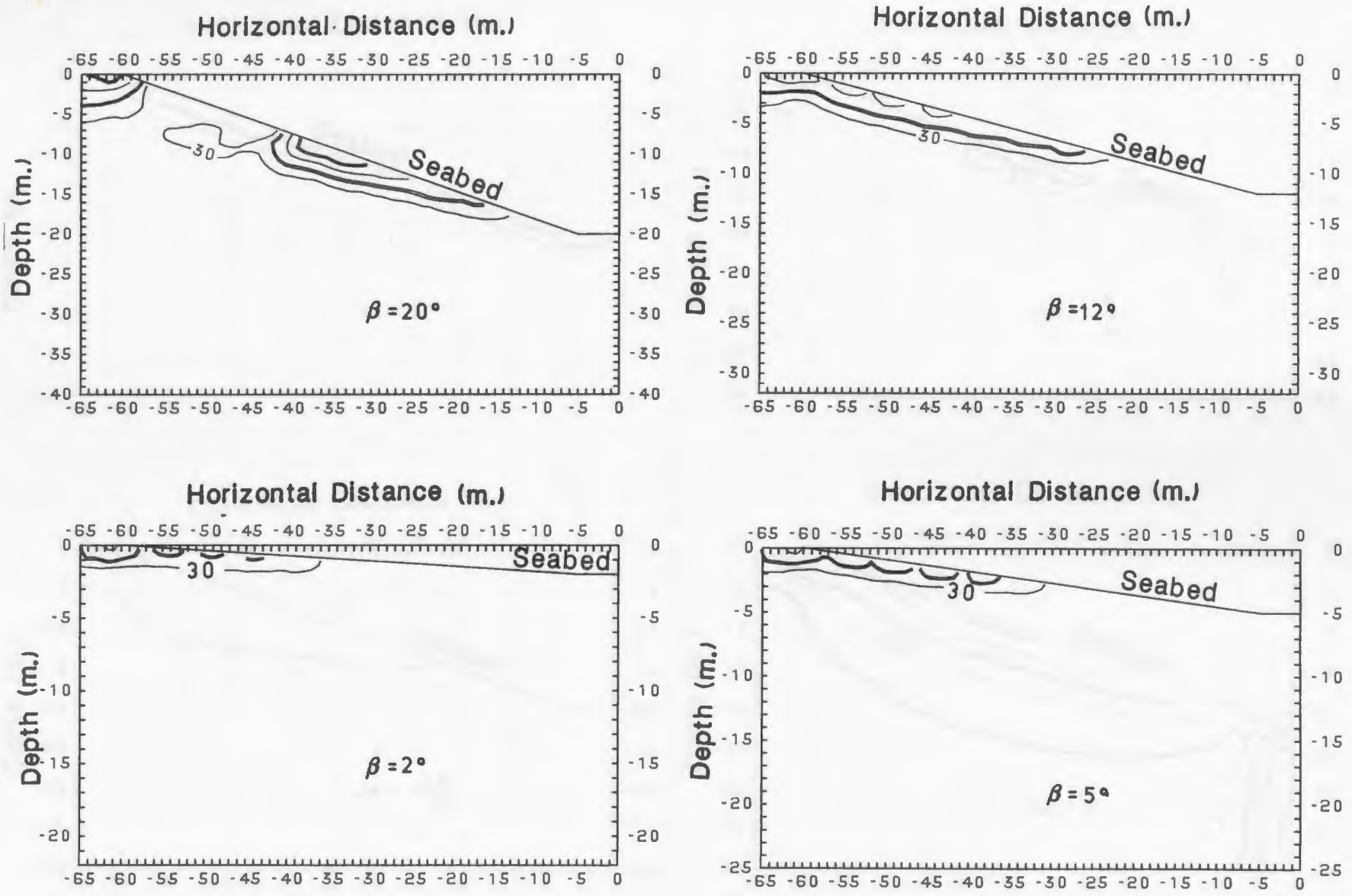

Figure 8.14: Stress Angle Contours(degrees): Coarse Sand, $L = 300$ m, $\omega t = \frac{\pi}{2}$, $K = 1.0$

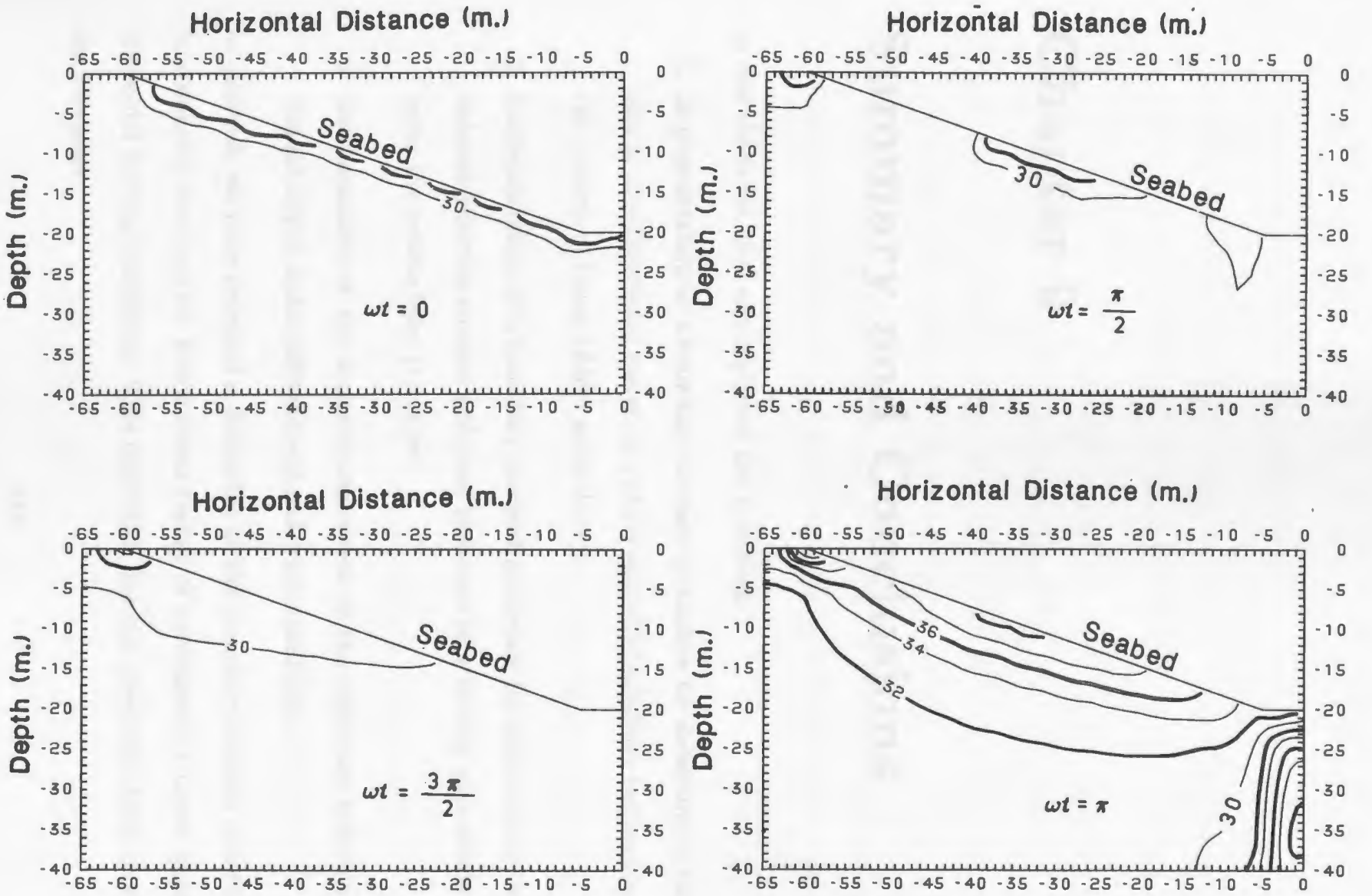

Figure 8.15: Stress Angle Contours(degrees): Coarse Sand, $L = 300$ m, $\beta = 20^o$, $K = 2.0$

Chapter 9

Summary and Conclusions

In this thesis we have accomplished the following:

1. Implementation of a boundary element procedure for determining the forces due to uni-directional waves on a plane seabed of arbitrary inclination within the context of linear (Airy) wave theory.

2. Implementation of a boundary element procedure for determining the wave-induced effective stresses and pore pressures in a sloping poroelastic seabed using the results from (1) above.

3. Determination of the approximate extent of the minimum failure zones in various slopes under different soil and wave conditions.

In addition, we have provided a derivation of the boundary integral equations and fundamental solutions for Biot's linear theory of poroelasticity under quasi-static sinusoidal loading conditions. This derivatior has not previously been recorded in the literature.

The following conclusions may be drawn :

(a). The boundary element technique is very accurate, as evidenced by the comparisons made with analytic solutions for flat beds.

(b). As expected, for a given slope angle the longer wave lengths produce the greater failure zones and for a given wavelength, the greater failures are observed in the steeper slopes. Also, a wave that is relatively harmless in deep water can cause significant failure in shallower water.

(c). There is no significant difference in the extent of the failure zones for fine sand ($k_0 = 10^{-4} ms^{-1}$) and coarse sand ($k_0 = 10^{-2} ms^{-1}$) although in some cases the failure zone in fine sand is slightly deeper.

(d). It is necessary to evaluate the stability characteristics of the slope throughout the wave cycle in order to assess the likelihood of failure.

(e). For gentler slopes, of the order of 5° or less, the failure zones may be located with sufficient accuracy by using the analytic solution of Appendix I, i.e. we can avoid the complexity of the BEM for such cases.

(f). The failure profile is strongly dependent on the initial state of stress in the slope as determined by the conjugate stress ratio K. For normally consolidated soils, the failure zone decreases in sizes as K increases, with K remaining in the range for which $\sigma_x'^{(0)} < \sigma_z'^{(0)}$. In such soils the maximum wave-induced failure occurs in a manner analogous to active failure. For some overconsolidated soils we may have $\sigma_x'^{(0)} > \sigma_z'^{(0)}$ and in such cases the

maximum wave induced failure occurs in a manner analogous to passive failure. In these cases , larger K values mean that the in-situ soil condition is closer to passive failure.

Suggestions for Further Research

(1) In order to account for the volume changes of soil under cyclic loading modifications to the original Biot formulation are required, as suggested by Verruijt (1985). Perhaps the phenomenon of pore pressure buildup under cyclic loading may be analysed in this way. Further research is also required to model the non-linear, time dependent and anisotropic behaviour of soil.

(2) The propagation of the soil failure illustrated in this thesis needs to be studied by means of some form of elasto-plastic analysis.

(3) Wave-induced stresses of layered soils can be easily studied by the methods described in the thesis. It will be necessary to divide the domain into sub-domains, generate a system of equations for each sub-domain, and match boundary conditions at common boundaries.

(4) Earthquake-induced stresses in a poroelastic medium can be determined by including the acceleration terms in the governing equations. This would involve the derivation of a new boundary integral equation and fundamental solutions.

(5) The study of axisymmetric and three-dimensional problems is a fruitful extension of the methods presented herein.

References

- Abramowitz, M. and Stegun, I. (1972).*Handbook of Mathematical Functions*, Dover.

- Alliney, S. (1981).“ A Numerical Study of Water Waves on Sloping Beaches” *Applied Math. Modelling*, Vol. 5, pp. 321-328.

- Aramaki, G. and Yasuhara, K. (1985). “ Application of the Boundary Element Method for Axisymmetric Biot's Consolidation,” *Engineering Analysis*, Vol. 2, No. 4, pp. 184-191.

- Barends, F. and Calle, E. (1985). “ A Method to Evaluate the Geotechnical Stability of Offshore Structures Founded on a Loosely Packed Seabed Sand in a Wave Loading Environment,”*Behavior of Offshore Structures*, pp. 643-652.

- Bea, R.G. (1971). “ How Seafloor Slides Affect Offshore Structures,” *Oil and Gas Journal*, Nov. 1971. pp. 88-92.

- Bell, K.; Hansteen, O.; Larsen, P.; Smith, E. (1976). “ Analysis of a Wave-Structure-Soil System,”*Behavior of Offshore Structures*, pp. 846-863.

- Biot, M.A. (1941). “ General Theory of Three Dimensional Consolidation,” *Journal of Applied Physics*, Vol. 12, pp. 155-164.

- Biot, M.A. (1955). “ Theory of Elasticity and Consolidation for a Porous Anisotropic Solid,”*Journal of Applied Physics*, Vol. 26, pp. 182-185.

- Biot, M.A. (1956). “ Theory of Deformation of a Porous Viscoelastic Anisotropic Solid,” *Journal of Applied Physics*, Vol. 27, No. 5, pp. 459-467.

- Biot, M.A. (1962)." Mechanics of Deformation and Acoustic Propagation in Porous Media,"*Journal of Applied Physics*, Vol. 33, No. 4, pp. 1482-1498.
- Biot, M.A. (1963)." Theory of Stability and Consolidation of a Porous Medium Under Stress,"*Journal of Mathematics and Mechanics*, Vol. 12, No. 4, pp. 521-541.
- Biot, M.A. (1965).*Mechanics of Incremental Deformations*, New York, John Wiley&Sons.
- Biot, M.A. and Willis,D.G. (1957)."The Elastic Coefficients of the Theory of Consolidation",*Journal of Applied Mechanics*, Vol. 24, pp. 594-601.
- Bouckovalas, G.; Whitman, R.V.; Marr, W.A. (1984). " Permanent Displacement of Sand With Cyclic Loading,"*Journal of Geotechnical Engineering*, ASCE, Vol., 110 No. 11, pp. 1629-1653.
- Bowles, J. (1984). *Physical and Geotechnical Properties of Soils*, 2nd ed., McGraw Hill Book Co., New York, 578 pp.
- Brebbia, C.A., Telles,J.C.F. and Wrobel, L.C. (1984). *Boundary Element Techniques, Theory and Applications in Engineering*, Springer-Verlag.
- Cheng, A.H-D. and Liggett, J. (1984). " Boundary Integral Equation Method for Linear Porous-Elasticity With Applications to Soil Consolidation," *International Journal for Numerical Methods in Engineering*, Vol. 20,pp. 255-278.
- Cheng, A.H-D. and Liu, P. (1986). " Seepage Force on a Pipeline Buried in a Poroelastic Seabed Under Wave Loading," *Applied Ocean Research*, Vol. 8, No. 1, pp. 22-32.

- Chowdhury, R.N. (1978). *Slope Analysis*, Developments in Geotechnical Engineering, Vol. 22, Elsevier Scientific Publishing Co.,Amsterdam, 423 pp.

- Cleary, M.P. (1977)." Fundamental Solutions for a Fluid-Saturated Porous Solid,"*International Journal of Solids and Structures*, Vol. 13, pp. 785-806.

- Clukey, E.C. and Turcotte, B.R. (1984). " Experimental Study of Effective Stress Response of Sand Under Water Wave Loading," *Offshore Technology Conference*, 4695, pp. 413-421.

- Davies ,M.H. (1985)." Pore Pressure Development in Sand Beds,"*Proc. Canadian Coastal Conference*, St. John's, Nfld.

- Dean, R.G. and Dalrymple, R.A. (1984).*Water Wave Mechanics for Engineers and Scientists,* Chap. 9, Prentice Hall Inc., Englewood Cliffs, New Jercey.

- Eubanks, R.A. and Sternberg, E. (1956). "On the Completeness of the Boussinesq-Papkovich Stress Functions",*Journal of Rational Mechanics and Analysis*, Vol. 5, No. 5, pp. 735-746.

- Finn, W. and Lee, M. (1979). " Seafloor Stability Under Seismic and Wave Loading,"*Proc. Soil Dynamics in the Marine Enviornment*, ASCE Reprint 3604.

- Finn, W.; Siddharthan, R.; Martin, G. (1983). " Response of Seafloor to Ocean Waves,"*Journal of Geotechnical Engineering*, Vol. 109, No. 4, pp. 556-572.

- Ghaboussi, J. and Wilson, E.L. (1973). " Flow of Compressible Fluid in Porous Elastic Media," *International Journal for Numerical Methods in Engineering*, Vol. 5, pp. 419-442.

- Hardin, B. and Drnevich, V. (1972). " Shear Modulus and Damping in Soils: Design Equations and Curves," *Journal of the Soil Mechanics and Foundations Division*, Proc. ASCE, Vol. 98. No. SM7, pp. 667-692.

- Henkel, D.J. (1970). " The Role of Waves in Causing Submarine Landslides," *Geotechnique* 20, No. 1, pp.75-80.

- Ishihara, K. and Yamazaki, A. (1984)." Wave Induced Liquefaction in Seabed Deposits of Sand", in *Seabed Mechanics*, edited by Bruce Denness, Graham and Trotman, chapter 12.

- Katsube, N. and Carroll, M.M. (1987)." The Modified Mixture Theory for Fluid-Filled Porous Materials: Theory",*Journal of Applied Mechanics*, Vol. 54, pp. 35-40.

- Kokkinowrachos, K. and Asorakas, S. (1985). " Hydrodynamic Analysis of Large Offshore Structures on Porous Elastic Seabed," *Proc. Fourth International O.M.A.E. Symposium*, Vol. 1, Dallas, Texas, pp. 172-181.

- Kraft, L.; Helfrich, S.; Suhayda, J.; Marin, J. (1985). " Soil Response to Ocean Waves,"*Marine Geotechnology*, Vol. 6, No. 2, pp. 173-203.

- Kuroki, T. and Ito, T. (1982). " Boundary Element Method in Biot's Linear Consolidation,"*Applied Math. Modelling*, Vol. 6, pp. 105-110.

- Lai, N. and Dominguez, R. (1975). " Determination of Wave -Induced Pressures in the Soil Media Contiguous to a Buried Pipeline," *P.O.A.C. Conference,* pp. 1059-1069.

- Liu, P. (1985). " Wave -Induced Pressures Under Gravity Structure," *(ASCE) Journal of Waterway, Port, Coastal, and Ocean Engineering*, Vol. 111, No. 1, pp. 111-120.

- Macpherson, H. (1978). " Wave Forces on Pipeline Buried in Permeable Seabed," *Journal of Waterway, Port, Coastal, and Ocean Division*, Proc. ASCE, Vol. 104, No. WW4, pp. 407-419.

- Madsen, O.S. (1978). " Wave-Induced Pore Pressures and Effective Stresses in a Porous Bed," *Geotechnique* 28, No. 4, pp. 377-393.

- Mei, C.C. (1982). " Analytical Theories for the Interaction of Offshore Structures With a Poro-Elastic Seabed," *Behavior of Offshore Structures (BOSS)*, Proceedings of the Third International Conference, Vol. 1, pp. 358-370.

- Mei, C.C. and McTigue,D.F. (1984). " Stresses in a Submarine Topography Under Ocean Waves," *Journal of Energy Resources Technology*, Vol. 106, pp. 311-318.

- Meimon, Y. and Lassoudiere, F. (1985). " Application to Design of Marine Foundations of a Complete Model for Cyclic Behavior of Soils," *Behavior of OffShore Structures (BOSS)*, Amsterdam: Elsevier Science Publishers B.V., pp. 785-796.

- Mitchell, R.J.; Tsui, K.K.; Sangrey,D.A. (1972). " Failure of Submarine Slopes Under Wave Action," *Proc. ASCE, Thirteenth International Coastal Engineering Conference*, Vol. 2, pp. 1515-1541.

- Bleistein, N. (1984). *Mathematical Methods for Wave Phenomena*,Chap 6., Academic Press Inc., 341 pp.

- Moshagen, H. and Torum, A. (1975). " Wave-induced Pressures in Permeable Seabeds " *Journal of the Waterways, Harbors, and Coastal Eng. Div., Proc. ASCE,* Vol. 101, No. WW1, pp. 49-57.

- Moshagen, H. and Monkmeyer, P. (1979). " Wave-induced Seepage forces on Embedded Offshore Structures " *Civil Engineering in The Oceans IV (ASCE),* Vol. 2, pp. 758-773.

- Mukherjee, S. and Morjaria,M. (1984). " On the Efficiency and Accuracy of the Boundary Element Method and the Finite Element Method", *International Journal for Numerical Methods in Engineering,* Vol. 20, pp. 515-522.

- Munro, J.; Cudworth, C. ; Rodger, A. (1985). " Soil-Structure Interaction in the Dynamic Response of an Offshore Structure ," *Behaviour of Offshore Structures (BOSS)*, Elsevier Science Publishers B.V., Amsterdam, pp. 939-950

- Mynett, A.E. and Mei, C.C. (1982). " Wave-induced Stresses in a Saturated Poroelastic Seabed Beneath a Rectangular Caisson ," *Geotechnique*,32, No.3, pp. 235-247

- O' Donnell, T.P. (1982).“ The Effect of Waves on Structures Founded in a Permeable Seabed ,” *M.Sc. thesis*, Cornell University.

- Okusa, S. (1985). “ Wave-induced Stresses in Unsaturated Submarine Sediments,” *Geotechnique*, 35, No.4, pp. 517-532

- Oner, M. and Janbu, N. (1975). “ Dynamic Soil-Structure Interaction in Offshore Storage Tanks,” *Proc. Int. Symp. Soil Mechanics*, Istanbul, Bull. 9, Geotechnical Div., Norwegian Inst. of Technology.

- Potts, D.M. and Windle, D.(1985).“ A Numerical Study of the Foundation Behaviour of a Proposed North Sea Gravity Platform,” *Behaviour of Offshore Structures (BOSS)*, Elsevier Science Publishers B.V. Amsterdam, pp. 665-672.

- Predeleanu, M. (1981). “ Boundary Integral Method for Porous Media,” *Proc. of the Third Int. Seminar on Boundary Element Methods*, Irvine, California, ed. by C.A. Brebbia, pp. 325-334.

- Pre'vost, J.H.; Hughes, T.J.R.; Cohen, M.F. (1980).“ Analysis of Gravity Offshore Structure Foundations,” *Journal of Petroleum Technology*,Feb., pp. 199-209.

- Putnam, J.A. (1949). “ Loss of Wave Energy due to Percolation in a Permeable Sea Bottom ,” *Trans. of the American Geophysical Union*, Vol. 30, No. 3.

- Rahman, .M.S.; Seed, H.B.; Booker, J.R. (1977).“ Pore Pressure Development under Offshore Gravity Structures,” *Journal of the Geotechnical Eng. Div.*,

Proc. of the ASCE, Vol. 103, No. GT12.

- Rahman, M.S. and Layas, F.M. (1985).“ Probabilistic Analysis for Wave-induced Submarine Landslides,” *Marine Geotechnology*, Vol. 6, No. 1, pp. 99-115.

- Raman-Nair, W.W. (1985).“ Stress Analysis of a Porous Deformable Seabed Under Wave Loading,” *M. Eng. thesis*, Memorial University of Newfoundland.

- Sabin, G.C.W. (1989). “ The Behavior of a Poroelastic Seabed Under Normal and Shear Loads”, *Journal of Offshore Mechanics and Arctic Engineering*, Vol. 111, pp. 303-310.

- Sandhu, R.S. and Wilson, E.L. (1969). “ Finite Element Analysis of Seepage in Elastic Media,” *Journal of the Engineering Mechanics Div., Proc. of the ASCE*, Vol. 95, No. EM3, pp. 641-652

- Schapery, R.A. and Dunlap, W.A. (1978).“ Prediction of Storm-induced Sea Bottom Movement and Platform Forces,” *Proc. Tenth Offshore Technology Conference*, Houston, Vol. 3, pp. 1789-1796

- Seed, H.B. and Rahman, M.S. (1978). “ Wave-induced Pore Pressure in Relation to Ocean Floor Stability of Cohesionless Soils,” *Marine Geotechnology*, Vol. 3, No. 2, pp. 123-150

- Silvestri, V.; Soulie, M.; Marche, C.; Louche, D. (1985). “ Some Considerations on the Wave-induced Instability of the Seafloor,” *Proc. of the Fourth*

Int. Offshore Mechanics and Arctic Eng. Symposium, Dallas, Texas, pp. 81-91

- Simon, B.R.; Zienkiewicz, O.C.; Paul, D.K. (1984)." An Analytical Solution for the Transient Response of Saturated Porous Elastic Solids," *Int. Journal for Numerical and Analytical Methods in Geomechanics*, Vol. 8, pp. 381-398

- Sleath, J.A. (1970)." Wave-induced Pressures in Beds of Sand, " *Journal of the Hydraulics Div., Proc. of the ASCE*, Vol. 96, No. HY2, pp. 367-378

- Sleath,J.F.A.(1984). *Sea Bed Mechanics*, John Wiley and Sons, New York.

- Smith, I.M. and Hobbs, R. (1976). " Biot Analysis of Consolidation beneath Embankments," *Geotechnique*, 26, No. 1, pp. 149-171

- Sokolnikoff, I.S. (1956).*Mathematical Theory of Elasticity,* 2nd ed., McGraw Hill, Inc., New York.

- Sokolnikoff, I.S. and Redheffer, R.M. (1966). *Mathematics of Physics and Modern Engineering,* 2nd ed., McGraw Hill,Inc., New York.

- Spierenburg, S.E.J. (1985)." Geotechnical Aspects of Submarine Pipelines," in *Behaviour of Offshore Structures (BOSS)*, pp. 797-805, Elsevier Science Publishers B.V. Amsterdam

- Stoll, R.D. (1974)."Acoustic Waves in Saturated Sediments ", in *Physics of Sound in Marine Sediments*,ed. by L. Hampton, New York, Plenum Press, pp. 19-39.

- Stoker, J.J. (1957). *Water Waves*,Interscience Publishers, New York.

- Taylor, D.W. (1948). *Fundamentals of Soil Mechanics*, Wiley, New York, 700 pp.

- Terzaghi, K. (1956)." Varieties of Submarine Slope Failures," *Proc. of the Eighth Texas Conference on Soil Mechanics and Foundation Engineering*, Univ. of Texas at Austin.

- Verruijt, A. (1985). " The Influence of Soil Properties on the Behaviour of Offshore Structures," *Behaviour of Offshore Structures (BOSS)*, pp. 7-19, Elsevier Science Publishers B.V. Amsterdam.

- Wright, S.G. (1976)." Analyses for Wave Induced Seafloor Movements," *Proc. of the Eighth Annual Offshore Technology Conference*, Houston, Texas, paper no. 2427, pp. 41-53

- Yamamoto, T., Koning, H., Sellmeijer, H., and Van Hijum, E. (1978). " On the Response of a Poro-elastic Bed to Water Waves," *Journal of Fluid Mechanics*, Vol. 87, part 1, pp. 193 -206.

- Yamamoto, T. (1978)." Seabed Instability from Waves," *Proc. of the Tenth Annual Offshore Technology Conference*, Houston, Texas, Vol. 1, paper no. 3262, pp. 1819-1828.

- Yamamoto, T. (1983). " On the Response of a Coulomb-damped Poro-elastic Bed to Water Waves," *Marine Geotechnology*, Vol. 5, No. 2, pp. 93-130.

- Yamamoto, T.; Takahashi, S.; Schuckman, B. (1983)." Physical Modeling of Sea-Seabed Interactions," *Journal of Engineering Mechanics*, Vol. 109, No.

1, ASCE, pp. 54-72 . Discussion and closure on this paper in *Journal of Eng. Mech.*, Vol. 110, No. 1, 1984, pp. 666-670.

- Yamamoto, T. and Takahashi, S. (1985)." Wave Damping by Soil Motion," *Journal of Waterway, Port, Coastal and Ocean Engineering*, Vol. 111, No. 1, ASCE, pp. 62-77.

- Yokoo,Y.; Yamagata, K.; Nagaoka, H. (1971). " Finite Element Method Applied to Biot's Consolidation Theory," *Soils and Foundations*, Vol. 11, No. 1, pp.29-46

- Zaretskii, Yu. K. (1972). *Theory of Soil Consolidation*, translated from the Russian by Prof. S. Rosenblat, ed. by Robert L. Schiffman, Israel Program for Scientific Translation Ltd., Jerusalem.

- Zienkiewicz, O.C.; Leung, K.H.; Hinton, E.; Chang, C.T.(1982). " Liquefaction and Permanent Deformation under Dynamic Conditions- Numerical Solution and Constitutive Relations," in *Soil Mechanics- Transient and Cyclic Loads* , ed. by G.N. Pande and O.C. Zienkiewicz, chap. 5, John Wiley and Sons Ltd.

- Zienkiewicz, O.C. and Shiomi, T. (1984). " Dynamic Behaviour of Saturated Porous Media; The Generalized Biot Formulation and its Numerical Solution," *Int. Journal for Numerical and Analytical Methods in Geomechanics*, Vol. 8, pp. 71-96.

Appendix A

Fundamentals of Linear Wave Theory

Referring to Figure (4.1), we assume inviscid and hence irrotational flow above the seabed. Therefore there exists a velocity potential $\Phi(x, y, z, t)$ such that

$$\nabla^2 \Phi = 0 \tag{A.1}$$

In general, $\nabla^2 \equiv \frac{\partial^2}{\partial x^2} + \frac{\partial^2}{\partial y^2} + \frac{\partial^2}{\partial z^2}$. The z axis (not shown) is normal to the $x - y$ plane. We assume negligible flow into the seabed, i.e.

$$\frac{\partial \Phi}{\partial n} = 0 \quad \text{on } BC \tag{A.2}$$

We now determine the boundary condition at the water surface. The water surface may be represented by the equation

$$\zeta(x, y, z, t) = 0 \tag{A.3}$$

from which we have

$$\frac{d\zeta}{dt} \equiv \frac{\partial \zeta}{\partial x}\dot{x} + \frac{\partial \zeta}{\partial y}\dot{y} + \frac{\partial \zeta}{\partial z}\dot{z} + \frac{\partial \zeta}{\partial t} = 0 \tag{A.4}$$

on the water surface, where the dots denote differentation with respect to time t. This equation may be written

$$\underline{\nabla}\zeta \, \underline{\nabla}\Phi = -\frac{\partial \zeta}{\partial t} \tag{A.5}$$

on the water surface ,since

$$\underline{\nabla}\Phi = \begin{pmatrix} \dot{x} \\ \dot{y} \\ \dot{z} \end{pmatrix} \tag{A.6}$$

If $\eta(x, z, t)$ denotes the elevation of the water surface above the mean water level OA, then the equation of the water surface is given by $y = \eta(x, z, t)$ or

$$\eta(x, z, t) - y = 0 \tag{A.7}$$

From (A.3) and (A.7):

$$\zeta(x, y, z, t) = \eta(x, z, t) - y \tag{A.8}$$

from which we get

$$\frac{\partial \zeta}{\partial t} = \frac{\partial \eta}{\partial t} \tag{A.9}$$

$$\underline{\nabla}\zeta = \frac{\partial \eta}{\partial x}\underline{i} + (-\underline{j}) + \frac{\partial \eta}{\partial z}\underline{k} \tag{A.10}$$

Here $\underline{i}, \underline{j}, \underline{k}$ are unit vectors in the x, y, z directions respectively. Substituting (A.9) and (A.10) into (A.5) gives

$$\frac{\partial \eta}{\partial x}\frac{\partial \Phi}{\partial x} - \frac{\partial \Phi}{\partial y} + \frac{\partial \eta}{\partial z}\frac{\partial \Phi}{\partial z} = -\frac{\partial \eta}{\partial t} \tag{A.11}$$

on the water surface.

In linear wave theory we assume that the water surface elevation η is small compared to the wave length so that equation (A.11) may be applied at the mean water level $y = 0$. Further, we neglect the non-linear terms in (A.11) which thus becomes

$$\frac{\partial \Phi}{\partial y} = \frac{\partial \eta}{\partial t} \quad \text{at } y = 0 \tag{A.12}$$

Equation (A.12) is known as the linearized kinematic free surface condition. Another condition at the free surface may be deduced from the Bernoulli equation, which is

$$\frac{\partial \Phi}{\partial t} + \frac{1}{2} \underline{\nabla} \Phi \, \underline{\nabla} \Phi + \frac{p}{\rho_f} + gy = f(t) \tag{A.13}$$

where p is water pressure and ρ_f is water density; $f(t)$ is an arbitrary function of time t. If we consider a purely hydrostatic condition, $\Phi \equiv 0$, $p = -\rho_f g y$ for all time, so that $f(t)$ is indentically zero.

We write equation (A.13) at the water surface and neglect the non-linear term:

$$\frac{\partial \Phi}{\partial t} + g\eta = 0 \quad \text{at } y = \eta \text{ i.e. at } y = 0 \text{ approximately} \tag{A.14}$$

Equation (A.14) is called the linearized dynamic free surface condition.

The linear wave theory model is described by equation (A.1) with boundary conditions (A.2), (A.12) and (A.14). Equations (A.12) and (A.14) may be combined by eliminating η:

$$\frac{\partial^2 \Phi}{\partial t^2} + g \frac{\partial \Phi}{\partial y} = 0 \quad \text{at } y = 0 \tag{A.15}$$

To derive the velocity potential due to the incident wave, as given in equation (4.14), we consider a flat seabed, constant water depth h_0, and a wave of surface

elevation

$$\eta = \eta_0 e^{i(kx-\omega t)} \tag{A.16}$$

This represents a wave propagating in the positive or negative x direction according as $k > 0$ or $k < 0$. For the two dimensional problem, Φ is independent of z and we write

$$\Phi(x,y) = g(y)e^{i(kx-\omega t)} \tag{A.17}$$

Substituting in (A.1) gives

$$\frac{\mathrm{d}^2 g}{\mathrm{d}y^2} - k^2 g = 0$$

from which we have

$$g(y) = C\cosh(ky+\alpha) \tag{A.18}$$

Applying (A.2) on the seabed $y = -h_0$ implies that $\alpha = kh_0$, so that

$$\Phi(x,y) = C\cosh(ky + kh_0)e^{i(kx-\omega t)} \tag{A.19}$$

Now, using (A.14) we find that

$$C = -\frac{ig\eta_0}{\omega\cosh(kh_0)} \tag{A.20}$$

and hence

$$\Phi(x,y) = \frac{-ig\eta_0}{\omega\cosh(kh_0)}\cosh(ky + kh_0)e^{i(kx-\omega t)} \tag{A.21}$$

A dispersion relation is obtained by substituting (A.19) into (A.15), which gives:

$$\omega^2 = gk\tanh(kh_0) \tag{A.22}$$

For an incident wave propagating in the negative x direction we set $k = -k_0$, the negative real root of (A.22). This gives the incident velocity potential as

$$\Phi_I(x,y) = \frac{-ig\eta_0}{\omega\cosh(k_0h_0)}\cosh(k_0y + k_0h_0)e^{-i(k_0x+\omega t)} \tag{A.23}$$

Appendix B

The Roots of the Dispersion Relation (Linear Wave Theory)

The dispersion relation (4.12) is

$$\frac{\omega^2}{g} = k \tanh(kh_0) \tag{B.1}$$

This is of the form

$$\frac{a}{x} = \tanh\, x \tag{B.2}$$

where $x = kh_0$ and $a = \dfrac{w^2 h_0}{g} > 0$. The sketch graph Figure (B.1) shows that equation (B.2) has two real roots $x = \pm x_0$. Thus equation (B.1) has two real roots $\pm k_0 \equiv \pm \dfrac{x_0}{h_0}$. To obtain the imaginary roots of (B.1) we put $k = i\bar{k}$ where $\bar{k}$ is real. Then (B.1) becomes

$$-\frac{a}{x} = \tan x \tag{B.3}$$

where $x = \bar{k}h_0$, and $a = \dfrac{w^2 h_0}{g}$.

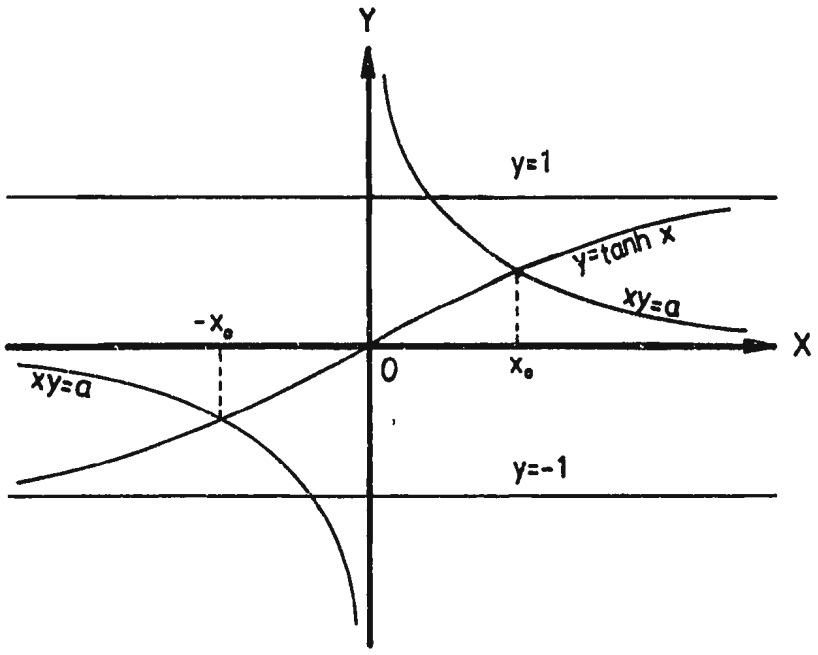

Fig.(B.1) Real roots of Dispersion Relation

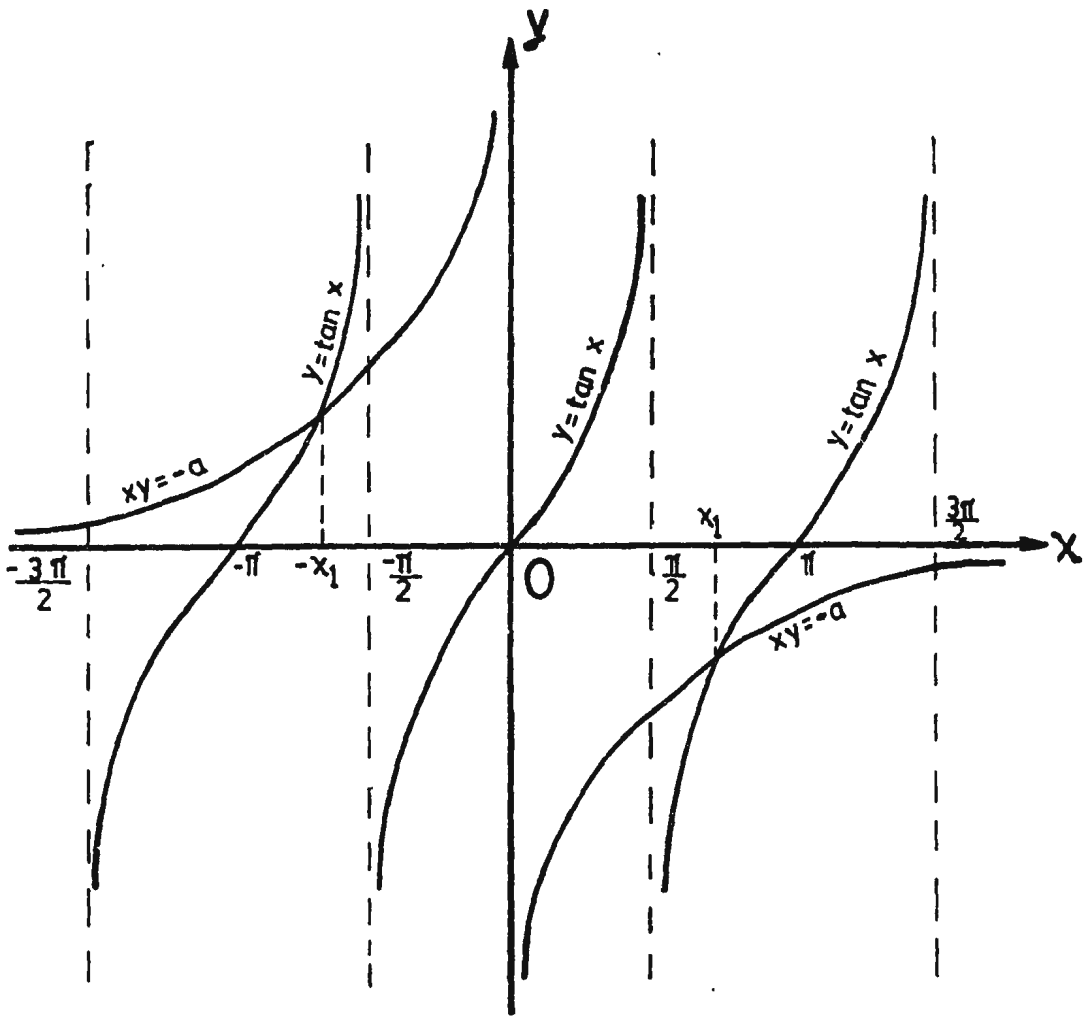

Fig.(B.2) Imaginary Roots of Dispersion Relation

The sketch graph Figure (B.2) shows that (B.3) has an infinity of roots $\pm x_1, \pm x_2, \ldots$ so that

$$\bar{k} = \pm\frac{x_1}{h_0}, \pm\frac{x_2}{h_0}, \ldots \tag{B.4}$$

i.e. the imaginary roots of (B.1) are given by $\pm ik_i$where

$$k_i = \frac{x_i}{h_0} \tag{B.5}$$

To obtain accurate values of the roots of (B.3), it is necessary to provide good estimates of these roots. From Figure (B.2) we note that the nth positive root of (B.3) is of the form

$$x_n = n\pi - y \tag{B.6}$$

where $y > 0$ and depends on n. Substituting (B.6) into (B.3) gives

$$\tan y - \frac{a}{n\pi - y} = 0 \tag{B.7}$$

The value of y is small and becomes smaller as n increases, so we may make the approximation $\tan y \approx y$. This renders equation (B.7) as

$$y^2 - n\pi y + a = 0$$

which has two positive roots:

$$y = \frac{\pi}{2}[n \pm \sqrt{n^2 - \frac{4a}{\pi^2}}] \quad \text{for } n > \frac{2}{\pi}\sqrt{a}$$

The root of interest is the smaller value, i.e.

$$y = \frac{\pi}{2}[n - \sqrt{n^2 - \frac{4a}{\pi^2}}] \quad \text{for } n > \frac{2}{\pi}\sqrt{a} \tag{B.8}$$

We therefore solve (B.7) for values of $n > \frac{2}{\pi}\sqrt{a}$, each time providing an estimate of y from (B.8). The nth root of (B.3) is then given by (B.6). For values of

$n < \frac{2}{\pi}\sqrt{a}$ we obtain the roots directly from (B.3) using $x_n = n\pi$ as an estimate. The imaginary roots of(B.1) are then $\pm\frac{ix_n}{h_0}, n = 1, 2, \cdots$. The equations (B.2), (B.3), (B.7), may be solved using the IMSL routine ZREAL.

Appendix C

Evaluation of the Integrals

(Potential Problem)

We refer to equations (4.33). We consider a typical element Γ_e as shown in Figure (C.1) with end points (x_e, y_e), (x_{e+1}, y_{e+1}). The direction of integration and the unit outward normal $\underline{n}$ are indicated in the figure. The direction of integration is such that the interior of the problem domain lies to the left. The element $\Gamma_e$is represented in terms of parameter ξ as follows:

On Γ_e

$$x = \frac{1}{2}(1-\xi)x_e + \frac{1}{2}(1+\xi)x_{e+1}$$
$$y = \frac{1}{2}(1-\xi)y_e + \frac{1}{2}(1+\xi)y_{e+1}$$
$$\text{where } -1 \leq \xi \leq 1 \qquad \text{(C.1)}$$

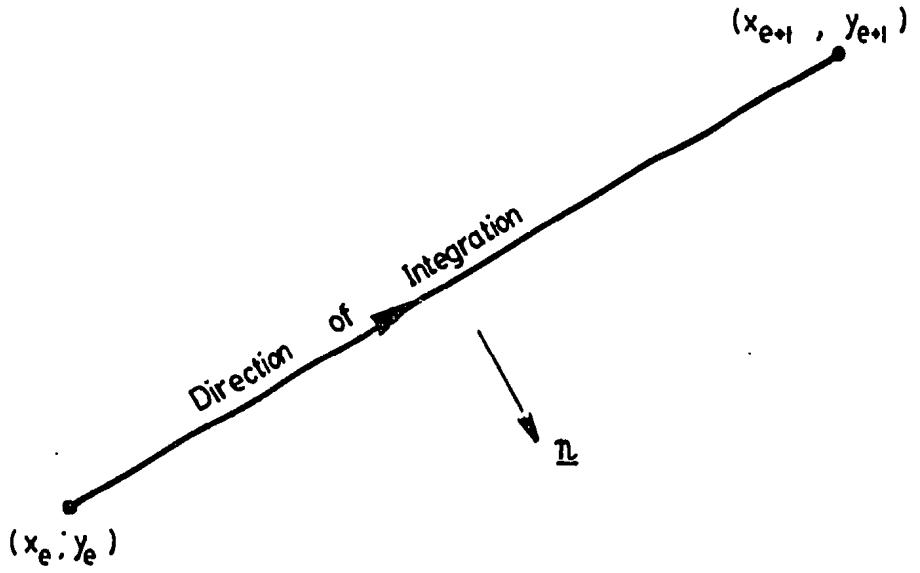

Fig.(C.1) Element Γ_e (Wave problem)

The line element ds is given by

$$\left(\frac{ds}{d\xi}\right)^2 = \left(\frac{dx}{d\xi}\right)^2 + \left(\frac{dy}{d\xi}\right)^2$$

from which we obtain

$$d\Gamma_e = ds = J_e d\xi \tag{C.2}$$

where

$$J_e = \frac{1}{2}[(x_{e+1} - x_e)^2 + (y_{e+1} - y_e)^2]^{\frac{1}{2}} \tag{C.3}$$

We have defined the distance r as $r = |\underline{x} - \underline{x}_j|$ where $\underline{x}$ is an arbitrary point on Γ_e and $\underline{x}_j$ is the position vector of node j. Since node j lies on the mid-point of element Γ_j we have the coordinates (x_0, y_0) of node j as:

$$x_0 = \frac{1}{2}(x_j + x_{j+1})$$
$$y_0 = \frac{1}{2}(y_j + y_{j+1})$$

Thus

$$r = [(x - x_0)^2 + (y - y_0)^2]^{\frac{1}{2}} \quad \text{for } x, y \in \Gamma_e$$
$$\frac{\partial r}{\partial x} = \frac{x - x_0}{r}; \quad \frac{\partial r}{\partial y} = \frac{y - y_0}{r} \tag{C.4}$$

The unit normal $\underline{n}$ is given by

$$\underline{n} = \begin{pmatrix} n_1 \\ n_2 \end{pmatrix} \text{ where}$$

$$n_1 = \frac{1}{2J_e}(y_{e+1} - y_e); \quad n_2 = \frac{1}{2J_e}(x_e - x_{e+1}) \tag{C.5}$$

If $e \neq j$, integration along Γ_e presents no difficulty. An integral of the form $\int_{\Gamma_e} f(r, r_{,i}, n_i) d\Gamma_e$ is transformed into one of the form $\int_{-1}^{1} g(\xi) d\xi$ by use of the formulae (C.1) to (C.5) and then straight-forward Gaussian integration is performed.

Integration along Γ_j, however, requires special consideration owing to the logarithmic singularity of the integrand. Putting $e = j$ in (C.1) to (C.5) we find that on Γ_j,

$$r = |\xi| J_j \tag{C.6}$$

$$\frac{\partial r}{\partial x} = \left(\frac{x_{j+1} - x_j}{2J_j}\right) \cdot \frac{\xi}{|\xi|} \; ; \; \frac{\partial r}{\partial y} = \left(\frac{y_{j+1} - y_j}{2J_j}\right) \frac{\xi}{|\xi|} \tag{C.7}$$

$$n_1 = \frac{y_{j+1} - y_j}{2J_j} \; ; \; n_2 = \frac{x_j - x_{j+1}}{2J_j} \tag{C.8}$$

Equations (C.7), (C.8) imply that

$$\frac{\partial r}{\partial n} = 0 \quad \text{on } \Gamma_j \tag{C.9}$$

We consider the integral

$$\begin{aligned} \int_{\Gamma_j} \ln r d\Gamma_j &= \int_{-1}^{1} \ln[|\xi| J_j] J_j d\xi \\ &= J_j \ln J_j \int_{-1}^{1} d\xi + J_j \int_{-1}^{1} \ln|\xi| d\xi \\ &= 2J_j \ln J_j + 2J_j \int_0^1 \ln \xi d\xi \\ &= 2J_j (\ln J_j - 1) \end{aligned} \tag{C.10}$$

We can now evaluate the integrals A_e and B_e. From (4.24)

$$\phi^* = -\frac{1}{2\pi} \ln r$$

$$\Rightarrow \frac{\partial \phi^*}{\partial n} = -\frac{1}{2\pi r} \frac{\partial r}{\partial n}$$

From (4.33):

$$A_e = \begin{cases} -\frac{1}{2\pi} \int_{\Gamma_e} \frac{1}{r} \frac{\partial r}{\partial n} d\Gamma_e & e \neq j \\ -\frac{1}{2\pi} \int_{\Gamma_j} \frac{1}{r} \frac{\partial r}{\partial n} d\Gamma_j + \frac{1}{2} & e = j \end{cases}$$

Using (C.9), this becomes

$$A_e = \begin{cases} -\frac{1}{2\pi}\int_{\Gamma_e} \frac{1}{r}\frac{\partial r}{\partial n} d\Gamma_e & e \neq j \\ \frac{1}{2} & e = j \end{cases} \tag{C.11}$$

Also, from (4.33) and (C.10)

$$B_e = \begin{cases} -\frac{1}{2\pi}\int_{\Gamma_e} \ln r \, d\Gamma_e & e \neq j \\ \frac{J_j}{\pi}(1 - \ln J_j) & e = j \end{cases} \tag{C.12}$$

As stated before, the integrals for $e \neq j$ can be simply evaluated using standard Gaussian quadrature.

Appendix D

Fundamental Solution (Laplace's Equation)

The following derivation is a classical one and can be found in any standard text on the boundary element method, e.g. Brebbia (1984). Referring to equations (4.23) or (5.34) we need to consider an equation of the form

$$\nabla^2\phi + k\Delta(\underline{x}, \underline{x}_p) = 0 \tag{D.1}$$

where k is a constant.

We recall the following familiar property of the delta function:

$$\int_\Omega \Delta(\underline{x} - \underline{x}_p)d\Omega = \begin{cases} 1 & \underline{x}_p \in \Omega \\ 0 & \underline{x}_p \in \Omega \end{cases} \tag{D.2}$$

where the integration is performed with respect to $\underline{x}$. We integrate (D.1) over a

circular region Ω, centre $\underline{x}_p$ and radius ϵ:

$$\int_\Omega \phi_{,ii}\, d\Omega + k = 0 \tag{D.3}$$

where we have used (D.2). By the divergence theorem,

$$\int_\Omega \phi_{,ii}\, d\Omega = \int_\Gamma \frac{\partial \phi}{\partial n} d\Gamma \tag{D.4}$$

where Γ is the boundary of Ω. From (D.3) and (D.4):

$$\int_\Gamma \frac{\partial \phi}{\partial n} d\Gamma = -k \tag{D.5}$$

We define polar coordinates with $\underline{x}_p$ as origin: $r = |\underline{x} - \underline{x}_p|$; θ is measured anti-clockwise from the x-axis through $\underline{x}_p$. On Γ, $r = \epsilon$, and $\dfrac{\partial \phi}{\partial n} = \dfrac{\partial \phi}{\partial r}$ so that (D.5) becomes

$$\int_0^{2\pi} \left(\frac{\partial \phi}{\partial r}\right)_{r=\epsilon} \epsilon\, d\theta = -k \tag{D.6}$$

Assuming that ϕ is independent of θ, we have

$$\left(\frac{\partial \phi}{\partial r}\right)_{r=\epsilon} = \frac{-k}{2\pi\epsilon} \tag{D.7}$$

which is satisfied by:

$$\phi = -\frac{k}{2\pi} \ln r \tag{D.8}$$

Appendix E

A Solution of Equation (5.108)

The equation is

$$\nabla^2 \eta_i - a^2 \eta_i = 0 \tag{E.1}$$

where a is a real or complex constant. We verify that a solution of (E.1) is

$$\eta_i = r_{,i} K_1(ar) \tag{E.2}$$

where $r = |\mathbf{x} - \mathbf{p}|$. We first note that for real or complex z, and integer n:

$$K_{n+1}(z) = K_{n-1}(z) + \frac{2n}{z} K_n(z) \tag{E.3}$$

$$\frac{d}{dz}[K_n(z)] = -\frac{1}{2}[K_{n-1}(z) + K_{n+1}(z)] \tag{E.4}$$

Also, since $r^2 = (x_i - p_i)(x_i - p_i)$,

$$\begin{aligned} r_{,j} &= \frac{x_j - p_j}{r} \\ r_{,ij} &= \frac{\delta_{ij}}{r} - \frac{r_{,i} r_{,j}}{r} \end{aligned} \tag{E.5}$$

$$r_{,jj} = \frac{1}{r}$$
$$r_{,j}\, r_{,j} = 1$$

We have from (E.2)

$$\begin{aligned}\eta_{i,j} &= r_{,i}\,[-K_0(ar) - \frac{1}{ar}K_1(ar)]ar_{,j} + r_{,ij}\,K_1(ar) \\ &= -ar_{,i}\,r_{,j}\,[K_0(ar) + \frac{2}{ar}K_1(ar)] + \frac{K_1(ar)}{r}\delta_{ij} \\ &= -ar_{,i}\,r_{,j}\,K_2(ar) + \frac{K_1(ar)}{r}\delta_{ij} \qquad \text{(E.6)}\end{aligned}$$

Also, using (E.5) it is easy to show that

$$(r_{,i}\,r_{,j}\,)_{,j} = \frac{r_{,i}}{r} \qquad \text{(E.7)}$$

Differentiating (E.6) with respect to x_j gives

$$\begin{aligned}\eta_{i,jj} &= -a\{r_{,i}\,r_{,j}\,[-K_1(ar) - \frac{2}{ar}K_2(ar)]ar_{,j} + K_2(ar)(r_{,i}\,r_{,j}\,)_{,j}\} \\ &\quad +\delta_{ij}\{\frac{1}{r}[-K_0(ar) - \frac{1}{ar}K_1(ar)]ar_{,j} - \frac{r_{,j}}{r^2}K_1(ar)\} \\ &= a\{ar_{,i}\,[K_1(ar) + \frac{2}{ar}K_2(ar)] - \frac{r_{,i}}{r}K_2(ar)\} \\ &\quad +\delta_{ij}\{-\frac{a}{r}r_{,j}\,K_0(ar) - \frac{2r_{,j}}{r^2}K_1(ar)\} \\ &= a\{ar_{,i}\,K_1(ar) + \frac{2r_{,i}}{r}K_2(ar) - \frac{r_{,i}}{r}K_2(ar) - \frac{r_{,i}}{r}K_0(ar) - \frac{2r_{,i}}{ar^2}K_1(ar)\} \\ &= a\{ar_{,i}\,K_1(ar) + \frac{r_{,i}}{r}[K_2(ar) - K_0(ar) - \frac{2}{ar}K_1(ar)]\} \\ &= a^2 r_{,i}\,K_1(ar) = a^2\eta_i\end{aligned}$$

i.e.

$$\nabla^2[r_{,i}\,K_1(ar)] = a^2[r_{,i}K_1(ar)]$$

Appendix F

Functions Required for Kelvin Function Approximations

These functions are defined in equations (6.21) to (6.27) and (6.28).

$$u_0(x) = \begin{cases} -\left[1 + \alpha_1 \left(\frac{x}{8}\right)^4 + \alpha_2 \left(\frac{x}{8}\right)^8 + \cdots + \alpha_7 \left(\frac{x}{8}\right)^{28}\right] & 0 < x \leq 8 \\ \\ 0 & x > 8 \end{cases}$$

$$v_0(x) = \begin{cases} \frac{\pi}{4}\left(\frac{x}{8}\right)^2 \left[\beta_1 + \beta_2 \left(\frac{x}{8}\right)^4 + \beta_3 \left(\frac{x}{8}\right)^8 + \cdots + \beta_7 \left(\frac{x}{8}\right)^{24}\right] & 0 < x \leq 8 \\ \quad + \left[a_0 + a_1 \left(\frac{x}{8}\right)^4 + a_2 \left(\frac{x}{8}\right)^8 + \cdots + a_7 \left(\frac{x}{8}\right)^{28}\right] & \\ \\ \sqrt{\frac{\pi}{2x}}\, e^{\nu(x)} \cos \lambda(x) & x > 8 \end{cases}$$

$$u_0'(x) = \begin{cases} \left(\frac{x}{8}\right)^2 \left[\beta_1 + \beta_2 \left(\frac{x}{8}\right)^4 + \beta_3 \left(\frac{x}{8}\right)^8 + \cdots + \beta_7 \left(\frac{x}{8}\right)^{24}\right] & 0 < x \leq 8 \\ 0 & x > 8 \end{cases}$$

$$v_0'(x) = \begin{cases} \frac{\pi}{4}\left[1 + \alpha_1 \left(\frac{x}{8}\right)^4 + \alpha_2 \left(\frac{x}{8}\right)^8 + \cdots + \alpha_7 \left(\frac{x}{8}\right)^{28}\right] & 0 < x \leq 8 \\ -\left(\frac{x}{8}\right)^2 \left[b_1 + b_2 \left(\frac{x}{8}\right)^4 + b_3 \left(\frac{x}{8}\right)^8 + \cdots + b_7 \left(\frac{x}{8}\right)^{24}\right] & \\ -\sqrt{\frac{\pi}{2x}}\, e^{\nu(x)} \sin \lambda(x) & x > 8 \end{cases}$$

$$u_1(x) = \begin{cases} \left(\frac{1}{2}\right) + \beta_1' \left(\frac{x}{8}\right)^4 + \beta_2' \left(\frac{x}{8}\right)^8 + \cdots + \beta_6' \left(\frac{x}{8}\right)^{24} & 0 < x \leq 8 \\ 0 & x > 8 \end{cases}$$

$$v_1(x) = \begin{cases} \frac{1}{8^2}\left[\beta_1 + \beta_2 \left(\frac{x}{8}\right)^4 + \beta_3 \left(\frac{x}{8}\right)^8 + \cdots + \beta_7 \left(\frac{x}{8}\right)^{24}\right] & 0 < x \leq 8 \\ +\frac{\pi}{4}\left[\alpha_1' \left(\frac{x}{8}\right)^2 + \alpha_2' \left(\frac{x}{8}\right)^6 + \cdots + \alpha_7' \left(\frac{x}{8}\right)^{26}\right] - g_0'(x) & \\ \frac{\sqrt{\pi}}{(2x)^{\frac{3}{2}}}\, e^{\nu(x)} \{s_\phi(x)[\sin \lambda(x) + \cos \lambda(x)] + t_\phi(x)[\sin \lambda(x) - \cos \lambda(x)]\} & x > 8 \end{cases}$$

$$u_1'(x) = \begin{cases} \alpha_1' \left(\frac{x}{8}\right)^2 + \alpha_2' \left(\frac{x}{8}\right)^6 + \cdots + \alpha_7' \left(\frac{x}{8}\right)^{26} & 0 < x \leq 8 \\ \\ 0 & x > 8 \end{cases}$$

$$v_1'(x) = \begin{cases} \frac{1}{8^2}\left[\alpha_1 \left(\frac{x}{8}\right)^2 + \alpha_2 \left(\frac{x}{8}\right)^6 + \cdots + \alpha_7 \left(\frac{x}{8}\right)^{26}\right] \\ -\frac{\pi}{4}\left[\frac{1}{2} + \beta_1' \left(\frac{x}{8}\right)^4 + \beta_2' \left(\frac{x}{8}\right)^8 + \cdots + \beta_6' \left(\frac{x}{8}\right)^{24}\right] - f_0'(x) & 0 < x \leq 8 \\ \\ \frac{\sqrt{\pi}}{(2x)^{\frac{3}{2}}} e^{\nu(x)}\{s_\phi(x)[\cos\lambda(x) - \sin\lambda(x)] + t_\phi(x)[\cos\lambda(x) + \sin\lambda(x)]\} \\ -\frac{1}{x^2} & x > 8 \end{cases}$$

$$u_2(x) = u_0(x) + 2u_1(x)$$

$$u_2'(x) = u_0'(x) + 2u_1'(x)$$

$$v_2(x) = v_0(x) + 2v_1(x)$$

$$v_2'(x) = v_0'(x) + 2v_1'(x)$$

$$u_3(x) = \begin{cases} \frac{1}{8\sqrt{2}}[(-\beta_1 - 2\alpha_1')\left(\frac{x}{8}\right) + (-\alpha_1 + 2\beta_1')\left(\frac{x}{8}\right)^3 \\ +(-\beta_2 - 2\alpha_2')\left(\frac{x}{8}\right)^5 + (-\alpha_2 + 2\beta_2')\left(\frac{x}{8}\right)^7 \\ +\cdots + (-\alpha_7 + 2\beta_7')\left(\frac{x}{8}\right)^{27}] & 0 < x \leq 8 \\ \\ 0 & x > 8 \end{cases}$$

$$w_3(x) = \begin{cases} \dfrac{1}{8\sqrt{2}}\left[\dfrac{\pi}{4}\left\{(\beta_1+2\alpha_1')\left(\dfrac{x}{8}\right)+(-\alpha_1+2\beta_1')\left(\dfrac{x}{8}\right)^3\right.\right. \\ \quad (\beta_2+2\alpha_2')\left(\dfrac{x}{8}\right)^5+(-\alpha_2+2\beta_2')\left(\dfrac{x}{8}\right)^7 \\ \quad +\cdots+\left.(-\alpha_7+2\beta_7')\left(\dfrac{x}{8}\right)^{27}\right\} \\ \quad +(b_1+2a_1')\left(\dfrac{x}{8}\right)+(a_1-2b_1')\left(\dfrac{x}{8}\right)^3 \\ \quad +(b_2+2a_2')\left(\dfrac{x}{8}\right)^5+(a_2-2b_2')\left(\dfrac{x}{8}\right)^7 \qquad 0<x\le 8 \\ \quad +\cdots+(a_7-2b_7')\left(\dfrac{x}{8}\right)^{27} \\ +\dfrac{2}{8^2}\left\{-\alpha_1\left(\dfrac{x}{8}\right)+\beta_2\left(\dfrac{x}{8}\right)^3-\alpha_2\left(\dfrac{x}{8}\right)^5+\beta_3\left(\dfrac{x}{8}\right)^7\right. \\ \quad \left.+\cdots+\beta_7\left(\dfrac{x}{8}\right)^{23}-\alpha_7\left(\dfrac{x}{8}\right)^{25}\right\}\Bigg] \\ \\ \dfrac{\sqrt{\pi}}{2x^{\frac{3}{2}}}\,e^{\nu(x)}\left[\cos\lambda(x)+\sin\lambda(x)+\right. \\ \left.\dfrac{2}{x}\left\{s_\phi(x)\sin\lambda(x)-t_\phi(x)\cos\lambda(x)\right\}\right]+\dfrac{\sqrt{2}}{x^3} \qquad x>8 \end{cases}$$

$$z_3(x) = \begin{cases} \dfrac{1}{\sqrt{2}}\left(a_0-2b_0'+\dfrac{1}{2}\right) & 0<x\le 8 \\ \\ 0 & x>8 \end{cases}$$

$$u_3'(x) = \begin{cases} \frac{1}{8\sqrt{2}}[(\beta_1 + 2\alpha_1')\left(\frac{x}{8}\right) + (-\alpha_1 + 2\beta_1')\left(\frac{x}{8}\right)^3 \\ \quad +(\beta_2 + 2\alpha_2')\left(\frac{x}{8}\right)^5 + (-\alpha_2 + 2\beta_2')\left(\frac{x}{8}\right)^7 \\ \quad +\cdots + (-\alpha_7 + 2\beta_7')\left(\frac{x}{8}\right)^{27}] & 0 < x \le 8 \\ \\ 0 & x > 8 \end{cases}$$

$$w_3'(x) = \begin{cases} \frac{1}{8\sqrt{2}}\left[\frac{\pi}{4}\left\{(\beta_1 + 2\alpha_1')\left(\frac{x}{8}\right) + (\alpha_1 - 2\beta_1')\left(\frac{x}{8}\right)^3\right.\right. \\ \quad +(\beta_2 + 2\alpha_2')\left(\frac{x}{8}\right)^5 + (\alpha_2 - 2\beta_2')\left(\frac{x}{8}\right)^7 \\ \quad \left.\left. +\cdots + (\alpha_7 - 2\beta_7')\left(\frac{x}{8}\right)^{27}\right\}\right. \\ \quad +(-b_1 - 2a_1')\left(\frac{x}{8}\right) + (a_1 - 2b_1')\left(\frac{x}{8}\right)^3 \\ \quad +(-b_2 - 2a_2')\left(\frac{x}{8}\right)^5 + (a_2 - 2b_2')\left(\frac{x}{8}\right)^7 & 0 < x \le 8 \\ \quad +\cdots + (a_7 - 2b_7')\left(\frac{x}{8}\right)^{27} \\ +\frac{2}{8^2}\left\{\alpha_1\left(\frac{x}{8}\right) + \beta_2\left(\frac{x}{8}\right)^3 + \alpha_2\left(\frac{x}{8}\right)^5 + \beta_3\left(\frac{x}{8}\right)^7\right. \\ \quad \left.\left. +\cdots + \beta_7\left(\frac{x}{8}\right)^{23} + \alpha_7\left(\frac{x}{8}\right)^{25}\right\}\right] \\ \\ \quad \frac{\sqrt{\pi}}{2x^{\frac{1}{2}}}\, e^{\nu(x)}\,[\cos\lambda(x) + \sin\lambda(x) + \\ \quad \frac{2}{x}\{s_\phi(x)\cos\lambda(x) + t_\phi(x)\sin\lambda(x)\}] - \frac{\sqrt{2}}{x^3} & x > 8 \end{cases}$$

$$z_3'(x) = \begin{cases} \dfrac{a_0 - 2b_0' + \frac{1}{2}}{\sqrt{2}} & 0 < x \leq 8 \\ \\ 0 & x > 8 \end{cases}$$

$$u_4(x) = u_3(x) + \frac{x}{\sqrt{2}}[u_1(x) + u_1'(x)]$$

$$w_4(x) = w_3(x) + \frac{x}{\sqrt{2}}[v_1(x) + v_1'(x)]$$

$$z_4(x) = z_3(x) + \frac{1}{\sqrt{2}}$$

$$u_4'(x) = u_3'(x) - \frac{x}{\sqrt{2}}[u_1(x) - u_1'(x)]$$

$$w_4'(x) = w_3'(x) - \frac{x}{\sqrt{2}}[v_1(x) - v_1'(x)]$$

$$z_4'(x) = z_3'(x) + \frac{1}{\sqrt{2}}$$

$$u_5(x) = u_0(x) + u_1(x)$$

$$v_5(x) = v_0(x) + v_1(x)$$

$$u_5'(x) = u_0'(x) + u_1'(x)$$

$$v_5'(x) = v_0'(x) + v_1'(x)$$

$$u_6(x) = 4u_3(x) + \frac{x}{\sqrt{2}}[u_1(x) + u_1'(x)]$$

$$w_6(x) = 4w_3(x) + \frac{x}{\sqrt{2}}[v_1(x) + v_1'(x)]$$

$$z_6(x) = 4z_3(x) + \frac{1}{\sqrt{2}}$$

$$u_6'(x) = 4u_3'(x) - \frac{x}{\sqrt{2}}[u_1(x) - u_1'(x)]$$

$$w_6'(x) = 4w_3'(x) - \frac{x}{\sqrt{2}}[v_1(x) - v_1'(x)]$$

$$z_6'(x) = 4z_3'(x) + \frac{1}{\sqrt{2}}$$

$$u_8(x) = \begin{cases} 1 & 0 < x \leq 8 \\ 0 & x > 8 \end{cases}$$

Functions needed for the above are as follows:

For $0 < x \leq 8$:

$$f_0(x) = a_0 + a_1\left(\frac{x}{8}\right)^4 + a_2\left(\frac{x}{8}\right)^8 + \cdots + a_7\left(\frac{x}{8}\right)^{28}$$

$$g_0(x) = b_1\left(\frac{x}{8}\right)^2 + b_2\left(\frac{x}{8}\right)^6 + \cdots + b_7\left(\frac{x}{8}\right)^{26}$$

$$f_0'(x) = a_1'\left(\frac{x}{8}\right)^2 + a_2'\left(\frac{x}{8}\right)^6 + \cdots + a_7'\left(\frac{x}{8}\right)^{26}$$

$$g_0'(x) = b_0' + b_1'\left(\frac{x}{8}\right)^4 + b_2'\left(\frac{x}{8}\right)^8 + \cdots + b_6'\left(\frac{x}{8}\right)^{24}$$

For $x > 8$:

$$\nu(x) = c_0 - c_1\left(\frac{8}{x}\right) + c_2\left(\frac{8}{x}\right)^2 - c_3\left(\frac{8}{x}\right)^3 + \cdots + c_6\left(\frac{8}{x}\right)^6 - \frac{x}{\sqrt{2}}$$

$$\lambda(x) = d_0 - d_1\left(\frac{8}{x}\right) + d_2\left(\frac{8}{x}\right)^2 - d_3\left(\frac{8}{x}\right)^3 + \cdots + d_6\left(\frac{8}{x}\right)^6 - \frac{x}{\sqrt{2}}$$

$$s_\phi(x) = (s_0+t_0)-(s_1+t_1)\left(\frac{8}{x}\right)+(s_2+t_2)\left(\frac{8}{x}\right)^2-(s_3+t_3)\left(\frac{8}{x}\right)^3+\cdots+(s_6+t_6)\left(\frac{8}{x}\right)^6$$

$$t_\phi(x) = (s_0-t_0)-(s_1-t_1)\left(\frac{8}{x}\right)+(s_2-t_2)\left(\frac{8}{x}\right)^2-(s_3-t_3)\left(\frac{8}{x}\right)^3+\cdots+(s_6-t_6)\left(\frac{8}{x}\right)^6$$

List of Coefficients

$$\alpha_1 = -64 \qquad \alpha_2 = 113.77777774$$

$$\alpha_3 = -32.36345652 \qquad \alpha_4 = 2.64191397$$

$$\alpha_5 = -0.08349609 \qquad \alpha_6 = 0.00122552$$

$$\alpha_7 = -0.00000901$$

$$\beta_1 = 16 \qquad \beta_2 = -113.77777774$$

$$\beta_3 = 72.81777742 \qquad \beta_4 = -10.56765779$$

$$\beta_5 = 0.52185615 \qquad \beta_6 = -0.01103667$$

$$\beta_7 = 0.00011346$$

$$\alpha_1' = -4 \qquad \alpha_2' = 14.22222222$$

$$\alpha_3' = -6.06814810 \qquad \alpha_4' = 0.66047849$$

$$\alpha_5' = -0.02609253 \qquad \alpha_6' = 0.00045957$$

$$\alpha_7' = -0.00000394$$

$$\beta_1' = -10.66666666 \qquad \beta_2' = 11.37777772$$

$$\beta_3' = -2.31167514 \qquad \beta_4' = 0.14677204$$

$$\beta_5' = -0.00379386 \qquad \beta_6' = 0.00004609$$

$$\beta_7' = 0$$

$a_0 = -0.57721566 \quad a_1 = -59.05819744$

$a_2 = 171.36272133 \quad a_3 = -60.60977451$

$a_4 = 5.65539121 \quad a_5 = -0.19636347$

$a_6 = 0.00309699 \quad a_7 = -0.00002458$

$b_1 = 6.76454936 \quad b_2 = -142.91827687$

$b_3 = 124.23569650 \quad b_4 = -21.30060904$

$b_5 = 1.17509064 \quad b_6 = -0.02695875$

$b_7 = 0.00029532$

$a'_1 = -3.69113734 \quad a'_2 = -21.42034017$

$a'_3 = -11.36433272 \quad a'_4 = 1.41384780$

$a'_5 = -0.06136358 \quad a'_6 = -0.00116137$

$a'_7 = -0.00001075$

$b'_0 = 0.21139217 \quad b'_1 = -13.39858846$

$b'_2 = 19.41182758 \quad b'_3 = -4.65950823$

$b'_4 = 0.33049424 \quad b'_5 = -0.00926707$

$b'_6 = 0.00011997 \quad b'_7 = 0$

$c_0 = 0$ $c_1 = 0.0110486$

$c_2 = 0$ $c_3 = -0.0000906$

$c_4 = -0.0000252$ $c_5 = -0.0000034$

$c_6 = 0.0000006$

$d_0 = -0.3926991$ $d_1 = -0.0110485$

$d_2 = -0.0009765$ $d_3 = -0.0000901$

$d_4 = 0$ $d_5 = 0.0000051$

$d_6 = 0.0000019$

$s_0 = 0.7071068$ $s_1 = -0.0625001$

$s_2 = -0.0013813$ $s_3 = 0.0000005$

$s_4 = 0.0000346$ $s_5 = 0.0000117$

$s_6 = 0.0000016$

$t_0 = 0.7071068$ $t_1 = -0.0000001$

$t_2 = 0.0013811$ $t_3 = 0.0002452$

$t_4 = 0.0000338$ $t_5 = -0.0000024$

$t_6 = -0.0000032$

Appendix G

Real and Imaginary Parts of the Poroelastic Fundamental Solutions

The real and imaginary parts of the fundamental solutions are defined in equation (6.30). The functions u_n, v_n, w_n and z_n used in the following take argument cr where the parameter c is defined from (6.16) as

$$c^2 = \frac{\omega f k H}{R(\lambda + 2\mu)}$$

The parameters R, k and H are given by (3.24), (5.118) and (5.121) respectively. The following dimensionless groups are useful in describing the fundamental

solutions

$$\Pi_a = \frac{\mu}{H} = \frac{1}{\frac{2(1-\nu)}{1-2\nu} + \frac{K_f}{\mu f}}$$

$$\Pi_b = \frac{K_f}{H} = \frac{\frac{K_f}{\mu}}{\frac{2(1-\nu)}{1-2\nu} + \frac{K_f}{\mu f}}$$

$$\Pi_c = \frac{1-2\nu}{2(1-\nu)} + \frac{\mu f}{K_f}$$

Thus in defining c, Π_a, Π_b and Π_c is necessary to know the following material constants: porosity f, permeability $k_0(ms^{-1})$, shear modulus of soil skeleton $\mu(Nm^{-2})$, Poisson's ratio of soil skeleton ν, density of pore water $\rho_f(kg\,m^{-3})$, bulk modulus of pore water $K_f(Nm^{-2})$.

The following dimensionless groups occur in the fundamental solutions. The symbol r_0 represents an arbitrary length.

$$\Pi_1 = \frac{H-\mu}{2H} = \frac{1}{2}(1-\Pi_a)$$

$$\Pi_2 = \frac{H+\mu}{2H} = \frac{1}{2}(1+\Pi_a)$$

$$\Pi_3 = \frac{ik_0K_fa^2\mu}{\omega f^2\rho_f g H^2} = \frac{\Pi_b^2\Pi_c}{f^2}$$

$$\Pi_4 = \frac{K_f a^2 r_0}{fH} \equiv -i\Pi_4'$$

where

$$\Pi_4' = \frac{\Pi_b c^2 r_0}{f}$$

$$\Pi_5 = \frac{ik_0a^2K_f\mu}{\omega f\rho_f g H} = \frac{\Pi_b\Pi_c}{f}$$

$$\Pi_6 = ar_0 \equiv (\frac{1-i}{\sqrt{2}})\Pi_6'$$

where

$$\Pi_6' = cr_0$$

$$\Pi_7 = \frac{2(H-\mu)}{H} = 2(1-\Pi_a)$$

$$\Pi_8 = \frac{\mu}{H} = \Pi_a$$

$$\Pi_9 = \frac{i2\mu K_f^2 k_0 a^3 r_0}{\omega f^2 \rho_f g H^2} \equiv (1-i)\Pi_9'$$

where

$$\Pi_9' = \frac{\sqrt{2}\Pi_b^2 \Pi_c c r_0}{f^2}$$

$$\Pi_{10} = \frac{K_f a^2 r_0^2}{fH} \equiv -i\Pi_{10}'$$

where

$$\Pi_{10}' = \frac{\Pi_b c^2 r_0^2}{f}$$

$$\Pi_{11} = \frac{K_f a^2 r_0}{fH} = -i\Pi_4'$$

$$\Pi_{12} = -i\Pi_{12}'$$

where

$$\Pi_{12}' = \frac{\rho_f g \omega r_0^2}{\mu k_0}$$

The functions defined in equation (6.30) are given below.

Function H_{ik}

For $i = 1, 2$

For $k = 1, 2$

$$H_{ik} = -\Pi_2 \delta_{ik} u_8 + \Pi_3 (u_2 r_{,i} r_{,k} - u_1 \delta_{ik})$$

For $k = 3$

$$H_{ik} = \Pi_4' r r_{,i} u_1'$$

For $i = 3$

For $k = 1, 2$

$$H_{ik} = \Pi_5 (-u_2 r_{,k} \frac{\partial r}{\partial n} + u_1 n_k)$$

For $k = 3$

$$H_{ik} = -c^2 r_0 r \frac{\partial r}{\partial n} u_1'$$

Function H'_{ik}

For $i = 1, 2$

For $k = 1, 2$

$$H'_{ik} = \Pi_3(u'_2 r_{,i} r_{,k} - u'_1 \delta_{ik})$$

For $k = 3$

$$H'_{ik} = -\Pi'_4 r r_{,i} u_1$$

For $i = 3$

For $k = 1, 2$

$$H'_{ik} = \Pi_5 \left(-u'_2 r_{,k} \frac{\partial r}{\partial n} + u'_1 n_k \right)$$

For $k = 3$

$$H'_{ik} = c^2 r_0 r \frac{\partial r}{\partial n} u_1$$

Function G_{ik}

For $i = 1, 2$

For $k = 1, 2$

$$G_{ik} = \Pi_1 r_{,i} r_{,k} + \Pi_2 \delta_{ik} [\ln(\frac{c}{2}) - (1 - u_8) \ln \left(\frac{cr}{2}\right)] + \Pi_3 (v_2 r_{,i} r_{,k} - v_1 \delta_{ik})$$

For $k = 3$

$$G_{ik} = \Pi_4' r r_{,i} v_1'$$

For $i = 3$

For $k = 1, 2$

$$G_{ik} = \Pi_5 (-v_2 r_{,k} \frac{\partial r}{\partial n} + v_1 n_k)$$

For $k = 3$

$$G_{ik} = -c^2 r_0 r \frac{\partial r}{\partial n} v_1'$$

Function G'_{ik}

For $i = 1, 2$

For $k = 1, 2$

$$G'_{ik} = \Pi_3(v'_2 r_{,i} r_{,k} - v'_1 \delta_{ik})$$

For $k = 3$

$$G'_{ik} = -\Pi'_4 r r_{,i} v_1$$

For $i = 3$

For $k = 1, 2$

$$G'_{ik} = \Pi_5(-v'_2 r_{,k} \frac{\partial r}{\partial n} + v'_1 n_k)$$

For $k = 3$

$$G'_{ik} = -c^2 r_0 r \frac{\partial r}{\partial n} v_1$$

Function P_{ik}

For $i = 1, 2$

For $k = 1, 2$

$$P_{ik} = \Pi'_9\{(\frac{\partial r}{\partial n}\delta_{ik} + r_{,i}n_k)(u_3 + u'_3) - \frac{\partial r}{\partial n}r_{,i}r_{,k}(u_6 + u'_6) + r_{,k}n_i(u_4 + u'_4)\}$$

For $k = 3$

$$P_{ik} = \Pi'_{10}\{-u'_2(2r_{,i}\frac{\partial r}{\partial n} - n_i) + u'_0 n_i\}$$

For $i = 3$

For $k = 1, 2$

$$P_{ik} = \Pi'_4 r_{,k} r u'_1$$

For $k = 3$

$$P_{ik} = \Pi'_{12} u'_0$$

Function P'_{ik}

For $i = 1, 2$

For $k = 1, 2$

$$P'_{ik} = \Pi'_9 \left\{ - \left(\frac{\partial r}{\partial n} \delta_{ik} + r_{,i} n_k \right) (u_3 - u'_3) + \frac{\partial r}{\partial n} r_{,i} r_{,k} (u_6 - u'_6) - r_{,k} n_i (u_4 - u'_4) \right\}$$

For $k = 3$

$$P'_{ik} = \Pi'_{10} \{ u_2 (2 r_{,i} \frac{\partial r}{\partial n} - n_i) + u_0 n_i \}$$

For $i = 3$

For $k = 1, 2$

$$P'_{ik} = -\Pi'_4 r_{,k} r u_1$$

For $k = 3$

$$P'_{ik} = -\Pi'_{12} u_0$$

Function Q_{ik}

For $i = 1, 2$

For $k = 1, 2$

$$Q_{ik} = \Pi'_9 \left\{ \left(\frac{\partial r}{\partial n}\delta_{ik} + r_{,i}n_k\right)(w_3 + w'_3) - \frac{\partial r}{\partial n} r_{,i}r_{,k}(w_6 + w'_6) + r_{,k}n_i(w_4 + w'_4) \right\}$$

For $k = 3$

$$Q_{ik} = \Pi'_{10} \left\{ -v'_2\left(2r_{,i}\frac{\partial r}{\partial n} - n_i\right) + v'_0 n_i \right\}$$

For $i = 3$

For $k = 1, 2$

$$Q_{ik} = \Pi'_4 r_{,k} r v'_1$$

For $k = 3$

$$Q_{ik} = \Pi'_{12} v'_0$$

Function Q'_{ik}

For $i = 1, 2$

For $k = 1, 2$

$$Q'_{ik} = \Pi'_9\{-(\frac{\partial r}{\partial n}\delta_{ik} + r_{,i}n_k)(w_3 - w'_3) + \frac{\partial r}{\partial n}r_{,i}r_{,k}(w_6 - w'_6) - r_{,k}n_i(w_4 - w'_4)\}$$

For $k = 3$

$$Q'_{ik} = \Pi'_{10}\{v_2(2r_{,i}\frac{\partial r}{\partial n} - n_i) - v_0 n_i\}$$

For $i = 3$

For $k = 1, 2$

$$Q'_{ik} = -\Pi'_4 r_{,k} r v_1$$

For $k = 3$

$$Q'_{ik} = -\Pi'_{12} v_0$$

Function Z_{ik}

For $i = 1, 2$

For $k = 1, 2$

$$\begin{aligned} Z_{ik} = & - \Pi_7 c r_0 \frac{\partial r}{\partial n} r_{,i} r_{,k} - \Pi_8 c r_0 \left(\frac{\partial r}{\partial n}\delta_{ik} + r_{,i} n_k - r_{,k} n_i\right) \\ & + \Pi_9' \left[\left(\frac{\partial r}{\partial n}\delta_{ik} + r_{,i} n_k\right)(z_3 + z_3') - \frac{\partial r}{\partial n} r_{,i} r_{,k}(z_6 + z_6') \right. \\ & + \left. r_{,k} n_i (z_4 + z_4')\right] \end{aligned}$$

For $k = 3$

$$Z_{ik} = 0$$

For $i = 3$

$$Z_{ik} = 0 \text{ for } k = 1, 2, 3$$

Function Z'_{ik}

For $i = 1,2$

For $k = 1,2$

$$Z'_{ik} = \Pi'_9 \left[- \left(\frac{\partial r}{\partial n} \delta_{ik} + r_{,i} n_k \right) (z_3 - z'_3) + \frac{\partial r}{\partial n} r_{,i} r_{,k} (z_6 - z'_6) - r_{,k} n_i (z_4 - z'_4) \right]$$

For $k = 3$

$$Z'_{ik} = 0$$

For $i = 3$

$$Z'_{ik} = 0 \text{ for } k = 1,2,3$$

Appendix H

Functions Required for the Evaluation of Interior Effective Stresses and Pore Pressure

These functions are the integrands occurring in equations (6.60)and (6.61). In the following,

$$\eta \equiv \frac{2\nu}{1-2\nu} \text{ where } \nu \text{ is Poisson's ratio of the solid skeleton}$$

$$a^2 = -ic^2 \ , \ a = e^{-\frac{i\pi}{4}}c = \frac{c}{\sqrt{2}}(1-i)$$

K_0 and K_1 are the modified Bessel functions of the second kind of orders 0 and 1 respectively.

$$K_0(ar) \ = \ ker(cr) - i\,kei(cr)$$

$$K_1(ar) = -\frac{1}{\sqrt{2}}[ker'(cr) + kei'(cr)] + \frac{i}{\sqrt{2}}[kei'(cr) - ker'(cr)]$$

where ker, kei, ker', kei' are the Kelvin functions.

$$\begin{aligned} F_1(ar) &= \frac{2}{a^2r^2} - K_0(ar) - \frac{2}{ar}K_1(ar) \\ &= -ker(cr) + \frac{2}{cr}kei'(cr) \\ &\quad +i[\frac{2}{c^2r^2} + kei(cr) + \frac{2}{cr}ker'(cr)] \end{aligned}$$

The functions $D_{\alpha kj}, S_{\alpha kj}, \tilde{\bar{u}}^{*3}_{\alpha}, \tilde{\bar{T}}^{*3}_{\alpha}$ are defined below.

Function $D_{\alpha kj}$

For $\alpha = 1,2$

For $k = 1,2$ and $j = 1,2$

$$\begin{aligned} D_{\alpha kj} \;=\; & -\Pi_1 \frac{1}{r}(2r_{,\alpha}\delta_{kj} + r_{,k}\delta_{\alpha j} + r_{,j}\delta_{\alpha k} - 4r_{,\alpha}r_{,j}r_{,k}) \\ & +\Pi_2 \frac{1}{r}(r_{,j}\delta_{\alpha k} + r_{,k}\delta_{\alpha j}) \\ & +\Pi_3\{\frac{2}{r}F_1(ar)[r_{,\alpha}\delta_{kj} + r_{,k}\delta_{\alpha j} + r_{,j}\delta_{\alpha k} - 4r_{,\alpha}r_{,j}r_{,k}] \\ & +2aK_1(ar)r_{,\alpha}r_{,j}r_{,k}\} \\ & -\eta r_{,\alpha}\delta_{kj}[\frac{1}{r}(\Pi_1 - \Pi_2) - \Pi_3 aK_1(ar)] \end{aligned}$$

For $\alpha = 3$

For $k = 1,2$ and $j = 1,2$

$$\begin{aligned} D_{\alpha kj} = -\Pi_5 \Bigg\{ & \frac{2}{r}F_1(ar)\left[\frac{\partial r}{\partial n}(\delta_{kj} - 4r_{,k}r_{,j}) + r_{,k}n_j + r_{,j}n_k\right] \\ & +a\frac{\partial r}{\partial n}K_1(ar)[2r_{,j}r_{,k} + \eta\delta_{kj}]\Bigg\} \end{aligned}$$

Function $S_{\alpha kj}$

For $\alpha = 1,2$

For $k = 1,2$ and $j = 1,2$

$$
\begin{aligned}
S_{\alpha kj} \;=\; & r_0\Pi_7\frac{1}{r^2}\{\frac{\partial r}{\partial n}(2r_{,\alpha}\delta_{kj} + r_{,k}\delta_{\alpha j} + r_{,j}\delta_{\alpha k} - 8r_{,\alpha}r_{,j}r_{,k}) \\
& + r_{,\alpha}(r_{,k}n_j + r_{,j}n_k)\} \\
& + r_0\Pi_8\frac{1}{r^2}\{2(n_j\delta_{\alpha k} + n_k\delta_{\alpha j}) - 2r_{,j}(\frac{\partial r}{\partial n}\delta_{\alpha k} + r_{,\alpha}n_k) \\
& - 2r_{,k}(\frac{\partial r}{\partial n}\delta_{\alpha j} + r_{,\alpha}n_j) - 2(\delta_{kj} - 2r_{,k}r_{,j})n_\alpha\} \\
& + 2(1-i)\Pi_9'\{\frac{F_1(ar)}{ar^2}[4\frac{\partial r}{\partial n}(6r_{,\alpha}r_{,k}r_{,j} - r_{,\alpha}\delta_{kj} - r_{,k}\delta_{\alpha j} - r_{,j}\delta_{\alpha k}) \\
& + n_\alpha\delta_{kj} + n_k\delta_{\alpha j} + n_j\delta_{\alpha k} \\
& - 4(r_{,\alpha}r_{,k}n_j + r_{,\alpha}r_{,j}n_k + r_{,k}r_{,j}n_\alpha)] \\
& + \frac{K_1(ar)}{r}[\frac{\partial r}{\partial n}(r_{,j}\delta_{\alpha k} + r_{,\alpha}\delta_{kj} + r_{,k}\delta_{\alpha j} - 8r_{,\alpha}r_{,k}r_{,j}) \\
& + r_{,\alpha}(r_{,k}n_j + r_{,j}n_k) + n_\alpha(3r_{,k}r_{,j} - \delta_{kj})] \\
& + aK_0(ar)[-\frac{\partial r}{\partial n}r_{,\alpha}r_{,k}r_{,j} + r_{,k}r_{,j}n_\alpha]\} \\
& + \eta\delta_{kj}\{2r_0\Pi_8\frac{1}{r^2}(n_\alpha - 2r_{,\alpha}\frac{\partial r}{\partial n}) \\
& + (1-i)\Pi_9'[\frac{K_1(ar)}{r}(n_\alpha - 2r_{,\alpha}\frac{\partial r}{\partial n}) \\
& + aK_0(ar)(n_\alpha - r_{,\alpha}\frac{\partial r}{\partial n})]\}
\end{aligned}
$$

For $\alpha = 3$

For $k = 1,2$ and $j = 1,2$

$$S_{\alpha kj} = -i\Pi_4'\{(1+\eta)\delta_{kj}K_0(ar) + F_1(ar)(\delta_{kj} - 2r_{,k}r_{,j})\}$$

Function $\tilde{\tilde{u}}_\alpha^{*3}$

For $\alpha = 1,2$

$$\tilde{\tilde{u}}_\alpha^{*3} = \frac{1}{2} i \Pi_4' r r_{,\alpha} [F_1(ar) + K_0(ar)]$$

For $\alpha = 3$

$$\tilde{\tilde{u}}_\alpha^{*3} = -\frac{(1-i)}{\sqrt{2}} \Pi_6' \frac{\partial r}{\partial n} K_1(ar)$$

Function $\tilde{\tilde{T}}_\alpha^{*3}$

For $\alpha = 1,2$

$$\tilde{\tilde{T}}_\alpha^{*3} = -i\Pi_{10}' \left\{ \left(2r_{,\alpha} \frac{\partial r}{\partial n} - n_\alpha \right) F_1(ar) + K_0(ar) n_\alpha \right\}$$

For $\alpha = 3$

$$\tilde{\tilde{T}}_\alpha^{*3} = -i\Pi_{12}' K_0(ar)$$

Appendix I

Wave loading of a Flat Homogeneous Isotropic Poroelastic Seabed - Analytic Solution

For the case of a flat seabed, it is possible to determine by analytic means the wave induced effective stresses and pore pressures. We present here a summary of the technique used by the author in his M.Eng thesis (Raman-Nair, 1985). It was demonstrated that for sand beds the acceleration terms may be deleted from the governing equations. We thus obtain from (3.17) and (3.18), for no body forces,

$$\tau_{ij,j} = 0 \tag{I.1}$$

$$-p_{,i} = \frac{\rho_f g}{k_0} \dot{w}_i \tag{I.2}$$

where

$$w_i = f(U_i - u_i)$$

We also recall from (3.5) and (3.26) the constitutive laws in the form

$$\tau_{ij} = 2\mu e_{ij} + \delta_{ij}\lambda e - \delta_{ij} p \tag{I.3}$$

$$-p = \frac{(1-f)}{f} K_f e + K_f \varepsilon \tag{I.4}$$

where we have used the fact that $K_\tau \to \infty$,so that $\alpha \approx 1$. Substituting (I.3) into (I.1) gives

$$\mu u_{i,jj} + (\lambda + \mu) u_{j,ji} = p_{,i} \tag{I.5}$$

We shall rewrite equation (I.2) in terms of the soil displacement vector u_i (rather than w_i). Differentiating (I.2) with respect to x_i gives

$$-p_{,ii} = \frac{\rho_f g f}{k_0} \frac{\partial}{\partial t}(\varepsilon - e) \tag{I.6}$$

From (I.4):

$$K_f(\varepsilon - e) = -p - \frac{K_f}{f} e$$

Substituting this into (I.6) gives:

$$\frac{k_0}{\rho_f g} \nabla^2 p = \frac{f}{K_f} \frac{\partial p}{\partial t} + \frac{\partial e}{\partial t} \tag{I.7}$$

This is the so-called storage equation derived in a different way by Verruijt (1969) and Biot (1941).

The system of equations (I.5) and (I.7) must be solved subject to appropriate boundary conditions. We take the x-axis on the flat seabed and parallel to the

direction of propagation of the wave. The z-axis is vertically downward into the soil. The problem domain is two dimensional in the $x-z$ plane and is illustrated in Figure (I.1). The boundary conditions are:

$$\text{(a) } \tau'_{zz} = \tau'_{xz} = 0 \quad \text{at } z = 0$$

$$\text{(b) } p(\text{ in bed }) = P_0 e^{i(kx-\omega t)}$$

where P_0 is the amplitude of the wave induced pressure on the seabed, k is the wave number and ω is the circular wave frequency.

$$\text{(c) } u_1 = u_2 = 0 \quad \text{at } z = z_0$$

where u_1 and u_2 denote the x and z components of the soil displacement vector $\underline{u}$.

$$\text{(d) } \frac{\partial p}{\partial z} = 0 \quad \text{at } z = z_0$$

The value of P_0 is determined from the wave velocity potential Φ which is given by:

$$\Phi(x,z,t) = \frac{i\eta_0 g}{\omega}[\cosh k(z+h) - \frac{\omega^2}{kh}\sinh k(z+h)]e^{i(kx-\omega t)} \tag{I.8}$$

where η_0 is the wave amplitude. Then from Bernoulli's equation,

$$P_0 e^{i(kx-\omega t)} = -\rho_f \frac{\partial \Phi}{\partial t} \quad \text{at } z = 0$$

so that

$$P_0 = \rho_f \eta_0 g[\cosh(kh) - \frac{\omega^2}{gk}\sinh(kh)] \tag{I.9}$$

In view of the dispersion relation

$$\omega^2 = gk\tanh(kh)$$

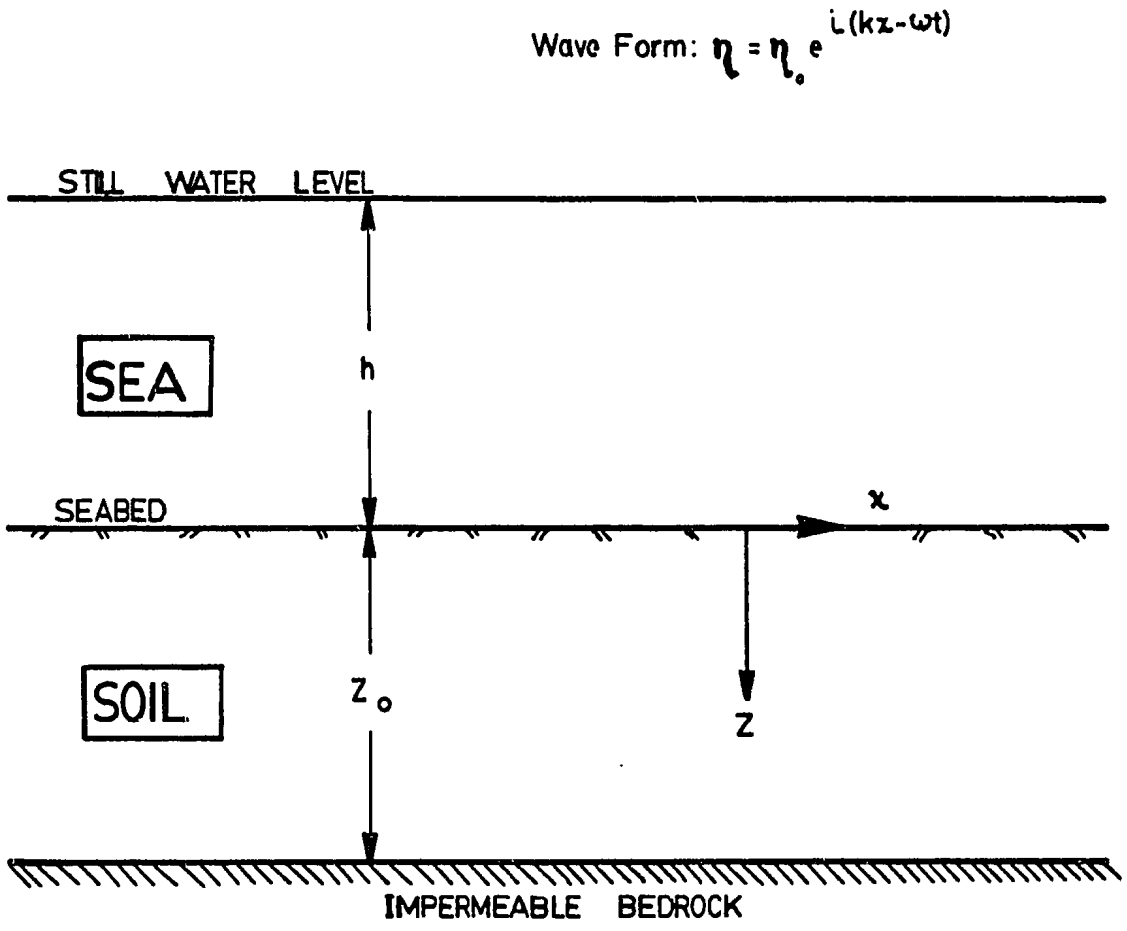

FIG.(I.1) Wave Loading of Flat Seabed

we can write (I.9) more compactly as

$$P_0 = \frac{\rho_f \eta_0 g}{\cosh(kh)} \tag{I.10}$$

Equation (I.5) is satisfied by the function

$$u_i = (\phi + x_j \psi_j)_{,i} - 4(1-\nu)\psi_i \tag{I.11}$$

where

$$\nu = \frac{\lambda}{2(\lambda+\mu)} \text{ (Poisson's ratio)}$$

provided that

$$\frac{2\mu(1-\nu)}{1-2\nu}(\nabla^2\phi + x_j\nabla^2\psi_j)_{,i} - 4\mu(1-\nu)\nabla^2\psi_i = p_{,i} \tag{I.12}$$

Equation (I.11) is the well known Papkovich-Neuber solution of the equilibrium equations of theory of elasticity, ϕ and ψ_i being functions of x, z , and t. Any one of the functions ϕ, ψ_1, ψ_2 may be taken to be zero without loss of completeness provided that the coordinate system is chosen in an appropriate way and 4ν is not a positive integer. We choose

$$\psi \equiv 0 \text{ and } \psi_2 \equiv \psi$$

Then equations (I.12) become

$$2\mu\beta\frac{\partial}{\partial x}(\nabla^2\phi + z\nabla^2\psi) = \frac{\partial p}{\partial x} \tag{I.13}$$

$$2\mu\beta\frac{\partial}{\partial z}(\nabla^2\phi + z\nabla^2\psi) - 4\mu(1-\nu)\nabla^2\psi = \frac{\partial p}{\partial z} \tag{I.14}$$

where

$$\beta = \frac{1-\nu}{1-2\nu} \tag{I.15}$$

Equations (I.13) and (I.14) represent equation (I.5) in terms of the functions ϕ and ψ. Using (I.11), we express (I.7) in terms of ϕ and ψ:

$$\frac{k_0}{\rho_f g}\nabla^2 p - \frac{f}{K_f}\frac{\partial p}{\partial t} = \frac{\partial}{\partial t}\left[\nabla^2\phi + z\nabla^2\psi - 2(1-2\nu)\frac{\partial\psi}{\partial z}\right] \tag{I.16}$$

It can be shown (Raman-Nair, 1985) that the solution of (I.13), (I.14) and (I.16) is of the form

$$\phi(x,z,t) = [(a_1 + a_2 z)e^{-kz} + (a_3 + a_4 z)e^{kz} + a_5 e^{-k'z} + a_6 e^{k'z}]e^{i(kx-\omega t)} \tag{I.17}$$

$$\psi(x,z,t) = (Be^{-kz} + De^{kz})e^{i(kx-\omega t)} \tag{I.18}$$

where

$$\begin{aligned} B &= \frac{-4\mu\beta a_2}{\alpha_0} \\ D &= \frac{-4\mu\beta a_4}{\alpha_0} \\ \alpha_0 &= -2(1-\nu)[\frac{f}{K_f} + \frac{1}{2\mu\beta}]^{-1} \end{aligned}$$

and

$$p(x,z,t) = (A_1 e^{-kz} + A_2 e^{kz} + A_3 e^{-k'z} + A_4 e^{k'z})e^{i(kx-\omega t)} \tag{I.19}$$

where

$$\begin{aligned} A_1 &= -4\mu\beta k a_2 \\ A_2 &= 4\mu\beta k a_4 \\ A_3 &= 2\mu\beta[(k')^2 - k^2]a_5 \\ A_4 &= 2\mu\beta[(k')^2 - k^2]a_6 \\ (k')^2 &= k^2 - \frac{i\omega}{c} \\ c &= \frac{k_0}{\rho_f g}\left[\frac{f}{K_f} + \frac{1}{2\mu\beta}\right]^{-1} \end{aligned}$$

Using the constitutive laws the effective stress components τ'_{ij} are written in terms of ϕ and ψ:

$$\begin{aligned}\tau'_{ij} &= 2\mu[\phi_{,ij} + z\psi_{,ij} - (1-2\nu)(\psi_{i,j} + \psi_{j,i})] \\ &\quad + \delta_{ij}\left(\frac{2\mu\nu}{1-2\nu}\right)[\nabla^2\phi + z\nabla^2\psi - 2(1-2\nu)\frac{\partial\psi}{\partial z}]\end{aligned} \tag{I.20}$$

Hence the effective stress components and pore pressure can be expressed in terms of the six constants $a_1, a_2, \cdots a_6$. The six boundary conditions lead to an equation of the form

$$[A]\underline{x} = \underline{b} \tag{I.21}$$

where

$$\underline{x} = (a_1, a_2, a_3, a_4, a_5, a_6)^T$$

$$\underline{b} = (0, 0, \frac{P_0}{2\mu\beta}, 0, 0, 0)^T$$

The elements a_{ij} of the matrix $[A]$ are given by

$$\begin{aligned}a_{11} &= k^2 \\ a_{12} &= -2k\beta[1 + \frac{4(1-\nu)\mu}{\alpha_0}] \\ a_{13} &= k^2 \\ a_{14} &= -a_{12} \\ a_{15} &= k^2 + \beta[(k')^2 - k^2] \\ a_{16} &= a_{15} \\ a_{21} &= -k \\ a_{22} &= 1 + \frac{4(1-\nu)\mu}{\alpha_0} \\ a_{23} &= k\end{aligned}$$

$$
\begin{aligned}
a_{24} &= a_{22} \\
a_{25} &= -k' \\
a_{26} &= k' \\
a_{31} &= 0 \\
a_{32} &= -2k \\
a_{33} &= 0 \\
a_{34} &= 2k \\
a_{35} &= (k')^2 - k^2 \\
a_{36} &= a_{35} \\
a_{41} &= e^{-kz_0} \\
a_{42} &= z_0 e^{-kz_0}(1 - \frac{4\mu\beta}{\alpha_0}) \\
a_{43} &= e^{kz_0} \\
a_{44} &= z_0 e^{kz_0}(1 - \frac{4\mu\beta}{\alpha_0}) \\
a_{45} &= e^{-k'z_0} \\
a_{46} &= e^{k'z_0} \\
a_{51} &= -ke^{-kz_0} \\
a_{52} &= [-kz_0 + 1 + (kz_0 + 3 - 4\nu)\frac{4\mu\beta}{\alpha_0}]e^{-kz_0} \\
a_{53} &= ke^{kz_0} \\
a_{54} &= [kz_0 + 1 + (-kz_0 + 3 - 4\nu)\frac{4\mu\beta}{\alpha_0}]e^{kz_0} \\
a_{55} &= -k'e^{-k'z_0} \\
a_{56} &= k'e^{k'z_0} \\
a_{61} &= 0
\end{aligned}
$$

$$a_{62} = 2k^2 e^{-kz_0}$$

$$a_{63} = 0$$

$$a_{64} = 2k^2 e^{kz_0}$$

$$a_{65} = -k'[(k')^2 - k^2]e^{-k'z_0}$$

$$a_{66} = k'[(k')^2 - k^2]e^{k'z_0}$$

Appendix J

Stress Angle Contours

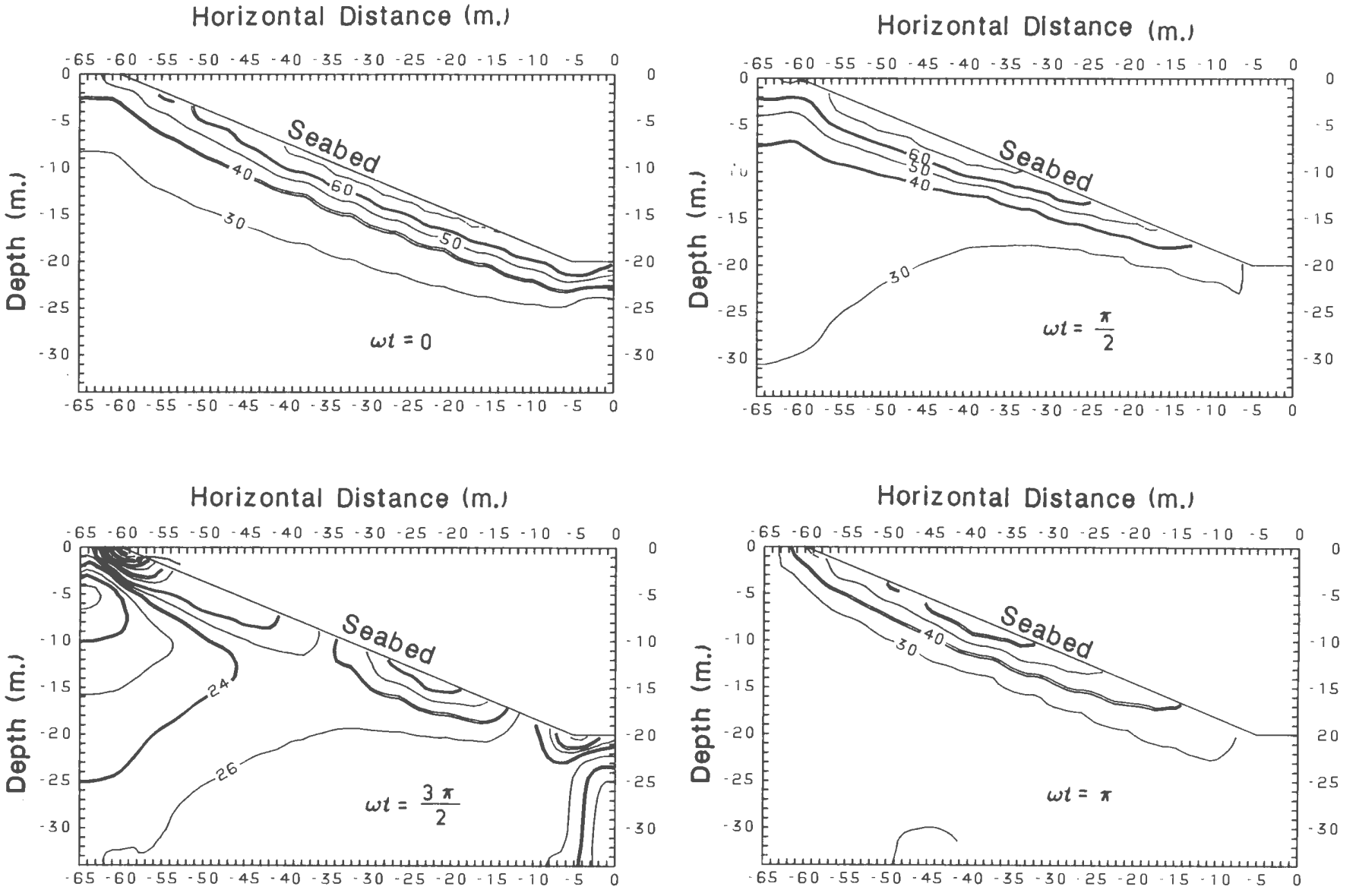

Figure J.1: Stress Angle Contours(degrees): Fine Sand, $K = 0.5$, $L = 300$ m, $\beta = 20^o$
$l_0 = 14$ m, $l_0' = 34$ m

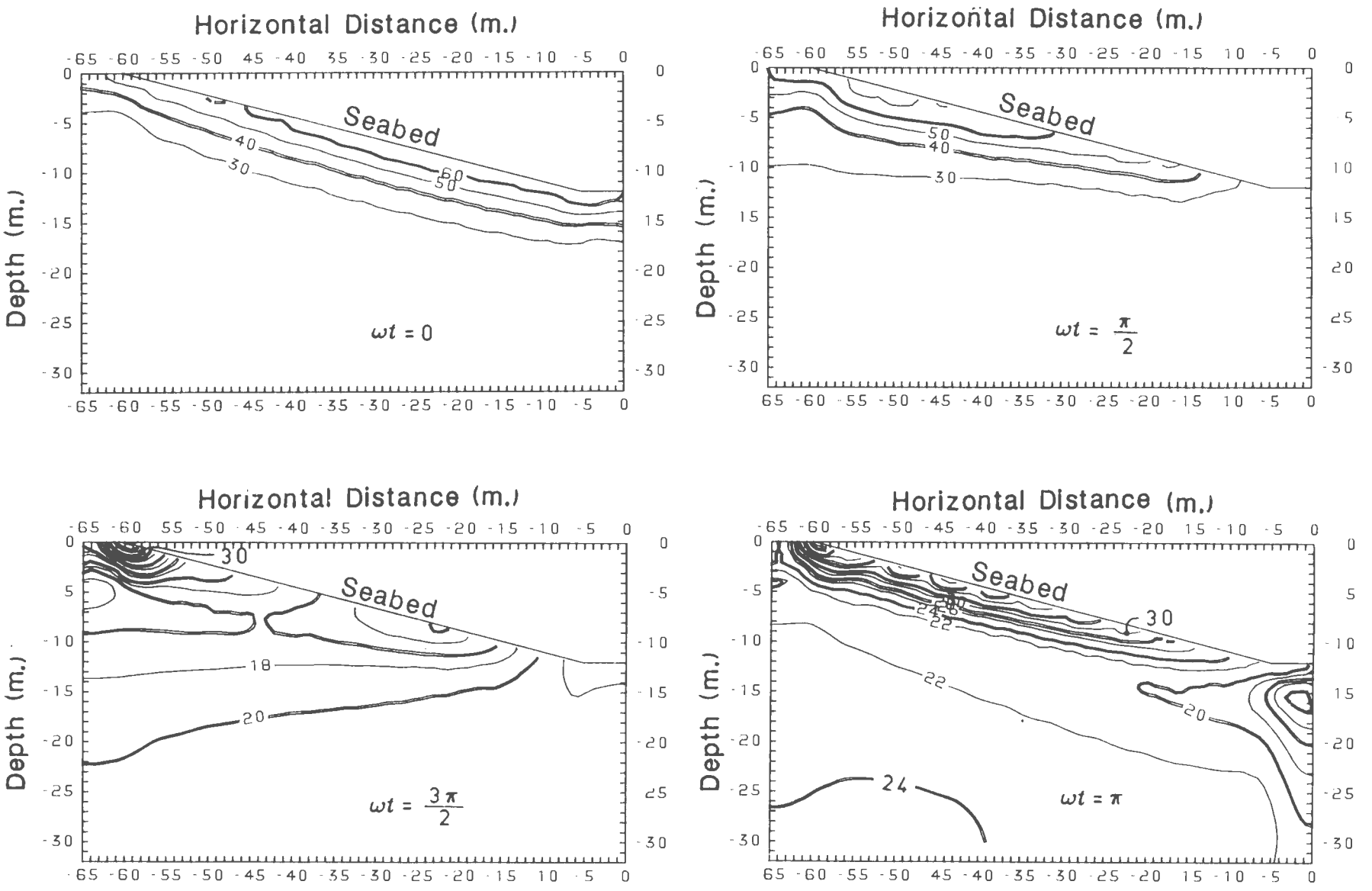

Figure J.2: Stress Angle Contours(degrees): Fine Sand, $K = 0.5$, $L = 300$ m, $\beta = 12^{o}$

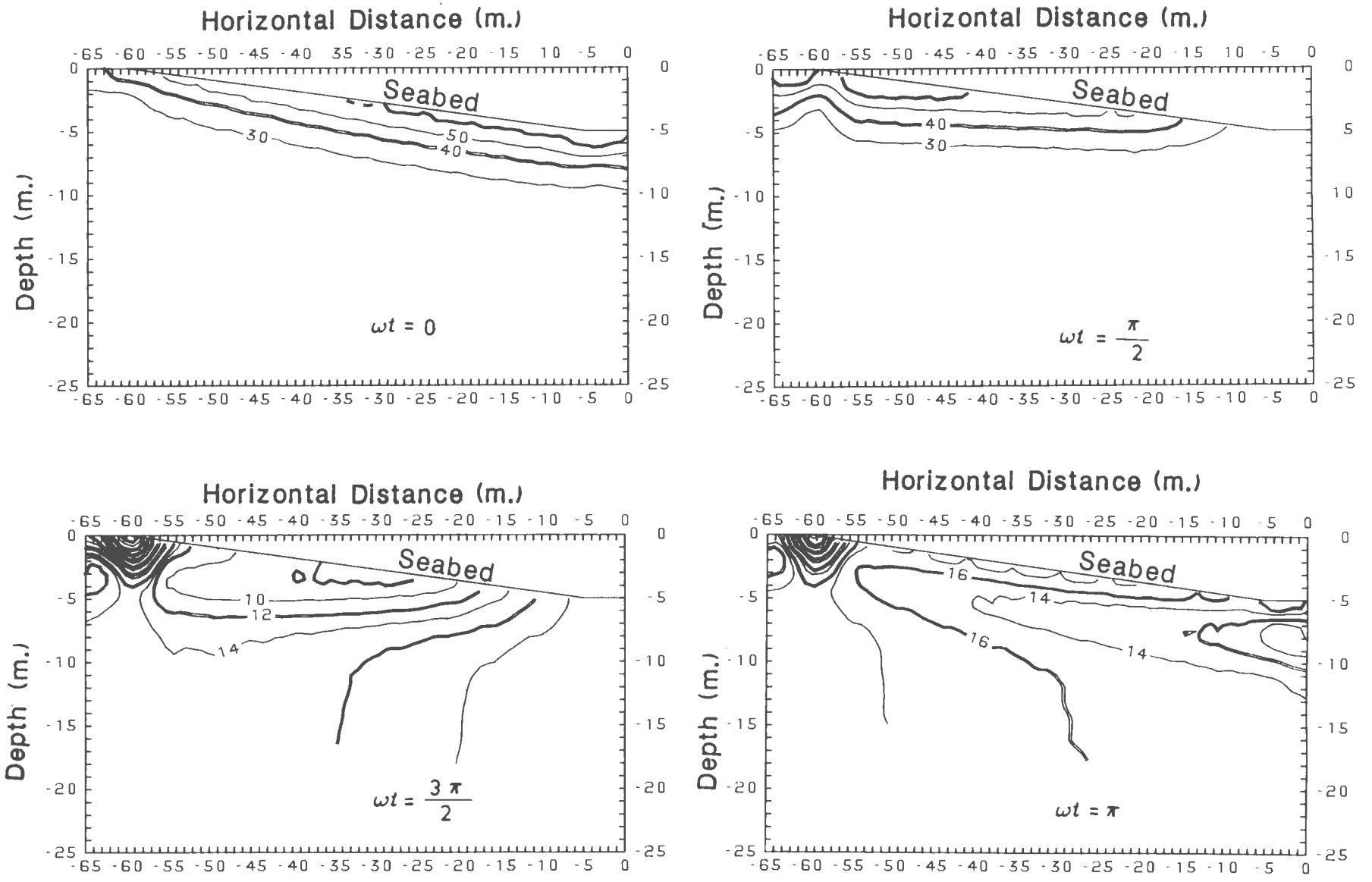

Figure J.3: Stress Angle Contours(degrees):Fine Sand, $K = 0.5$, $L = 300$ m, $\beta = 5^o$

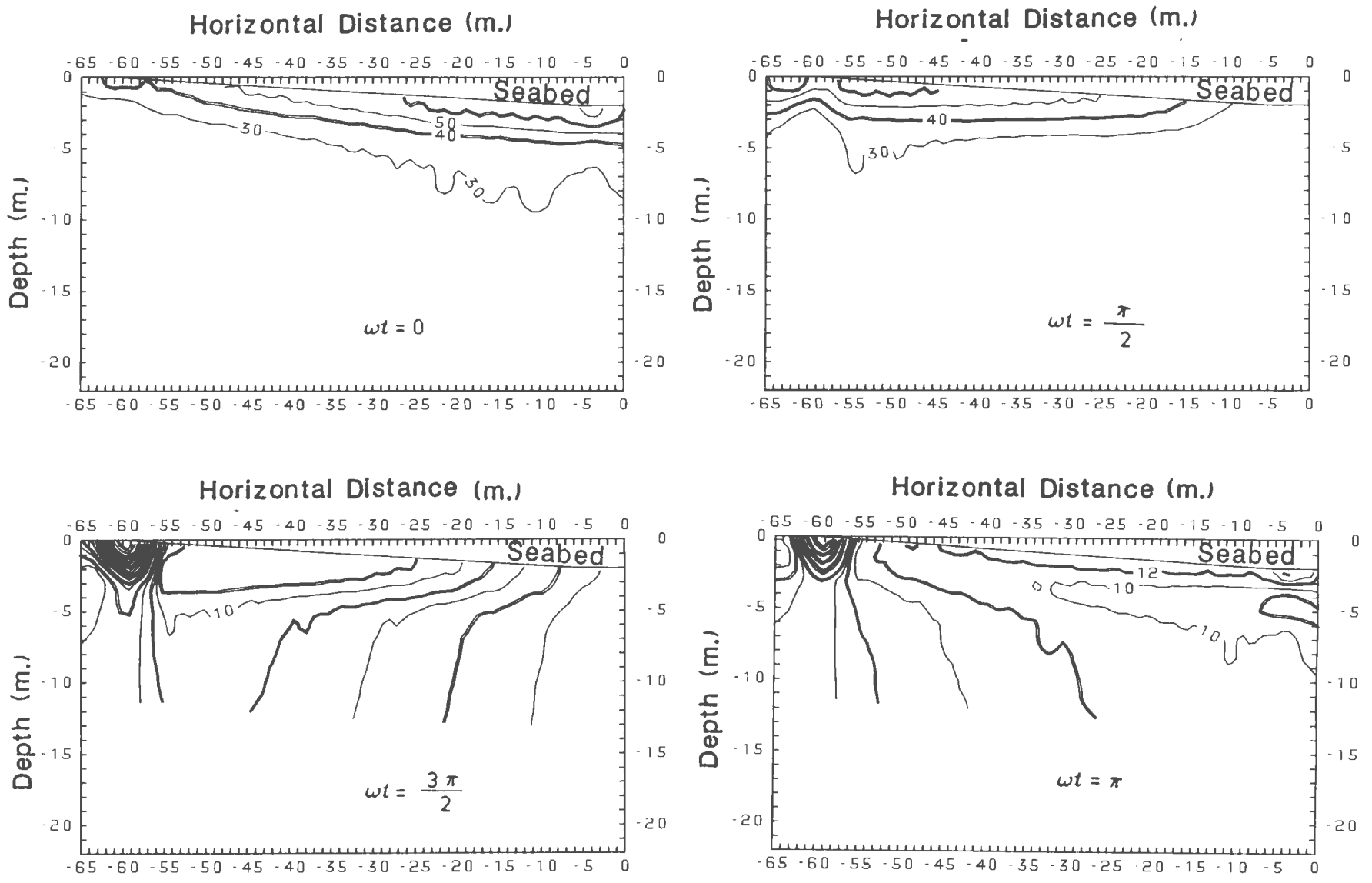

Figure J.4: Stress Angle Contours(degrees):Fine Sand,$K = 0.5$, $L = 300$ m, $\beta = 2^o$

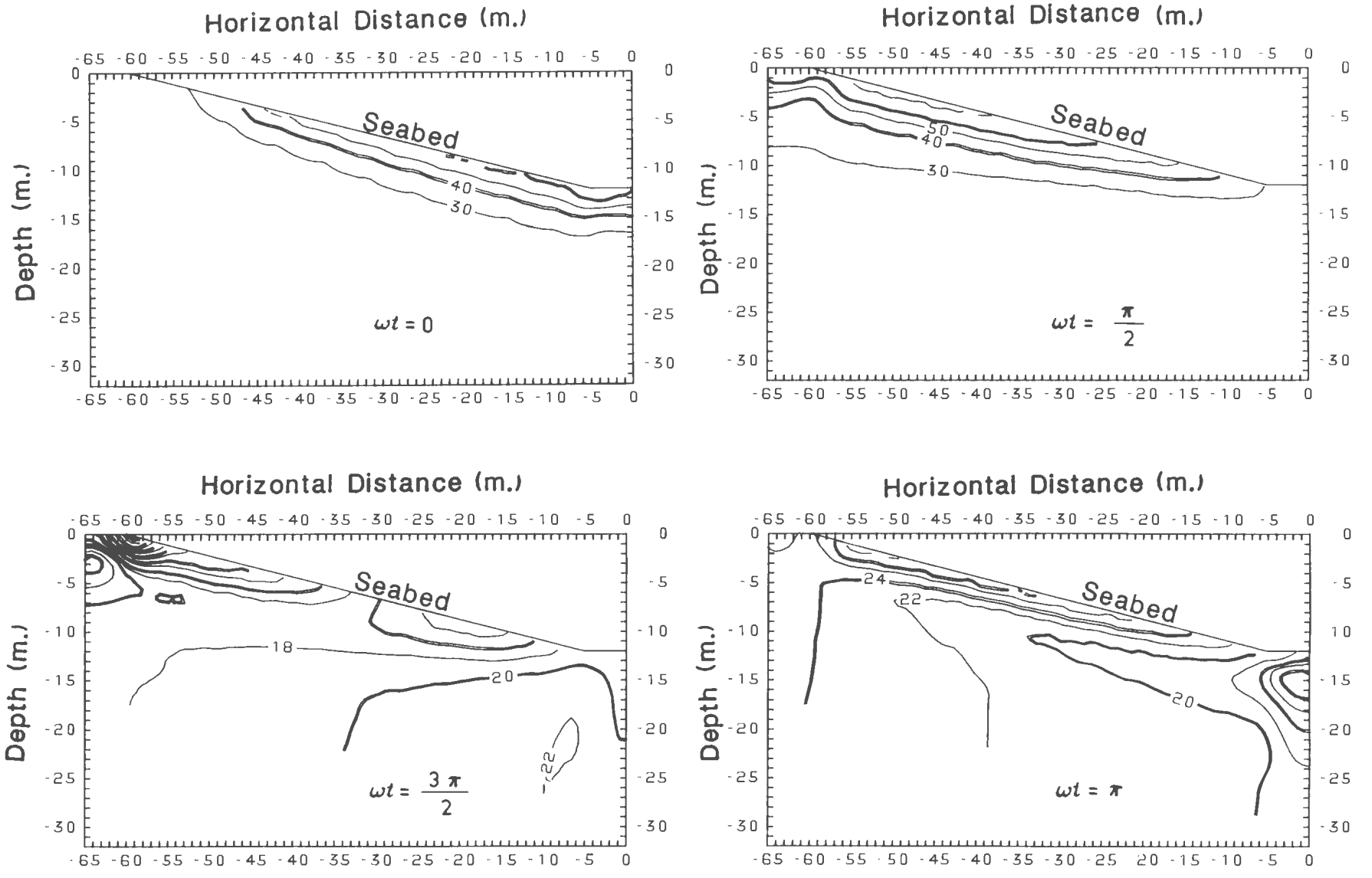

Figure J.5: Stress Angle Contours(degrees):Fine Sand,$K = 0.5$, $L = 225$ m, $\beta = 12^o$

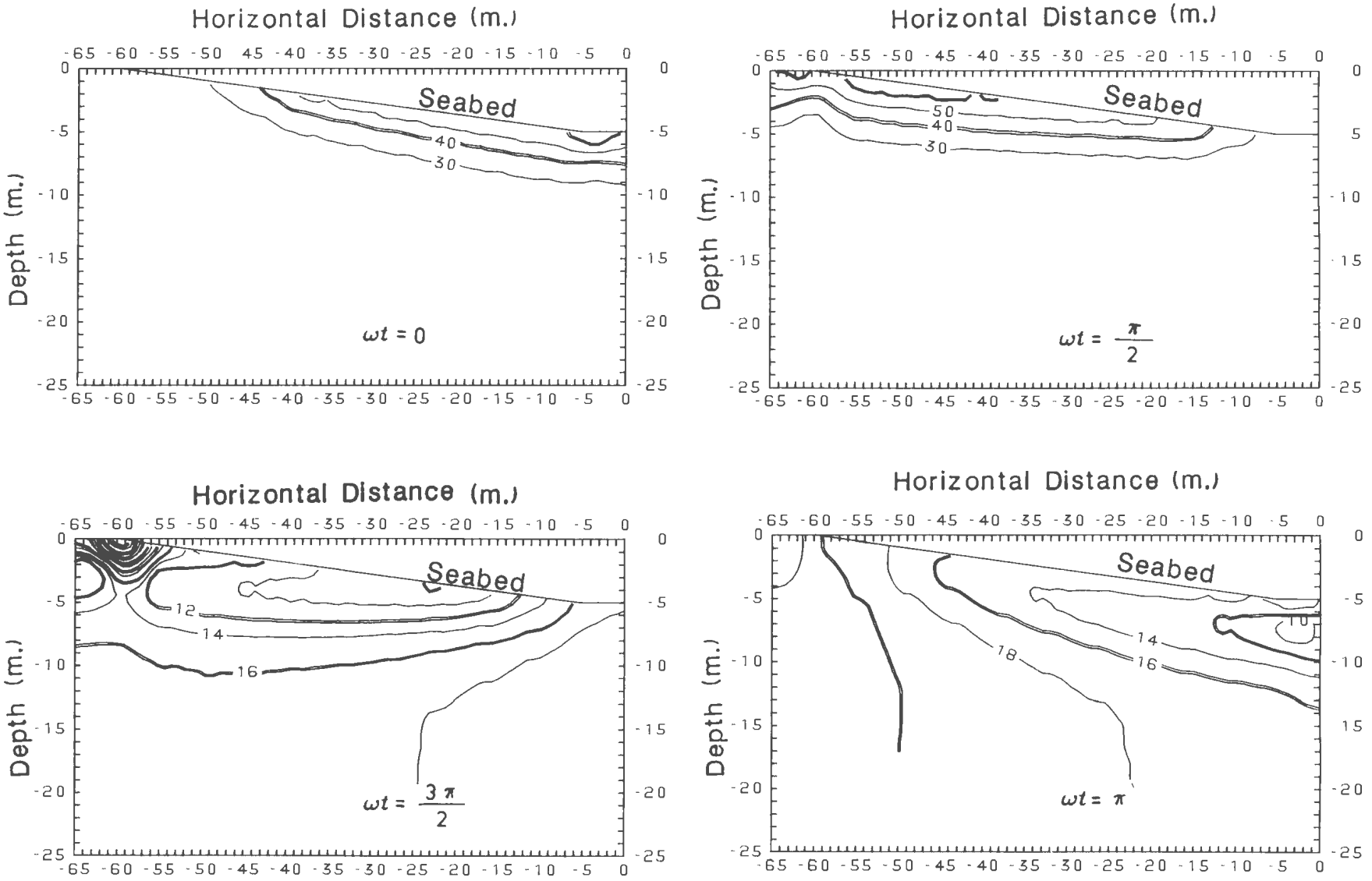

Figure J.6: Stress Angle Contours(degrees):Fine Sand,$K = 0.5$, $L = 225$ m, $\beta = 5^o$

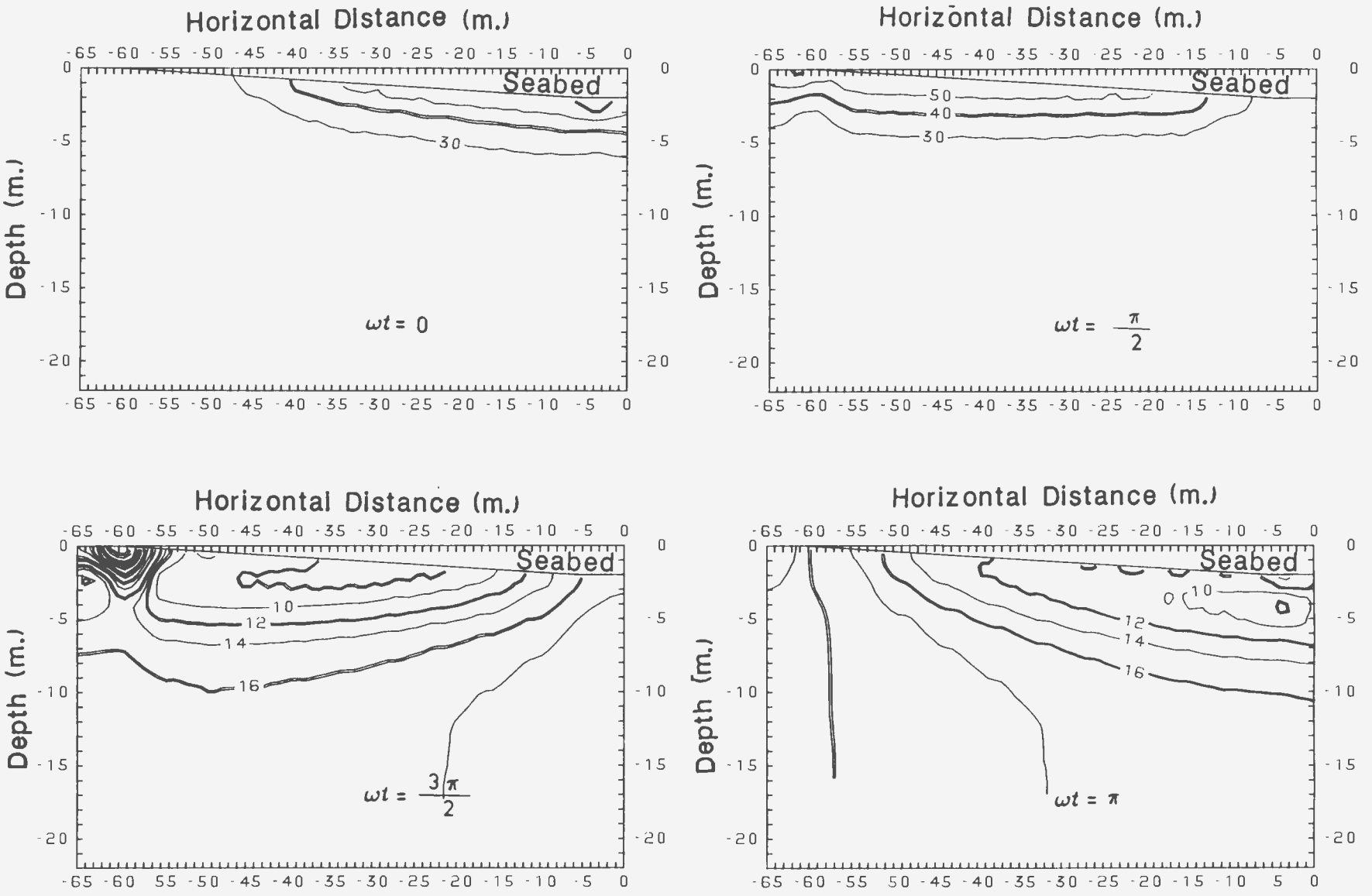

Figure J.7: Stress Angle Contours(degrees):Fine Sand,$K = 0.5$, $L = 225$ m, $\beta = 2^o$

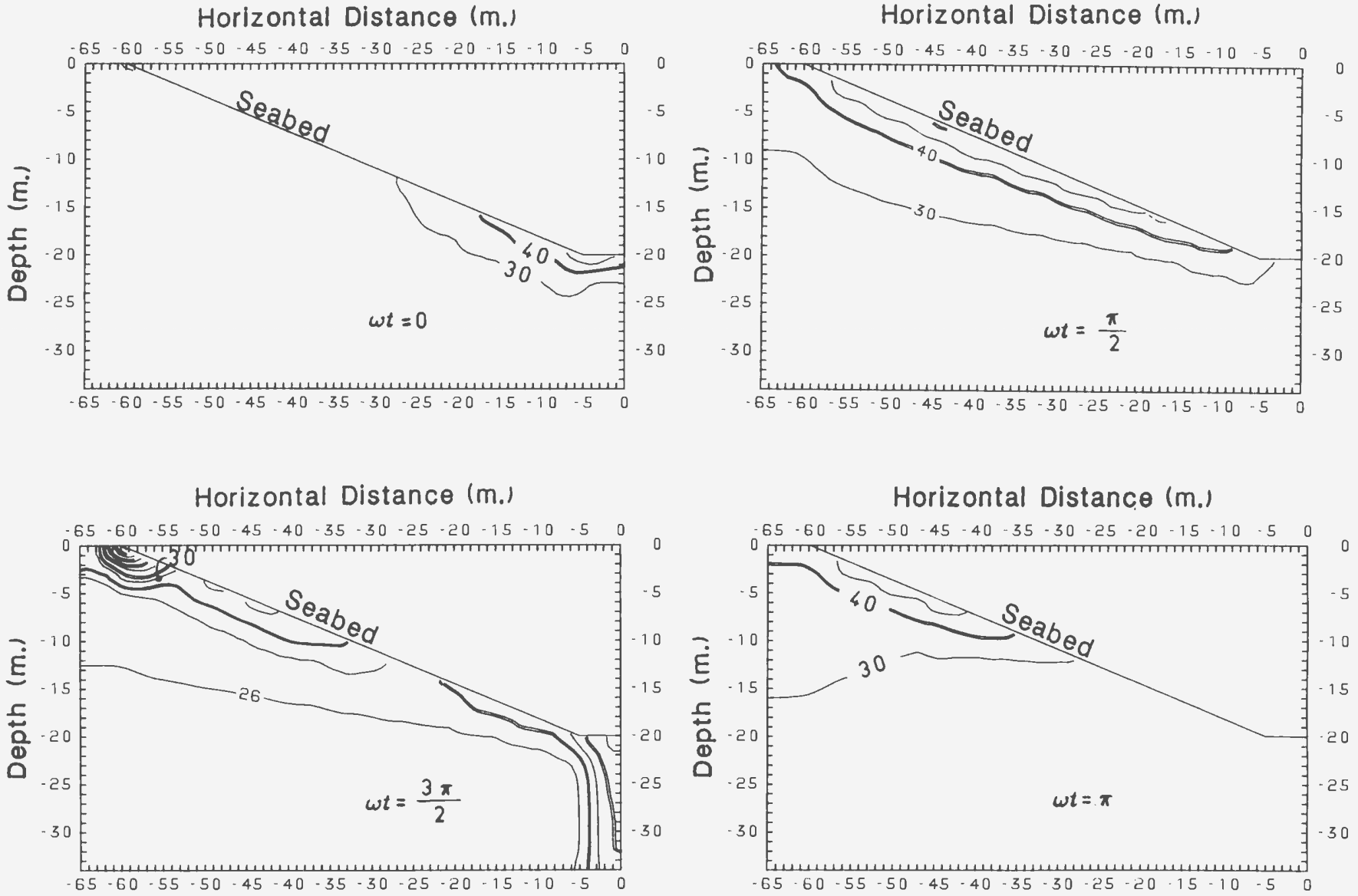

Figure J.8: Stress Angle Contours(degrees):Fine Sand,$K = 0.5$, $L = 150$ m, $\beta = 20^o$

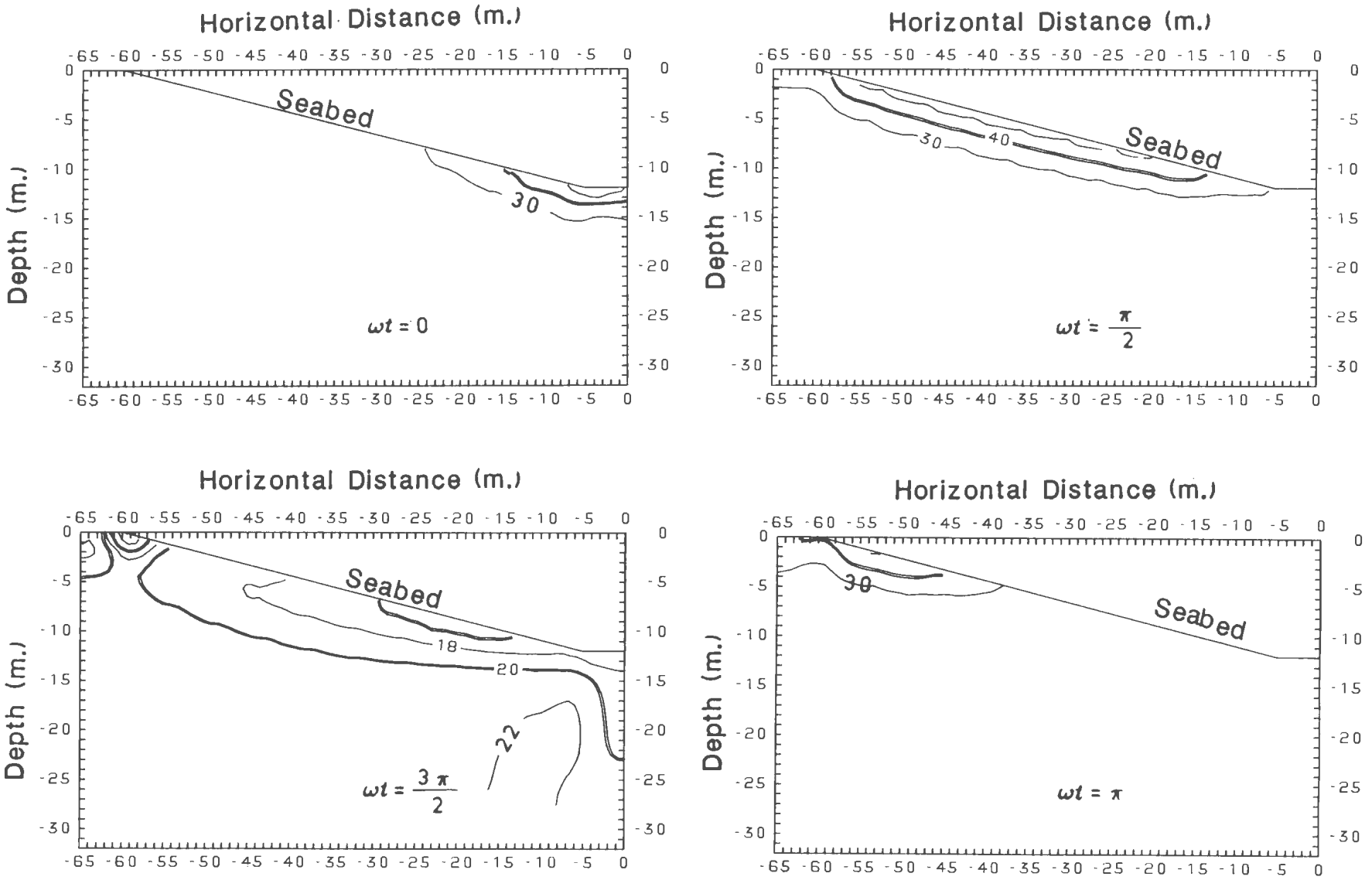

Figure J.9: Stress Angle Contours(degrees):Fine Sand,$K = 0.5$, $L = 150$ m, $\beta = 12^o$

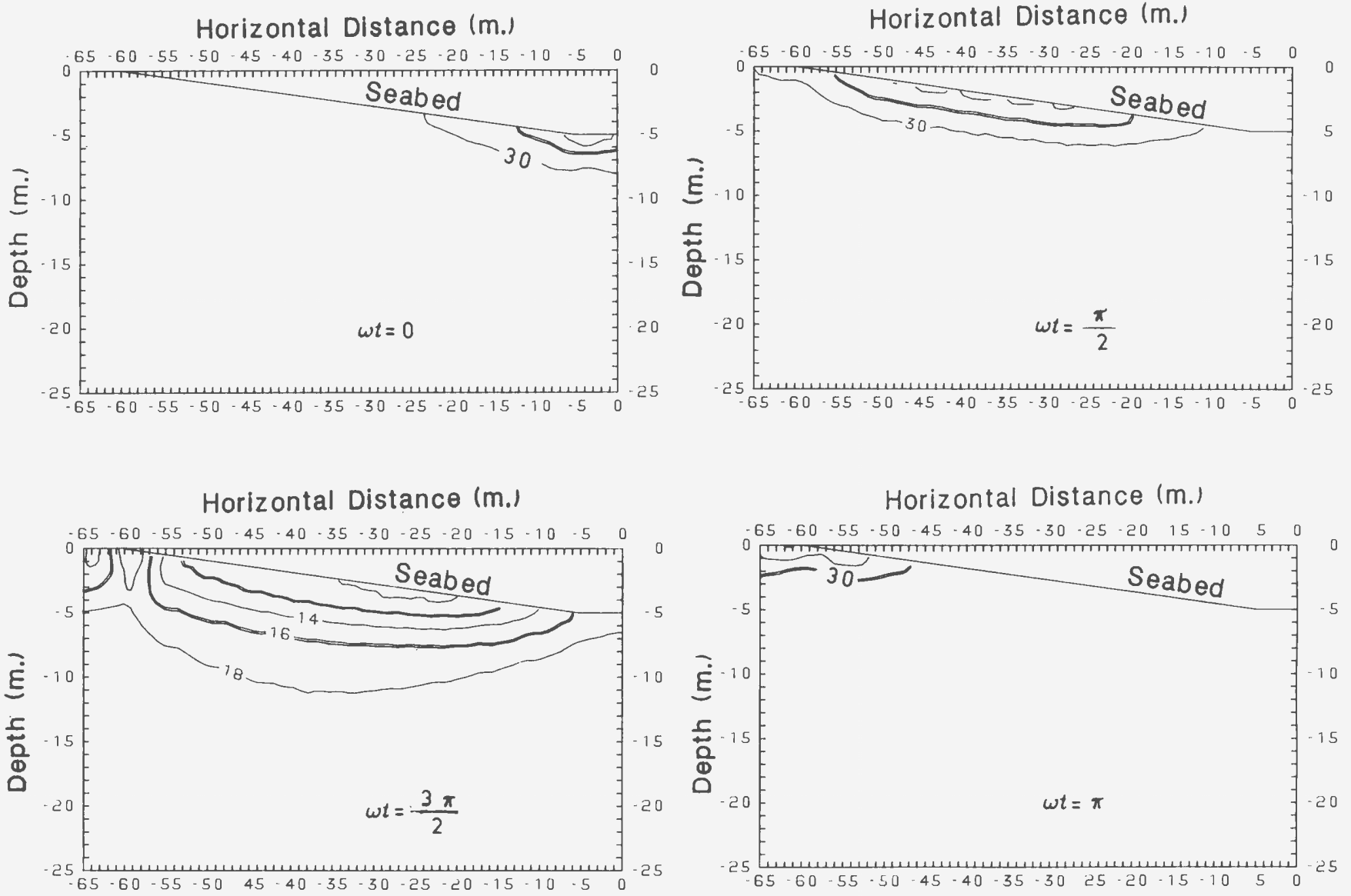

Figure J.10: Stress Angle Contours(degrees):Fine Sand,$K = 0.5$, $L = 150$ m, $\beta = 5^o$

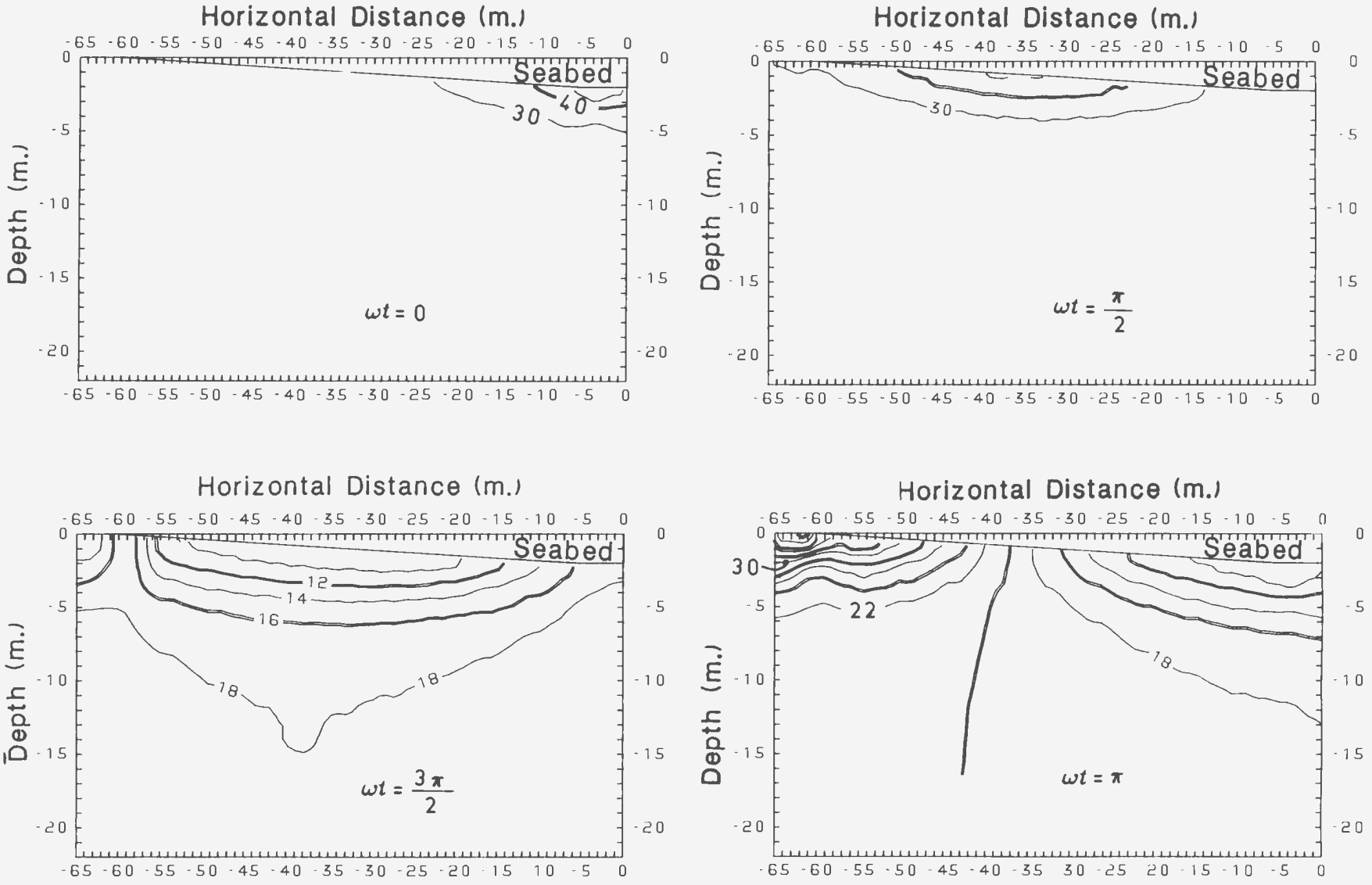

Figure J.11: Stress Angle Contours(degrees):Fine Sand,$K = 0.5$, $L = 150$ m, $\beta = 2^o$

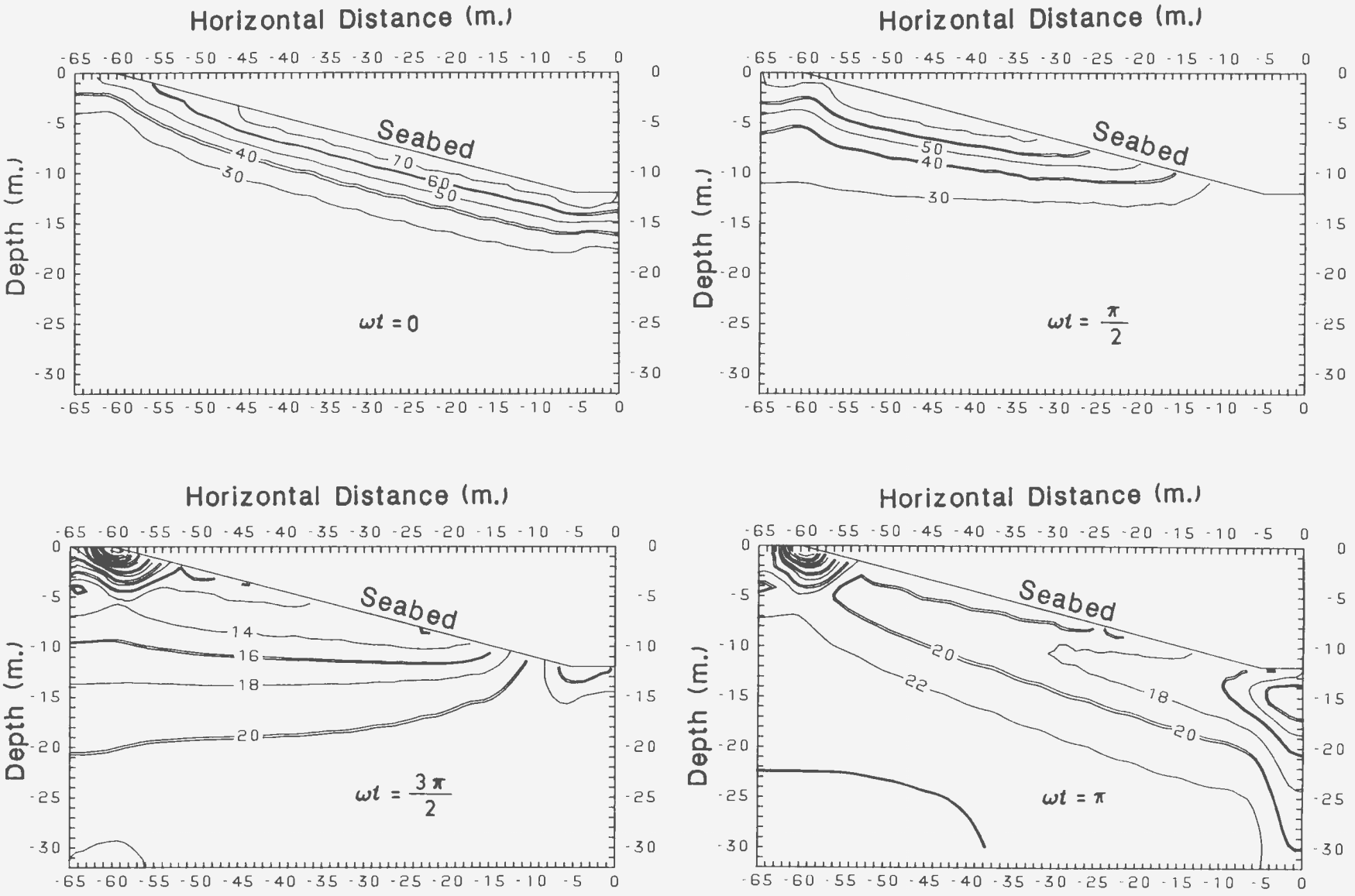

Figure J.12: Stress Angle Contours(degrees):Coarse Sand,$K = 0.5$, $L = 300$ m, $\beta = 12^o$

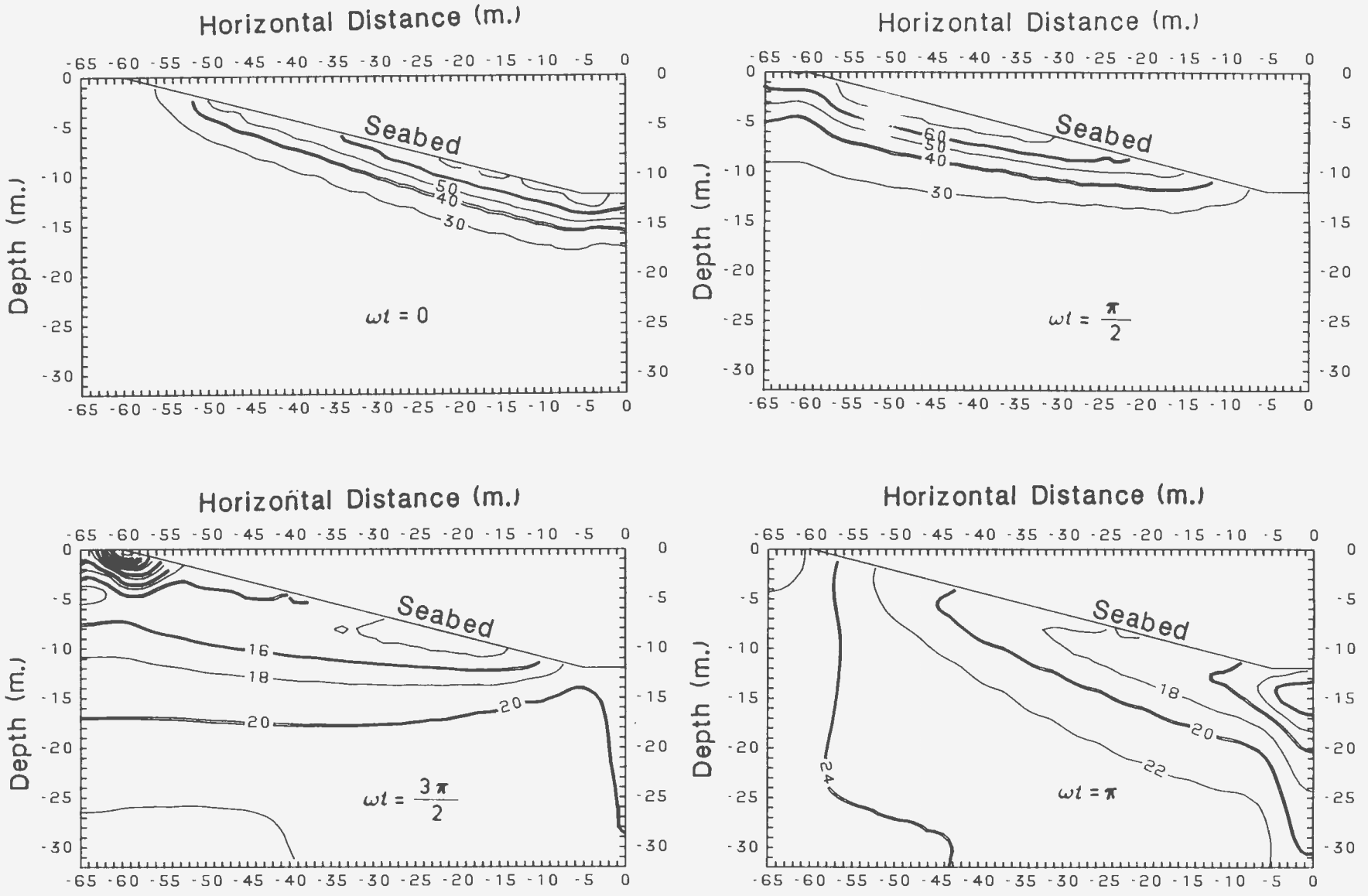

Figure J.13: Stress Angle Contours(degrees):Coarse Sand,$K = 0.5$, $L = 225$ m, $\beta = 12^{o}$

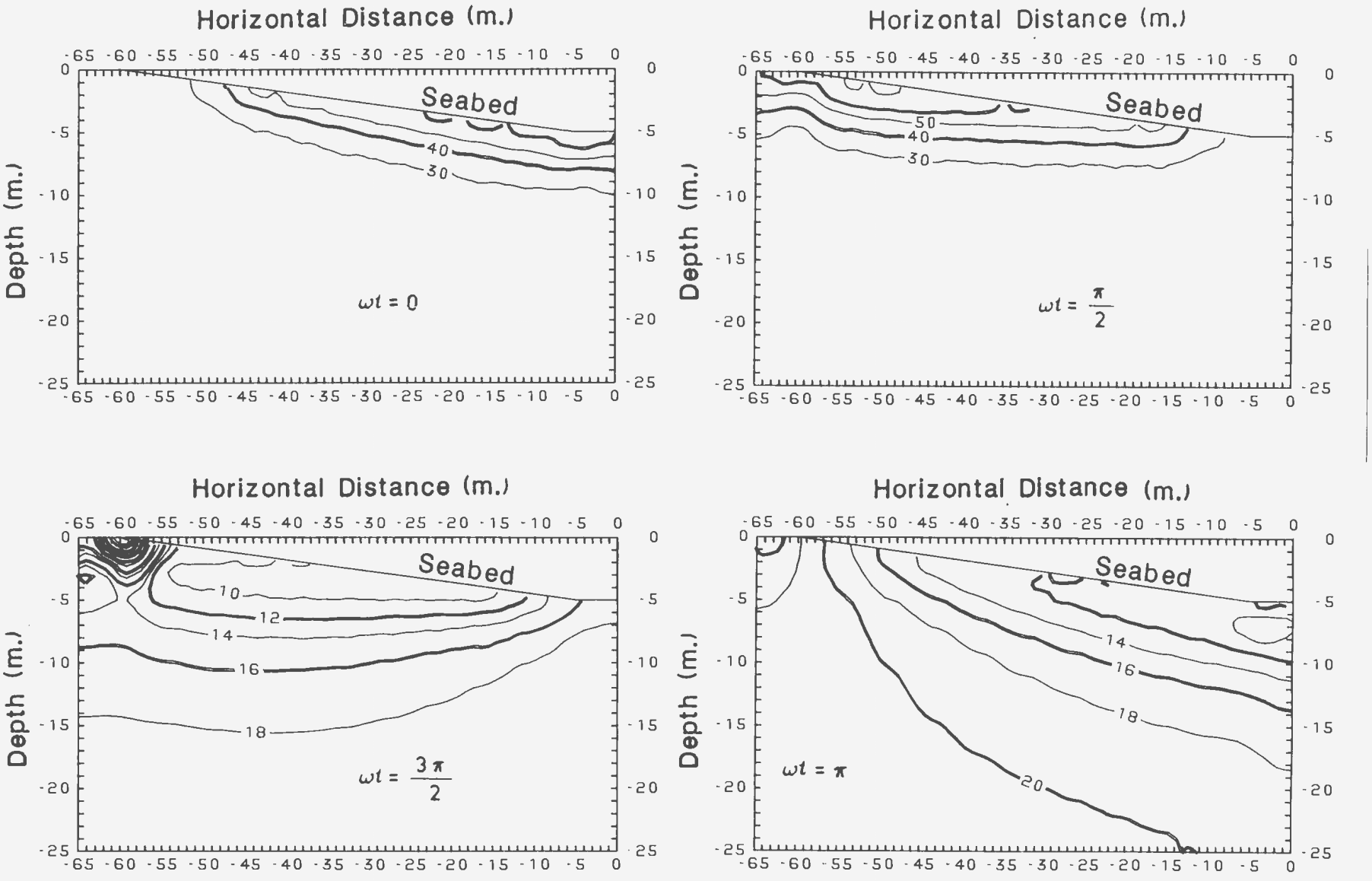

Figure J.14: Stress Angle Contours(degrees):Coarse Sand, $K = 0.5$, $L = 225$ m, $\beta = 5^o$

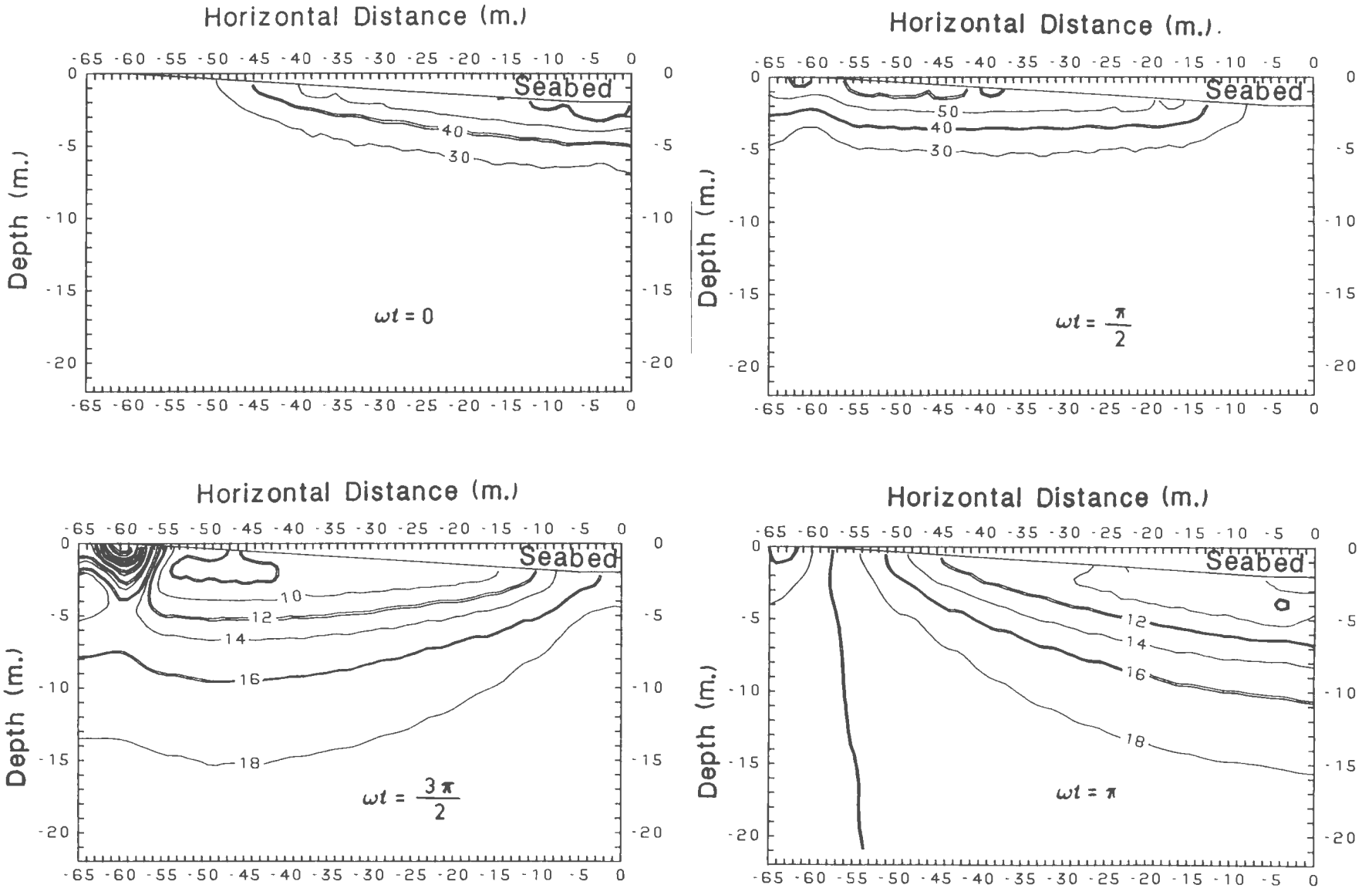

Figure J.15: Stress Angle Contours(degrees):Coarse Sand,$K = 0.5$, $L = 225$ m, $\beta = 2^o$

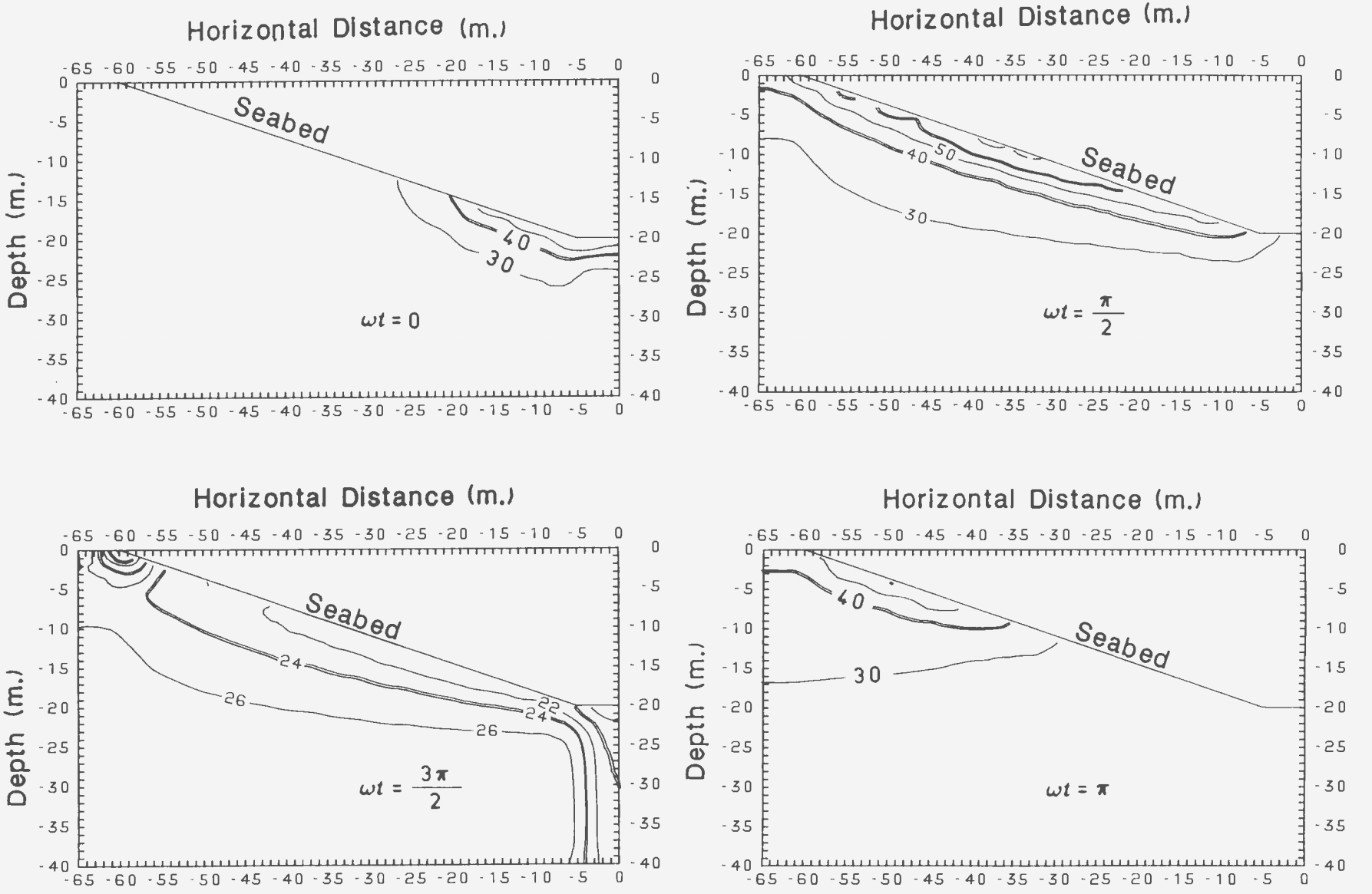

Figure J.16: Stress Angle Contours(degrees):Coarse Sand,$K = 0.5$, $L = 150$ m, $\beta = 20^o$

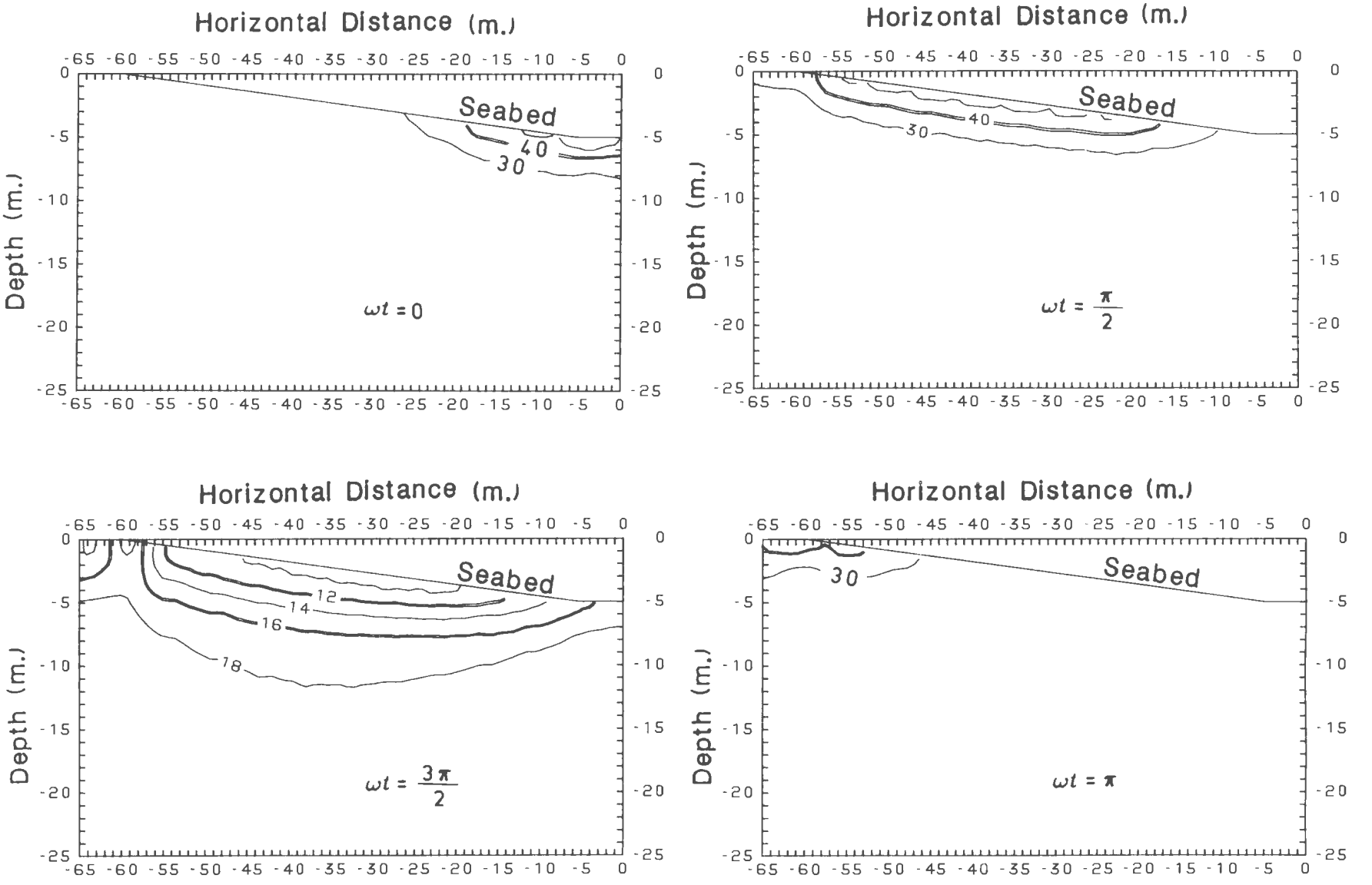

Figure J.17: Stress Angle Contours(degrees):Coarse Sand,$K = 0.5$, $L = 150$ m, $\beta = 5^o$

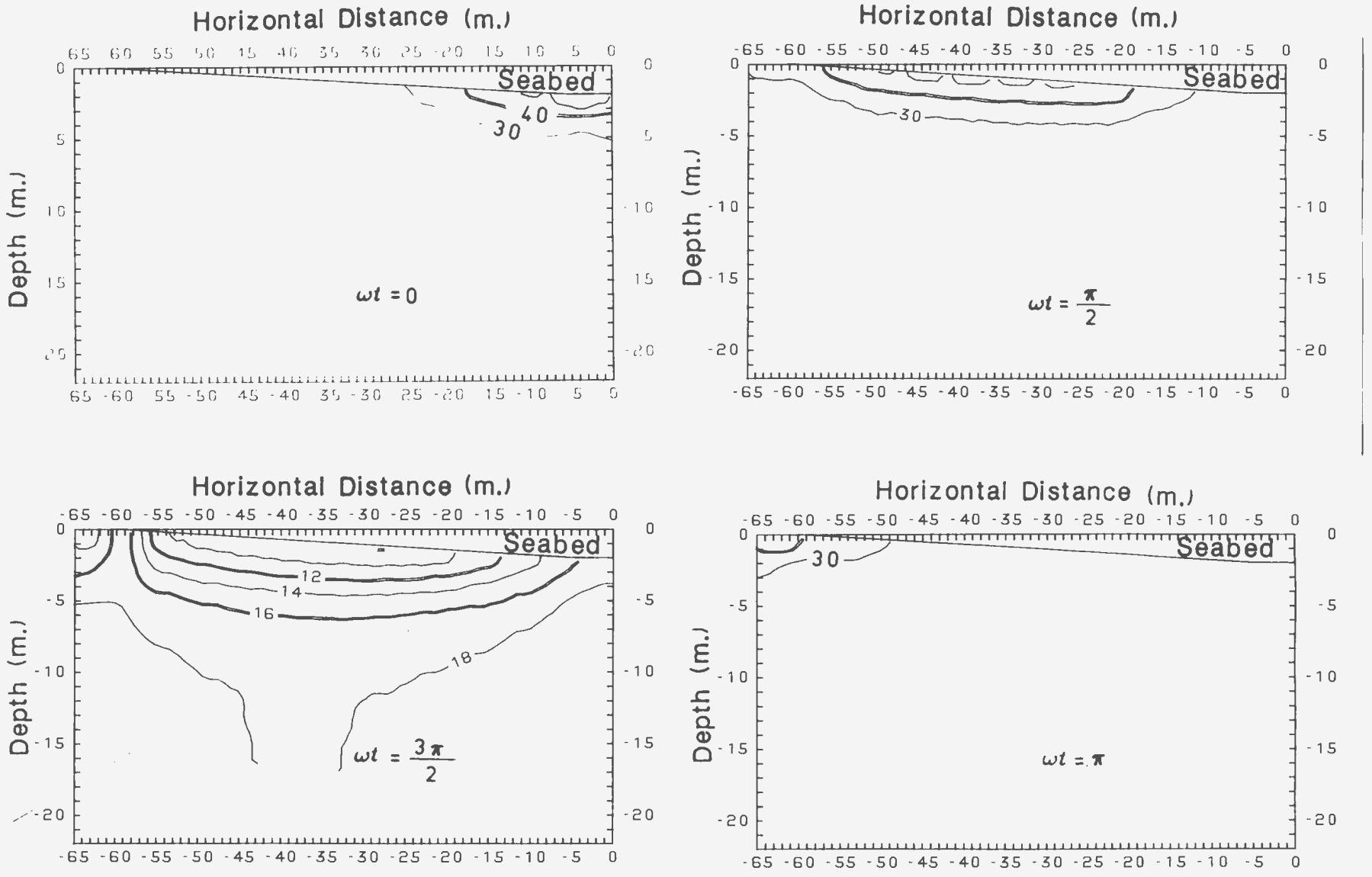

Figure J.18: Stress Angle Contours(degrees):Coarse Sand, $K = 0.5$, $L = 150$ m, $\beta = 2^o$

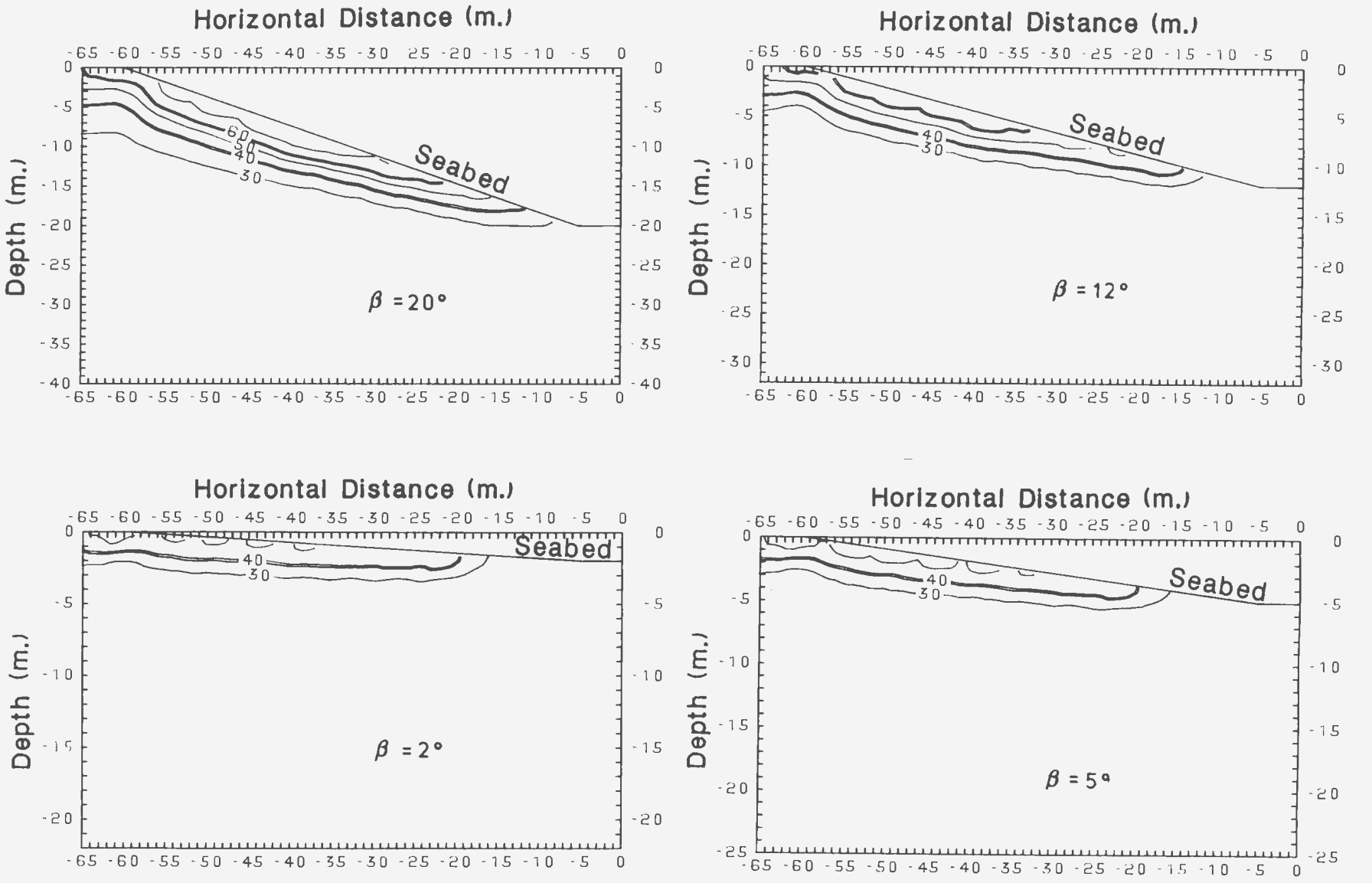

Figure J.19: Stress Angle Contours(degrees):Coarse Sand, $L = 225$ m, $\omega t = \frac{\pi}{2}$, $K = 0.7$

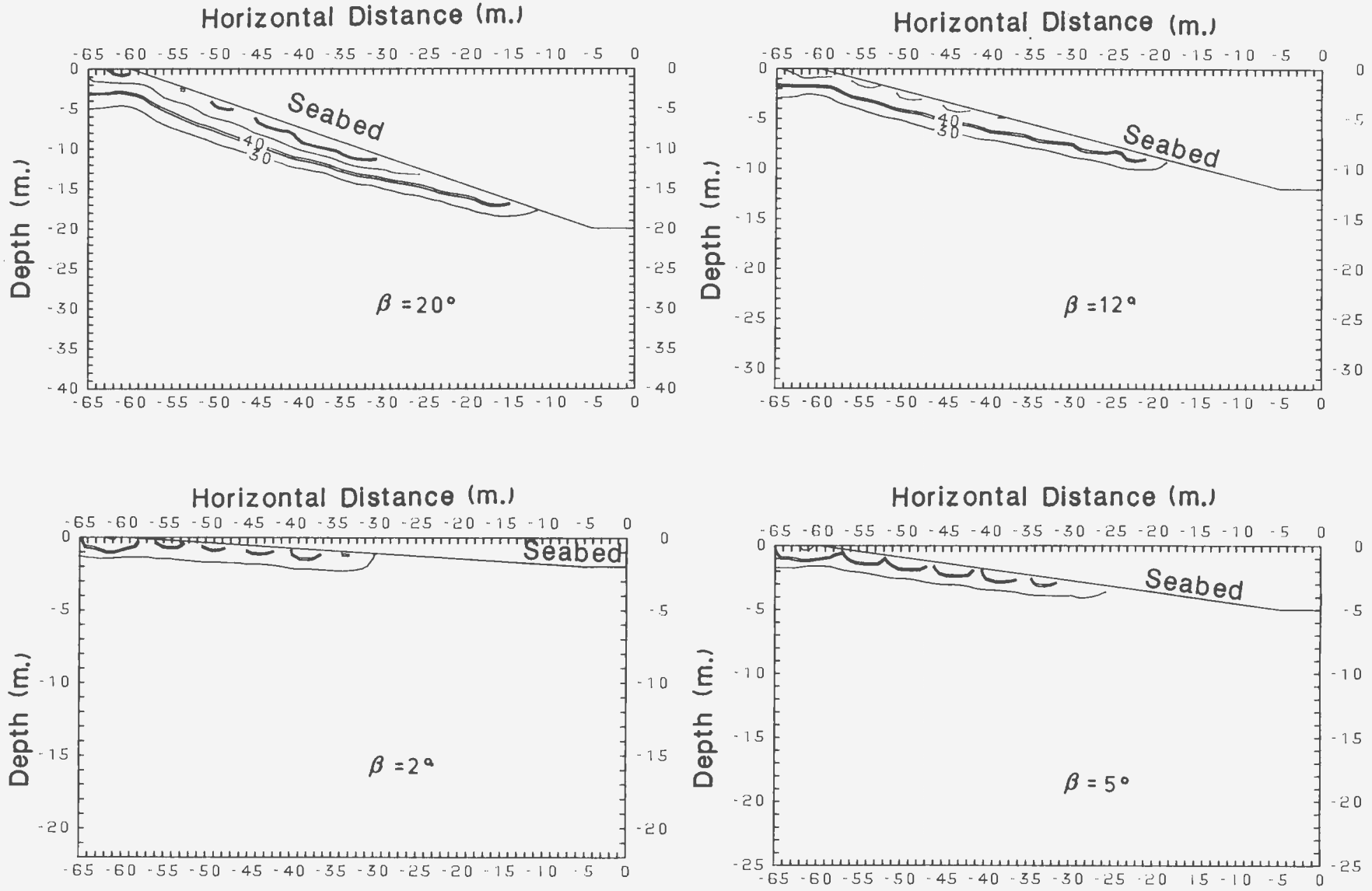

Figure J.20: Stress Angle Contours(degrees):Coarse Sand, $L = 225$ m, $\omega t = \frac{\pi}{2}$, $K = 1.0$

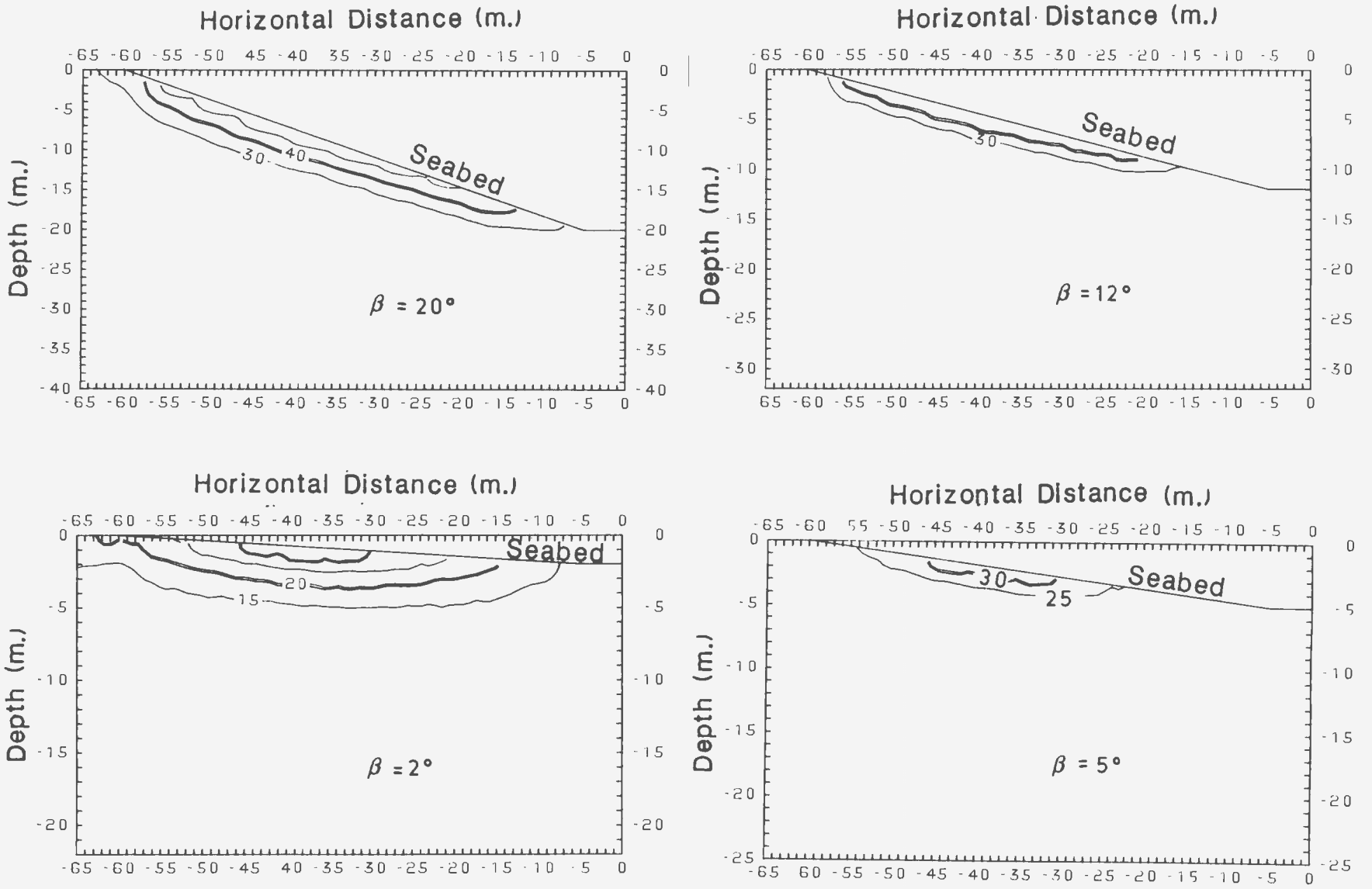

Figure J.21: Stress Angle Contours(degrees):Coarse Sand, $L = 150$ m, $\omega t = \frac{\pi}{2}$, $K = 0.7$

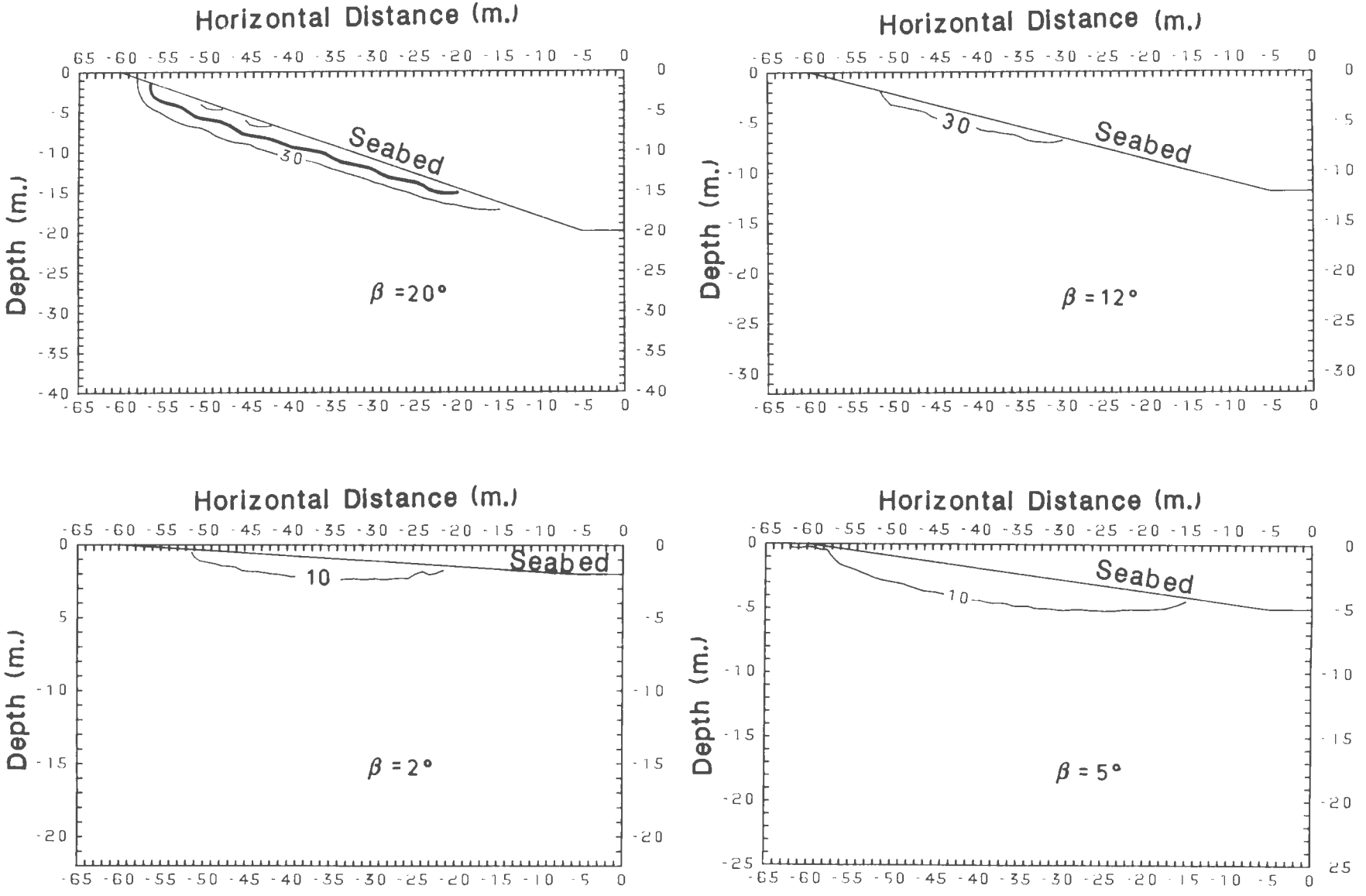

Figure J.22: Stress Angle Contours(degrees):Coarse Sand, $L = 150$ m, $\omega t = \frac{\pi}{2}$, $K = 1.0$